Modélisation 3D et simulation multimodalité de la correction percutanée des CIA sinus venosus

Clément Batteux

THESE DE DOCTORAT

NNT : 2024UPASQ072

université PARIS-SACLAY

Modélisation 3D et simulation multimodalité de la correction percutanée des CIA type sinus venosus

3D modeling and multimodality simulation of sinus venosus defects' transcatheter correction

Thèse de doctorat de l'université Paris-Saclay

École doctorale n° 569 Innovation thérapeutique : du fondamental à l'appliqué (IFTA)
Spécialité de doctorat : sciences chirurgicales
Graduate School : Santé et Médicaments. Référent : Faculté de Pharmacie

Thèse préparée dans l'unité de recherche Hypertension Pulmonaire : Physiopathologie et Innovation thérapeutique (Université Paris-Saclay, INSERM), sous la direction de **Sébastien Hascoet**, Docteur en médecine, titulaire de l'HDR.

Thèse soutenue à Paris-Saclay, le 18 Décembre 2024, par

Clément BATTEUX

Composition du Jury

Membres du jury avec voix délibérative

Damien BONNET PU-PH, Hôpital Necker, Université Paris Cité	Président
Pamela MOCERI PU-PH, HDR, CHU de Nice, Université Côte d'Azur	Rapporteur & Examinatrice
Bruno LEFORT MCU-PH, HDR, CHU de Tours, Université de Tours	Rapporteur & Examinateur
Claire BOULETI PU-PH, CHU de Poitiers, Université de Poitiers	Examinatrice
Alain FRAISSE PU-PH, Royal Brompton Hospital, Université Londres	Examinateur
Jurgen HOERER Professeur, Centre du Cœur de Munich, Université Technologique de Munich	Examinateur
Magalie LADOUCEUR PU-PH, Hôpitaux Universitaires de Genève, Université de Genève	Examinatrice
Caroline OVAERT PU-PH, CHU de Marseille, Université de Marseille	Examinatrice

Titre : Modélisation 3D et simulation multimodalité de la correction percutanée des CIA type sinus venosus

Mots clés : Cardiopathie congénitale, Anatomie, Sinus venosus, Modélisation tri-dimensionnelle, Simulation préopératoire, Cathétérisme cardiaque interventionnel

Résumé : La communication inter-atriale type sinus venosus (CIA-SV) est une cardiopathie congénitale rare décrite comme une communication inter-atriale haute associée à un retour veineux pulmonaire anormal dans la veine cave supérieure.

La correction percutanée des CIA-SV est une nouvelle technique de cathétérisme interventionnel qui consiste à tunnéliser la veine cave supérieure à l'oreillette droite avec un stent couvert, dans le but de fermer la communication entre les deux oreillettes et de rediriger les veines pulmonaires anormales vers l'oreillette gauche à la face postérieure du stent. Les 3 objectifs clés de l'intervention sont la stabilité du stent implanté, l'absence de shunt résiduel et l'absence d'obstacle sur les veines pulmonaires redirigées.

Fort du succès de la première correction française en 2020, ce travail de thèse a débuté par la création d'un programme global de simulation de l'intervention basé sur la modélisation d'un jumeau numérique et son impression 3D, ayant pour objectif la planification et l'optimisation de cette nouvelle intervention.

Une simulation préopératoire de l'intervention était d'abord effectuée sur jumeau numérique afin d'évaluer au cas par cas sa faisabilité, et de choisir le matériel optimal à sa réalisation.

La simulation était ensuite effectuée sur le cœur imprimé, sur un banc d'essai perfusé et progressivement amélioré. Le banc d'essai a vu l'intégration des outils de guidage similaires à ceux utilisés in vivo en salle de cathétérisme, comme l'échographie trans-oesphagienne, la fusion d'image et le cone-beam de contrôle permettant une simulation dans des conditions semblables à la procédure in-vivo.

La simulation sur jumeau numérique a été depuis intégrée dans le processus décisionnel de l'éligibilité des patients référés pour CIA-SV (étude prospective Optivenosus en cours, NCT 05865119).

Les nombreux variants anatomiques de la CIA-SV rendent sa description anatomique aléatoire. A partir d'une cohorte débutant en 2010, nous avons pu constituer une base de données de 250 patients ayant une CIA-SV. Après collecte et analyse des scanners préopératoires, une reconstruction 3D de la malformation était effectuée, permettant d'établir une importante banque 3D de CIA-SV (200 patients).

Cette série a fait l'objet d'une analyse anatomique tridimensionnelle permettant une analyse des variants anatomiques, la mesure de leurs interconnexions et la classification de ce groupe hétérogène de cardiopathie. Cela a constitué le deuxième volet de ce travail de thèse.

Grâce au programme de simulation et aux progrès dans la compréhension anatomique, le troisième volet de cette thèse, centré sur la recherche clinique et le développement, a participé à la création de nouveaux dispositifs médicaux dédiés, spécifiquement designés pour l'intervention (stent Optimus XXL, société Andratec). La création de ces nouveaux stents a permis de lancer une étude prospective nationale afin d'évaluer la sécurité et l'efficacité et la sécurité du dispositif (étude Optivenosus).

Les 3 parties de ce travail ont été sans cesse interconnectées et cela a permis d'améliorer la connaissance et le traitement de cette cardiopathie.

Les perspectives sont nombreuses grâce à une sélection de plus en plus large des patients, garantie par un taux de succès satisfaisant sans mortalité répertoriée depuis le lancement du programme.

La modélisation tridimensionnelle des cardiopathies congénitales assure donc une meilleure visualisation et compréhension des variants anatomiques. Elle permet également la navigation à l'intérieur du jumeau numérique pour l'analyse de régions précises.

La simulation préopératoire virtuelle et physique sur banc d'essai permet elle, un entrainement des opérateurs et une meilleure compréhension de challenges et des points critiques de l'opération afin d'en optimiser les taux de succès et d'en minimiser les risques.

Title : 3D modeling and multimodality simulation of sinus venosus defects' transcatheter correction

Keywords : Congenital heart disease, Anatomy, Sinus venosus, Three-dimensional modelisation, Pre-operative simulation, Interventional cardiac catheterization

Abstract : Sinus venosus defect (SVD) is a rare congenital heart defect described as a high inter-atrial communication associated with abnormal pulmonary venous return into the superior vena cava.

Trans-catheter correction of SVD is a novel interventional catheterization technique that involves tunneling the superior vena cava to the right atrium with a covered stent, aiming to close the communication between the two atria and redirect the abnormal pulmonary veins to the left atrium at the posterior side of the stent. The three key objectives of the intervention are the stability of the implanted stent, the absence of residual shunt, and the absence of obstruction in the redirected pulmonary veins.

Building on the success of the first French correction in 2020, this thesis work began with the creation of a comprehensive simulation program for the procedure based on the modeling of a digital twin and its 3D printing, with the goal of planning and optimizing this new intervention. A preoperative simulation of the procedure was first performed on the digital twin to assess its feasibility on a case-by-case basis and to select the optimal equipment for its execution. The simulation was then conducted on the printed heart, using a perfused test bench that was progressively improved. The test bench incorporated guidance tools similar to those used in vivo in the catheterization laboratory, such as transesophageal echocardiography, image fusion, and cone-beam control, allowing for simulation under conditions akin to the in vivo procedure. The digital twin simulation has since been integrated into the decision-making process for the eligibility of patients referred for SVD trans-catheter correction (ongoing prospective study Optivenosus, NCT 05865119).

The numerous anatomical variants of SV-ASD render its anatomical description variable. From a cohort starting in 2010, we were able to establish a database of 250 patients with SVD. After collecting and analyzing preoperative scans, a 3D reconstruction of the malformation was performed, allowing for the establishment of a significant 3D bank of SVD cases (200 patients). This series underwent three-dimensional anatomical analysis to examine anatomical variants, measure their interconnections, and classify this heterogeneous group of heart defects. This constituted the second part of this thesis work.

Thanks to the simulation program and advances in anatomical understanding, the third part of this thesis, focused on clinical research and development, contributed to the creation of new dedicated medical devices specifically designed for the intervention (Optimus XXL stent, Andratec company). The development of these new stents has enabled the launch of a national prospective study to evaluate the safety and efficacy of the device (Optivenosus study).

The three components of this work have been continuously interconnected, leading to improved knowledge and treatment of this heart defect. There are numerous prospects for expansion, thanks to an increasingly broad selection of patients, guaranteed by a satisfactory success rate without recorded mortality since the program's launch.

Three-dimensional modeling of congenital heart defects thus ensures better visualization and understanding of anatomical variants. It also allows navigation within the digital twin for the analysis of specific regions. The virtual and physical preoperative simulation on the test bench enables training for operators and a better understanding of the challenges and critical points of the operation, optimizing success rates and minimizing risks.

MOTS CLÉS

Cardiopathie congénitale
Anatomie
Sinus venosus
Modélisation tri-dimensionnelle
Simulation préopératoire
Cathétérisme cardiaque interventionnel

KEY WORDS

Congenital heart disease
Anatomy
Sinus venosus
Three-dimensional modelisation
Pre-operative simulation
Interventional cardiac catheterization

LABORATOIRE D'ACCUEIL

Unité Inserm 999 : Hypertension Pulmonaire : Physiopathologie et Nouvelles Thérapies

FINANCEMENT DE LA THÈSE

2020/2021
Bourse Hélène de Marsan (Cardiologie Pédiatrique ou congénitale) soutenue par l'AREMCAR de la Société Française de Cardiologie.
"*Modélisation tridimensionnelle et simulation multi-modalité de la fermeture percutanée des communication inter-atriales type sinus venosus*"
Montant : 15 000 euros

Le reste de la thèse a été auto-financé, le doctorant étant salarié de l'Hôpital Marie Lannelongue et a mené cette thèse dans le cadre de la « formation tout au long de la vie ».

LIENS D'INTÉRÊTS

Le doctorant n'a pas de conflits d'intérêts pour ce travail.

REMERCIEMENTS

A madame **Pamela Moceri**, je vous remercie d'avoir accepté d'être rapporteur de cette soutenance de thèse. Au cours de nos échanges en congrès où vous modériez des sessions dans lesquelles j'intervenais, mais aussi en réunion pluri-disciplinaire sur des dossiers difficiles, vous avez toujours fait preuve envers vos pairs d'une bienveillance et d'une rigueur sans failles, nous permettant d'échanger avec sérénité, sérieux, et confiance. Merci également pour votre expertise renommée dans la prise en charge des adultes porteurs de cardiopathie congénitales, et plus particulièrement ceux atteints d'hypertension pulmonaire, maladie centrale ayant conduit à la naissance de ce travail doctoral. Acceptez de trouver ici le témoignage de mon respect sincère.

A monsieur **Bruno Lefort**, je vous remercie d'avoir accepté d'être rapporteur de cette thèse de doctorat. Je vous remercie pour l'accueil enthousiaste de ma sollicitation l'été dernier, de faire partie du jury de cette thèse. Votre engagement auprès des patients porteurs de cardiopathie congénitale, votre leadership naturel et bienveillant auprès de tous nos jeunes pairs, sont des exemples pour aborder ma pratique médicale et universitaire dans les années à venir. Votre rigueur et détermination en salle de cathétérisme, toujours pour le bien du patient, est une source d'inspiration. Acceptez de trouver ici le témoignage de ma sincère amitié.

A monsieur **Damien Bonnet**, je vous remercie d'avoir accepté de juger ce travail doctoral et d'en être le président. C'est un véritable honneur et plaisir de vous compter parmi les membres de mon jury. Je vous remercie de m'avoir ouvert la porte de votre bureau à l'été 2017, de m'avoir donné la possibilité de travailler à Necker sous votre direction, et d'avoir toujours été humainement juste dans nos échanges professionnels. Votre bienveillance et votre confiance à mon égard sont inestimables. Merci aussi pour votre empathie envers les patients, ainsi que pour votre dévouement à notre chère spécialité. Acceptez de trouver ici le témoignage de ma sincère reconnaissance.

A madame **Claire Bouleti**, je vous remercie d'avoir accepté de juger cette thèse doctorale. Votre implication dans le domaine de la cardiologie de l'adulte et vos travaux universitaires sont une source d'inspiration. Votre expertise et jugement apporteront j'en suis sûr, une valence très bénéfique à ce doctorat et sa soutenance. Veuillez accepter mon respect dévoué.

A madame **Magalie Ladouceur**, je vous remercie d'avoir accepté d'être membre du jury de ma soutenance de thèse. Votre expertise et votre dévouement dans la prise en charge des cardiopathies congénitales de l'adulte est admirable. Vous avez modéré ma première communication orale quand interne, je m'intéressais à la modélisation 3D des cardiopathies congénitales. C'est donc avec émotion que je vous remercie et vous demande de trouver le témoignage de ma reconnaissance.

A madame **Caroline Ovaert,** je vous remercie d'avoir accepté avec enthousiasme de juger cette thèse. Votre carrière, votre énergie, votre détermination, sont tous autant d'exemples pour les générations actuelles et futures. Votre implication dans les associations et fédérations nationales et internationales de notre spécialité (et sur-spécialité) est inspirante et source d'énergie. Merci d'accepter le témoignage de mon respect amical.

A monsieur **Alain Fraisse,** je vous remercie de prendre part à la soutenance en tant que membre avec voix délibérative. La passion et l'ingéniosité avec laquelle vous pratiquez votre métier est une source d'admiration. L'intérêt que vous avez porté à mon travail de thèse, ainsi que l'enthousiasme partagé lors de nos différents échanges constructifs ont été plus que bénéfiques à la conduite de ce travail. Veuillez accepter le témoignage de mon amitié et de mon grand respect.

A monsieur **Jurgen Hoerer**, je vous remercie de traverser les frontières pour juger avec impartialité mon travail. De votre accueil à Munich à votre bienveillance à Vienne, toutes nos rencontres ont été pour moi une grande joie. Je vous remercie de votre implication et professionnalisme dans la prise en charge chirurgicale des patients congénitaux, mais aussi d'avoir cru en notre projet de traitement percutanné des CIA sinus venosus, qui, soutenu par un chirurgien de renommée internationale, a pu

s'émanciper et se construire avec toute la sérénité nécessaire. Veuillez accepter le témoignage de ma sincère admiration.

A monsieur **Sébastien Hascoet**, je vous remercie d'avoir dirigé pendant 4 ans ce travail de thèse. Que de chemin parcouru depuis notre première rencontre où nous avons posé les bases d'une collaboration professionnelle que j'espère longue et fructueuse, comme en témoigne ce chemin doctoral. Merci d'avoir cru en mon projet profesionnel, puis en mon aptitude au cathétérisme des cardiopathies congénitales. Merci également pour votre implication sans faille ni relâche dans la prise en charge des patients porteurs de cardiopathie congénitale, d'où qu'ils viennent. Votre dévouement et passion m'obligent respect, admiration et amitié. Veuillez trouver ici le témoignage de ma reconnaissance sincère.

A Ivan Bouzguenda, sans qui rien n'aurait été.

A mes mentors, pierres angulaires du médecin accompli que je suis aujourd'hui : Olivier Guilluy, Géry Hannebicque, Jean-François Piéchaud, Joy Zoghbi, Emre Belli, Damien Bonnet, Jérôme Petit, Sébastien Hascoet.

A mes compagnons de route et amis à vie, rencontrés sur les bancs de la fac et de l'hôpital : Antoine Schernberg, Remy Hamdam, Ghita Badidi, Gabriel Miget, Harry Etienne, Pierre-Marie Duret, Julien Hannebicque, Victor Housset, Domenico Sirico.
A Arshid Azarine pour son sourire sa musique sa good vibe.

A tous les employés de l'Hôpital Marie Lannelongue (internes, médecins, chefs de service, paramédicaux, brancardiers, agents d'entretien, personnel administratif, personnel de la communication, personnel de l'informatique, personnel du PC sécurité, personnel du self) pour leur gentillesse, bienveillance, et participation à rendre le quotidien agréable.
A notre devise commune à tous : *patient first.*

A toute les équipes du département de recherche clinique, du département de la recherche préclinique (#Malic) ainsi qu'à Vlad Ciobotaru pour son ingéniosité hors pair.

A tou(te)s les stagiaires ingénieur(e)s rencontrés autour de ce projet.

A tous les organismes ayant participé, financièrement ou institutionnellement, de près ou de loin, à la conduite de ce travail, notamment la fondation Hôpital Saint Joseph.

A nos patients qui ont cru au « projet sinus venosus », avec espoir, parfois déception, souvent enthousiasme, toujours confiance.

A l'amicale de la restauration.
Au foot le dimanche matin 10h.
A Minorque.

A mes amis, ceux pour toujours.

A ceux tellement dans mon cœur qu'ils n'ont plus de vrai prénoms (Mimi, Nono, Albich, Cécé, FF, Clix, Kuc, Nugget, sagesse, JT, Conin, KD, Will.i.am, Loulou, Nanou, Stephou)

A ma famille, ouvrière, immigrée, citoyenne, républicaine
A ma sœur Marion et son compagnon Simon, parents de mes merveilleux neveux Alix et Léandre.
A Marie-France et mon père que j'aime tellement.
A ma mère Chantal Batteux, que j'aime, et à qui cet accomplissement universitaire est dédié.
A tous mes grands-parents, là-haut : il faut se reposer maintenant.
A ma grand-mère Hélène, qui me manque chaque jour.

TABLE DES MATIÈRES

LISTE DES ABBRÉVIATIONS

AEPC : Association Européenne de Cardiologie Pédiatrique
AMM : autorisation de mise sur le marché
ANSM : agence nationale de santé du médicament ANSM
AO : aorte
AP : artère pulmonaire
CAM : champs aléatoires de Markov
CAV: canal atrio-ventriculaire
CBCT: cone-beam computed tomography
CEC: circulation extra-corporelle
CEO: chief executive officer (président directeur général)
CIA: communication inter-atriale
CRF: case report form (eCRF: electronic CRF)
DICOM: digital imaging and communication in medicine
DSS : digital signature standard
ECG : électrocardiogramme
ETO : échographie trans-oesophagienne
ETT : échographie trans-thoracique
FA : fibrillation atriale
HML : Hôpital Marie Lannelongue
HTAP : hypertension artérielle pulmonaire
IFSBM : Institut de Formation Supérieure Biomédicale
IFTA : Innovation Thérapeutique : du Fondamental à l'Appliqué
IRM : imagerie par résonnance magnétique
JCA : jonction cavo-atriale
MALIC : Marie Lannelongue Innovation Center
MPR : multi planar Reconstruction
M3C : Malformation Cardiaque Congénitale Complexe
NIFTI : neuroimaging informatics technology initiative
OD : oreillette droite
OG : oreillette gauche
OP: ostium primum
OS: ostium secundum
PAP : pressions artérielles pulmonaires
PME : petite et moyenne entreprise
PRME : projet de recherche médico-économique
PTFE : poly-tétrafluoroéthylène
QP/QS : débit pulmonaire/débit systémique
RCP : réunion de concertation pluri-disciplinaire
ROI : region of interest
RVPA : retour veineux pulmonaire anormal
SC : sinus coronaire
SLA: stereolithograph apparatus
SLS: selective laser sintering
STL: Standard Tessellation Language

STROBE: Strengthening the Reporting of Observational Studies in Epidemiology
SV : sinus venosus
TDR : trouble du rythme
TPU : thermo-polyuréthane
TVI : tronc veineux innominé
UV : ultra-violet
UW : unité Wood
VAV : valve auriculo-ventriculaire
VCI : veine cave inférieure
VCS : veine cave supérieure
VCSD : veine cave supérieure droite
VCSG : veine cave supérieure gauche
VD : ventricule droit
VG : ventricule gauche
VP : veine pulmonaire
VPSG : veine pulmonaire supérieure gauche
2D : deux dimensions
3D : trois dimensions
4D : quatre dimensions

LISTE DES FIGURES

INTRODUCTION

I. Communications inter-atriales

1. Généralités

Les communications inter-atriales (CIA) forment un groupe de malformations cardiaque congénitale rassemblant les anomalies de la septation atriale et des retours veineux aboutissant à un shunt à l'étage atrial. Il y a 5 types anatomiques de CIA (Figure 1) : les CIA ostium secundum (OS), les CIA ostium primum (OP), les CIA sinus venosus (SV), les CIA à travers le toit du sinus coronaire fenestré (SC) et les CIA basses ou « low septal defect ».

Le foramen ovale perméable, du fait de son caractère embryologique constant et de sa prévalence élevée dans la population générale, n'est pas considéré comme une cardiopathie congénitale. Les CIA sont diagnostiquées dans 1/1000 naissances vivantes.[1] La prévalence des CIA OS est plus importante chez la femme (70%) alors que le sex-ratio est équilibré pour les autres formes de CIA.

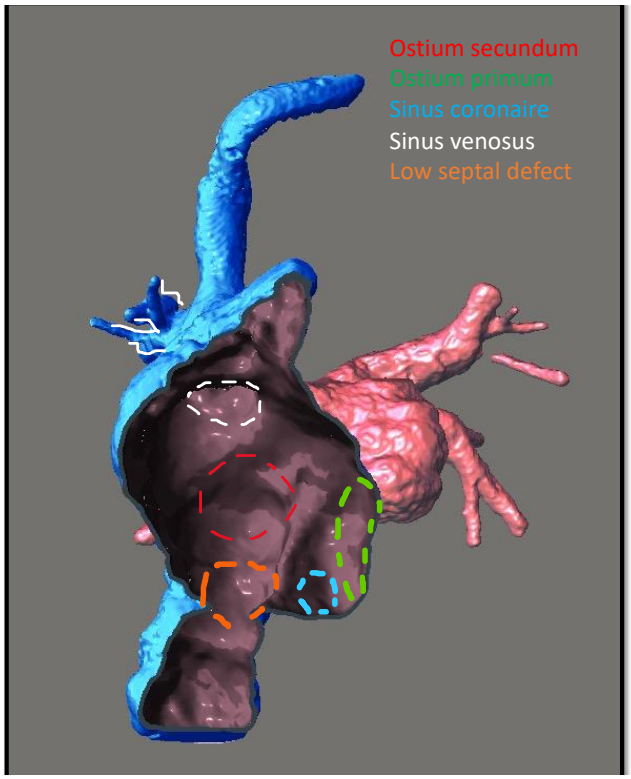

Figure 1 : modélisation 3D du septum inter-atrial et localisation des différentes formes anatomiques de CIA

Les CIA sont souvent sporadiques. Il existe des formes familiales liées à des mutations de gènes connus (Nkx2.5, GATA4, TBX5, MYH6)[2-11]. Parfois, les CIA sont intégrées à un syndrome génétique tel que le syndrome de Holt Oram (dysplasie atrio-digital associant anomalies musculo-squelettique et cardiaques) où une CIA est présente dans 2/3 des cas.[12] On note une incidence plus élevée des CIA chez les enfants de femmes âgées, et en cas d'exposition maternelle à certains toxiques (tabac, hyperglycémie, antidépresseurs).[13-16]

2. Embryologie

A la 4ème semaine de la vie fœtale, l'oreillette primitive unique se cloisonne par le développement du septum primum. Ce croissant musculaire naissant à la partie postéro-supérieure de l'oreillette primitive, croit vers le bourgeon endocardique atrio-ventriculaire supérieure entre les composants droit et gauche en cours de développement. Le bord libre du septum primum est recouvert d'un tissu mésenchymateux qui fusionne avec le bourgeon endocardique supérieure. Durant la même période, une protrusion mésenchymateuse dorsale appelée l'épine vestibulaire, située à la droite de l'orifice veineux pulmonaire primitif, entre dans la partie postérieure du cœur et croit vers le bourgeon endocardique inférieure[17]. Durant cette période de croissance de l'épine vestibulaire et du septum primum, les bourgeons endocardiques supérieur et inférieur fusionnent divisant le canal atrioventriculaire en un orifice mitral et un orifice tricuspide. Le septum primum, l'épine vestibulaire et les bourgeons endocardiques délimitent l'ostium primum mettant en communication l'oreillette droite et gauche. Avant que cet ostium primum ne puisse se fermer, une déhiscence appelée l'ostium secundum se forme par apoptose cellulaire dans le septum primum à sa partie postéro-supérieure. L'ostium secundum permet la persistance d'un shunt inter-atrial droite-gauche, indispensable durant la vie fœtale, lorsque l'ostium primum disparait à J34 par fusion des bords mésenchymateux du septum primum, de l'épine vestibulaire et des bourgeons atrio-ventriculaires. Entre J36 et J42, à la droite du septum primum se développe ensuite le septum secundum, par invagination de la paroi musculaire de l'oreillette à sa partie postéro-supérieure entre

la veine cave supérieure et la veine pulmonaire primitive. Le septum secundum constitue un clapet qui vient fermer l'ostium secundum après la naissance.
Les veines pulmonaires se développent à partir du mésocarde dorsal et leur connexion à l'oreillette gauche provient de la fusion entre le plexus vasculaire pulmonaire atrial et la veine pulmonaire primitive de façon concomitante au développement du septum secundum. La connexion des veines systémiques à l'oreillette droite se fait par des mécanismes de prolifération/apoptose entre le sinus veineux et l'oreillette droite. La corne droite du sinus veineux se développe en veines caves supérieure et inférieure droites, alors que la corne gauche involue de manière partielle le plus souvent (ne donnant que le sinus coronaire), ou non, avec persistance d'une veine cave supérieure gauche, abouchée au sinus coronaire. Des reliquats embryologiques membraneux persistent dans l'oreillette droite : la valve d'Eustachi à la jonction entre l'oreillette droite et la veine cave inférieure et la valve de Thébésius à la jonction entre l'oreillette droite et le sinus coronaire.

3. Physiopathologie

La physiopathologie des CIA dépend du sens et de l'importance du shunt atrial. Les déterminants de ce shunt sont la taille du défect, le rapport de compliance entre les deux ventricules et les éventuelles lésions associées.[18]
A la naissance, les résistances vasculaires pulmonaires sont élevées, la compliance ventriculaire droite est faible, superposable à celle du ventricule gauche. Il n'y a donc pas de shunt significatif à travers une CIA, même large. Un shunt unidirectionnel à travers une CIA chez un nouveau-né doit faire rechercher une anomalie associée. Si le shunt est gauche droite, cela peut être un obstacle du cœur gauche ou une coarctation aortique. Si le shunt est droite gauche, cela peut être un obstacle ou atrésie sur les valves pulmonaire ou tricuspide, une persistance de résistance vasculaire pulmonaire élevée ou un retour veineux pulmonaire anormal total.
Après la naissance, les résistances vasculaires diminuent progressivement. La post-charge du VD baisse en conséquence et donc la compliance VD s'améliore. Le shunt est gauche-droite à travers la CIA et il augmente proportionnellement à l'amélioration de la compliance du VD. Le shunt gauche-droite est responsable d'un hyperdébit pulmonaire et les cavités cardiaques droites se dilatent progressivement. La bonne

compliance du ventricule droit lui permet de se dilater facilement sans épaississement pariétal (phénomène de remodelage excentrique), tout en conservant une fonction systolique normale. Le volume d'éjection systolique VD est augmentée et le VD est hyperkinétique. La surcharge volumique des cavités droites en diastole conduit à un mouvement paradoxal du septum interventriculaire en protodiastole. Cette physiopathologie n'entraine le plus souvent aucune symptomatologie dans l'enfance et chez l'adulte jeune.

Chez l'adulte, la dilatation de l'OD et secondairement de l'OG peut-être le substrat de troubles du rythme supra-ventriculaires, à type de type flutter et fibrillation atriale. L'hyperdébit pulmonaire prolongé peut de façon inconstante entrainer un remodelage vasculaire pulmonaire avec hypertrophie de la média et prolifération intimale puis fibrose vasculaire. Ces lésions aboutissent à une augmentation des résistances vasculaires pulmonaires et à une hypertension artérielle pulmonaire (HTAP), augmentant la post-charge du VD. Le VD s'hypertrophie et sa compliance s'altère. A l'extrême, une inversion du shunt de la droite vers la gauche survient (syndrome d'Eisenmenger).[19]

Avec la sénescence, en l'absence d'HTAP, le shunt gauche-droite augmente. Cela est expliqué par l'altération de la compliance VG liée à l'augmentation plurifactorielle des résistances vasculaires systémiques et à une dysfonction diastolique du VG favorisée par l'âge et des comorbidités comme le diabète, l'hypertension artérielle ou la sténose valvulaire aortique. Dans ces conditions, l'hyperdébit pulmonaire est plus important et responsable de symptômes avec une dyspnée, même avec un défect de taille moyenne.

Dans le cas particulier de la CIA SV, le shunt gauche-droite est aggravé par le RVPA. Parfois, une partie du flux de la veine cave supérieure se draine dans l'OG étant donné la position haute du défect et est responsable d'une désaturation systémique modérée (shunt droite-gauche).[20]

4. Différentes formes anatomiques

a. CIA ostium secundum

La CIA OS est liée à un excès d'apoptose ou à une apoptose anarchique du septum primum. Le défect peut être unique ou multiple, de taille variable.[21,22]

L'évolution naturelle peut être la fermeture spontanée complète dans la prime enfance pour les petits défects, la stabilité, ou voir l'élargissement pour les défects larges. Plus un défect est large plus il peut s'élargir durant la croissance, et moins la fermeture spontanée est probable. Il est admis que la découverte chez un nourrisson d'une CIA OS de plus de 10 mm a très peu de chance de se fermer spontanément.[23-25]

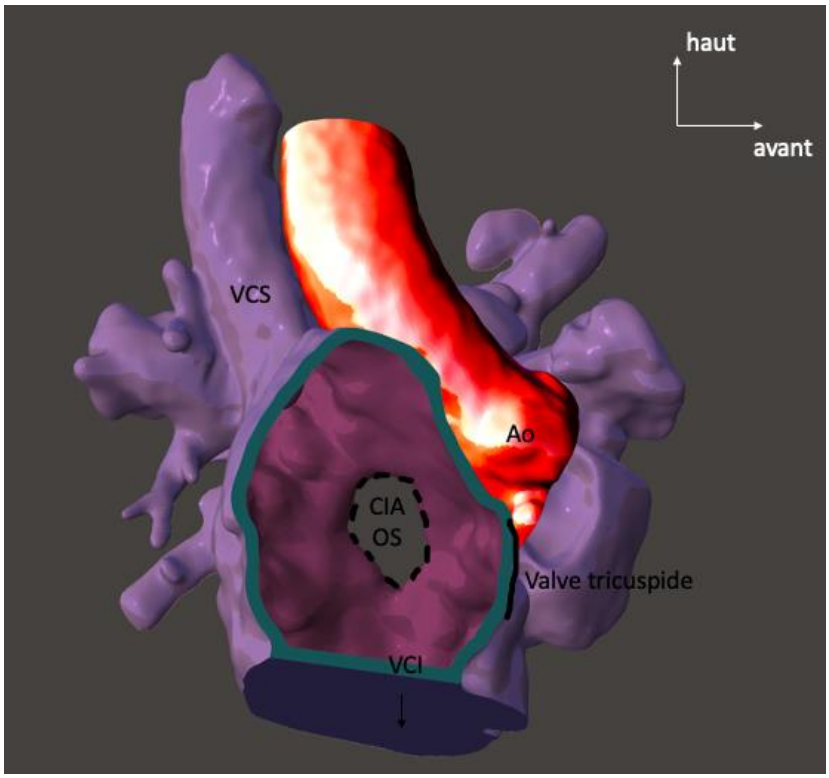

Figure 2vue 3D d'une CIA ostium secundum par l'oreillette droite.

VCS et VCI : veine cave supérieure et inférieure, Ao : aorte.

b. CIA ostium primum

La CIA OP s'intègre dans le spectre des canaux atrio-ventriculaire (CAV), et résulte d'une anomalie de septation atrio-ventriculaire. La CIA OP est systématiquement associée à un alignement des valves atrio-ventriculaires et à une fente de la valve atrio-ventriculaire gauche.

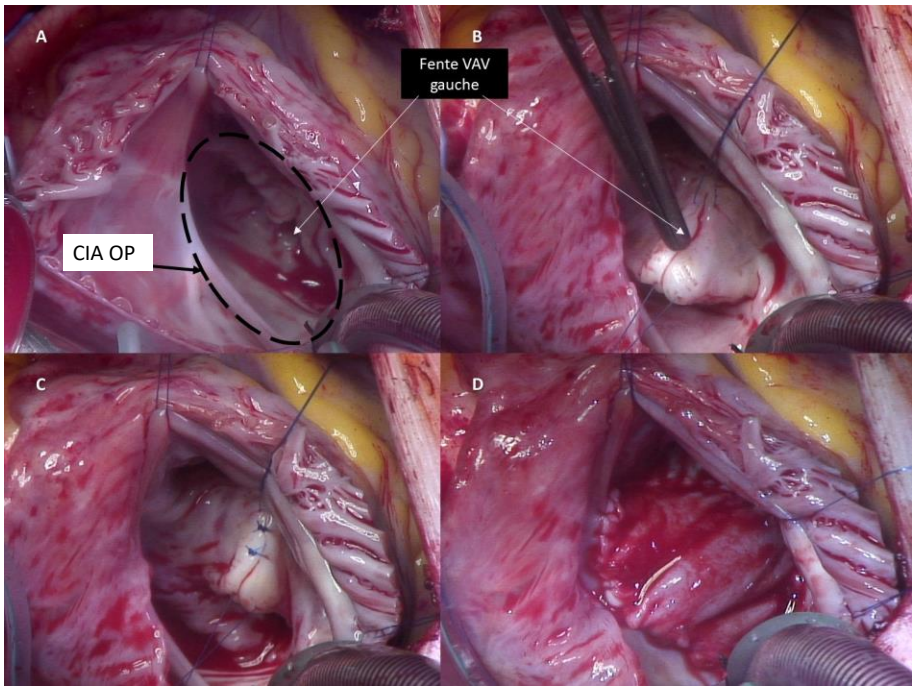

Figure 3: Vue chirurgicale par l'oreillette droite d'une CIA ostium primum

A : defect central en regard des valves auriculoventriculaire et fente ouverte de la VAV gauche.

B : suture de la fente de la VAV gauche. C : fente de la VAV gauche suturée. D : CIA ostium primum fermée par un patch.

c. CIA low septal defect

Cette forme particulière de CIA OS consiste en un défaut de septation de la portion basse du septum primum, au voisinage de la veine cave inférieure. Dans cette forme, il n'y a pas d'anomalie du retour veineux pulmonaire, et la fermeture spontanée est peu probable. Il y a une continuité entre la veine cave inférieure et l'oreillette gauche.

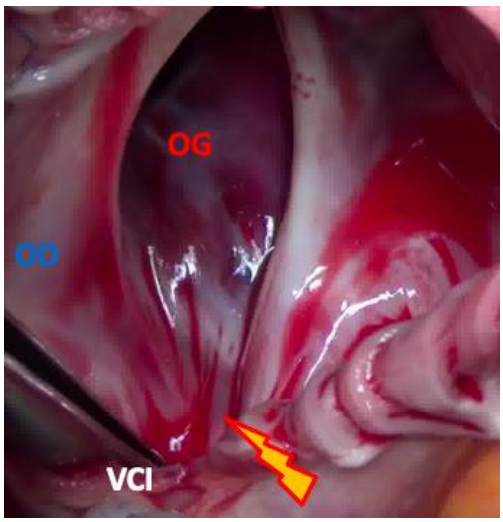

Figure 4: vue chirurgicale d'une CIA low septal defect

OG : oreillette gauche OD : oreillette droite VCI : veine cave inférieure Éclair : déficit de la berge inférieure

d. CIA sinus venosus

Les CIA SV représentent 10% des CIA. Elle est le résultat d'une séquence embryologique pathologique. Une fusion anormale des parois d'une veine cave et d'une (ou de plusieurs) veines pulmonaires droites se produit. Un défect dit « sinus venosus » se forme par apoptose de la paroi fusionnée commune. Ce défect SV n'est donc pas située dans le septum primum mais au-dessus (dans la forme supérieure).[26,27]

La CIA SV supérieure est associée à un retour veineux pulmonaire anormal (RVPA) supérieur droit vers la veine cave supérieure. Il n'est pas rare que plusieurs veines pulmonaires supérieures segmentaires se drainent également dans la veine cave supérieure, parfois relativement haut, à proximité de l'abouchement de la veine azygos.

Très rarement, la CIA SV est inférieure, très basse dans le septum, associée à un RVPA d'une veine pulmonaire inférieure droite au pied de la veine cave inférieure.[28, 29]

Les CIA SV ne se ferment jamais spontanément.

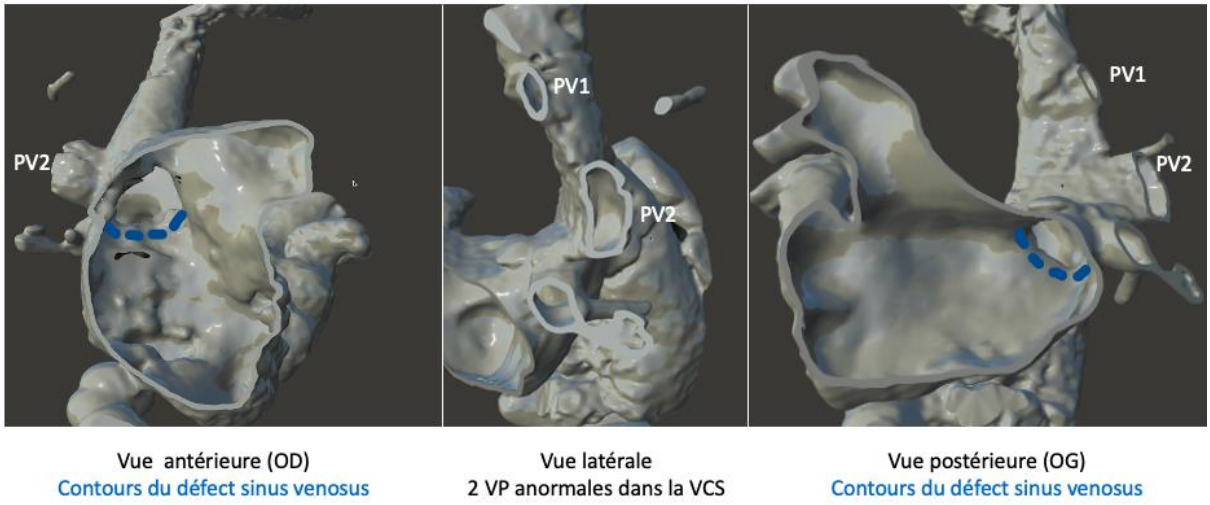

Figure 5: modélisation 3D d'une CIA type sinus venosus

Légende : PV1 et PV2 : veines pulmonaire 1 et 2. OD oreillette droite. OG oreillette gauche.

e. *CIA du sinus coronaire*

Le sinus coronaire, qui chemine le long de la paroi inférieure de l'oreillette gauche et qui s'abouche à l'oreillette droite à la partie antéro-inférieure du septum inter-atrial, est normalement séparé de l'oreillette gauche par un « toit » complet imperméable. Dans la CIA SC, le toit du sinus coronaire peut être fenestré partiellement ou totalement, du fait d'une apoptose anormale. Cette fenestration met alors en communication l'oreillette gauche et l'oreillette droite[30,31]. Ce défect est souvent mais inconstamment associée à la persistance d'une veine cave supérieure gauche abouchée au sinus coronaire.[32]

Lorsque la déhiscence du toit du sinus coronaire est totale, le shunt inter-atrial gauche-droite se fait par l'orifice du sinus coronaire et il s'y associe un shunt droite-gauche par incorporation totale du sinus coronaire dans l'oreillette gauche. Ce shunt droite-gauche est habituellement négligeable sauf lorsqu'il persiste une veine cave supérieure gauche.

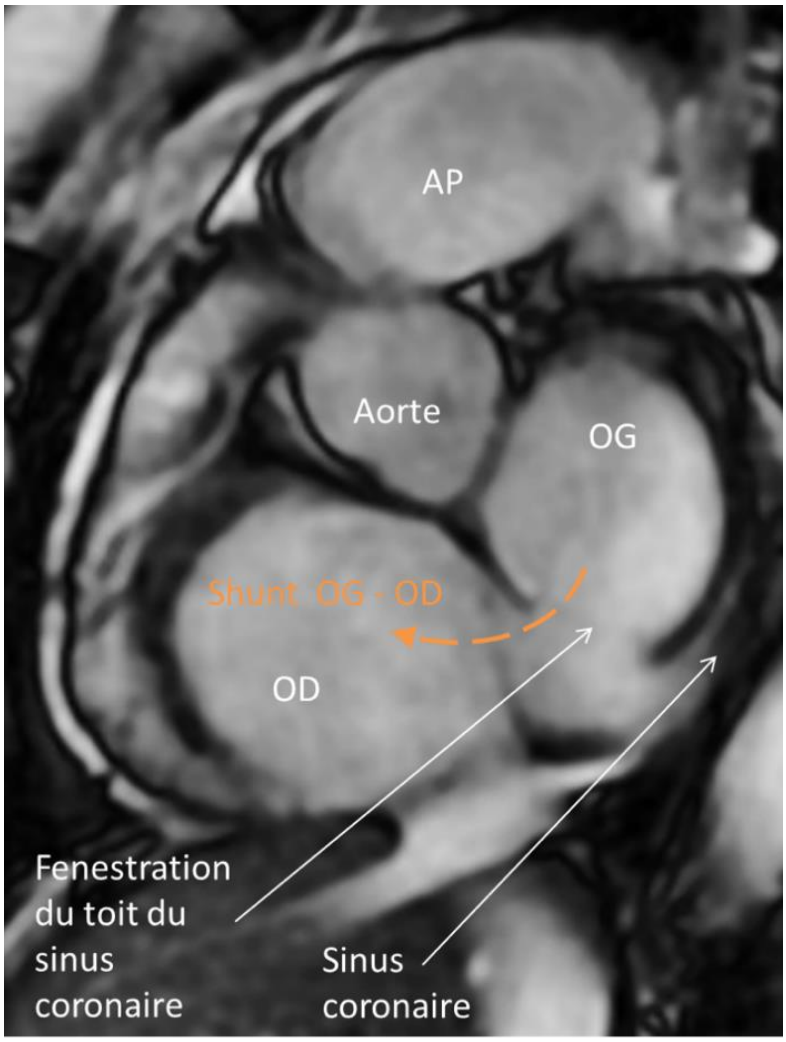

Figure 6 : vue IRM (coupe sagittale) d'une CIA du sinus coronaire.

OG OD : oreillette gauche et droite, AP artère pulmonaire.

5. Complications à long terme des CIA

a. Troubles du rythme supraventriculaire

Chez les patients ayant une CIA non opérée, l'incidence des troubles du rythme supra-ventriculaires augmente avec l'âge. Près d'1/3 des patients de plus de 40 ans développeront une arythmie. Les arythmies les plus fréquemment observées sont le flutter commun passant par l'isthme cavo-tricuspide et la fibrillation atriale[33,34]. Ces troubles du rythme seront d'autant plus fréquents que la CIA sera fermée tardivement avec dilatation évoluée des massifs auriculaires droit et gauche.

Une ablation de ces troubles du rythme pourra être proposée, idéalement avant fermeture du défect en cas de fermeture percutanée envisagée pour faciliter l'accès à l'oreillette gauche pour la fibrillation atriale. Une chirurgie rythmique de type Cox-Maze peut aussi être envisagée associée à une correction chirurgicale. Le taux de succès sera supérieur à 98% pour le flutter. Pour la fibrillation atriale, il sera plus faible, entre 50 et 90% avec les techniques actuelles, dépendant de l'ancienneté de la fibrillation et du niveau de dilatation des massifs auriculaires. Les formes familiales de CIA associée à une mutation NKX2.5, en plus d'être associées à des troubles conductifs, entrainent un risque majoré de fibrillation atriale et de mort subite.[2]

La fermeture de CIA, lorsqu'elle est précoce et percutanée, diminue la survenue de ces troubles du rythme, mais ne la supprime pas. [35-36]

Pour les arythmies récidivant après fermeture, la ponction trans-septale restera toutefois possible à travers la prothèse ou en bordure de prothèse mais devra être discutée au cas par cas.[37] Au décours d'une fermeture chirurgicale, la ponction trans-septale est réalisable après un délai post-opératoire acceptable permettant la cicatrisation de la zone opératoire.

Chez les patients opérés par chirurgie, en plus des deux troubles du rythme sus-cités, peuvent se développer des flutters incisionnels (par réentrée autour des zones de sutures opératoires ou des patchs mis en place)). Ils sont accessibles à une ablation percutanée qui doit être proposée précocement devant une excellente efficacité (> 95%) avec une très faible mortalité dans des centres expérimentés [38] .Des troubles

conductifs peuvent survenir très rarement par lésion du tissu de conduction, principalement dans les CIA ostium primum. [39,40.]

Figure 7.

Il est estimé que 60% des patients avec fibrillation atriale et opérés d'une CIA referont de la fibrillation atriale [41].

L'incidence tardive d'arythmies supra-ventriculaires et de fibrillation atriale après correction chirurgicale dans l'enfance reste supérieure à la population normale, mais est nettement plus basse que chez les patients non opérés ou opérés à l'âge adulte[34].

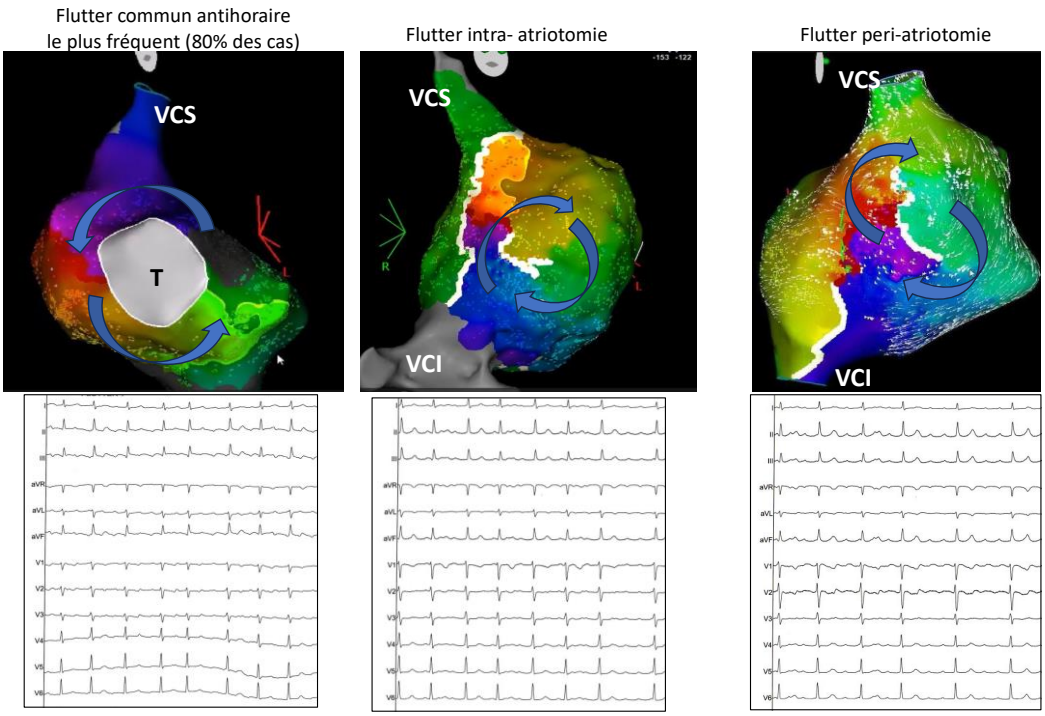

Figure 7: visualisation cartographique des différents circuits de flutter après fermeture de chirurgicale de CIA

VCS et VCI : veine cave supérieure et inférieure, T : tricuspide

b. Hypertension pulmonaire

La CIA peut être découverte sur un bilan d'HTAP qui en est une complication tardive [42,43]

L'étude histologique montre que cette HTAP se rapproche de l'HTAP primitive par atteinte de la micro-vascularisation pulmonaire.

Son apparition est probablement favorisée par une susceptibilité génétique.

Très rare chez les enfants elle survient plus souvent chez l'adulte jeune, notamment chez les femmes. La grossesse peut être un facteur déclenchant ou d'aggravation rapide de cette HTAP.

Les autres facteurs de risque connus sont l'importance du shunt et le type sinus venosus.[44]

L'HTAP associée à la CIA entraine une baisse de la capacité fonctionnelle. Le pronostic est moins bon qu'une CIA sans HTAP mais l'évolution reste lente. L'évolution vers le syndrome d'Eisenmenger, forme la plus avancée d'HTAP associée à un défect intracardiaque, est devenue exceptionnelle, en particulier depuis la fermeture précoce des défects. Ce dernier est associé à une dysfonction diastolique sévère du VD et se révèle donc par une désaturation fixe liée à une inversion permanente du shunt atrial. La fermeture de la CIA est contre-indiquée en cas de syndrome d'Eisenmenger car on supprimerait une « soupape » pour la dysfonction diastolique droite.

La fermeture précoce des CIA prémunie du développement de l'HTAP. Les observations d'HTAP apparue après fermeture précoce de shunt atrial sont rarissimes.[45]

c. Accidents vasculaires cérébraux

D'origine ischémique, l'AVC sur shunt inter-atrial survient lorsque deux conditions sont présentes ensembles : un thrombus veineux périphérique ou intracardiaque (dans l'oreillette ou l'auricule droit) et une inversion du shunt en droite gauche, même transitoire, ce qui peut survenir sur effort de toux, effort de poussée.[46]

`

6. Traitement des CIA

a. Traitement chirurgical

La CIA a été la première cardiopathie réparée « à cœur ouvert » sous circulation extracorporelle (CEC) en 1953. L'intervention a été réalisée à Philadelphie chez une patiente de 18 ans à l'aide la machine dite « de Gibbon ». La durée de CEC a été de 45 minutes [47].

b. *Traitement endovasculaire*

La fermeture percutanée d'une CIA a été réalisée pour la première fois chez le chien en 1974 par King. 2 ans plus tard l'intervention était réalisée chez une femme de 17 ans avec une prothèse de 35 mm de diamètre[48]. Au fil du temps, le matériel s'est simplifié, le diamètre des gaines a diminué et le la composition des prothèses s'est améliorée. Cette méthode est alors devenue technique de référence pour la fermeture des CIA OS. Le principe de fermeture percutanée repose sur le déploiement d'une prothèse en nitinol (métal auto-expansible à mémoire de forme constitué d'un alliage de titane et de nickel) composé de deux disques reliés entre eux centralement (Figure 8).

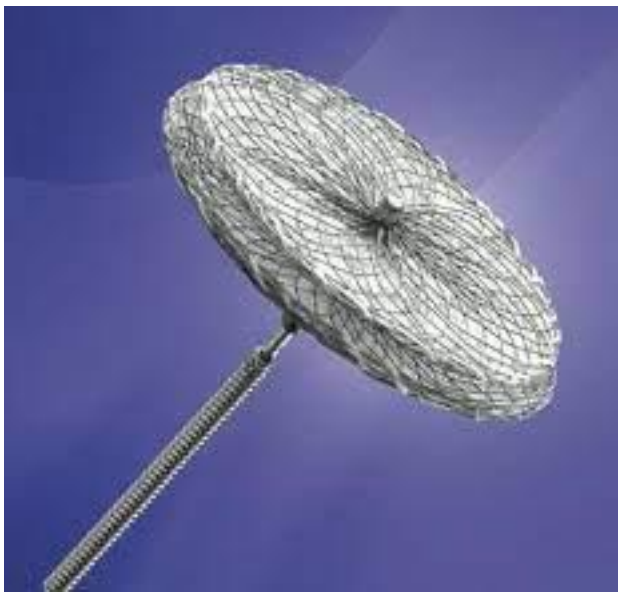

Figure 8 : Prothèse à double disque (Amplatzer Septal Occluder, Abbott)

c. *Indications*

i. Nourissons

L'indication de fermeture des CIA chez le nourrisson est exceptionnelle et doit être discutée au cas par cas si une augmentation progressive de pressions pulmonaires est identifiée ou s'il est associé d'autres anomalies favorisant une cyanose par un shunt inversé (antécédent de sténose pulmonaire, anomalie d'Ebstein par exemple). La fermeture sera alors le plus souvent chirurgicale.

ii. Enfants

Chez l'enfant, l'indication de fermeture est retenue devant une dilatation des cavités droites. Cette dilatation est le reflet d'un shunt gauche droit significatif, et en l'absence

de prise en charge, le patient sera exposé à la survenue de complications à l'âge adultes.

L'âge optimal de fermeture chirurgicale chez l'enfant se situe à partir de 5 ans, donc une fois atteint un poids de 15-20 kg environ, et avant l'entrée en cours préparatoire si possible. L'âge de fermeture percutanée peut être décalé au cas par cas après 5 ans afin d'attendre un poids et une dimension septale cardiaque suffisante pour insérer une prothèse de grand diamètre si la CIA est large ; ce décalage n'aura que peu d'impact sur la scolarité de l'enfant en raison du temps d'hospitalisation court.

iii. Adultes

Chez l'adulte symptomatique ou asymptomatique avec des cavités droites dilatées, la fermeture de CIA doit être systématiquement envisagée car elle améliorera le statut fonctionnel et prémunira de la survenue des complications. Il faudra s'assurer au préalable de l'absence d'HTAP.

L'hypertension artérielle pulmonaire sans syndrome d'Eisenmenger n'est pas une contre-indication absolue à la fermeture d'une CIA. Dans cette situation, une analyse hémodynamique détaillée au cathétérisme doit est nécessaire avant la fermeture du défect.

d. CIA ostium secundum

Le mode de fermeture de choix est endovasculaire.

L'abord est veineux fémoral. Le premier temps du geste consiste en une exploration des cavités droites avec prise des pressions étagées puis en une mesure du défect réel à l'aide d'un ballon de calibration (Figure 9). Ensuite, une gaine est amenée par la veine cave inférieure jusque dans l'oreillette droite puis traverse la CIA pour s'arrêter dans l'oreillette gauche. La montée et le positionnement de la large gaine est sécurisé et orientée par un guide positionné dans une veine pulmonaire gauche. Cette gaine servira à l'acheminement et au déploiement de la prothèse de fermeture de CIA. Le premier disque de la prothèse s'ouvre dans l'oreillette gauche puis le cathétériseur manœuvre pour venir plaquer ce disque sur le versant gauche du septum inter-atrial. Bien ancré, il peut alors déployer le second disque dans l'oreillette droite qui une fois extrait de la gaine, vient se plaquer sur le versant droit du septum, et ainsi occlure le défect.(Figure 10) Lorsque les deux disques sont positionnés de part et d'autre du septum, une manœuvre de mobilisation (retrait-poussée ou test de Minnesota) est effectuée pour valider la bonne stabilité de la prothèse. La prothèse peut alors être

libérée de la gaine sous contrôle de l'échographie et de la fluoroscopie (Figure 10). La gaine est ensuite retirée et un pansement compressif au pli de l'aine sera maintenu jusqu'au lendemain. Ce geste doit être couvert par une anticoagulation efficace et par une antibioprophylaxie systématique. Cette méthode de fermeture après calibration au ballon permet d'effectuer ce geste sous anesthésie locale chez les adultes car l'ETO n'est pas nécessaire. D'autres centres proposent la fermeture de CIA sans ballon de calibration mais avec une mesure du défect par ETO, donc sous anesthésie générale.

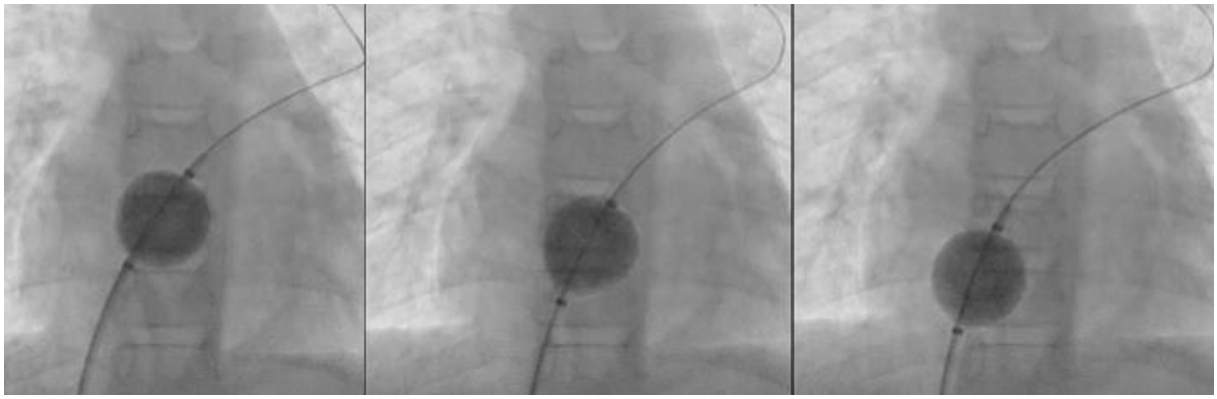

Figure 9 : calibration de la CIA au ballon semi-compliant (Medtech Equalizer 27 mmm, Boston)

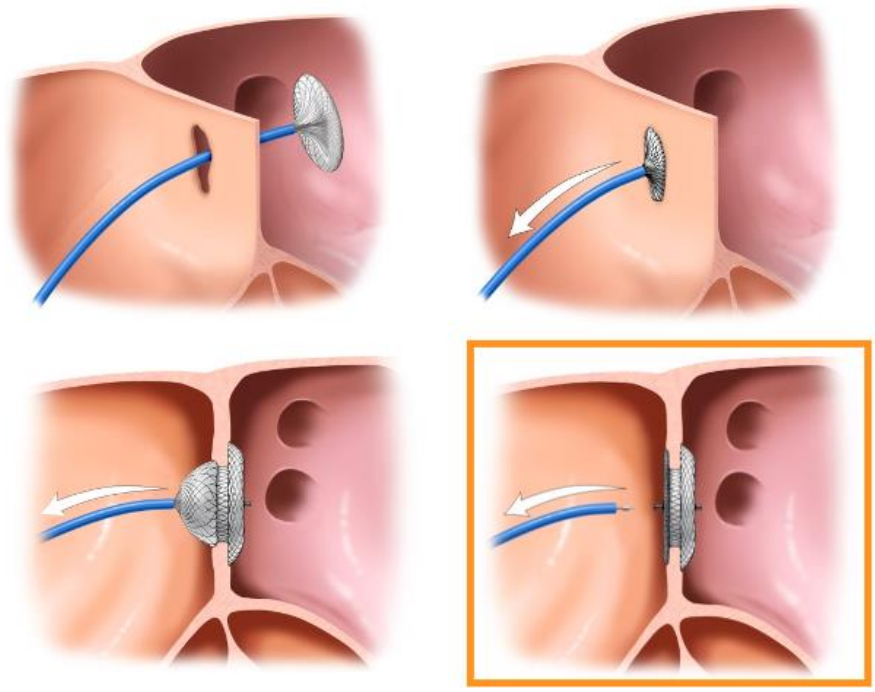

Figure 10 : Étapes du positionnement et du déploiement de la prothèse de fermeture de CIA.

Les complications immédiates de la fermeture percutanée sont : [49, 50.]

-l'embolisation de la prothèse, rare. Celle-ci pourra être extraite au lasso percutané ou par chirurgie.

-les complications au point de ponction (thrombose, faux anévrysme, hématome)
- le bloc auriculo-ventriculaire exceptionnel
Les complications tardives sont :
-l'érosion du mur aortique par la prothèse avec risque de tamponnade
-le shunt résiduel
- la thrombose de la prothèse.
-l'endocardite infectieuse sur matériel prothétique, exceptionnelle.
La fermeture d'une CIA chez un adulte ayant fait au préalable des troubles du rythme supraventriculaire ne protège pas contre la récidive des troubles du rythme qui peuvent évoluer à leur propre compte.
La durée d'hospitalisation après fermeture percutanée est habituellement de 24h, et un contrôle échographique pour s'assurer du bon positionnement de la prothèse et de l'absence d'épanchement, ainsi qu'un ECG seront réalisés le jour de la sortie et 1 semaine après la procédure.

Lorsque la fermeture percutanée d'une CIA ostium secundum n'est pas envisagée (défects multiples, défect trop large, berges trop petites, la prise en charge est chirurgicale.
Cette procédure est toujours effectuée sous circulation extra-corporelle, avec clampage aortique et atriotomie droite. Les CIA ostium secundum, ostium primum, low septal défect et sinus coronaire sont fermées par suture simple ou par patch de péricarde ou de dacron (Figure 11).
L'abord chirurgical est classiquement la sternotomie médiane, mais partir de l'âge de 10 kg, l'abord chirurgical par thoracotomie latérale droite des CIA type ostium secundum sans RVPA peut s'envisager pour des considérations esthétiques, mais au prix d'un risque de douleur postopératoire immédiate un peu plus accru.
Les complications immédiates sont celles classiques de la chirurgie à cœur ouvert : accident de CEC, lésion du tissu de conduction (nœud sinusal, nœud auriculo-ventriculaire), lésion du nerf phrénique, troubles rythmiques supraventriculaires transitoires (essentiellement fibrillation auriculaire chez l'adulte), infection du site opératoire mais la mortalité est quasi-nulle.
A plus long terme, un risque de troubles de rythme supra-ventriculaire (flutter commun, ré-entrée incisionelle puis fibrillation auriculaire) est noté jusqu'à 40% des cas, en rapport avec l'incision de l'oreillette droite et le patch de fermeture du défect.

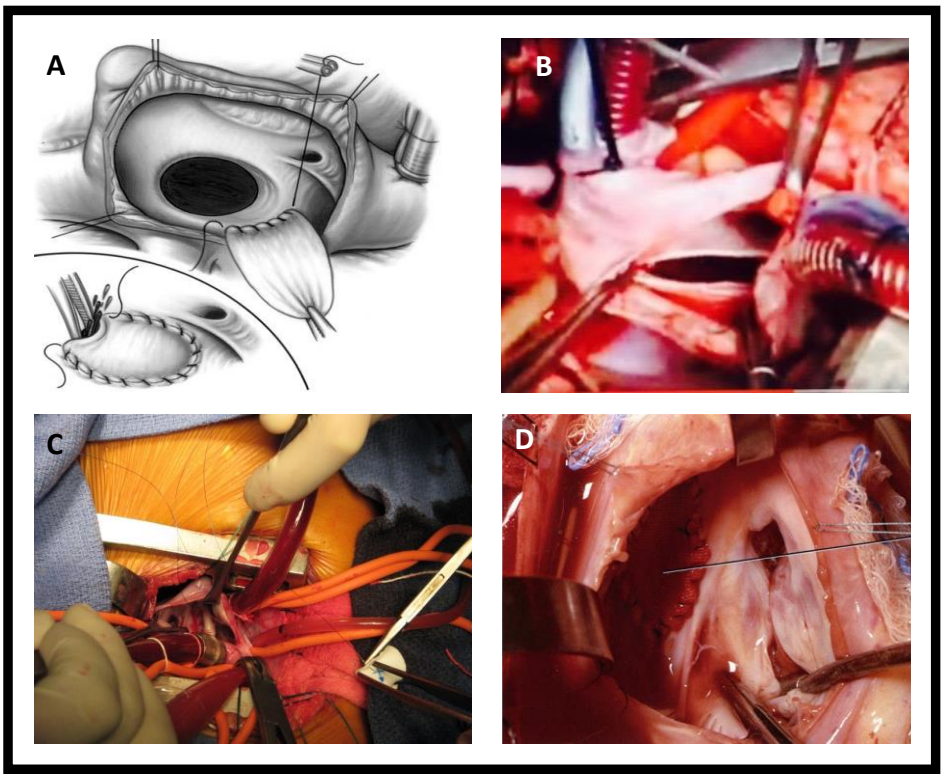

Figure 11 : Chirurgie des CIA ostium secundum.

Les CIA ostium primum, sinus venosus inférieure, et low septal defect ne peuvent pas être fermées par voie percutanée. Le traitement percutané des CIA du sinus coronaire est parfois possible.

Leur fermeture chirurgicale expose à des risques spécifiques : lésions des voies de conduction auriculoventriculaires dans la CIA ostium primum, sténose de la VCI dans les CIA low septal defect et sinus venosus inférieur.

7. Suivi à long terme

Quelle que soit la méthode de fermeture, le pronostic à long terme est bon, avec une mortalité proche de zéro et des ré-interventions sporadiques. L'espérance de vie est semblable à celle de la population générale pour les CIA prises en charge dans la petite enfance.[50, 51]

Le suivi postopératoire rapproché initial pourra être espacé progressivement à deux contrôles par décennie ; mais un suivi à vie est néanmoins indiqué.

Les arythmies préalables à la fermeture peuvent évoluer à leur propre compte quel que soit le mode de fermeture[34]. Si une communication inter-atriale a été fermée chirurgicalement dans l'enfance, le risque de troubles du rythme à l'âge adulte reste

supérieur à celui de la population générale saine appariée et justifie d'une surveillance rythmologique à vie [34].

8. Cas particuliers

a. Hypertension pulmonaire

La fermeture précoce des CIA prémunie du développement de l'HTAP. Les observations d'HTAP apparue après fermeture précoce de shunt atrial sont rarissimes. [43, 52.]

Dans la situation extrême du syndrome d'Eisenmenger, la fermeture du défect est contre-indiquée et ne sera qu'exceptionnellement envisagée une éventuelle transplantation pulmonaire (Stratégie « transplant and repair »)[53, 54.]

Dans la situation du développement d'une HTAP mais avec shunt gauche droite persistant, la prise en charge est moins consensuelle mais doit dans tous les cas reposer sur une évaluation hémodynamique approfondie avec calcul des résistances vasculaires pulmonaires par la méthode de Fick. [55-57.]

Pour cela, plusieurs outils seront utilisés au cours de la phase diagnostic du cathétérisme.

-la mesure de la consommation en oxygène sous canopy : grâce à une console dédiée, les échanges gazeux mesurés sous cloche permettent de calculer de manière fiable les débits et index cardiaques et d'utiliser ces valeurs pour calculer les résistances vasculaires. En raison du shunt, la méthode de calcul du débit cardiaque par thermodilution n'est pas applicable.

Les critères prédictifs de succès d'une fermeture de CIA dans ces situations sont : un Qp/Qs >1.5, des résistances vasculaires pulmonaires <5 U.Wood/m2, des PAP moyenne <40 mmHg et des pressions de remplissage basses. [58-60]

Si les résistances vasculaires pulmonaires sont < 3 UW avec un shunt gauche droite significatif, la fermeture du défect est recommandée permettant le plus souvent une normalisation des pressions pulmonaires. [58, 61.]

Si les résistances vasculaires sont < 5 UW avec un shunt gauche droite significatif, de base ou sous traitement anti-hypertenseur pulmonaire (stratégie « treat and repair »), la fermeture du défect peut être considérée. Si les résistances vasculaires sont > 5 UW, la fermeture du défect est le plus souvent contre-indiquée hormis quelques rare cas sélectionnés avec shunt gauche droit persistant très important.

Le traitement médicamenteux de l'HTAP sera poursuivi ou instauré si on observe au cathétérisme droit la persistance d'une HTAP documentée au moins 6 mois après la fermeture.[52]

b. Sujet âgé

Chez les sujets âgés ayant une CIA, la découverte est souvent faite en présence de symptômes ou complications. L'apparition tardive de symptômes après une longue période asymptomatique et avec des cavités cardiaques équilibrées s'explique par l'apparition chez le sujet âgé d'une dysfonction diastolique du ventricule gauche sous l'influence de plusieurs facteurs : hypertension artérielle, diabète, coronaropathie. Cette situation entraine une majoration du shunt gauche-droite. La fermeture percutanée des CIA du sujet âgé est le plus souvent proposée en absence d'HTAP importante car elle permet le plus souvent une amélioration clinique.[62] Cependant, lors de la fermeture, il peut y avoir une élévation brutale des pressions de remplissage gauche. Il est nécessaire dans ce cas d'ajouter un traitement diurétique avant et/ou durant la procédure.

II. Communications type sinus venosus

1. Embryologie et controverses

L'origine embryologique des CIA sinus venosus est débattue.

La malformation a été décrite pour la première fois par Peacock en 1858 comme un défect au dessus de la fosse ovale chez un enfant de 6 ans [63]. Le retour veineux pulmonaire n'est alors pas mentionné, probablement car la pièce anatomique extraite du thorax l'a été sa sans les veines pulmonaires.

En 1955, Lewis[64] expose pour la première fois les critères anatomiques liés cette malformation particulière. Le défect se situe au-dessus de la fosse ovale, il n'a pas de berges bien délimitées et il s'associe fréquemment à un retour veineux pulmonaire anormal du poumon droit.

Cette malformation est nommée pour la première fois Sinus Venosus en 1956 par Ross[65], qui en propose l'explication embryologique suivante : La cardiopathie serait due à une absorption incomplète du sinus veineux systémique par l'oreillette droite, entrainant une communication entre le sinus veineux systémique et le vestibule de l'OG, à proximité de la zone normale d'implantation des veines pulmonaires droites. Il atteste alors que cette malformation n'est pas une communication inter-atriale (atrial septal défect) et propose le terme de sinus venosus éefect.

En 1958, Shaner [66] suppose que les segments terminaux des veines pulmonaires droites et de la veine cave supérieure sont si proches qu'ils ont un mur commun. Une fistule de ce mur commun pourrait alors conduire à la formation des communications type sinus venosus.

La théorie d'une connexion bi-atriale de la VCS est également très forte à cette époque.

Anderson[67] propose ensuite une explication embryologique : il s'agirait d'une anomalie de connexion du système veineux systémique et veineux pulmonaire du poumon droit avec les veines concernées conservant une connexion à l'OG.

A partir de ces suppositions, une controverse scientifique entre Anderson d'un côté et Stella et Richard Van Praagh de l'autre, va naitre.

En 1994 Van Praagh [68] se demande encore ce qu'est le défect des Sinus Venosus, si celui-ci existe vraiment *(what is the defect of sinus venosus, if any?).*

A partir d'analyses échographiques et d'étude post-mortem sur pièces anatomiques, il postule que la malformation est expliquée par la déhiscence d'un mur commun séparant les veines pulmonaires et la veine cave supérieure, créant la malformation et pouvant expliquer à la fois le défect quand il existe, et à la fois le retour veineux pulmonaire anormale.

Il propose alors une classification de la malformation en 2 groupes.

Le premier groupe, supérieur, concernerait la déhiscence du mur postérieur commun entre la veine cave supérieure et la veine pulmonaire supérieure droite, et aurait pour conséquence l'unroofing de cette veine qui se drainera dans la veine cave supérieure ou dans la jonction cavo-atriale. Cet unroofing pourrait alors se prolonger vers le septum situé au-dessus de la fosse ovale, entrainant le défect.

Le second groupe concernerait la déhiscence du mur commun entre la veine pulmonaire et l'oreillette droite, et entrainerait un unroofing complet des veines pulmonaires droites dans l'oreillette droite.

Une veine cave supérieur gauche serait alors trouvée dans 13% des cas du groupe 1 et 50% des cas du groupe 2.

Il expose également que vu depuis l'oreillette gauche, le défect occupe la zone normale occupée par la veine pulmonaire supérieure droite à son abouchement dans l'OG.

Selon cette théorie, la fistule ou déficience du mur commun provoque l'unroofing +- étendu des veines pulmonaires avec l'OD ou la veine cave supérieure.

L'unroofing veineux pulmonaire constitue donc lui-même la communication entre l'OG et l'OD, de la même manière que dans la CIA du sinus coronaire (unroofed coronary sinus).

Il rajoute que lorsque l'unroofing est très limité en taille, la veine semble être connectée autant à l'OD qu'à l'OG et donc que ce n'est pas une CIA au sens propre

Quand il y a plusieurs VP concernées, il pense que la déficience du mur commun s'étend sur toute la zone de RVPA concernée.

En 1997 dans Heart [69], Anderson atteste que le sinus venosus est une association constante d'un defect extra-septal et d'un retour veineux pulmonaire.

Il réfute la théorie de Van Praagh sur la déhiscence du mur postérieur commun en affirmant que ce mur commun n'existant pas dans un cœur normal, il ne peut pas exister dans un cœur anormal. (Figure 12).

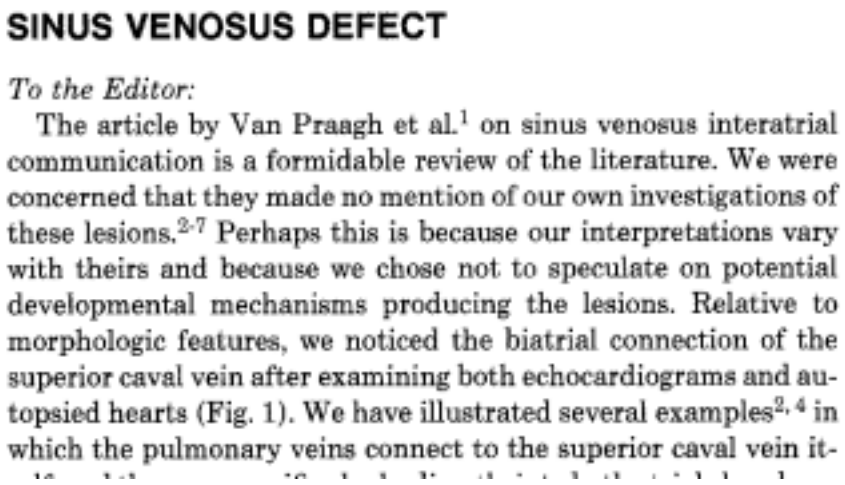

SINUS VENOSUS DEFECT

To the Editor:

The article by Van Praagh et al.[1] on sinus venosus interatrial communication is a formidable review of the literature. We were concerned that they made no mention of our own investigations of these lesions.[2-7] Perhaps this is because our interpretations vary with theirs and because we chose not to speculate on potential developmental mechanisms producing the lesions. Relative to morphologic features, we noticed the biatrial connection of the superior caval vein after examining both echocardiograms and autopsied hearts (Fig. 1). We have illustrated several examples[2, 4] in which the pulmonary veins connect to the superior caval vein it-

Figure 12 : Extrait d'une letter to the editor[70] d'Anderson concernant les théories de Van Praagh.

Il affirme que dans un cœur normal, les tissus séparant l'OD et l'OG en dehors de la fosse ovale sont fibromusculaires ou adipeux. Le pôle antérosupérieur de la fosse ovale étant formé lui par une inflexion des murs des deux atriums (extensive fold), il pense alors que la communication type sinus venosus est liée à un défaut d'infolding du mur séparant les deux oreillettes. En conséquence de ce défaut d'infolding, l'abouchement de la veine cave supérieur au massif auriculaire se ferait avec un over-riding (entre l'OD et l'OG), responsable d'une communication inter-atriale en dehors de la fosse ovale.

En résumé, la malformation serait due à une anomalie de la structure pariétale et non pas de la structure septale. Le défaut d'infolding du mur pariétal créerait le défect et l'over-riding fréquemment rencontré.

A ce stade, les messages communs clés de ces observations et controverses sont relativement simples.

1 : la CIA sinus venosus n'est pas un atrial septal défect.

2 : le diagnostic positif se fait grâce au caractère intact de la fosse ovale.

En 2021, Anderson ré-insiste sur le fait que cette communication particulière ne soit pas un atrial septal defect[71]. Il décrit également la communication non pas comme un simple trou, mais comme un espace conique volumique. Il met l'over-riding de la veine

cave supérieure au centre du de la description anatomique et embryologique de la malformation.

En 2022, l'origine embryologique finalement supposée serait une fistule veino-veineuse entrainant la communication inter-auriculaire[72].
En effet, des collatérales existeraient entre les veines pulmonaires et le système veineux systémique adjacent, y compris dans le développement d'un cœur normal.
L'explication de la cardiopathie résiderait alors d'un pont veino-veineux avec des veines pulmonaires ayant toutefois conservé le drainage vers l'oreillette gauche, produisant ainsi une communication extra-septale.

2. Anatomie

Une CIA sinus venosus est donc anatomiquement déterminée par deux critères :
-un défect haut situé entre les deux oreillettes du cœur, en dehors de la région de la fosse ovale, plus particulièrement en arrière et au-dessus de cette dernière.
-un retour veineux pulmonaire anormal du poumon droit dans la veine cave supérieure.
Ces deux caractéristiques expliquent que la malformation est responsable d'un shunt gauche droit dit « double ». Le shunt se fait effectivement par le défect lui-même, mais également par la veine pulmonaire anormale connectée à la veine cave supérieure.

Le point clé du diagnostic réside en l'intégrité de la fosse ovale.
Il existe dans les descriptions anatomiques de nombreuses variations concernant : le nombre de veines pulmonaires concernées, la taille et l'orientation du défect si celui-ci peut être déterminé, l'over-riding de la veine cave supérieur, l'association d'une veine cave supérieure gauche. (Figure 13)

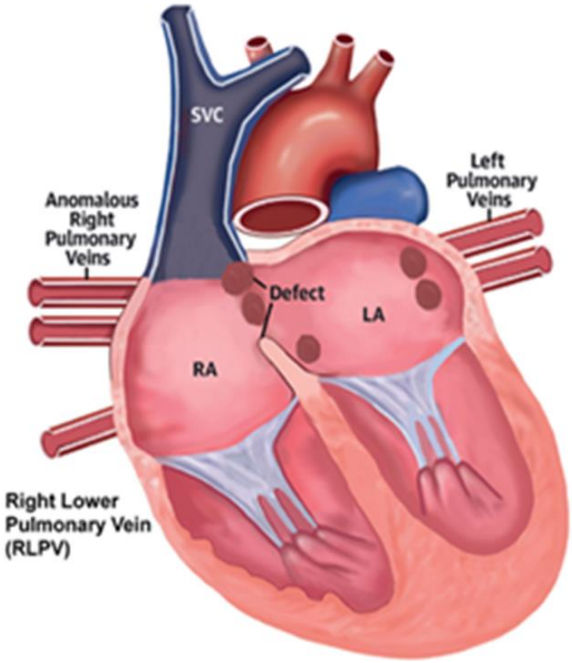

Figure 13 : Anatomie des CIA sinus venosus

LA et RA: left and right atrium (oreillette droite et gauche)
SVC: superior vena cava (veine cave supérieure)
Hansen JH & al Transcatheter Correction of Superior Sinus Venosus Atrial Septal Defects as an Alternative to Surgical Treatment. J Am Coll Cardiol 2020.

Pour aller plus loin, Chowdhury et Anderson[72] (2022) déterminent plusieurs concepts permettant de décrire la malformation. Ces derniers sont décrits à partir de coupes scannographiques axiales, sagittales et obliques.

-L'over-riding déjà évoqué n'étant pas mesuré de manière standard, il est proposé d'utiliser la même méthode que dans la tétralogie de Fallot, en prolongeant ici virtuellement le septum inter-atrial afin de déterminer un pourcentage d'over-riding de la veine cave supérieure avec l'OG.
Il est alors déterminé que 30% des patients ne présentent pas d'over-riding, et qu'un over-riding >50% n'est retrouvé chez qu'une infime partie des patients.
L'over-riding de la VCS n'est donc pas un critère obligatoire pour caractériser la malformation.
D'autres concepts sont également proposés et décrits
-La zone d'implantation des veines pulmonaires anormales : considérée comme connectée à la jonction cavo-atriale si l'orifice est à – de 5 mm du pôle supérieure de

la jonction. A l'inverse, elles sont considérées comme haute si leur orifice est à + de 2 cm du pole supérieur de la jonction cavo-atriale.
-l'extension caudale du défect, déterminée comme présente si la taille supéro-inférieure du défect sur une vue scanner orthogonale modifiée, est mesurée à plus de 25 mm.

La nécessité d'optimiser la compréhension embryologique et la description anatomique s'est renforcée ces dernières années avec le développement d'une nouvelle technique de correction percutanée des communication type sinus venosus. Des publications croissantes sur la description anatomique, à l'orée de la nouvelle technique de correction, ont tenté d'en améliorer la compréhension et la classification de cette cardiopathie à la fois singulière mais comportant de nombreuses variabilité inter-individuelles.

3. Examens complémentaires[74]

a. Échocardiographie Trans-Thoracique (ETT)

Le diagnostic peut être évoqué par l'échocardiographie transthoracique (ETT) montrant deux signes anatomiques directs : une communication inter-atriale anormalement haute en relation avec la zone de la veine cave supérieure (VCS) et un ou plusieurs retours veineux pulmonaires anormaux dans la VCS.
La vue sous-costale peut être très utile pour retrouver ces signes chez les patients avec une bonne échogénicité. Des signes indirects, expliqués par la physiopathologie, doivent être recherchés pour analyser les conséquences de la pathologie ou pour guider le cardiologue vers le diagnostic final : dilatation des cavités droites, shunt gauche droit auriculaire en Doppler couleur et, dans certains cas, hypertension pulmonaire modérée à sévère sur la fuite de la valve tricuspide ou de la valve pulmonaire. Figure 14.
Bien que l'ETT soit un outil efficace, d'autres techniques d'imagerie sont utilisées pour préciser l'anatomie, comme l'angioscanner cardiaque ou l'imagerie par résonance magnétique (IRM). Ce besoin d'imagerie complémentaire s'explique par la grande variabilité des anomalies anatomiques rencontrées et par les difficultés à visualiser précisément les retours veineux pulmonaires anormaux à l'ETT.

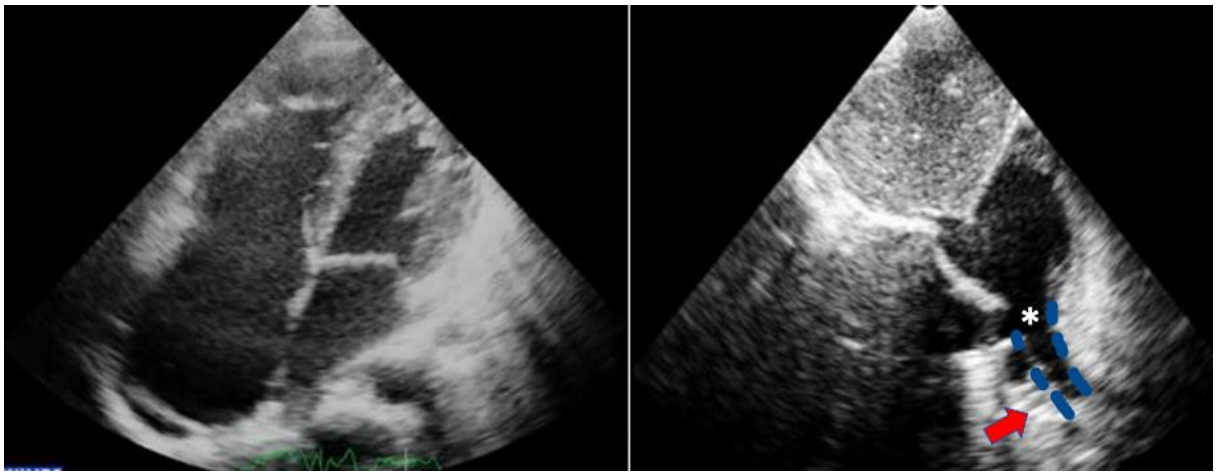

Figure 14 : échographie trans-thoracique (CIA sinus venosus)

Gauche (coupe apicale 4 cavité) : septum inter-atrial semblant intact mais cavités droites très dilatées.

Droite (coupe sous costale bi-cavale) : visualisation de la CIA haut située (étoile), avec la VCS arrivant à cheval sur la CIA (trait pointillé bleu). On visualise le retour veineux pulmonaire anormal d'une veine pulmonaire droite dans la veine cave supérieure (flèche rouge).

b. Angioscanner thoracique injecté

La tomodensitométrie cardiaque reste l'outil d'imagerie de choix pour évaluer les communications type sinus venosus.

Concernant son exécution, un process de synchronisation apparaît comme recommandé ; en effet, plus l'acquisition est précise (donc synchronisée), plus l'analyse du défect et des retours veineux pulmonaires peut être fine ; le nombre de veines concernées, l'existence d'un collecteur de veines pulmonaires, l'orientation et la hauteur du drainage anormal dans la VCS sont des points importants pour caractériser cette pathologie singulière sur le plan anatomique. Figure 15.

L'injection de contraste dans le bras gauche est recommandée pour rechercher une veine cave supérieure gauche associée et analyser l'anatomie du tronc veineux innominé. Ces paramètres pourraient être manqués avec une injection dans le bras droit et sont très importants concernant la stratégie thérapeutique.

L'angioscanner cardiaque est également le meilleur examen d'imagerie pour convertir les images en coupes en un modèle 3D de la malformation en raison de sa bonne résolution spatiale.

Grâce à des logiciels de modélisation 3D, il est désormais possible et facile de créer un modèle 3D fiable de la malformation du patient. Avec cette nouvelle approche, l'anatomie des CIA type sinus venosus révèle un large panel de variabilité anatomique parmi les patients.

De nos jours, cette analyse anatomique personnalisée pour chaque patient est cruciale pour l'éligibilité à une procédure percutanée. De plus, la technologie 3D permet d'imprimer la malformation afin de simuler l'intervention sur banc d'essai.

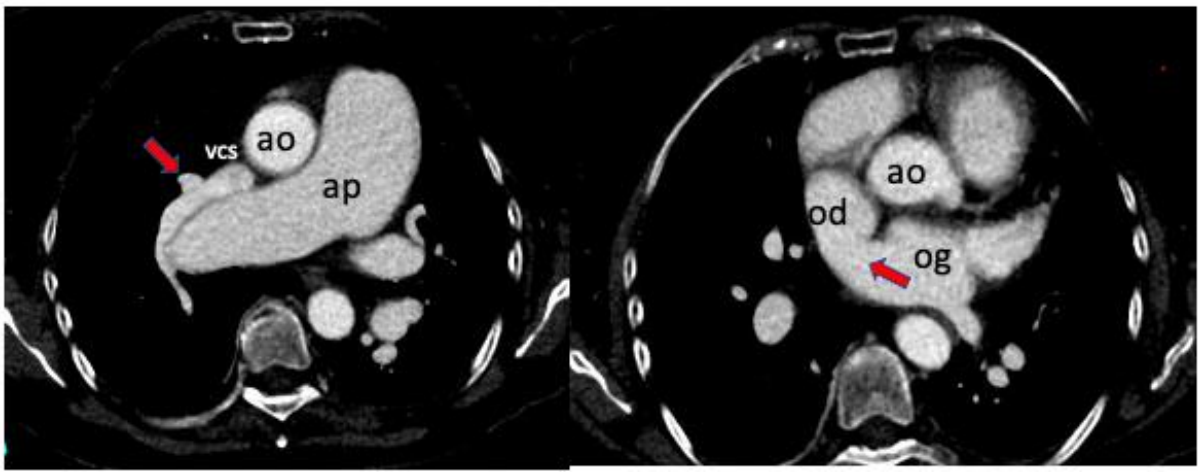

Figure 15 : angioscanner en coupe axiale d'une CIA sinus venosus.

VCS veine cave supérieure, AP artère pulmonaire, Ao Aorte, OD et OG oreillettes droite et gauche.

c. *IRM Cardiaque*

Bien que la résolution spatiale de l'IRM reste moins précise que celle du scanner cardiaque, cet examen d'imagerie peut fournir beaucoup d'informations concernant la cardiopathie.

Le diagnostic anatomique peut être établi et une étude hémodynamique peut être réalisée avec une analyse de flux 4D. Cet outil récent est efficace pour évaluer le shunt (sa direction et son intensité) et ses conséquences (dilatation des cavités droites, surcharge vasculaire pulmonaire) ;

Il participe donc au processus de décision de traitement chez les adultes. La limite de cet examen est le besoin d'immobilité pendant l'acquisition, ce qui n'est pas facile à obtenir chez les enfants ou les adultes claustrophobes.

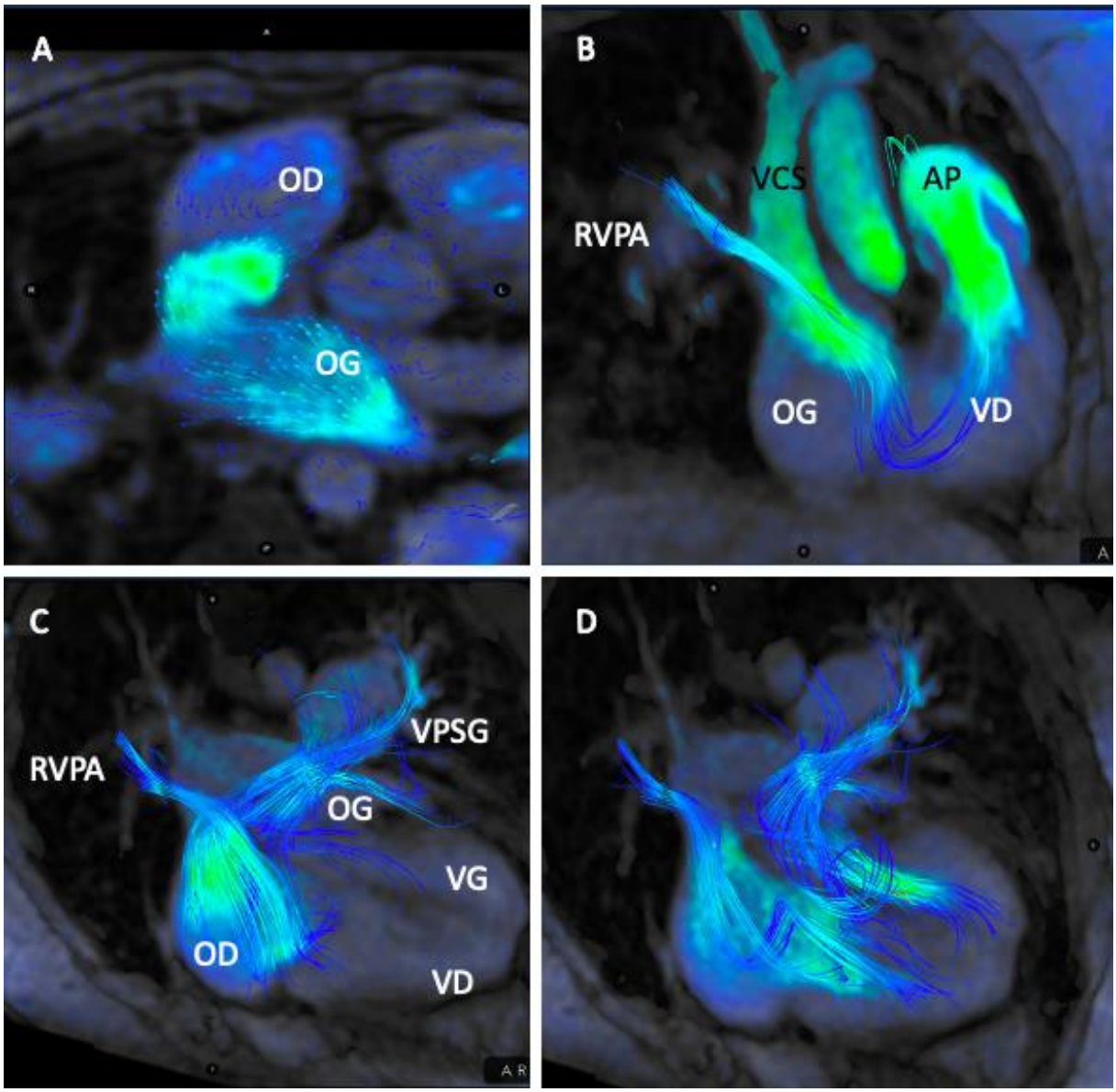

Figure 16 : IRM 4D d'une CIA type sinus venosus

VCS veine cave supérieure, RVPA retour veineux pulmonaire anormal, VPSG veine pulmonaire supérieure gauche, VG VD ventricule gauche et droit, OD OG oreillette droite et gauche.

d. Autres outils d'imagerie

i. Cathétérisme cardiaque

Le diagnostic CIA type sinus venosus peut parfois être découvert fortuitement lors d'un examen de cathétérisme. Dans cette situation, l'étude hémodynamique découvre un shunt gauche droit avec enrichissement du sang artériel pulmonaire et peut révéler une hypertension pulmonaire modérée à sévère. Une cyanose discrète sur l'étude

d'oxymétrie sanguine peut être trouvée dans l'oreillette gauche en raison de la relation étroite de l'oreillette gauche et de la veine cave supérieure. La fluoroscopie et les angiographies des artères pulmonaires montrent le drainage anormal d'une veine pulmonaire dans la VCS et l'anatomie du retour veineux systémique et pulmonaire doit être précisée. Le tronc veineux innominé, la veine cave supérieure gauche, les dimensions de la VCS droite sont également des paramètres importants à analyser concernant la stratégie thérapeutique endovasculaire.

ii. Échocardiographie Trans-Œsophagienne (ETO)

Bien que l'ETO ne soit pas un examen d'imagerie de première ligne pour diagnostiquer les CIA sinus venosus, il est aujourd'hui obligatoire de l'utiliser en direct lors de la correction percutanée. Comme pour les communications inter-atriales classiques, c'est un outil utile pour guider la procédure.
Concernant les CIA sinus venosus, grâce à la vue postérieure, il est possible de voir toutes les veines pulmonaires droites précisément et dynamiquement, ainsi que d'évaluer la relation de chaque veine pulmonaire anormale avec le défect et la veine cave supérieure.
De cette manière, cet outil dynamique permet de guider la correction percutanée et d'être conscient du risque d'occlusion ou de sténose de la veine pulmonaire pendant la procédure ; de plus, il peut évaluer la correction partielle ou totale du shunt de gauche à droite après la mise en place du stent couvert.

4. Traitement chirurgical historique

La chirurgie à cœur ouvert implique le plus souvent la mise en préalable d'une circulation extra-corporelle ainsi que l'arrêt cardiocirculatoire.
Elle est le plus souvent réalisée par un abord de sternotomie (de face) et rarement par thoracotomie latérale droite.

Selon les particularités anatomiques et la hauteur de la communication entre les cavités droites et gauches, différentes techniques ont été décrites[75, 76].

-La ligature simple de la connexion anormale, décrite par Laboux et al en 1968[77] en cas de connexion bi-atriale de la veine cave supérieure, permet de forcer le flux cave

s'écouler directement dans l'oreillette droite. Cette technique ancienne ne nécessitait pas d'arrêt circulatoire mais exposait à la persistance d'une shunt gauche droit pas la veine pulmonaire haut située.

-La mise en place d'un patch de tunnélisation en PTFE entre la veine pulmonaire anormale et la VCS droite, nécessitant un arrêt circulatoire.

-la technique de double patch décrite par Shapiro et Enjalbert en 1967[78] : le premier patch sépare la veine pulmonaire de la VCS. Le deuxième patch permet d'élargir la veine cave supérieure au niveau de sa portion rétrécie.

Ces techniques de tunnélisation doivent veiller à préserver la jonction cavo-atriale et plus particulièrement l'artère du nœud sinusal. (Figure 17)

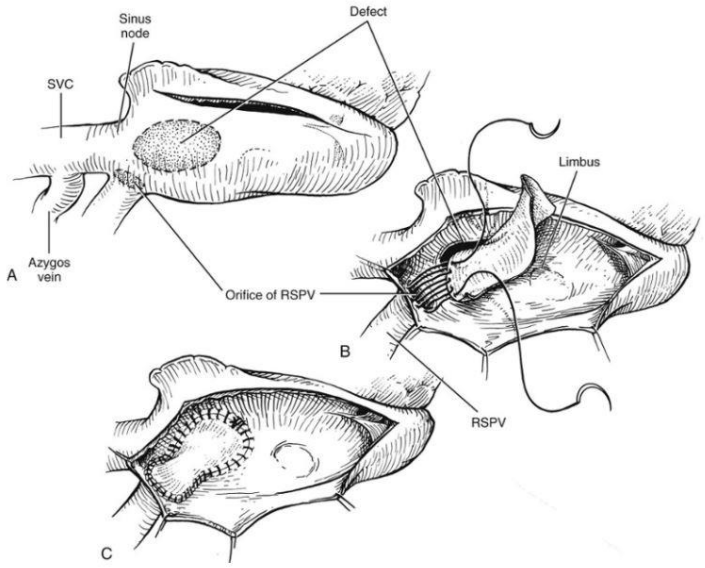

Figure 17 : tunnélisation par patch (Kirklin/Barratt-Boyes cardiac sugery)

SVC: superior vena cava, RSPV : right superior pulmonary vein.

-l'intervention de Warden[79] consiste en la section suture de la veine cave supérieure juste au-dessus du RVPA avec anastomose (directe ou par tube) de la veine cave supérieure à l'auricule droit. S'y associe la fermeture de la communication par un patch tunnélisant le retour veineux pulmonaire à l'OG. Figure 18.

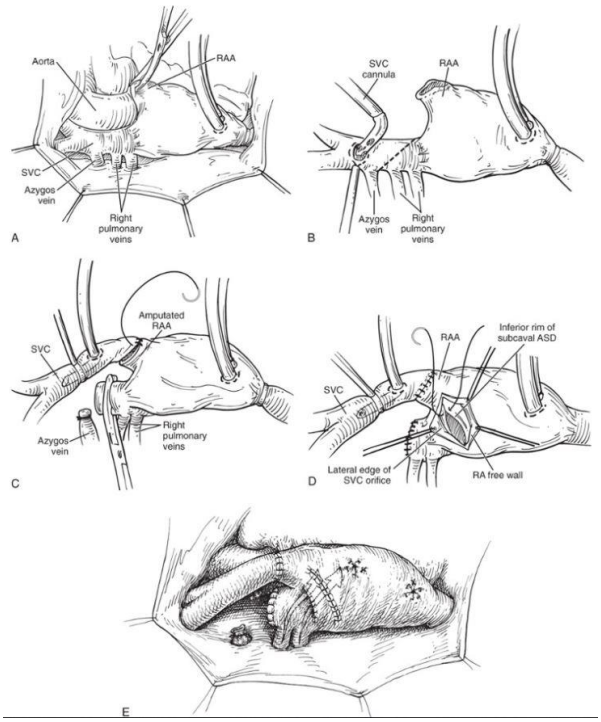

Figure 18 : intervention de Warden (Kirklin/Barratt-Boyes cardiac sugery)

Legende : SVC superior vena cava (veine cave supérieure), RSPV right superior pulmonary vein (veine pulmonaire supérieure droite), RA right atrium (oreillette droite).

Les résultats à long terme des deux dernières techniques sont excellents et la survie comparable à celle de la population générale [80].

Toutefois, en plus des complications classiques communes aux chirurgies des CIA (shunt résiduel, trouble conductifs, accidents de circulation extracorporelle, infections, épanchement), des complications spécifiques aux CIA sinus venosus sont rencontrées : sténose des veines pulmonaire ou de la veine cave supérieure, déhiscence de patch entrainant un shunt résiduel, arythmie supra ventriculaire.

5. Traitement percutané novateur

Récemment, une correction percutanée des CIA sinus venosus a été développé en alternative au gold standard, la chirurgie[73, 81.] Cette technique consiste en le placement d'un stent couvert depuis la veine cave supérieure jusqu'à l'oreillette droite, afin de rediriger le flux du retour veineux pulmonaire anormal vers l'oreillette gauche, à travers la communication, à la face postérieure du stent. Figure 19.

De manière obligatoire, le flux cave est alors séparé du flux veineux pulmonaire, et ainsi indépendamment drainé vers l'oreillette droite. Ainsi, le double shunt gauche droit (lié au défect et lié au RVPA) peut être totalement corrigé. Figure 20 et 21.

La première correction percutanée a été effectuée par Abdullah[81] en 2011 puis décrite par Garg et al[82] en 2014.

Depuis, la technique s'est développée et répandue de manière internationale. On estime aujourd'hui que plus de 400 correction percutanée de CIA type sinus venosus ont été effectuées dans le monde.

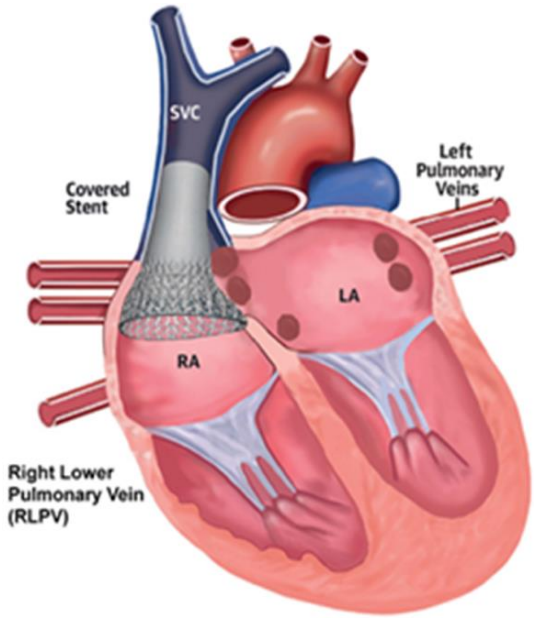

Figure 19 : Concept de la correction percutanée des CIA type sinus venosus par stent couvert [73].

Hansen JH & al Transcatheter Correction of Superior Sinus Venosus Atrial Septal Defects as an Alternative to Surgical Treatment. J Am Coll Cardiol 2020.

Un stent est place dans la veine cave supérieure pour séparer le flux cave du flux veineux pulmonaire. Le retour veineux pulmonaire est redirigé à la face postérieure du stent couvert, à l'oreillette gauche

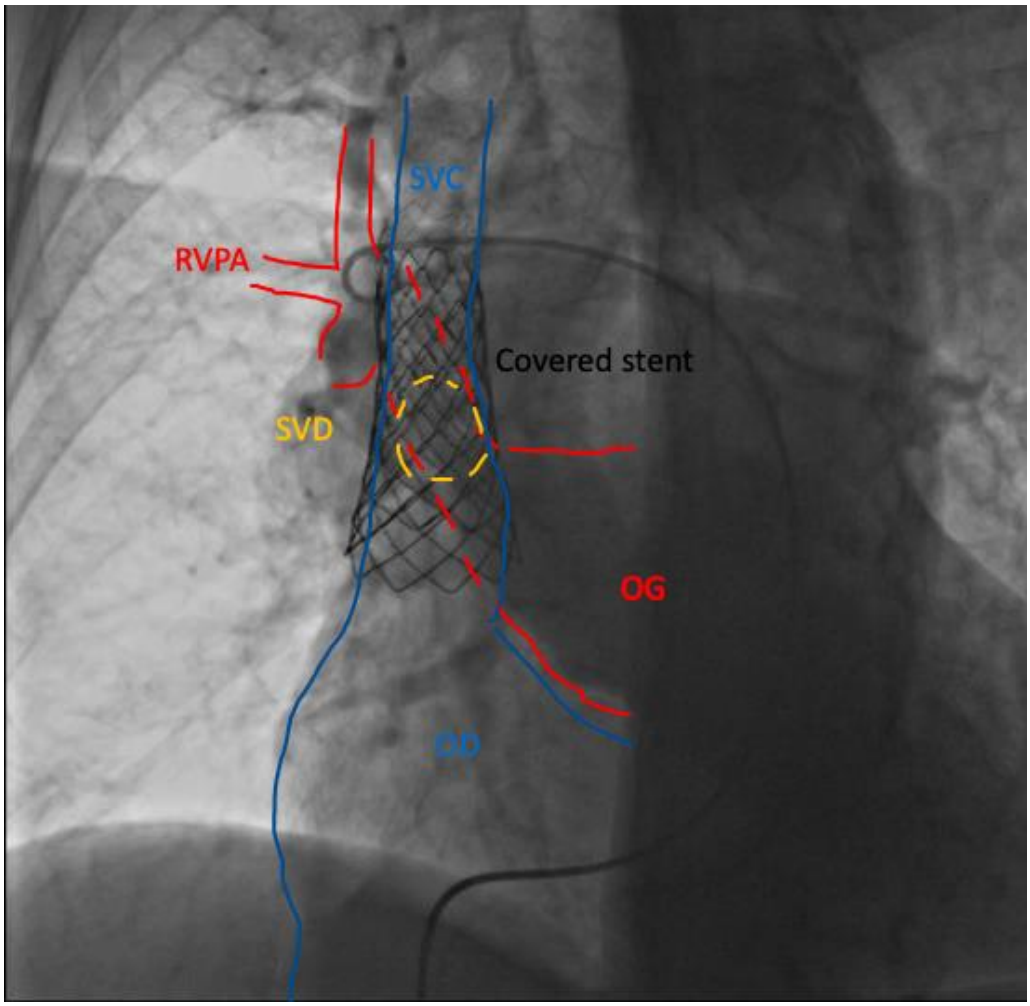

Figure 20 : Projection sur écran de scopie du concept de correction percutanée.

RVPA : retour veineux pulmonaire anormal. SVC : superior vena cava. SVD : sinus venosus defect. OG OD oreillette gauche et droite.
Covered stent : stent couvert pour corriger la malformation

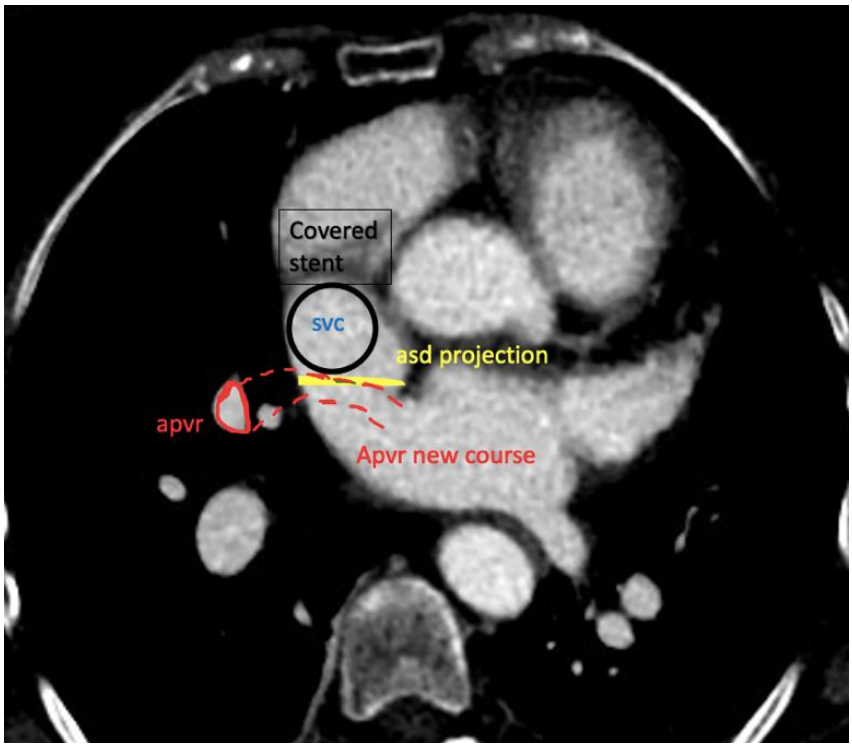

Figure 21 : Projection sur coupe scanner axiale du concept de correction percutanée.

APVR : retour veineux pulmonaire anormal. ASD : Communication type sinus venosus. SVC : veine cave supérieure. LA : left atrium, RA : right atrium
Covered stent : stent couvert pour corriger la malformation

Les structures anatomiques à analyser dans la communication type sinus venosus sont nombreuses et leurs caractéristiques géométriques peuvent varier d'un patient à l'autre.

Cette nouvelle technique n'est envisageable qu'après une étude anatomique précise de la malformation cardiaque et de ses structures adjacentes, spécifiquement pour chaque patient.

La visualisation 3D de la cardiopathie apparait nécessaire pour déterminer la faisabilité de l'intervention chez les patients.

Les composants anatomiques clés suivants doivent être précisés afin d'envisager la faisabilité de la correction chez un patient.

-le défect lui-même, si tant est qu'il soit définissable ce qui on le verra n'est pas toujours le cas. Il est tout de même nécessaire de déterminer l'espace de communication, sa dimension, sa forme et sa relation avec la veine cave supérieure.

-l'oreillette droite, son volume et sa morphologie.

-La veine cave supérieure, ses diamètres étagés, sa longueur, sa forme, sa relation avec le tronc veineux innominé et la veine azygos ainsi que sa relation avec la zone de communication.
-la jonction cavo-atriale, correspondant à la zone d'abouchement de la veine cave supérieure à l'oreillette droit.
-le retour veineux pulmonaire, le nombre de veines concernées, le nombre d'ostia, leur orientation, leur hauteur dans la veine cave supérieure ou la jonction cavo-atriale, l'angulation de connexion, sa distance avec l'espace de communication.
Comme cela a été expliqué en introduction, la description anatomique claire, la classification, et les paramètres clés à intégrer dans la décision de correction percutanée ne sont pas encore clairement établi ni explorés.

Les résultats de cette nouvelle technique sont décrits et prometteurs et les complications majeures sont les suivantes [83, 84] :
L'embolisation du stent pouvant nécessiter une intervention chirurgicale urgente.
Le shunt résiduel pouvant être localisé à différents endroits autour du stent.
La sténose du RVPA, par compression intrinsèque du trajet veineux pulmonaire lié à une tro forte impaction du stent ou à un conflit anatomique préexistant.

Sur le plan technique, la procédure se prépare de manière standardisée [85].
Anesthésie et Accès : La procédure est réalisée sous anesthésie générale avec un accès veineux double (fémoral + jugulaire).
Guidage par Imagerie : L'échocardiographie trans-oesophagienne (ETO) est obligatoire, et le guidage par fusion d'image multimodale aide à la procédure.
Création d'un Rail : Établir un rail rigide à l'aide d'un guide rigide pour faciliter l'introduction de divers ballons de calibration et du stent dans la zone cible, permettant une précision et une stabilité indispensable au déroulement de l'intervention. Figure 22.
Ponction Trans-Septale : elle peut être nécessaire pour accéder au retour veineux pulmonaire depuis l'oreillette gauche pour monitorer voir protéger depuis l'oreillette gauche une veine pulmonaire à risque de sténose lié au déploiement du stent.

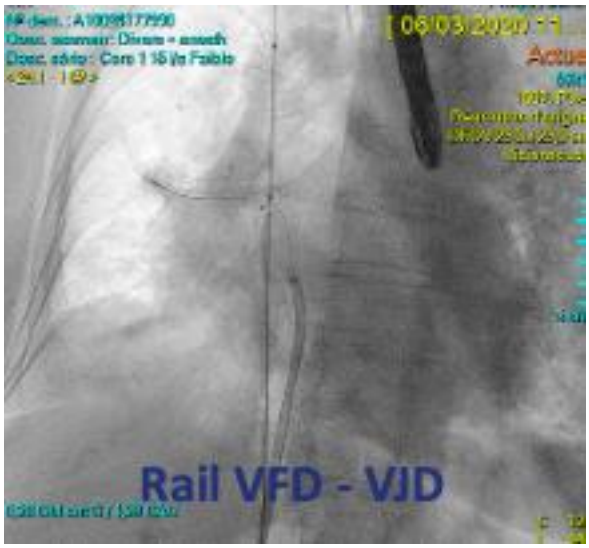

Figure 22 : rail rigide entre la veine fémorale droite (VFD) et la veine jugulaire droite (VJD).

La première étape de l'intervention consiste à mesurer les dimensions (diamètre et longueur) de la veine cave supérieure. Cela permettra de choisir les dimensions du stent à implanter ensuite. Cette étape s'effectue à l'aide d'angiographie et de ballons de calibrations. Figure 23.

Les ballons compliants (mous) permettent d'évaluer la distensibilité spontanée de la veine cave supérieure. En effet, les dimensions rapportées par le scanner préopératoire doivent être vérifiées car peuvent varier, du fait d'une distensibilité variable liée à plusieurs facteurs supposés (âge, fragilité ou élasticité des tissus, condition d'hydratation et de précharge).

Au cours des tests au ballon compliant, le risque de sténose de ou des veine(s) pulmonaire(s) à tunnéliser peut également être apprécié par différentes techniques (angiographie dans la veine, monitoring de pression avant/après gonflement du ballon, analyse de flux doppler par échographie trans-oesophagienne au cours de l'inflation du ballon).

Les ballon semi-compliants (plus durs) peuvent ensuite être utilisés pour simuler la place prise par le futur stent à positionner et ainsi reproduire les modifications hémodynamiques similaires à lorsque le stent de taille choisie sera implanté. Le choix de la taille du stent à implanter sera ainsi affiné et le risque de sténose de veine pulmonaire pourra ainsi être confirmé ou infirmé, de même que le risque éventuel de shunt résiduel à travers la CIA normalement occluse.

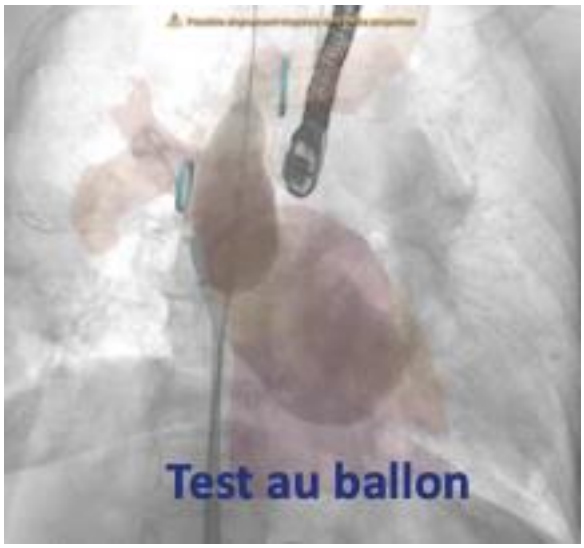

Figure 23 : test au ballon pour mesure de la distensibilité de la veine cave supérieure

Objectif complémentaire : évaluation du risque d'occlusion du retour veineux pulmonaire anormal.

À tout moment, un risque authentifié de sténose de veine pulmonaire pourra conduire à la réalisation d'une ponction trans-septale afin de protéger la veine pulmonaire à risque, depuis l'oreillette gauche (sa destination finale). Figure 24.

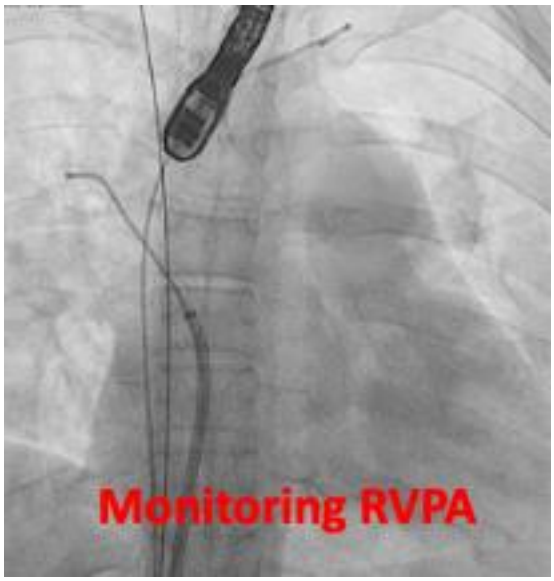

Figure 24 : surveillance du RVPA depuis l'oreillette gauche

La longueur du stent sera alors déterminée. Sa longueur devra être suffisante pour assurer une occlusion de la CIA à son pôle caudal et assurer une redirection de la veine pulmonaire à son pôle crânial.

Le ballon de déploiement sur lequel le stent sera serti puis déployé sera également choisi en fonction des tests sus-cités avec pour objectif principal une bonne impaction du stent afin d'éviter son glissement, et donc son embolie.

L'acheminement du stent et son déploiement en zone cible sera alors réalisé de manière précautionneuse, avec des contrôles réguliers concernant sa position, son absence d'occlusion de la veine pulmonaire et son efficacité concernant la suppression du shunt. Figure 25 et 26.

Figure 25 : Déploiement du stent couvert par inflation en zone cible.

Un flairing de la partie inférieure du stent au niveau de l'oreillette droite est parfois nécessaire pour permettre d'élargir cette partie, et ainsi obtenir une bonne impaction du stent autour de la jonction cavo-atriale, afin de diminuer le risque de shunt résiduel.
Un contrôlé du résultat final sera effectué selon plusieurs modalités
-angiographie dans l'artère pulmonaire droite, avec graphie numérisée et temps tardif, permettant de visualiser les veines pulmonaires droites redirigées à l'oreillette gauche, et de contrôler l'absence de shunt résiduel.
-angiographie direct dans la veine pulmonaire redirigée si celle ci a été protégée après ponction trans-septale. Sa perméabilité sans sténose sera évaluée, ainsi que l'absence de gradient de pression sur son nouveau trajet jusqu'à l'oreillette gauche.

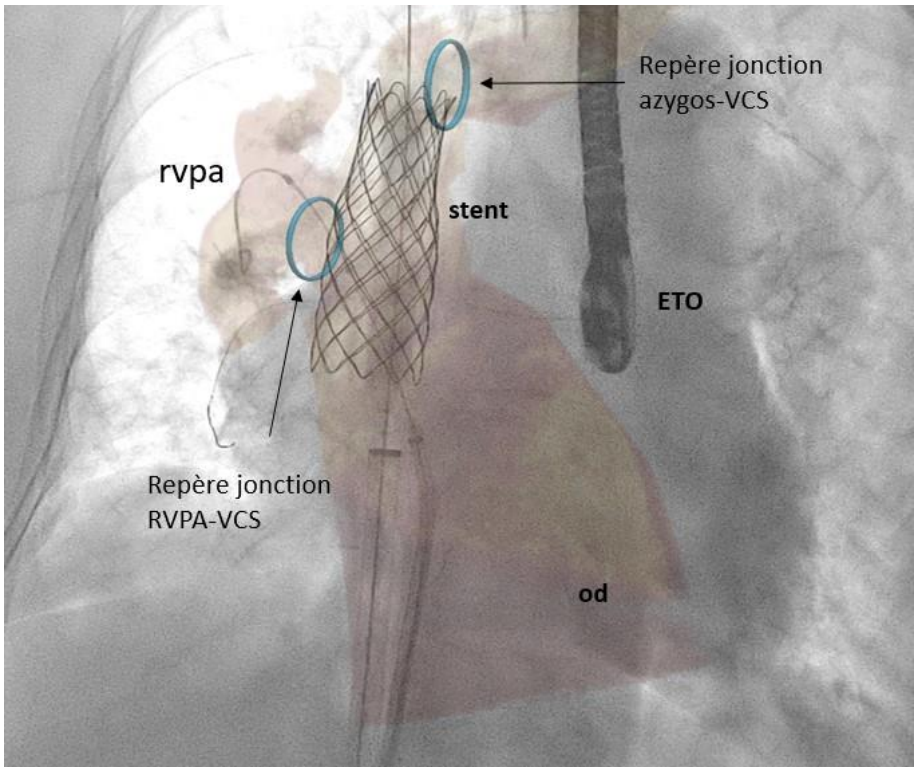

Figure 26 : correction percutanée d'une CIA sinus venosus, avec aide de l'imagerie multimodalité

Ici : fusion scanner 3D et fluoroscopie.

RVPA : retour veineux pulmonaire anormal, OD oreillette droite, ETO échographie trans-oesophagienne, VCS veine cave supérieure)

Les points importants de cette nouvelle technique sont les suivants

-choix de la bonne taille et du bon diamètre du stent.

-stabilité du stent et ancrage dans la veine cave supérieure : le stent doit être bien fixé notamment dans sa partie supérieure au niveau de la veine cave supérieure.

-rapport du stent avec le TVI.

-correction partielle ou totale du shunt, qui dépend de la taille de la CIA et du degré d'évasement du stent dans l'oreillette droite.

-écoulement libre du flux des VP dans l'OG, validé par l'absence d'augmentation des pressions dans les VP après l'implantation du stent.

6. Evolution à long terme et indications de correction

Sans traitement, l'évolution des CIA sinus venosus est la même que les autres CIA.

Le double shunt gauche droit lié aux caractéristiques de la malformation peut accélérer la survenue des complications de type surcharge vasculaire pulmonaire, hypertension pulmonaire, et arythmie supra-ventriculaire[51, 52, 55].

Le traitement des CIA sinus venosus doit donc être préférentiellement effectué au diagnostic si possible. Pour éviter la survenue des complications, le traitement est proposé chez les enfants afin de les en prémunir. Dans ce cas, le plus fréquent reste encore la prise en charge chirurgicale, car la correction percutanée ne peut théoriquement s'envisager qu'une fois la croissance du patient achevée.

Dans la pratique quotidienne, le traitement est souvent envisagé chez l'adulte, du fait du diagnostic tardif de cette cardiopathie.

Quand une complication survient, le bénéfice de la correction doit être mis en balance avec le risque de l'intervention.

Par exemple, dans le cas l'hypertension artérielle pulmonaire installée et fixée, la correction devient contre indiquée car la suppression du shunt sera délétère car supprimera une soupape intracardiaque à la majoration potentielle de l'hypertension artérielle pulmonaire.

Comme pour les autres CIA, une stratégie de traitement puis réparation (« treat and repair ») pourra être tentée[53] : elle consiste en la tentative de baisse des pressions pulmonaires grâce à des traitements médicamenteux qui parfois abaissent les pressions et résistances pulmonaires de telle sorte que la correction de la cardiopathie devient alors secondairement envisageable.

Concernant les troubles du rythme supra ventriculaire, ils peuvent avoir pour origine l'oreillette droite (flutter) ou l'oreillette gauche (fibrillation auriculaire). La correction de la malformation dans ce cas ne devra être envisagée qu'en prenant en considération la potentielle nécessité d'ablation rythmologique ultérieure[86].

Dans ce cas, les projets d'ablation endo-cavitaire des arythmies peuvent retarder de quelques mois la correction de la cardiopathie, permettant d'avoir encore accès à l'oreillette gauche grâce à la communication OD-OG toujours existante.

Pour le cas particulier de la fibrillation atriale[87], une attention particulière devra être portée à l'anatomie et au substrat arythmogènes, potentiellement concernés par la malformation anatomique (retour veineux pulmonaire anormal et jonction cavo-atriale).

III. Modélisation 3D

1. Principes

La modélisation 3D consiste à convertir en volume 3D une structure anatomique, un organe ou une région anatomique d'intérêt.

En médecine, les images acquises d'une région d'intérêt étudiée par les différents examens complémentaires le sont souvent en coupes (plus ou moins fines). C'est le cas des images obtenues par ultrasons (échographie), rayons x (tomodensitométrie) et par résonnance magnétique (IRM).

L'interprétation de ces examens par les médecins et radiologues se fait le plus souvent sur ces coupes fines qui défilent sur écran, présenté selon l'axe d'acquisition des images par l'appareil.

Cette interprétation requiert donc une connaissance préalable et de la région étudiée, et des structures avoisinantes de cette dernière.

De plus, l'interprétation des images requiert un repérage clair par le lecteur concernant l'axe d'acquisition de l'examen ainsi que les axes de lecture des coupes qui peuvent être variables.

Le plus souvent, les examens en coupes sont interprétés dans les 3 axes dimensionnels principaux (axial, frontal, sagittal). Figure 27.

Figure 27 : coupes scanner avec visualisation simultanée en 3 axes orthogonaux axial, frontal, sagittal (X ;Y ;Z).

Ce mode de lecture et d'analyse entraine un biais inter-individuel net dans l'interprétation de sa représentation mentale par l'opérateur. Ce biais peut être favorisé

par divers paramètres (connaissances personnelles, acuité, capacité de vision dans l'espace, capacité ou non de reconstruire mentalement en 3D une image 2D donnée selon plusieurs plans).

A partir d'une analyse en coupe, les axes de lecture peuvent également être modifiés à souhait pour analyser une région souhaitée dans son intégralité, alors qu'elle n'est pas visible en totalité selon un axe pré-défini.
Cette reconstruction d'images 2D à l'intérieur d'un volume prédéfini selon un plan choisi par l'opérateur est appelé reconstruction multi-planaire (Multi Planar Reconstrution, MPR). Figure 28.

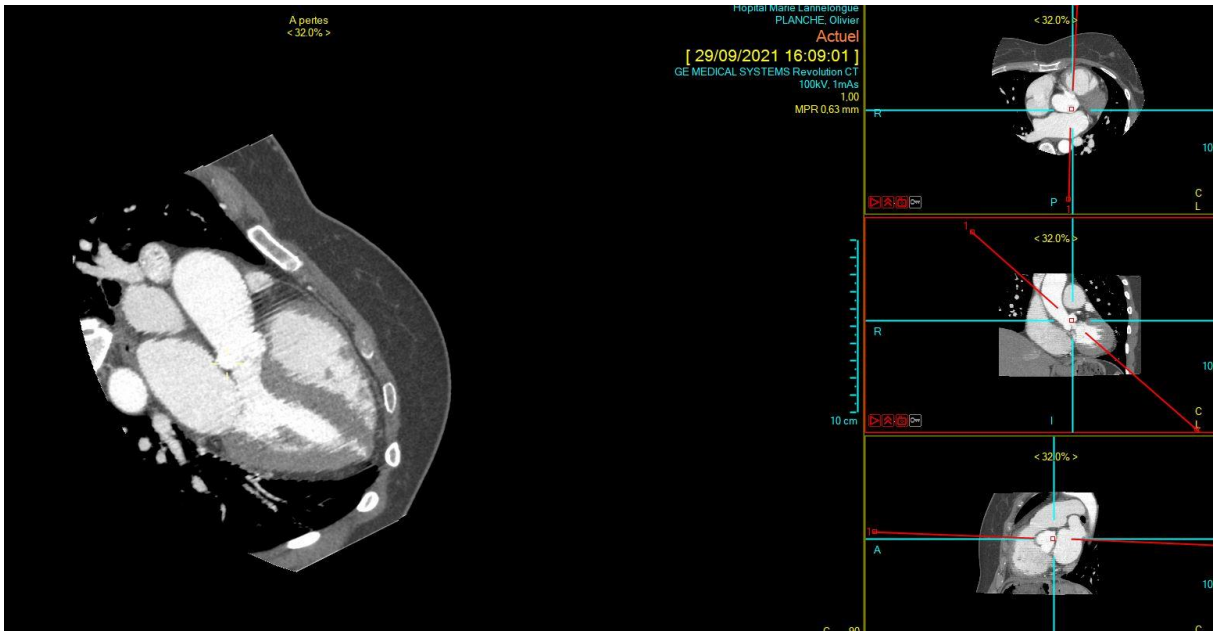

Figure 28 : Image reconstruite d'une voie d'éjection gauche (ventricule gauche - aorte) selon axe orthogonal modifié en MPR.

Un point d'intérêt sur une image en coupe (2 dimensions) correspond à un pixel, et quel que soit son plan de lecture, ce pixel garde une coordonnée dans l'espace précise en constante selon l'axe 3D (x ;y ;z). En vue en coupe, il est néanmoins toujours visualisé en 2 dimensions. Figure 29.

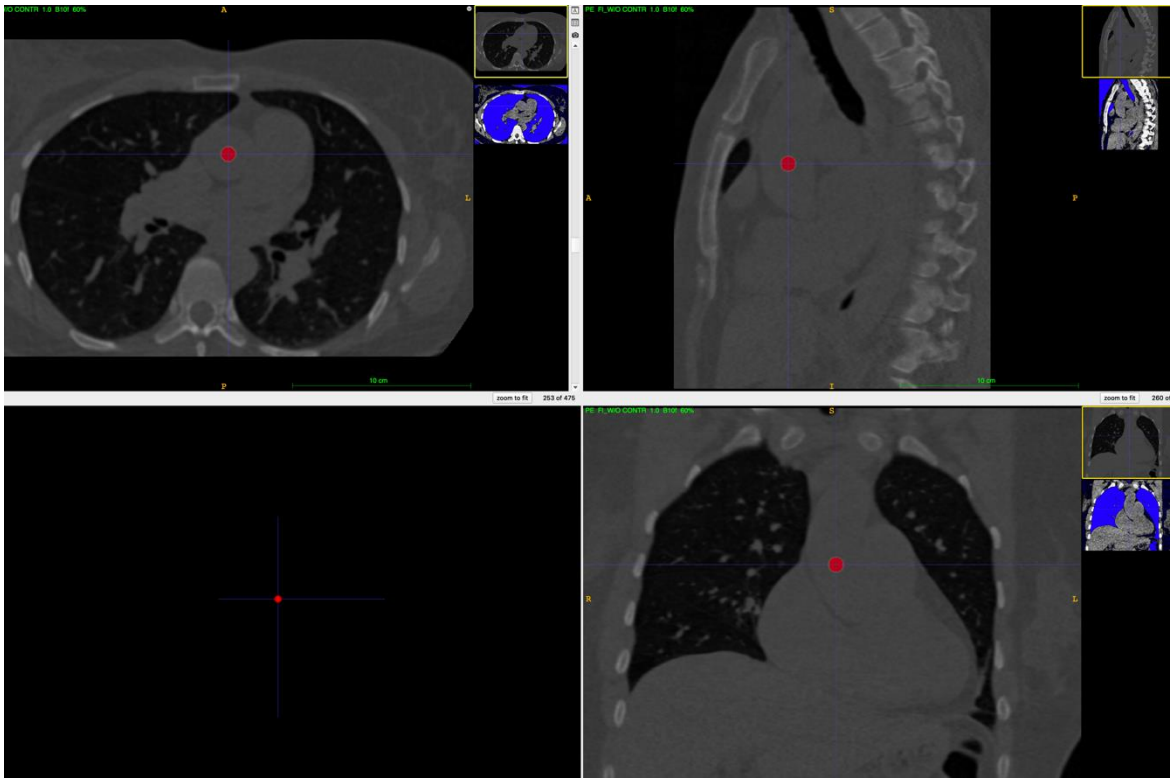

Figure 29 : Image d'un point d'intérêt dans un plan 3D et sur les 3 axes orthogonaux standards.

Grâce à la modélisation 3D, un pixel est transformé en un volume appelé voxel. Le voxel garde les mêmes coordonnées 3D dans l'axe (x ;y ;z) que son pixel correspondant, mais est visualisé dans les 3 dimensions de manière simultanée. De plus, il est constitué d'une surface, d'arêtes et de sommet. Élargi à une structure anatomique d'intérêt, une image devient donc un volume anatomique.

Les images d'un organe d'intérêt sur coupes empilées peuvent ainsi être transformées en un volume 3D de cet organe. Figure 30.

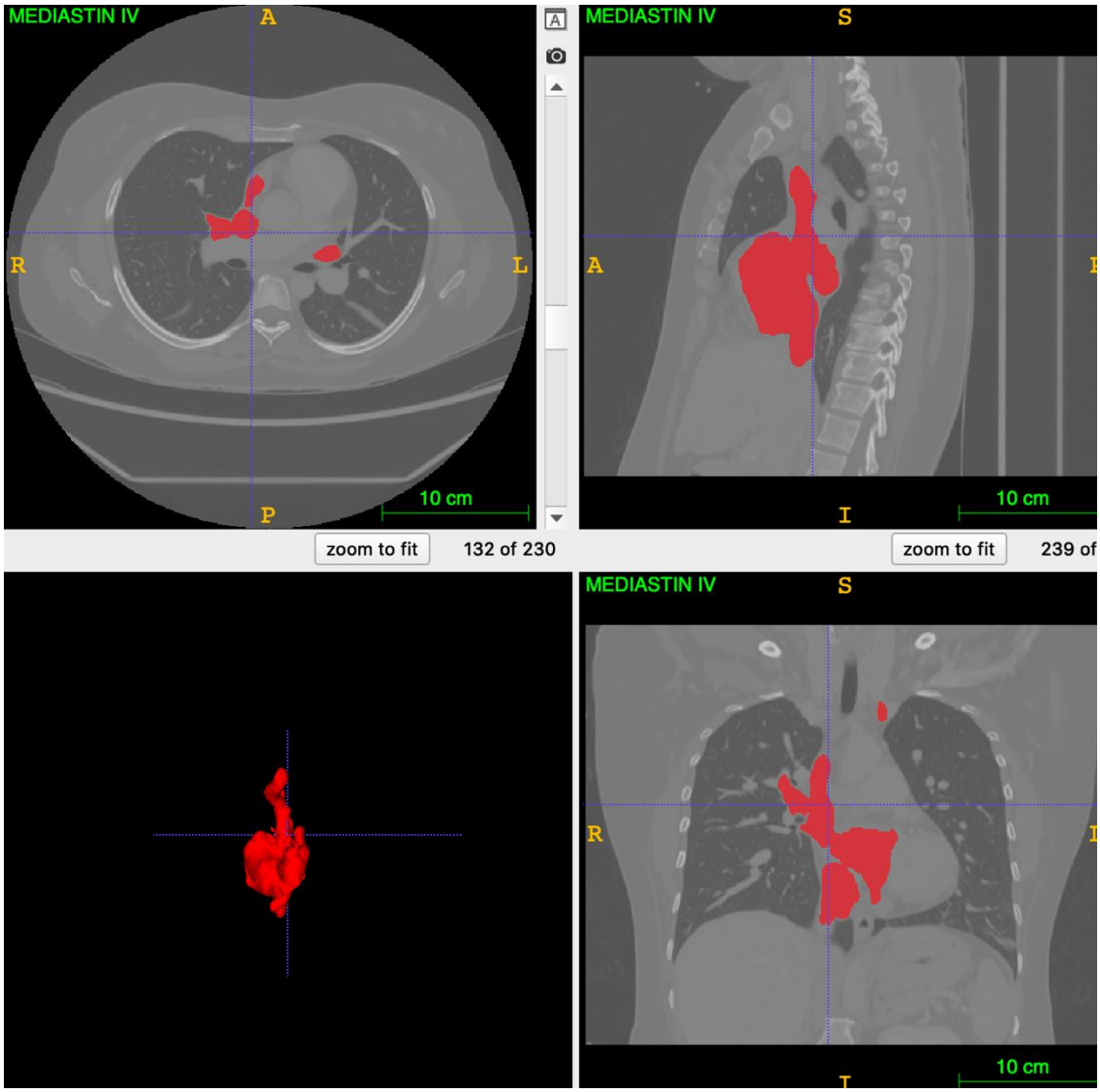

Figure 30 : Image d'un Volume 3D complet après segmentation semi-automatique (logiciel ITK-snap).

Les bénéfices potentiels de la visualisation d'une région d'intérêt en 3D plutôt qu'en coupe sont les suivants :

-tous les lecteurs du volume présenté lisent une information plus globale, plus complète et plus univoque. Le biais d'interpretation est donc fortement diminué.

-tous les facteurs confondant la lecture et l'interpretation de l'image peuvent être supprimés, permettant une attention plus particulière sur la région d'intérêt elle-même.

-à la vision en surface s'ajoute une navigation à l'intérieur de la région d'intérêt, plus profonde et donc plus précise.

-l'axe de lecture de l'image 3D peut être modifié à l'infini et de manière plus facilement centrée sur le modèle lui-même (la région d'intérêt). Cela permet une vision ciblée et

précise, autour et à l'intérieur de la région étudiée. Cela implique d'avoir déterminé comme l'iso-centre des axes, le centre du modèle lui-même.

La tomodensitométrie est actuellement l'examen médical permettant la modélisation 3D d'une région anatomique la plus précise, en raison de ses meilleures performances en termes de résolution spatiale.

2. Volume Rendering

Le Volume Rendering est une fonctionnalité intégrée dans la majorité des logiciels d'imagerie médicale en coupe, permettant l'obtention rapide d'images en 3D à partir des coupes acquises. Ce processus offre une visualisation en trois dimensions de l'anatomie, tout en éliminant les structures environnantes qui pourraient nuire à la vision et l'analyse (technique de cropping). Bien que cette approche soit rapide et accessible, elle présente l'inconvénient de limiter l'autonomie de l'utilisateur dans l'utilisation et l'extraction des informations obtenues.
En effet, avec cet outil, l'opérateur peut visualiser l'image 3D, la faire tourner selon un des 3 axes (x ;y ;z) et zoomer à l'intérieur. La modification du volume par l'opérateur lui-même est souvent impossible, de même que son extraction en tant que volume. Des photos ou captures d'écran peuvent être collectées, mais souvent cela consiste finalement à revenir en arrière dans le processus d'analyse (d'un volume, on revient à une image en 2 dimensions). Figure 31.

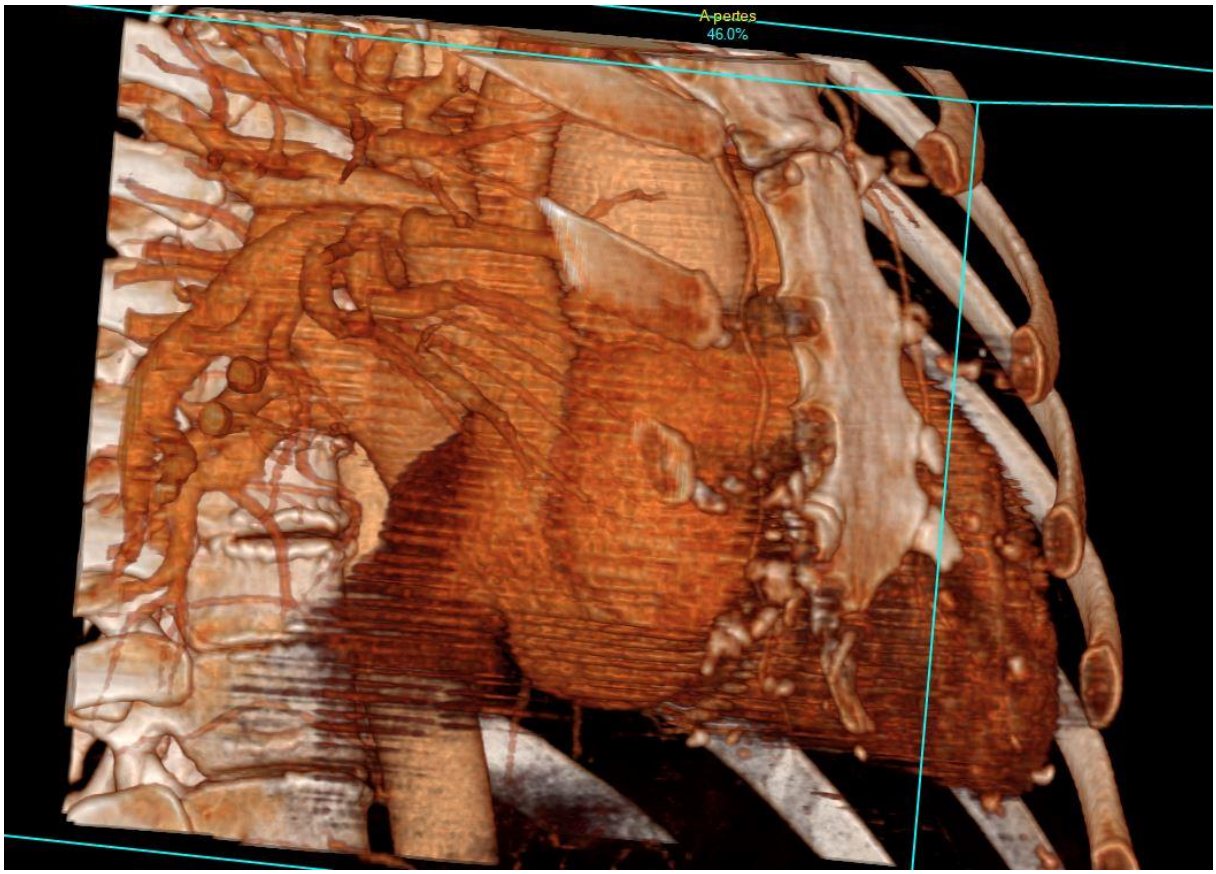

Figure 31 :Iimage d'une CIA sinus venosus en 3D après application de la fonction volume rendering.

3. Segmentation automatique

La segmentation automatique consiste, via des calculs algorithmiques et mathématiques sophistiquées, en l'extraction d'un examen en coupe permettant d'obtenir un volume 3D de la région d'intérêt.

Les méthodes de segmentation automatique peuvent être classées en fonction de leur approche. Les méthodes basées sur des modèles génératifs traitent la segmentation comme un problème d'inférence statistique, où la segmentation est considérée comme une variable latente. Ces méthodes peuvent être univariées, utilisant des modèles de mélanges finis pour décrire les intensités d'image des différents segments, ou multivariées, prenant en compte les dépendances entre pixels grâce aux champs aléatoires de Markov (CAM). Ces dernières modélisent la distribution des intensités sur l'ensemble d'une image, ce qui permet une segmentation plus précise en tenant compte des relations spatiales entre les pixels [88].

En résumé, la segmentation automatique facilite la modélisation 3D rapide, mathématique et automatique d'une structure, tout en répondant à la complexité des données d'imagerie.

L'opérateur n'a aucune influence sur la création du modèle, ce qui d'une part supprime le potentiel d'un biais de modélisation, mais qui d'autre part, expose à des limites de résultat liées à la qualité de l'examen de référence sur lequel se base la modélisation. Figure 32.

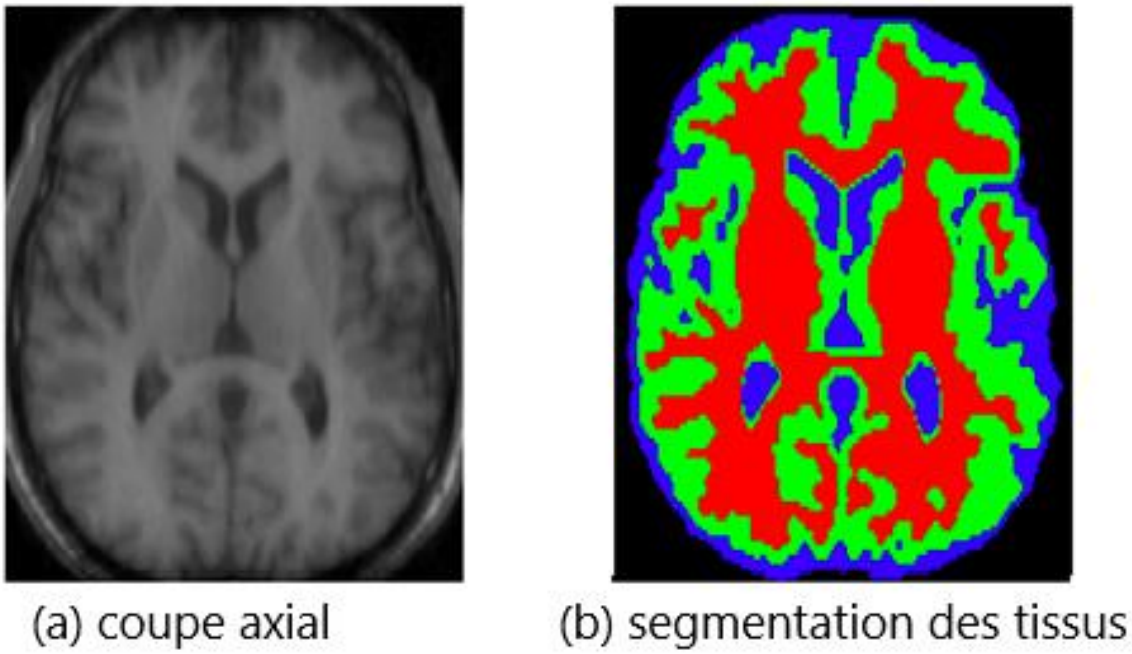

Figure 32 : segmentation automatique de la substance grise et de la substance blanche [89].

4. Segmentation manuelle

La segmentation manuelle, bien qu'utile, est souvent coûteuse et chronophage, nécessitant l'expertise de spécialistes. Par exemple, dans le domaine de la neuro-imagerie, la segmentation manuelle des tissus cérébraux est complexe et sujette à variabilité inter-annotateurs.

5. Segmentation semi-automatique

La segmentation semi-automatique est une approche intermédiaire entre la segmentation manuelle et automatique, utilisée dans le traitement des images

médicales. Elle combine l'interaction de l'utilisateur avec des algorithmes avancés pour améliorer la précision et l'efficacité de l'extraction des structures anatomiques.

Dans ce processus, un professionnel de santé initie la segmentation en définissant des régions d'intérêt ou en annotant des structures clés. L'algorithme, ensuite, exploite ces informations pour segmenter automatiquement le reste de l'image, ce qui permet de réduire le temps de travail tout en conservant le contrôle de l'utilisateur sur les résultats. Cette méthode est particulièrement utile dans des contextes où des variations complexes dans les données d'image peuvent compromettre les résultats d'une segmentation entièrement automatique.

La segmentation semi-automatique est largement utilisée dans divers domaines, notamment la cardiologie, l'oncologie et la neuro-imagerie, où des structures anatomiques précises sont essentielles pour le diagnostic et le traitement. Par exemple, dans le cas de tumeurs, cette méthode permet d'obtenir des contours précis qui peuvent être critiques pour la planification chirurgicale ou le suivi des traitements[90].

Les algorithmes de segmentation semi-automatique peuvent inclure des techniques de contours actifs, des modèles de Markov, ou des réseaux de neurones qui s'appuient sur des données d'apprentissage préalable.

La segmentation semi-automatique allie donc expertise humaine et puissance algorithmique, permettant une flexibilité et une adaptabilité face à la variabilité des images médicales analysées.

Quelle que soit la méthode de segmentation choisie, le modèle 3D obtenu est donc un nuage de voxels interconnectés dont le format le plus fréquemment utilisé est le STL (Standard Tesselaltion Language).

6. Applications en médecine

Lecture et compréhension 3D homogénéisée

En lisant l'anatomie sur une imagerie en coupe, le médecin reconstruit cérébralement, spontanément, consciemment ou non, et selon son propre mode opératoire, le volume 3D correspondant à analyser. Une variabilité inter-individuelle est donc quasi obligatoire, que ce soit dans le regard, la reconstruction mentale, et la figuration finale de la représentation que chacun se fait d'une région anatomique.

La présentation directe, partagée, sur écran, du modèle 3D anatomique univoque, permet de supprimer cette variabilité interindividuelle d'interprétation, et ainsi

homogénéiser la vision et la compréhension anatomique entre les opérateurs concernés[92].

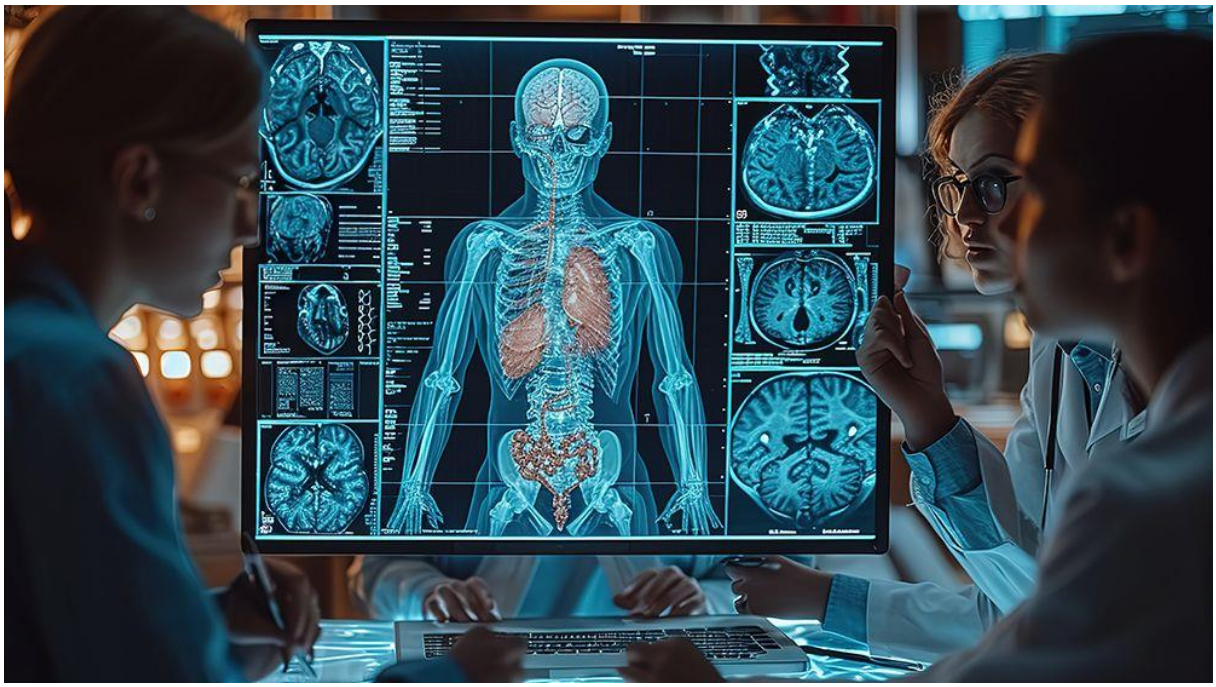

Figure 33 : Amélioration de l'échange entre médecin grâce à la technologie 3D.

www.enseigner.ulaval.ca

Simulation opératoire virtuelle

Le travail médical sur modèle 3D permet également d'envisager des simulations de traitement sur l'écran de travail. Cela est très utile en chirurgie ou en cathétérisme interventionnel, ou la conséquence d'une action thérapeutique (mise en place d'un stent ou d'une valve dans un conduit, résection d'une partie d'organe) peut être visualisée sur écran, et ainsi analysée, adaptée et préparée.

Figure 34 : simulation opératoire via l'utilisation du logiciel Avatar médical. https://sante.sorbonne-universite.fr

Préparation et aide opératoire concrète

Cette technologie permet dans certains cas une préparation opératoire concrète, par exemple la planification d'un plan de coupe en chirurgie orthopédique ou maxillo-faciale. Elle peut aussi aider à la préparation de prothèse à insérer dans l'organisme du patient, comme c'est le cas en chirurgie vasculaire (cf chapitre sur l'impression 3D et le banc d'essai).[93]

A l'avenir, on peut imaginer que les tissus synthétiques (patch en dacron pour fermer les communications intracardiaques par exemple), seront aussi pré-préparés en amont sur la base d'une modélisation 3D préalable du cœur.

Toutes ces applications de simulation virtuelle et d'aide opératoire offertes par la modélisation 3D tendent à amener la prise en charge des patients vers une médecine personnalisée, sur-mesure.

Figure 35 : impression 3D d'une prothèse de remplacement de mandibule en chirurgie maxillo-faciale. www.medicalexpo.fr (xilloc/product)

Enseignement

L'enseignement médical bénéficie également de manière significative des technologies de modélisation 3D[93] : cela permet un apprentissage de l'anatomie par l'étudiant de façon plus réaliste et vivante. Les planches d'anatomie et les dissections d'organes à visée d'enseignement pourraient au fur et à mesure être prochainement remplacées par des banques virtuelles d'organes et de modèles de pathologie.
Les applications destinées à l'information du grand public et des patients sont également des champs d'applications concrets de cette technologie.

Réalité augmentée

Les progrès sont tels dans le domaine de la 3 dimension en médecine, que l'étape suivante a déjà débuté, avec la réalité augmentée[94]. Cette dernière a pour vocation d'inclure le principe du mouvement voir le direct-live dans l'analyse et le traitement de l'image avec des champs d'applications nombreux dans des domaines médicaux variés.
Cette technologie s'utilise via un casque de réalité virtuelle et nécessite un support informatique conséquent (hardware) pas toujours aisé à mettre en place dans des endroits spécifiques comme le bloc opératoire.

Figure 36 : réalité augmentée. Le HoloLens 2 de Microsoft utilisé au bloc opératoire. (Crédits photos : Microsoft)

7. Fusion d'image

La fusion d'images multimodale est une technologie associant la modélisation 3D et le suivi en temps réel des images produites par fluoroscopie au cours d'une intervention en cathétérisme.

Elle constitue une avancée technologique cruciale par l'intégration des données d'imagerie classiques (scanner, échographie) à la baie de cathétérisme sur laquelle est réalisée en live l'intervention[95].

Ce processus repose sur l'alignement spatial des images provenant de différentes sources, permettant de superposer en temps réel des informations anatomiques détaillées préalables sur le flux de travail interventionnel live.

En pratique, cela implique l'utilisation de techniques de registration d'images, qui corrigent les variations de perspective et de position entre les différentes modalités, assurant ainsi une correspondance précise des structures anatomiques provenant de deux sources différentes.

Une étape pré-procédurale appelée « recalage » est nécessaire pour obtenir une fusion d'image fiable dans l'espace au cours de l'intervention. Ce recalage consiste en la détermination de points fixes disponibles communs et concordants sur les deux examens d'imagerie sources (la fluoroscopie, et l'autre examen choisi).

Cette détermination de points fixes communs doit se faire dans deux plans différents, orthogonaux l'un de l'autre, afin que le logiciel de guidage puisse faire bouger l'image additionnée de manière simultanée et exactement identique au mouvement de l'image

donnée par la fluoroscopie, quel que soit son axe d'acquisition au cours de l'intervention.

Par exemple, la fusion entre la tomodensitométrie et la fluoroscopie permet, en live au cours du cathétérisme (guidé par fluoroscopie), la superposition du modèle 3D (segmenté préalablement grâce au scanner).[96]
Les bénéfices de cette approche sont significatifs en salle de cathétérisme, notamment pour les interventions complexes.
La visualisation intégrée permet une navigation précise sur la base de différents repères provenant de sources différentes, et optimise ainsi le guidage de l'opérateur vers les régions d'intérêt au cours de l'intervention, réduisant les risques de lésions vasculaires ou d'atteinte des tissus environnants.
Cette technologie permet également l'apposition sur le masque additionné et projeté, de repères d'intérêt dont l'opérateur va se servir tout au long de l'intervention, améliorant encore son guidage et sa concentration sur des objectifs opératoires prédéfinis.

La fusion d'image est également possible entre l'échographie trans-oesophagienne et la fluoroscopie[97]. Par exemple, l'échographie peut fournir des informations en temps réel sur la localisation et la morphologie flux sanguins, tandis que la fluoroscopie permet de visualiser la progression du cathéter dans le système vasculaire. Ensemble, ces modalités offrent une image complète qui améliore la prise de décision en cours d'intervention.

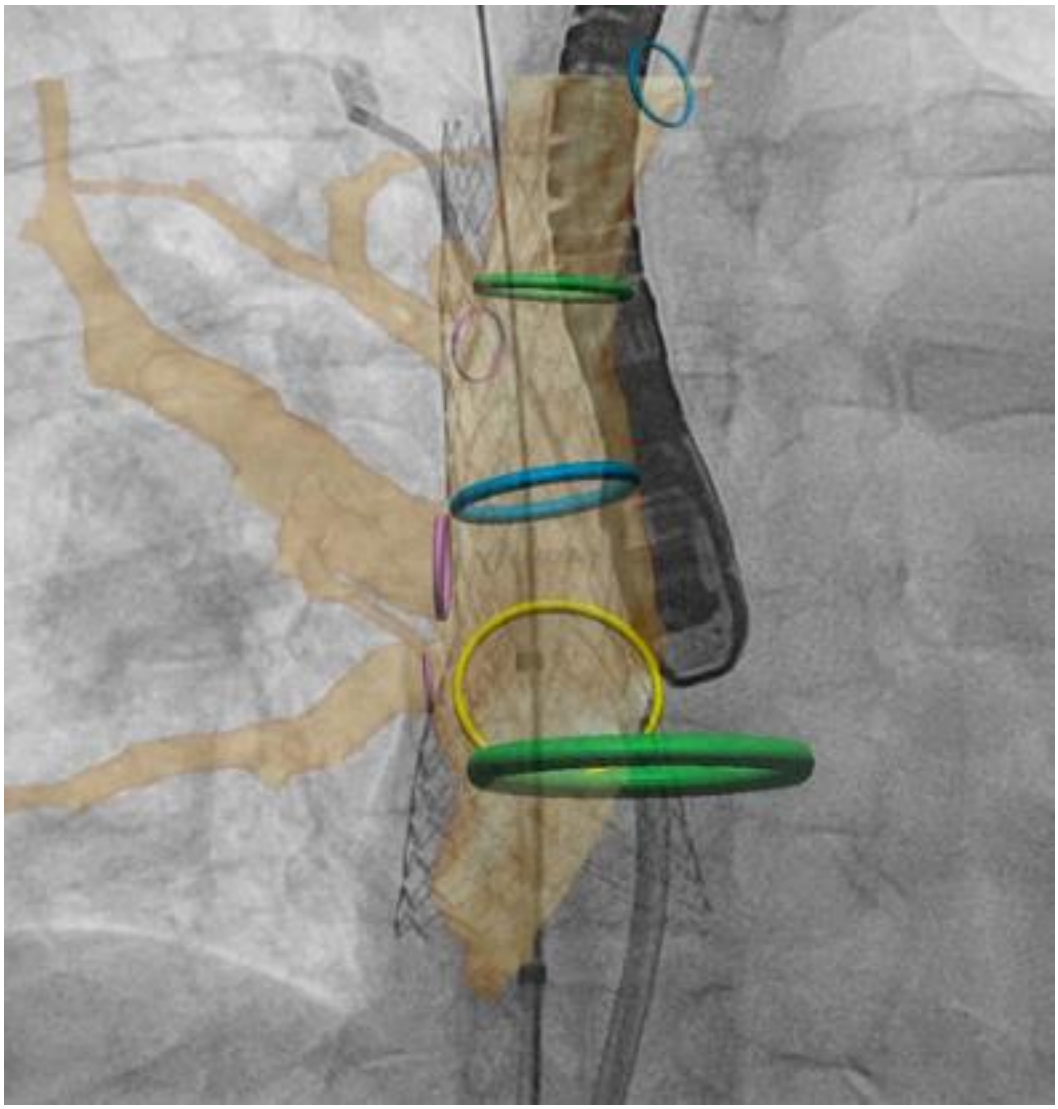

Figure 37 : fusion d'image en salle de cathétérisme (fluoroscopie + angioscanner)

IV. 3D printing et benchtesting

Il est possible à partir de pièces anatomiques modélisée en 3D et disponible sous le format STL, d'imprimer en 3 dimensions les sujets souhaités, ce qui permet d'ajouter à une utilisation sur écran, une utilisation physique de la pièce souhaitée.

Cette utilisation physique d'un modèle imprimé en médecine part de l'analyse simple dans la main, vers le partage entre différents opérateurs à des fins d'homogénéisation de réflexion sur un cas. Elle peut aboutir à la simulation physique d'une intervention, parfois sur un banc d'essai interventionnel connecté, permettant de reproduire une intervention dans les conditions du réel, sur un objet imprimé comparable à l'organe opéré dans la vraie vie [98, 99].

1. Techniques d'impression

Plusieurs techniques d'impression existent, permettant l'utilisation de différents matériaux afin d'obtenir la pièce anatomique imprimée finie. En cardiologie interventionnelle, à des fins de simulation sur banc d'essai, les modèles imprimés flexibles seront privilégiés[100-102].

L'objectif de la technique d'impression à choisir est d'obtenir le matériau adéquat répondant au cahier des charges souhaité.

Le modèle imprimé devra donc au mieux, être élastique, souple, translucide, radio-transparent, échogène. De plus, il devra résister à l'eau et à la contrainte (traction et cisaillement), en gardant une distensibilité semblable au tissu humain. De plus, il devra garder une bonne résolution spatiale pour être comparable au sujet imprimé, et éventuellement avoir une mémoire de forme permettant sa réutilisation.

A ces fins, les 3 principaux matériaux utilisés avec des techniques d'impressions propres sont :

-le thermo-polyuréthane qui utilise la technique du « selective laser sintering » (SLS) : le modèle s'imprime par durcissement et fusion de poudre très fine sous l'effet d'un laser

Les avantages de cette technique sont la faible utilisation de consommable et l'absence de support nécessaires pour imprimer les modèles. Les inconvénients résident en le fait que le modèle est peu résistant à l'eau, et n'est pas transparent.

-le polyjet est un autre procédé d'impression par dépose couche par couche de résine molle et transparente. Son impression nécessite de nombreux support, une phase de post-traitement longue et le modèle obtenu est souvent fragile.

-le stereolithograph apparatus (SLA) est un procédé qui utilise une lumière UV qui va solidifier une couche de résine photopolymère liquide. Le post-traitement de cette technologie nécessite un nettoyage dans un solvant, puis le traitement par ultraviolet afin de durcir le modèle.

L'avantage théorique de cette technique est l'obtention de modèles transparents ce qui permet une visualisation directe du testing procédural. Sa solidité et son comportement dans un banc d'essai reste à évaluer.

2. Applications du banc d'essai en cardiologie interventionnelle

Les progrès en modélisation 3D et en simulation sur banc d'essai sont devenus des outils performants pour la planification pré-procédurale en cardiologie interventionnelle, notamment concernant les procédures complexes[103].

Par exemple, les simulations sur banc d'essai sont publiées pour les fermetures d'auricule gauche[104-107], les revalvulations pulmonaires percutanées[108, 109], les fermetures de fuite para-prothétique[110], ainsi qu'en chirurgie vasculaire interventionnelle[111].

Les avantages d'une approche 3D avec simulation pré-procédurale sur jumeau numérique et sur banc d'essai pour les sessions « hands-on » sont nombreux : amélioration et accélération de la courbe d'apprentissage des médecins interventionnels, évaluation des risques et de la faisabilité d'une intervention spécifique, incluant l'anticipation des complications. Cette approche favorise également le développement de nouveaux dispositifs médicaux, et facilite les procédures d'autorisation par les organismes de contrôle de santé pour valider des projets thérapeutiques novateurs.

REVIEW 1: Sinus venosus ASDs : imaging and percutaneous closure

C Batteux, A Azarine, C Karsenty, J Petit, V Ciobotaru, P Brenot, S Hascoet

Reference bibliographique 74

Abstract traduit en français

Objectif de la revue

La correction percutanée de la communication inter-atriales type sinus venosus par implantation d'un stent couvert est une nouvelle technique prometteuse et peu invasive. La caractérisation anatomique préopératoire et la sélection rigoureuse des patients semblent essentielles au succès de la procédure, et de nouveaux outils d'imagerie sont utilisés à cet effet. Nous proposons ici de décrire et d'analyser toutes ces caractéristiques récentes.

Constatations récentes

Les CIA sinus venosus présentent une grande variabilité de caractéristiques anatomiques, qui doivent être décrites et analysées à l'aide de nombreux outils d'imagerie, y compris la technologie 3D. La correction percutanée est un défi, mais elle peut accélérer la récupération clinique par rapport à la chirurgie cardiaque conventionnelle à cœur ouvert. La faisabilité de la correction percutanée repose sur une étude anatomique préopératoire précise et sur un guidage en temps réel utilisant un processus de fusion d'image multimodale.

Résumé

La modélisation 3D des CIA type sinus venosus est indispensable pour comprendre le large éventail anatomique rencontré dans cette pathologie. L'orientation par fusion d'image multimodale est très utile pour réaliser la correction percutanée des CIA sinus venosus chez les patients sélectionnés.

Current Cardiology Reports (2021) 23:138
https://doi.org/10.1007/s11886-021-01571-7

STRUCTURAL HEART DISEASE (RJ SIEGEL AND NC WUNDERLICH, SECTION EDITORS)

Sinus Venosus ASDs: Imaging and Percutaneous Closure

C. Batteux[1] · A. Azarine[1] · C. Karsenty[2] · J Petit[1] · V. Ciobotaru[1] · P. Brenot[1] · S. Hascoet[1]

Accepted: 17 May 2021

Abstract
Purpose of the review Percutaneous closure of sinus venosus atrial septal defects (ASD) using covered stent implantation is a new and promising minimally invasive technique. New imaging tools are used to ensure preoperative anatomical characterization and preoperative guidance, which are key procedural success factors. Here we will describe and analyze these recent developments.
Recent findings Sinus venosus ASDs present a wide variety of anatomical features which must be described and analyzed using various imaging tools, including 3D technology. Percutaneous closure is challenging, but can hasten clinical recovery compared to the gold-standard conventional open-heart surgery. The feasibility of percutaneous closure relies on precise preoperative anatomical study and on real-time guidance using a multimodal fusion imaging process.
Summary Three-dimensional modeling of sinus venosus ASD is essential to understand the large anatomical panel encountered in this pathology. Multimodal fusion imaging guidance is very useful for performing sinus venosus ASD percutaneous closure in selected patients.

Keywords Sinus venosus · Congenital heart disease · Percutaneous closure · 3D technology · Multimodal fusion imaging

Introduction

Imaging and treatment of sinus venosus atrial septal defects (ASD) has seen a significant paradigm shift over the past few years as a result of two innovations: first, improvements in three-dimensional (3D) technology in the field of congenital heart disease (CHD), and second, the development of a percutaneous closure procedure using a covered stent and blood flow redirection technique.

As these two approaches are now starting to be used worldwide, this study aims to review and analyze the current and future position of these novel tools in the global consideration of sinus venosus ASD pathology.

A Large Imaging Panel for a Wide Anatomical Spectrum

Sinus venosus ASD is characterized by high ASD and an abnormal pulmonary vein return (PVR) in the superior vena cava (SVC). There are numerous imaging diagnostic tools available to describe this type of CHD [1].

This article is part of the Topical Collection on *Structural Heart Disease*

✉ C. Batteux
c.batteux@ghpsj.fr

A. Azarine
aazarine@ghpsj.fr

C. Karsenty
clement.karsenty@hotmail.fr

J Petit
j.petit@ghpsj.fr

V. Ciobotaru
vciobotaru@yahoo.fr

P. Brenot
p.brenot@ghpsj.fr

S. Hascoet
hascoets@gmail.com

[1] Hôpital Marie Lannelongue, Cardiologie congénitale, chirurgie cardiaque congénitale et cardiologie interventionnelle, Centre de référence M3C cardiopathies congénitales complexes, Groupe Hospitalier Paris Saint Joseph, Paris Saclay University, Le Plessis Robinson, France

[2] Centre Hospitalo-Universitaire de Toulouse. Service de cardiologie pédiatrique et congénitale. Institut des Maladies Métaboliques et Cardiovasculaires, Université de Toulouse, INSERM U1048, I2MC, Toulouse, France

Published online: 19 August 2021

Transthoracic Echocardiography (TTE)

Diagnosis can be made by transthoracic echocardiography (TTE) showing two direct anatomical signs: high unusual ASD in relation to the SVC area, and drainage from one or several abnormal pulmonary veins in the SVC [2, 3].

The subcostal view is essential for identifying these signs in patients with good echogenicity. Indirect signs, explained by the physiopathology, have to be searched to analyze the consequences of the pathology or to guide the cardiologist to the final diagnosis: right chamber dilatation, left-to-right atrial shunt in color Doppler, and in some cases moderate to severe pulmonary hypertension (PH) on tricuspid valve (TV) or pulmonary valve (PV) regurgitation.

Although TTE is an effective tool, other imaging techniques are used to enhance visualization of the global anatomy, such as cardiac computed tomography (CT) or magnetic resonance imaging (MRI). This need for complementary imaging is explained by the large variability in anatomical anomalies encountered and by the difficulties in precisely visualizing the abnormal PVR by TTE [4] (Fig. 1).

Cardiac CT

Cardiac CT remains the best imaging tool for assessing sinus venosus ASD [5–7].

Regarding its execution, a gating process appears to be essential. Indeed, the more precise (gated) the acquisition, the more accurate the analysis of the defect and the abnormal PVR can be; the number of veins concerned, the existence of a PVR collector, and the orientation and height of the abnormal drainage in the SVC are concerning elements that characterize this singular pathology anatomically.

Left-arm contrast injection is recommended to identify a left SVC and to analyze the anatomy of the innominate vein. These parameters could be missed with a right-arm injection and are a very important consideration in the choice of treatment= [8, 9].

Thanks to its good spatial resolution, cardiac CT is the best imaging modality for converting slice images into a 3D model of the malformation. With 3D modeling software, it is now possible and easy to create a reliable 3D model of the malformation. Therefore, the anatomy of sinus venosus ASDs can

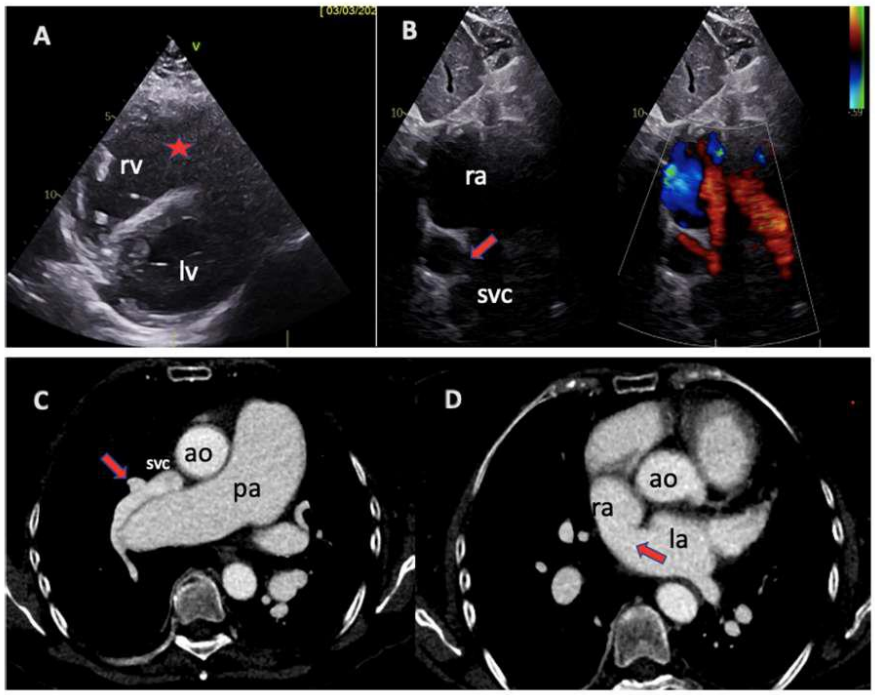

Fig. 1 Transthoracic echocardiography and cardiac CT findings in sinus venosus ASD. **A**, **B** Transthoracic echocardiography findings. **A** Right ventricle dilatation in short axis (*star*). **B** ASD in subcostal view (*arrow*) pulmonary vein close to the ASD (Doppler flow). **C**, **D** Cardiac CT findings. **C** Abnormal pulmonary vein return in SVC (*arrow*). **D** Particular ASD in relation to SVC (*arrow*). *RA* right atrium, *LA* left atrium, *RV* right ventricle, *LV* left ventricle, *SVC* superior vena cava, *AO* aorta

reveal a wide spectrum of anatomical variability among patients.

Nowadays, this personalized anatomical analysis for each patient is crucial in determining who is eligible for a percutaneous procedure and who is not. Moreover, 3D technology enables the clinician to obtain an image of the malformation in order to evaluate the feasibility of percutaneous closure in a "close-to-reality" situation. It also enables practitioners to optimize, in "real-time" mode, the percutaneous procedure using 3D guidance software (see above) [10•] (Fig. 1).

Cardiac MRI

While MRI spatial resolution remains less precise than that of CT, this imaging exam can provide much information regarding sinus venosus ASD. Nevertheless, the anatomical diagnosis can be confirmed, and a hemodynamic study can be performed with 4D flow analysis. This recently developed tool is effective for assessing the left-to-right shunt and its consequences (right chamber dilatation, pulmonary blood overflow), and contributes to the treatment decision in adults. It also enables an evaluation of the proportion of left-to-right shunt induced by the ASD on one side, and the abnormal PVR on the other side.

Limits of this exam include the need for immobility during acquisition, which is not easy for children or claustrophobic adults [11–13] (Fig. 2).

Other Imaging Tools

Cardiac Catheterization

Sinus venosus ASD diagnosis can sometimes be discovered fortuitously during a catheterization exam. In this situation, hemodynamic study identifies a left-to-right shunt and can reveal moderate to severe pulmonary hypertension; light cyanosis on blood oximetry can be found in the left atrium due to the close relationship between the ASD and the SVC. Fluoroscopy and pulmonary artery angiograms show the abnormal PVR drainage in the SVC, and the anatomy of systemic and pulmonary venous return has to be precise. The innominate vein, left SVC, and right SVC dimensions are important parameters in determining the treatment strategy.

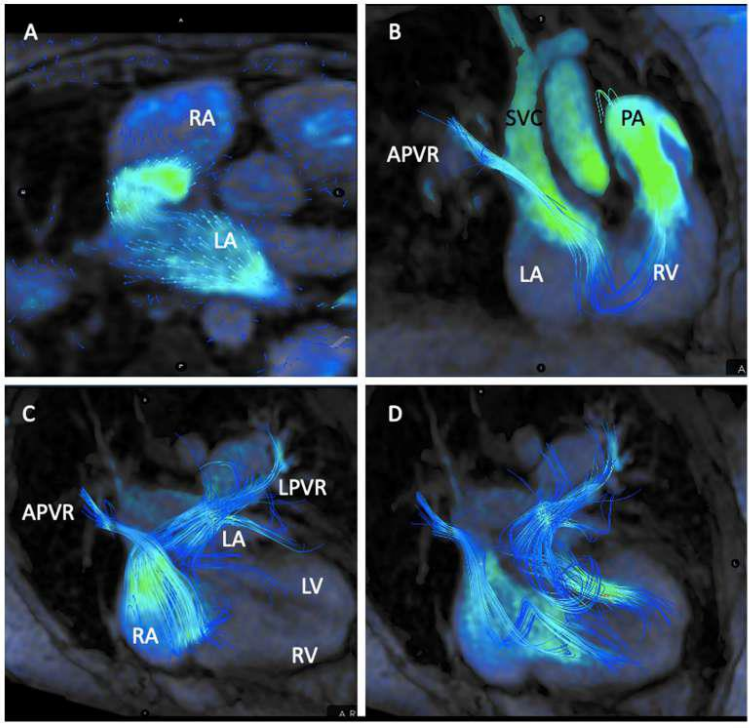

Fig. 2 Cardiac 4D-flow MR images of sinus venosus ASD. **A** Axial view: left-to-right shunt through the defect is demonstrated by velocity vectors. **B** Right chamber sagittal view. Streamlines show the pathway of incoming blood flow from anomalous pulmonary venous return (APVR) to SVC, RA, RV, and finally PA, during diastole. **C**, **D** Four-chamber views during systole (**C**) and diastole (**D**). Streamlines show blood flow pathways from APVR and superior LPVR. During systole (**C**), both flows arrive in the RA, through ASD for LPVR, while during diastole (**D**), superior LPVR flow goes to LV and APVR flow goes to RV. *APVR* anomalous pulmonary venous return, *LPVR:* Left pulmonary venous return, *PA* pulmonary artery, *LA* left atrium, *RA* right atrium, *LV* left ventricle, RV right ventricle

Transesophageal Echocardiography (TEE)

Even if TEE is not a major imaging modality for the diagnosis of sinus venosus ASD, it is currently required for use in real time during percutaneous closure. As described with classic ASDs, it is a useful tool for guidance during the procedure [14].

Concerning sinus ASDs, the back-view offered by this tool makes it possible to visualize all the right pulmonary veins precisely and dynamically, and to evaluate the relationship between each abnormal vein and the defect and the SVC. In this way, this dynamic tool helps to guide the percutaneous closure and to identify any PV occlusion or stenosis risk during the procedure; moreover, it can accurately assess partial or total suppression of the left-to-right shunt after stent deployment. [15–18].

A Recent Percutaneous Correction Procedure

Surgical treatment of sinus venosus ASD has historically involved the Warden procedure, which consists in a section-anastomosis of the SVC (the upper PVR abnormal return) to the right atrial appendage by tunneling of the PVR to the left atrium through the ASD [19]. Major related adverse surgical events reported are SVC anastomosis stenosis and pulmonary vein stenosis around the tunneling patch (Fig. 3).

The first case of sinus venosus ASD percutaneous correction was published in 2014 by Garg et al., and has since been performed in several countries. Around 50 cases have been reported to date [20••, 21].

The approach consists in placing a covered stent from the SVC to the right atrium, to ensure that the abnormal PVR can no longer flow to the right atrium, but can only flow to the left atrium through the posterior part of the ASD; the abnormal PVR is thus excluded from the upper systemic return. Therefore, this is not precisely an ASD closure, but more of a blood flow redirection. We believe this technique could have been inspired by a surgical procedure [22, 23••].

The technique, under general anesthesia and TEE guidance, consists in creating a stabilization rail with a stiff wire from a right femoral vein access to a right jugular vein access. This rail makes it possible to route the covered stent in the desired position up to the SVC with good stability and precision. Abnormal pulmonary vein(s) have to be catheterized from the left atrium after a transseptal puncture and left femoral vein access. This makes it possible to monitor the lack of increasing pressure in the concerned vein during the stent deployment, to assess the left-to-right shunt correction after stent deployment, and to eventually protect a PV from stenosis during stent inflation with a balloon protection system.

Transhepatic access has been performed for patients with no femoral access [24].

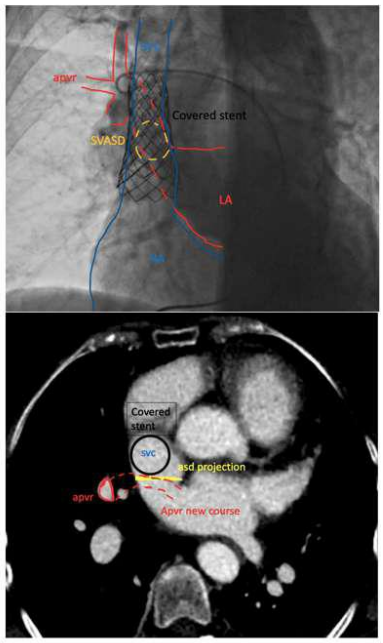

Fig. 3 Concept of sinus venosus ASD percutaneous closure. *Top*: Concept of sinus venosus percutaneous closure on angiography figure. *Bottom*: Concept of sinus venosus percutaneous closure on CT slice figure. *APVR* abnormal pulmonary vein return, *SVASD* sinus venosus atrial septal defect, *LA* left atrium, *RA* right atrium, *SVC* superior vena cava

The benefits of this endovascular procedure, compared to open-heart surgery, include less morbidity, faster recovery, and shorter hospital stay. Nevertheless, this approach must be performed in a tertiary center with surgical resources to anticipate any failure. Since its creation, the technique has evolved and is still eligible for simplification [25]. The early results based on selected patients look excellent [26, 27].

Major immediate risks of this procedure have to be considered [23••]:

- Stent instability and migration can occur in cases where the stent deployment does not perfectly fit the anchoring site in the SVC. To prevent this risk, the anchoring zone in the SVC has to be as long as possible, and the diameter of the stent deployment has to be increased a bit compared to the SVC diameter. The device dimensions (length, diameter) have to be perfectly chosen and adapted to each patient's anatomy. Stent migration can lead to the need for immediate surgery, as endovascular capture of this consequent embolized device appears impossible.

- Pulmonary vein stenosis/occlusion can occur during the covered stent deployment. The new channel created for the PVR flow to the left atrium is represented anteriorly by the posterior part of the stent and posteriorly by the PVR itself. The obstruction of this channel can cause significant damages such as pulmonary hypertension and pulmonary edema. To avoid this major event, patient eligibility for percutaneous procedure has to be carefully considered based on prior precise 3D anatomical evaluation. During the procedure, pressure and TEE monitoring of the at-risk PVR are mandatory. Then, stent inflation has to be carried out cautiously and progressively. A protection balloon can also be inflated in the PVR to protect the channel from obstruction and to mold the covered stent in a way to keep the channel large and open.
- Residual shunt can occur due to an insufficient ASD covering from the stent. The residual shunt can involve the inferior part of the defect if the stent is deployed too high. It can also involve the lateral part of the defect if the stent deployment is not as large as the hole dimension. In this case, the residual shunt can be corrected by stent flaring with a secondary hyperinflation of the inferior part of the stent with a large balloon [18].

As the percutaneous procedure is efficient but quite new, indication and patient eligibility have to be carefully assessed to ensure that the risk of adverse events is as low as possible. Given this concern, today the procedure appears to be reserved for adult patients. However, growth considerations and device implantation in a non-definitive SVC in children are being studied: evolutive devices should be one of the solutions in the future.

Within an adult population, we are facing a large anatomical variability concerning the ASD and the abnormal PVR, so patient selection should be stringent, and only done after a precise anatomical study [23••].

Here, three-dimensional virtual simulation and multimodal fusion imaging appear to be very helpful for assessing the feasibility and eligibility of the percutaneous procedure for each patient, and for guiding the procedure itself to prevent the occurrence of major adverse events.

Multimodal Imaging Simulation and Guidance

3D Modeling and Virtual Simulation

Nowadays, 3D modeling is widely used in medicine within all specialties. Applied to CHD and its infinite anatomical variability, this technology offers strong assistance to physicians for anatomical description and understanding. In the field of sinus venosus ASD, 3D technology is helpful for precisely determining the position of the defect and its relationship with SVC, and the abnormal PVR in the SVC (Fig. 4, Video 1).

Beyond analysis of the malformation itself, it is also possible to simulate the closure procedure on 3D models on screen [28–30].

Using a Standard Tessellation Language (STL) model of a covered stent, simulation is carried out by placing the stent in the optimal position on the 3D model of the sinus venosus ASD. This approach offers many benefits regarding the preparation and organization of the real procedure.

- It can more clearly determine which patient is eligible for percutaneous closure and which patient is not, supported by anatomical findings and reliable projection.
- It helps in choosing the optimal dimension of the device to implant. By adjusting the device on the 3D simulation model, the physician can determine the optimal length and diameter of the stent, which is very important in choosing the type of stent.
- This simulation tool also enables a focused and personalized approach and aids in defining major potential risks for each individual patient. It is indeed clear that certain patients are more at risk for PV occlusion and others for residual shunt, and this predilection can be highlighted by a 3D simulation tool.

At the end of this predictive pre-procedural work, a comprehensive plan for the percutaneous procedure will be in place, with a suitable and personalized roadmap tailored for each patient.

3D printed models

The evolution of 3D printing in recent years has made it possible to produce reliable 3D printed models of CHD. Various printing technologies are available, including fusion deposit modeling (FDM), stereolithography (SLA), digital light processing (DLP), and selective laser sintering (SLS), and there is significant variability in the price, time, and manpower required to obtain a printed model. Globally, this tool is used more and more frequently; with regard to sinus venosus ASD, it offers the physician the possibility for "hands-on" manipulation of CHD. Moreover, it is possible to anticipate percutaneous closure by testing different stents in the malformation. It can also inform and educate patients and associates. This way of viewing and touching a CHD appears to be a major change in the global understanding of and approach to CHD for physicians [31] (Fig. 5).

3D Fusion Imaging Guidance

When anatomical findings during pre-procedural work identify eligibility for percutaneous closure, a multimodal fusion

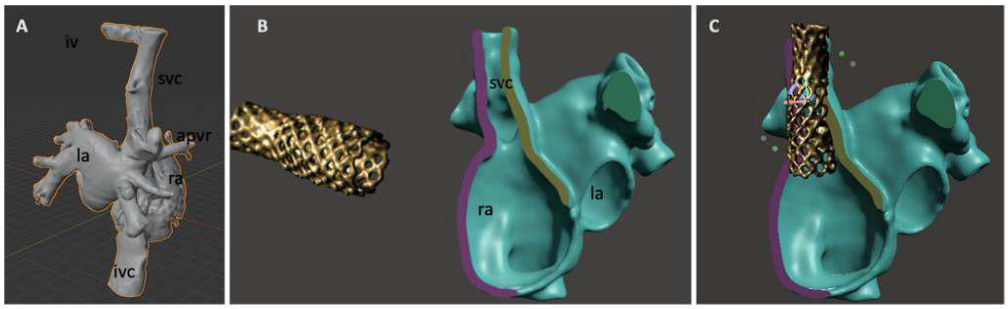

Fig. 4 Sinus venosus ASD percutaneous closure simulation. **A** 3D modeling of sinus venosus atrial septal defect, permitting 3D geometric analysis. **B** On-screen simulation of the percutaneous closure. **C** Choice of the optimal position and dimension of the stent in the superior vena cava. *IV* innominate vein, *IVC* inferior vena cava, *SVC* superior vena cava, *APVR* abnormal pulmonary vein return

imaging process is used and appears to be very helpful in the cath lab during the live procedure (Fig. 6).

The concept is to merge fluoroscopy and angiography with different imaging exams during the procedure in real time and to use this tool for guidance.

The guidance provided during the procedure is twofold: On one hand, it provides the physician with global vision and landmarks of the malformation to easily achieve the objective. On the other hand, it enables the procedure to be performed more safely and with permanent additional control, to lower the risk of major event occurrence.

Fusion of Fluoroscopy and 3D Model

This fusion imaging tool is helpful in obtaining, a volume rendering of a CHD from a cardiac CT projected in real time during the procedure. It needs to be planned before the intervention, and comprises several steps: segmentation of the model, volume rendering, and landmark positioning. In the cath lab during the procedure, the 3D model has to be cushioned with the fluoroscope using static anatomical structures like the manubrium sterni or vertebras, for example. When the 3D model is merged with fluoroscopy, the fusion projection enables the operator to obtain efficient guidance inside the malformation, and also helps to focus on important landmarks. This latter tool is very useful throughout the procedure. It also provides virtual landmarks like the ASD position and the connection zone of the SVC with the right atrium, which are all important factors to control during stent positioning and deployment to avoid PV stenosis and residual shunt (Video 2).

If there were one drawback to highlight with this fusion process, it would be that it is not real "live" imaging, because the cardiac CT is not continuous and instantaneous. The operator needs to be highly focused on distinguishing what is live from what is static. Moreover, a second cushion is also sometimes necessary to obtain a reliable projection of the 3D model on the fluoroscopy screen throughout the procedure [29, 30].

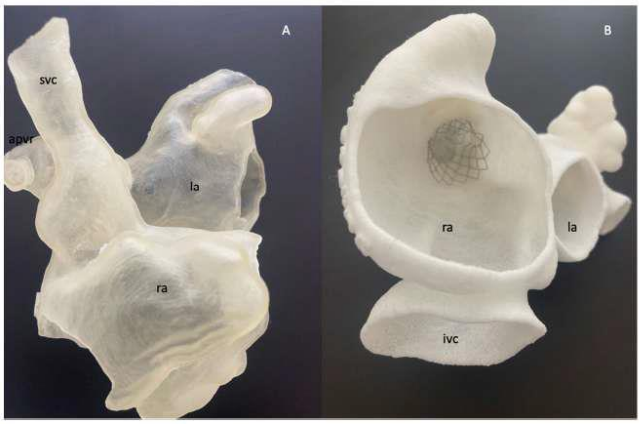

Fig. 5 3D printed models of sinus venosus ASD. **A** Silicon model (polyjet technology). **B** Polyurethane model (TPU technology) with non-covered stent implantation for testing. *IVC* inferior vena cava, *SVC* superior vena cava, *APVR* abnormal pulmonary vein return, *LA* left atrium, *RA* right atrium

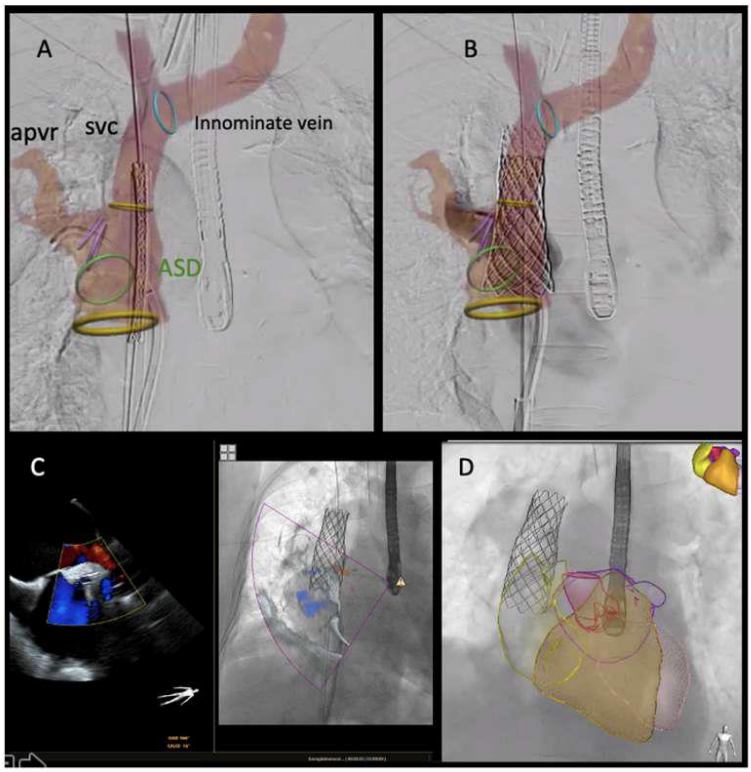

Fig. 6 Multimodal fusion imaging. **A**, **B** Fusion between 3D model and fluoroscopy (VesselNavigator, Philips, Hanover). **A** Stent positioning. *Green circle*: projection of the ASD. *Yellow circles*: landmarks for optimal stent positioning for stability and covering. **B** Angiographic control after stent deployment showing the lack of residual shunt. **C**, **D** Fusion between TEE and fluoroscopy (EchoNavigator, Philips, Hanover). **C** Control of the free blood flow from superior right abnormal PVR to left atrium during stent deployment. **D** 4D TEE fusion with fluoroscopy after stent deployment

Fusion of Fluoroscopy and TEE

This dynamic fusion tool makes it possible to combine TEE with fluoroscopy, and appears to be helpful during stent deployment. It helps in redirecting the abnormal PV flow to the LA instantaneously and continuously and aids in the early detection of an obstruction. Moreover, it makes it possible to control the left-to-right shunt suppression or persistence after stent deployment in real time. This tool is very valuable for precisely guiding the operator during the procedure. Indeed, it provides important imaging and hemodynamic control during stent deployment and helps the operator to determine whether to stop stent inflation immediately or to continue [17, 18, 29, 30] (Video 2).

Conclusion

Developments in 3D technology with regard to imaging exams in medicine have enabled a better understanding of complex pathologies thanks to a spatial anatomical approach. Applied to sinus venosus ASDs, this tool also makes it possible to prepare and guide new treatment modalities such as percutaneous correction. The success and value of this new procedure in the future will probably rely on the continuous improvement of 3D imaging tools coupled with precise anatomical eligibility assessment for each patient.

Supplementary Information The online version contains supplementary material available at https://doi.org/10.1007/s11886-021-01571-7.

Declarations

Conflict of Interest The authors declare that they have no conflict of interest.

Human and Animal Rights and Informed Consent This article does not contain any studies with human or animal subjects performed by any of the authors.

References

Papers of particular interest, published recently, have been highlighted as:
- • Of importance
- •• Of major importance

1. al Zaghal AM, Li J, Anderson RH, Lincoln C, Shore D, Rigby ML. Anatomical criteria for the diagnosis of sinus venosus defects. Heart. 1997;78(3):298–304. https://doi.org/10.1136/hrt.78.3.298.
2. Omomo Y, Mochizuki Y, Chino S, Oyama N, et al. Superior sinus-venosus atrial septal defect complicated by partial anomalous pulmonary venous connection detected by repeated transthoracic echocardiography in an adult. J Echocardiogr. 2020. https://doi.org/10.1007/s12574-020-00488-4.
3. Konstantinos C, Theodoropoulos AP, Masoero G, Papitsas M, et al. Superior sinus venosus atrial septal defect. J Geriatr Cardiol. . https://doi.org/10.11909/j.issn.1671-5411.2018.10.007.
4. Turner J, Turner MC, Kerut EK. Complementary echo and CCTA findings with superior sinus venosus atrial septal defect. Echocardiography. 2016;33(10):1600–1. https://doi.org/10.1111/echo.13319.
5. Otsuka M, Itoh A, Haze K. Sinus venosus type of atrial septal defect with partial anomalous pulmonary venous return evaluated by multislice CT. Heart. 2004;90(8):901. https://doi.org/10.1136/hrt.2003.031203.
6. White HD, Halpern EJ, Savage MP. Imaging of adult atrial septal defects with CT angiography. JACC Cardiovasc Imaging. 2013;6(12):1342–5. https://doi.org/10.1016/j.jcmg.2013.07.011.
7. Hoey ET, Lewis G, Yusuf S. Multidetector CT assessment of partial anomalous pulmonary venous return in association with sinus venosus type atrial septal defect. Quant Imaging Med Surg. 2014;4(5):433–4. https://doi.org/10.3978/j.issn.2223-4292.2014.07.08.
8. Rio PP, Mumpuni H, Anggrahini DW, Dinarti LK. Persistent left superior vena cava in atrial septal defect sinus venosus type: diagnosis with saline contrast echocardiography-a case series. Clin Case Rep. 2017;5(5):587–90. https://doi.org/10.1002/ccr3.883.
9. Disha B, Prakashini K, Shetty RK. Persistent left superior vena cava in association with sinus venosus defect type of atrial septal defect and partial pulmonary venous return on 64-MDCT. BMJ Case Rep. 2014;2014:bcr2013202999. https://doi.org/10.1136/bcr-2013-202999.
10. • Gertz ZM, Strife BJ, Shah PR, Parris K, Grizzard JD. CT angiography for planning of percutaneous closure of a sinus venosus atrial septal defect using a covered stent. J Cardiovasc Comput Tomogr. 2018;12(2):174-175. https://doi.org/10.1016/j.jcct.2017.09.007. **Here we have one of the first publications describing the benefit of planning percutaneous closure from CT, opening doors for multimodal fusion guidance. As this pathology presents significant anatomical variability, this personalized approach is used to tailor the treatment for each patient individually.**
11. Kafka H, Mohiaddin RH. Cardiac MRI and pulmonary MR angiography of sinus venosus defect and partial anomalous pulmonary venous connection in cause of right undiagnosed ventricular enlargement. AJR Am J Roentgenol. 2009;192(1):259–66. https://doi.org/10.2214/AJR.07.3430.
12. Ganigara M, Tanous D, Celermajer D, Puranik R. The role of cardiac MRI in the diagnosis and management of sinus venosus atrial septal defect. Ann Pediatr Cardiol. 2014;7(2):160–2. https://doi.org/10.4103/0974-2069.132509.
13. Isorni MA, Moisson L, Moussa NB, Monnot S, Raimondi F, Roussin R, et al. 4D flow cardiac magnetic resonance in children and adults with congenital heart disease: Clinical experience in a high volume center. Int J Cardiol. 2020;320:168–77. https://doi.org/10.1016/j.ijcard.2020.07.021.
14. Hascoët S, Hadeed K, Karsenty C, Dulac Y, Heitz F, Combes N, et al. Feasibility, Safety and Accuracy of Echocardiography-Fluoroscopy Imaging Fusion During Percutaneous Atrial Septal Defect Closure in Children. J Am Soc Echocardiogr. 2018;31(11):1229–37. https://doi.org/10.1016/j.echo.2018.07.012.
15. Hadeed K, Hascoët S, Karsenty C, Ratsimandresey M, Dulac Y, Chausseray G, et al. Usefulness of echocardiographic-fluoroscopic fusion imaging in children with congenital heart disease. Arch Cardiovasc Dis. 2018;111(6-7):399–410. https://doi.org/10.1016/j.acvd.2018.03.006.
16. Kronzon I, Tunick PA, Freedberg RS, Trehan N, Rosenzweig BP, Schwinger ME. Transesophageal echocardiography is superior to transthoracic echocardiography in the diagnosis of sinus venosus atrial septal defect. J Am Coll Cardiol. 1991;17(2):537–42. https://doi.org/10.1016/s0735-1097(10)80128-7.
17. Kabir SR, Simpson JM, Jones MI, Butera G, Qureshi SA, Rosenthal E. TEE Guidance During Transcatheter Treatment of Superior Sinus Venosus ASDs With Partial Anomalous Pulmonary Venous Drainage. JACC Cardiovasc Imaging. 2021:S1936-878X(20)31015-9. https://doi.org/10.1016/j.jcmg.2020.11.010.
18. Sivakumar K, Qureshi S, Pavithran S, Vaidyanathan S, Rajendran M. Simple Diagnostic Tools May Guide Transcatheter Closure of Superior Sinus Venosus Defects Without Advanced Imaging Techniques. Circ Cardiovasc Interv. 2020;13(12):e009833. https://doi.org/10.1161/CIRCINTERVENTIONS.120.009833.
19. Gustafson RA, Warden HE, Murray GF. Partial anomalous pulmonary venous connection to the superior vena cava. Ann Thorac Surg. 1995;60(6 Suppl):S614–7. https://doi.org/10.1016/0003-4975(95)00854-3.8604948.
20. •• Garg G, Tyagi H, Radha AS. Transcatheter closure of sinus venosus atrial septal defect with anomalous drainage of right upper pulmonary vein into superior vena cava–an innovative technique. Catheter Cardiovasc Interv. 2014;84(3):473–7. https://doi.org/10.1002/ccd.25502. **This is the first published case of sinus venosus ASD percutaneous closure.**
21. Meier B, Gloekler S, Dénéréaz D, Moschovitis A. Percutaneous repair of sinus venosus defect with anomalous pulmonary venous return. Eur Heart J. 2014;35(20):1352. https://doi.org/10.1093/eurheartj/ehu088.
22. Nicholson IA, Chard RB, Nunn GR, Cartmill TB. Transcaval repair of the sinus venosus syndrome. J Thorac Cardiovasc Surg. 2000;119(4 Pt 1):741–4. https://doi.org/10.1016/S0022-5223(00)70009-2.
23. •• Hansen JH, Duong P, Jivanji SGM, Jones M, Kabir S, Butera G, et al. Transcatheter Correction of Superior Sinus Venosus Atrial Septal Defects as an Alternative to Surgical Treatment. J Am Coll Cardiol. 2020;75(11):1266–78. https://doi.org/10.1016/j.jacc.2019.12.070. **This publication provides comprehensive information regarding our topic. It increases anatomical selection, planning, and technical considerations. Moreover, it describes results and follow-up in a number of patients. As percutaneous closure is a relatively new procedure, this publication assesses the feasibility and safety of the process in selected patients.**
24. Alkhouli M, Campsey DM, Higgins L, Badhwar V, Diab A, Sengupta PP. Transcatheter Closure of a Sinus Venosus Atrial Septal Defect Via Transhepatic Access. JACC Cardiovasc Interv. 2018;11(14):e113–5. https://doi.org/10.1016/j.jcin.2018.02.021.
25. Kempny A, Gatzoulis MA. Percutaneous repair of sinus venosus ASD: the end of congenital cardiac surgery? EuroIntervention. 2018;14(8):843–5. https://doi.org/10.4244/EIJV14I8A150.
26. Riahi M, Velasco Forte MN, Byrne N, Hermuzi A, Jones M, Baruteau AE, et al. Early experience of transcatheter correction of

superior sinus venosus atrial septal defect with partial anomalous pulmonary venous drainage. EuroIntervention. 2018;14(8):868–76. https://doi.org/10.4244/EIJ-D-18-00304.

27. Abdullah HAM, Alsalkhi HA, Khalid KA. Transcatheter closure of sinus venosus atrial septal defect with anomalous pulmonary venous drainage: Innovative technique with long-term follow-up. Catheter Cardiovasc Interv. 2020;95(4):743–7. https://doi.org/10.1002/ccd.28364.
28. Tandon A, Burkhardt BEU, Batsis M, Zellers TM, Velasco Forte MN, Valverde I, et al. Sinus Venosus Defects: Anatomic Variants and Transcatheter Closure Feasibility Using Virtual Reality Planning. JACC Cardiovasc Imaging. 2019;12(5):921–4. https://doi.org/10.1016/j.jcmg.2018.10.013.
29. Batteux C, Meliani A, Brenot P, Hascoet S. Multimodality fusion imaging to guide percutaneous sinus venosus atrial septal defect closure. Eur Heart J. 2020;41(46):4444–5. https://doi.org/10.1093/eurheartj/ehaa292.
30. Butera G, Sturla F, Pluchinotta FR, Caimi A, Carminati M. Holographic Augmented Reality and 3D Printing for Advanced Planning of Sinus Venosus ASD/Partial Anomalous Pulmonary Venous Return Percutaneous Management. JACC Cardiovasc Interv. 2019;12(14):1389–91. https://doi.org/10.1016/j.jcin.2019.03.020.
31. Thakkar AN, Chinnadurai P, Breinholt JP, Lin CH. Transcatheter closure of a sinus venosus atrial septal defect using 3D printing and image fusion guidance. Catheter Cardiovasc Interv. 2018;92(2):353–7. https://doi.org/10.1002/ccd.27645.

REVIEW 2 : Transcatheter closure of superior sinus venosus defects

Alban-Elouen Baruteau, MD, PHD; Sébastien Hascoet, MD, PHD ; Sophie Malekzadeh-Milani, MD ; Clément Batteux, MD ; Clément Karsenty, MD, PHD ; Vlad Ciobotaru, MD ; Jean-Benoit Thambo, MD, PHD ; Alain Fraisse, MD, PHD ; Younes Boudjemline, MD, PHD ; Zakaria Jalal, MD, PHD.

Reference bibliographique 112

Abstract traduit en français

La CIA sinus venosus est une communication entre l'oreillette droite et l'oreillette gauche située au-dessus de la fosse ovale, immédiatement en dessous de la jonction de la veine cave supérieure et de l'oreillette droite. Il est systématiquement associé à un retour veineux pulmonaire anormal partiel de la veine pulmonaire supérieure droite. La réparation chirurgicale a été la méthode de référence pour fermer cette communication. Introduite en 2014, la correction percutanée est progressivement devenue une alternative sûre et efficace à la chirurgie chez les patients soigneusement sélectionnés, bien que l'expérience mondiale demeure limitée. Cet article fournit une évaluation du processus de sélection des patients ainsi qu'une description détaillée de la procédure, accompagnée d'une revue complète de ses résultats.

JACC: CARDIOVASCULAR INTERVENTIONS VOL. 16, NO. 21, 2023

PUBLISHED BY ELSEVIER

STATE-OF-THE-ART REVIEW

Transcatheter Closure of Superior Sinus Venosus Defects

Alban-Elouen Baruteau, MD, PhD,[a,b,c,d] Sébastien Hascoet, MD, PhD,[e] Sophie Malekzadeh-Milani, MD,[f] Clément Batteux, MD,[e] Clément Karsenty, MD, PhD,[g,h] Vlad Ciobotaru, MD,[e,i] Jean-Benoit Thambo, MD, PhD,[j,k] Alain Fraisse, MD, PhD,[j] Younes Boudjemline, MD, PhD,[m] Zakaria Jalal, MD, PhD[j,k]

ABSTRACT

Superior sinus venosus defect is a communication between the right and left atrium located above the upper margin of the oval fossa, immediately inferior to the junction of the superior vena cava and the right atrium. It is systematically associated with partial anomalous pulmonary venous drainage, especially of the right upper pulmonary vein. Surgical repair has been the gold standard approach to close that defect. Introduced in 2014, percutaneous closure has gradually become a safe and effective alternative to surgery in carefully selected patients, although worldwide experience remains limited. This article provides an appraisal of the patients' selection process and a step-by-step description of the procedure as well as a comprehensive review of its outcomes. (J Am Coll Cardiol Intv 2023;16:2587-2599) © 2023 by the American College of Cardiology Foundation.

Surgical correction is the gold standard management strategy for patients with sinus venosus defect (SVD) with partial anomalous pulmonary venous drainage (PAPVD). Transcatheter closure, by placing a long and large covered stent in the superior vena cava (SVC) with its lower end flared in the right atrium, has emerged as a feasible alternative to surgery in selected patients. Initially described by Abdullah et al at the annual Congenital and Structural Interventions in Frankfurt in 2013,[1,2] this procedure is poised to revolutionize the therapeutic approach to SVD.

Understanding the anatomy of the crossroads formed by the right upper pulmonary vein (RUPV)

From the [a]Nantes Université, Centre Hospitalier Universitaire Nantes, Department of Pediatric Cardiology and Pediatric Cardiac Surgery, Nantes, France; [b]Nantes Université, Centre Hospitalier Universitaire Nantes, Centre National de la Recherche Scientifique, Institut National de la Santé et de la Recherche Scientifique, l'institut du thorax, Nantes, France; [c]Nantes Université, Centre Hospitalier Universitaire Nantes, Institut National de la Santé et de la Recherche Scientifique, Centre d'Investigations Cliniques Femmes-Enfants-Adolescents 1413, Nantes, France; [d]Nantes Université, Institut National de Recherche pour l'Agriculture, l'Alimentation et l'Environnement, Unité Mixte de Recherche 1280, Physiologie des Adaptations Nutritionnelles, Nantes, France; [e]Malformations Cardiaques Congénitales Complexes-Hôpital Marie Lannelongue, Department of Pediatric Cardiology and Congenital Heart Disease, Groupe Hospitalier Paris Saint Joseph, BME Lab, Institut National de la Santé et de la Recherche Scientifique UMR-S 999, Université Parsis Saclay, Le Plessis Robinson, France; [f]Malformations Cardiaques Congénitales Complexes-Necker, Department of Congenital and Pediatric Cardiology, Hôpital Necker-Enfants Malades, Assistance Publique Hôpitaux de Paris, Université de Paris, Paris, France; [g]Department of Pediatrics, Centre Hospitalier Universitaire Toulouse, Université de Toulouse, Toulouse, France; [h]Institut des Maladies Métaboliques et Cardiovasculaires, Université de Toulouse, Toulouse, France; [i]Clinique des Franciscaines, 3Dheartmodeling, Nîmes, France; [j]Department of Pediatric and Adult Congenital Cardiology, Centre Hospitalier Universitaire Bordeaux, Bordeaux, France; [k]Electrophysiology and Heart Modeling Institute, Institut Hospital-Universitaire Liryc, Fondation Bordeaux Université, Bordeaux, France; [l]National Heart and Lung Institute, Imperial College London, Royal Brompton and Harefield Hospitals, London, United Kingdom; and the [m]Sidra Heart Center, Sidra Medicine, Weil Cornell Medical College, Doha, Qatar.

The authors attest they are in compliance with human studies committees and animal welfare regulations of the authors' institutions and Food and Drug Administration guidelines, including patient consent where appropriate. For more information, visit the Author Center.

Manuscript received February 21, 2023; revised manuscript received July 12, 2023, accepted July 18, 2023.

ISSN 1936-8798/$36.00 https://doi.org/10.1016/j.jcin.2023.07.024

JACC: CARDIOVASCULAR INTERVENTIONS VOL. 16, NO. 21, 2023
NOVEMBER 13, 2023:2587–2599

ABBREVIATIONS AND ACRONYMS

3D = 3-dimensional
ASD = atrial septal defect
CHD = congenital heart disease
CP = Cheatham-platinum
CT = computed tomography
LA = left atrium
PAPVD = partial anomalous pulmonary venous drainage
RA = right atrium
RIJV = right internal jugular vein
RUPV = right upper pulmonary vein
SVC = superior vena cava
SVD = sinus venosus defect
TEE = transesophageal echocardiography

ostium, the SVC orifice, the right atrium (RA), and the left atrium (LA) above the level of the unroofed atrial septum is key to appreciating the procedural concept. This article provides a comprehensive, up-to-date description of percutaneous management of SVD, detailing preprocedural screening, multimodality imaging for case planning and guidance, and procedural steps. It also summarizes a comprehensive overview of the contemporary clinical outcomes of the transcatheter SVD closure.

SUPERIOR SVD

DEFINITION: EPIDEMIOLOGY. An atrial septal defect (ASD) represents a direct communication between atrial chambers allowing shunting of blood between the systemic and pulmonary circulation. It is the second most common type of congenital heart disease (CHD) with an estimated prevalence of 1.4 per 1,000 individuals, accounting for 15.4% of CHD,[3] and the most common type of CHD diagnosed in adulthood, accounting for 25% to 30% of new diagnoses.[4] ASDs include several distinct defects in the cardiac termination of systemic and pulmonary veins (ie, sinus venosus and coronary sinus ASDs) and the interatrial septum (ie, primum ASDs and secundum ASDs). SVDs account for 5% of ASDs, and almost 90% of these are superior SVDs,[5] which are the most common interatrial communication outside the oval fossa.[6]

SUPERIOR SVD ANATOMY. The defect is located immediately inferior to the junction of the SVC and the RA (Figure 1). It is characterized by anomalous connection of 1 or more of the right-sided pulmonary veins.[7] It results from deficient infolding of the atrial wall that forms the posterior wall of the SVC and the anterior wall of the RUPV. The RUPV is no longer committed to the LA and drains into the RA at the mouth of the SVC.[8] In a series of 96 SVD patients, all patients had anomalous connection of the RUPV, whereas 92% and 18% also had anomalous connection of the right middle pulmonary vein and the right inferior pulmonary vein, respectively.[6] In a minority of patients, the defect showed significant caudal extension, having a superoinferior dimension >25 mm. Anomalous connection of the right inferior pulmonary vein was more common in those with significant caudal extension of the defect. The SVC over-rode the interatrial septum in 70% patients.[6]

HIGHLIGHTS

- Surgical repair is the standard of care for superior sinus venosus defect with partial anomalous pulmonary venous drainage. However, transcatheter closure is emerging as a safe and effective alternative in carefully selected patients.
- Knowledge of the anatomy of crossroads formed by the right upper pulmonary vein, superior vena cava, right atrium, and left atrium is key to appreciating the procedural concept.
- Optimal patient selection requires the integration of multimodality imaging, 3D modeling, and balloon interrogation of the superior vena cava.
- Modified techniques along with growing experience of interventionalists will further enhance safety and expand the role of transcatheter closure of SVD.

PATHOPHYSIOLOGY. SVD typically results in a left-to-right shunt. The direction and magnitude of blood flow through the defect are determined by the size of the defect and the compliances of both ventricles. Larger, long-standing defects result in an increased pulmonary:systemic flow ratio over 1.5, volume overload, and later pressure overload of the right heart, leading to right atrial and right ventricular dilatation with diastolic septal shift toward the left ventricle resulting in decreased left ventricular compliance.[5] This results in decreased left ventricular diastolic filling, increased pulmonary:systemic flow ratio through the atrial defect, and diminished systemic output. Superior SVD is commonly hemodynamically significant because it results from the conjunction of PAPVD and a usually large defect.[6] Both contribute to right ventricular enlargement because of volume overload.

INDICATIONS FOR CLOSURE. Indications for ASD closure should be discussed in a CHD multidisciplinary team according to guidelines.[9,10] In case of SVD, the indications for treatment include right heart volume overload with right-sided enlargement and a pulmonary:systemic blood flow ratio >1.5:1 by cardiac magnetic resonance or cardiac catheterization. Most SVD patients meet these criteria given the magnitude of shunts associated with that CHD. Other indications such as paradoxical embolism or brain

FIGURE 1 Superior SVD Anatomy

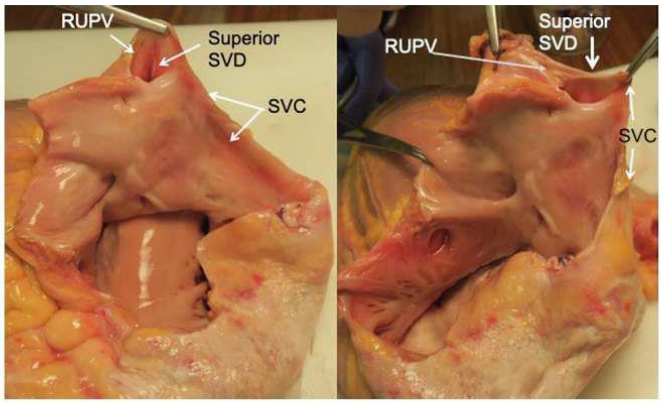

The defect is characterized by anomalous connection of the right upper pulmonary vein (RUPV), which drains into the right atrium at the mouth of the superior vena cava (SVC). SVD = sinus venosus defect. Courtesy of Lucile Houyel, M3C anatomic collection.

abscess may be considered on a case-by-case basis. Complete closure is contraindicated in irreversible pulmonary hypertension.

SURGICAL REPAIR. Surgical repair of SVD with PAPVD achieved excellent results when performed by experienced CHD surgeons with low operative mortality (<1%).[11-13] However, it carries the general morbidity of sternotomy and cardiopulmonary bypass and other major complications such as sinus node dysfunction requiring pacemaker implantation, pulmonary venous obstruction/occlusion, and SVC obstruction. A single-patch, double-patch, or the Warden technique (caval division technique) are performed. The double-patch technique uses 1 patch to close the ASD and another patch to enlarge the SVC at

FIGURE 2 The Warden Procedure

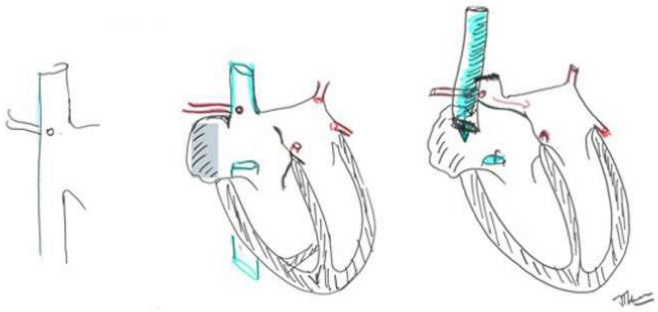

The superior vena cava (SVC) is divided above the anomalous pulmonary veins and anastomosed to the right atrial appendage. The residual SVC, now receiving only pulmonary venous blood, is baffled to the left atrium through the sinus venosus defect and in the process separates the atria.

CENTRAL ILLUSTRATION **Transcatheter Closure of Superior Sinus Venosus Defect With Partial Anomalous Pulmonary Venous Return**

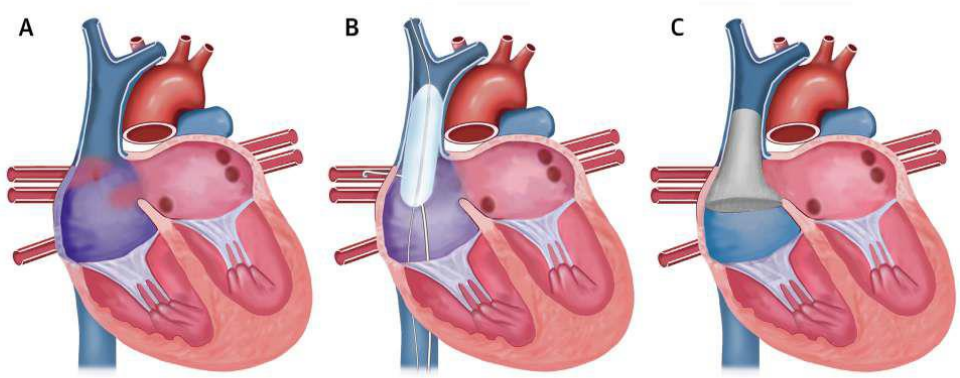

Baruteau A-E, et al. J Am Coll Cardiol Intv. 2023;16(21):2587-2599.

Transcatheter closure of a superior sinus venosus defect with partial anomalous pulmonary venous return has become a safe and efficient alternative to open heart surgery in carefully selected patients, although worldwide experience remains limited. (A) The procedural concept is based on the crossroad formed by the abnormally connected right pulmonary veins, the superior vena cava, the right atrium, and the left atrium above the level of the unroofed atrial septum. (B) Careful patient selection, especially balloon interrogation of the superior vena cava along with continuous monitoring of the right upper pulmonary vein pressure, is key. (C) The transcatheter approach consists in placing a long covered stent in the superior vena cava-right atrium junction to close the defect, diverting the superior vena cava flow to the right atrium and redirecting the right upper pulmonary vein flow around the stent into the left atrium.

the cavoatrial junction. The RA incision often extends onto the SVC so that the sinus node is at risk for iatrogenic dysfunction.[14] In the Warden technique (Figure 2), the SVC is divided above the anomalous pulmonary veins and anastomosed to the right atrial appendage. The residual SVC now receiving only pulmonary venous blood is baffled to the LA through the SVD and in the process separates the atria.[15] High connection of anomalous pulmonary veins to the SVC may warrant modification of the classic Warden operation in the form of an interpositional graft that can also thrombose. Unlike patch procedures, the Warden procedure avoids a cavoatrial incision and the risk of sinus node damage; however, SVC obstruction has been described.[16,17] A 2% to 8.6% rate of sinus node dysfunction and a 2.7% to 7.7% rate of pulmonary vein or SVC obstruction have been reported in a meta-analysis of over 900 patients.[18] However, individual series show higher complication rates, including a 35% incidence of sinus node dysfunction,[13] a 14% incidence of postoperative atrial fibrillation,[11] a 20% incidence of SVC narrowing or obstruction, and a 22.5% incidence of RUPV obstruction.[12]

TRANSCATHETER CLOSURE OF SVD WITH PAPVD

PROCEDURAL CONCEPT. Transcatheter closure of SVD consists in placing a long, covered stent in the SVC-RA junction to close the defect, divert the SVC flow to the RA, and redirect the RUPV flow around the stent into the LA (Central Illustration). This is facilitated by a detailed multifaceted preprocedural planning approach that includes balloon interrogation of the SVC,[19] patient-specific 3-dimensional (3D)-printed models with mock implantation of stents,[20,21] 3D modeling and virtual simulation,[22] 3D fusion imaging guidance,[23] and even holographic augmented reality.[24]

INDICATION FOR CLOSURE AND PATIENT SELECTION. Patients are carefully evaluated by a multidisciplinary CHD team. The main indication for closure is right heart volume overload regardless of symptoms.[9,10] Other indications such as paradoxical emboli may be considered on a case-by-case basis.[21] In centers with transcatheter SVD closure capabilities, patients

TABLE 1 Contraindications to Transcatheter SVD Correction

Absolute contraindications
Right pulmonary vein obstruction during balloon interrogation of the SVC in a patient in whom pulmonary vein balloon protection is expected to fail
Age <16 y, unless right SVC can accommodate at stent diameter of 16-18 mm
Relative contraindications
Patient with SVD and another indication for cardiac surgery
Large, hemodynamically significant "upper" RUPV considered suitable for surgical repair
Large interatrial defect with significant caudal extension
Anterior positioning of the abnormally connected right pulmonary veins
Short distance between the upper end of the RUPV and the bridging innominate vein

RUPV = right upper pulmonary vein; SVC = superior vena cava; SVD = sinus venosus defect.

referred for SVD intervention are usually systematically assessed for surgical correction or transcatheter closure.[2,25] Although this is an evolving field, current contraindications to the transcatheter approach are summarized in Table 1.

PREPROCEDURAL MULTIMODALITY IMAGING EVALUATION. All patients are initially assessed by transthoracic echocardiography and/or transesophageal echocardiography (TEE) to assess right ventricular dimension and function, defect position and size, pulmonary venous drainage, tricuspid regurgitation, and estimation of right ventricular systolic pressure.

Cross-sectional imaging aims at confirming the diagnosis and assessing the anatomy of the defect and surrounding structures. Electrocardiogram-gated multidetector cardiac computed tomography (CT) is key for assessing anatomical landmarks and accurate delineation of the defect size and shape; its relationship with abnormally connected pulmonary veins; their number; the diameter and height of the opening into the SVC; the existence of a pulmonary venous return collector; the existence of an "upper" RUPV; the orientation and heights of the abnormal drainage in the SVC; and the SVC size, length, and morphology.[22] Smaller RUPV branches draining into the SVC remote from the SVC-RA junction and usually higher than the main RUPV are not considered a contraindication for transcatheter closure, especially if the distance is thought to be too far for the pulmonary veins to be surgically addressed or if the vein size and cardiac magnetic resonance calculation of its flow volume are deemed to be hemodynamically insignificant.[2,26] On the contrary, when the "upper" RUPV is large, deemed to carry a significant portion of pulmonary blood flow or considered suitable for surgical repair, the Warden procedure is preferred.[26] Interruption of the inferior vena cava with azygos continuation should be ruled out. A left arm contrast injection is recommended to identify a left SVC and to analyze the anatomy of the innominate vein. Patients with a left SVC are usually good candidates for transcatheter SVD closure because the right SVC is smaller and often amenable to stent implantation. In addition, in case of the absence of a bridging innominate vein, transcatheter SVD closure may also be easier because of a longer landing zone, allowing for a better stent anchoring because of a higher implantation of the covered stent in the SVC.

Cardiac magnetic resonance is not routinely performed for case planning because of its lower spatial resolution than that of CT imaging. However, it has the advantage of allowing for hemodynamic study using 4-dimensional flow analysis, enabling assessment of the left-to-right shunt and its consequences (right chamber dilatation and pulmonary blood overflow); it is also useful to assess the left-to-right shunt induced by the ASD on one side and the abnormal pulmonary venous return on the other side.[22] Hence, it could be considered as a complementary imaging modality in selected cases.

PRINTED AND VIRTUAL 3D MODEL SIMULATION. 3D printing. Despite optimal preprocedural planning, the complex anatomical features of SVD and their variable morphology may result in procedural complications and failure. Three-dimensional printing technology can aid in minimizing these risks (Figures 3 and 4). This technique transforms medical images into a physical model using dedicated post-processing software. It replicates the anatomical, tissular, and biomechanical features of the studied structure. It can also be connected to a perfused system allowing hands-on simulation testing, which facilitates physician training and technique optimization in SVD closure and other transcatheter interventions for CHDs.[27]

Virtual 3D simulation. Using a similar post-processing protocol, CT scan data may also be converted to a 3D stereo lithography model that can be used for virtual simulation of the procedure. 3D volume rendering images of SVD allows a realistic assessment of the defect anatomical configuration, especially when creating a virtual tunnel from the anomalous pulmonary venous return to the LA. The 3D CT scan data set can also be merged with fluoroscopy to enhance procedural guidance. To obtain all

JACC: CARDIOVASCULAR INTERVENTIONS VOL. 16, NO. 21, 2023
NOVEMBER 13, 2023:2587–2599

FIGURE 3 Preprocedural Planning Using Virtual 3D Model Simulation

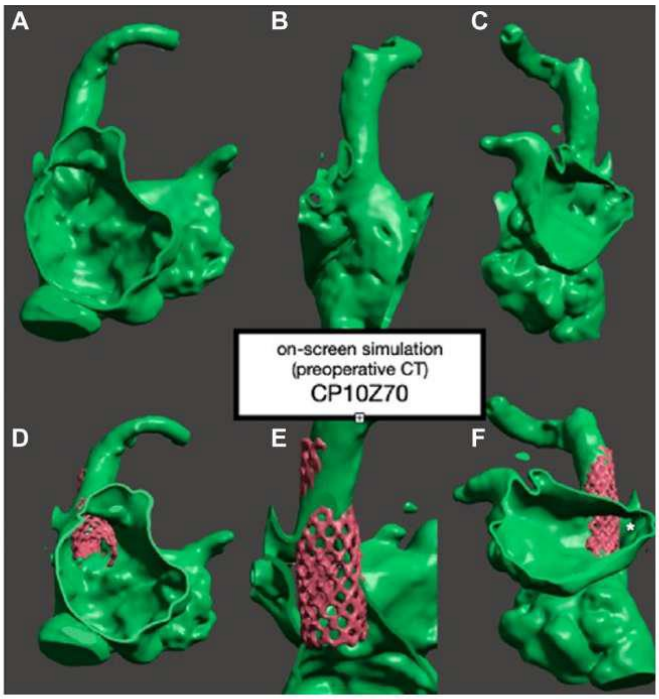

(A to C) Three-dimensional (3D) virtual modeling of the defect. (D to F) Virtual simulation of the implantation of a 7-cm 10-zig covered Cheatham-platinum (CP) stent (in red) showing effective closure of the sinus venosus defect with right upper pulmonary vein patency (white asterisk). CT = computed tomography.

needed information for procedural planning, the following specific CT acquisition techniques should be implemented: 1) the box of acquisition should cover all the thorax including the heart, the SVC, and the innominate vein; 2) submillimeter slices should be performed in order to increase spatial resolution; and 3) delay of acquisition should be targeted to have both opacifications of systemic venous return and pulmonary venous return.[22]

CATHETER-BASED SVD CORRECTION. Procedures are performed under general anesthesia with TEE and fluoroscopic guidance (**Figure 5**, Video 1). Vascular access is usually obtained in the right internal jugular vein (RIJV), the left and right femoral veins, and the left femoral artery. Transcatheter SVD closure via transhepatic access has also been reported and could be considered if central venous occlusions are present.[28] Antibiotic prophylaxis is recommended, and intravenous heparin is administered to maintain an activated clotting time >250 seconds. Real-time image fusion between echocardiography and biplane fluoroscopy can be used if available. In addition, 3D reconstruction converted from a CT scan can be aligned with fluoroscopy. RUPV pressure must be monitored throughout the procedure. A transseptal puncture may be performed using a Brockenbrough transseptal needle (St. Jude Medical) in an 8-F sheath to place a 5-F pigtail angiographic catheter in the RUPV; this allows for both serial venography and simultaneous LA and RUPV pressure monitoring via the sheath and the pigtail catheter, respectively.[2] The RUPV may also be accessed through the interatrial communication, which avoids the risk of transseptal

FIGURE 4 Preprocedural Planning Using Mock 3D Model Simulation

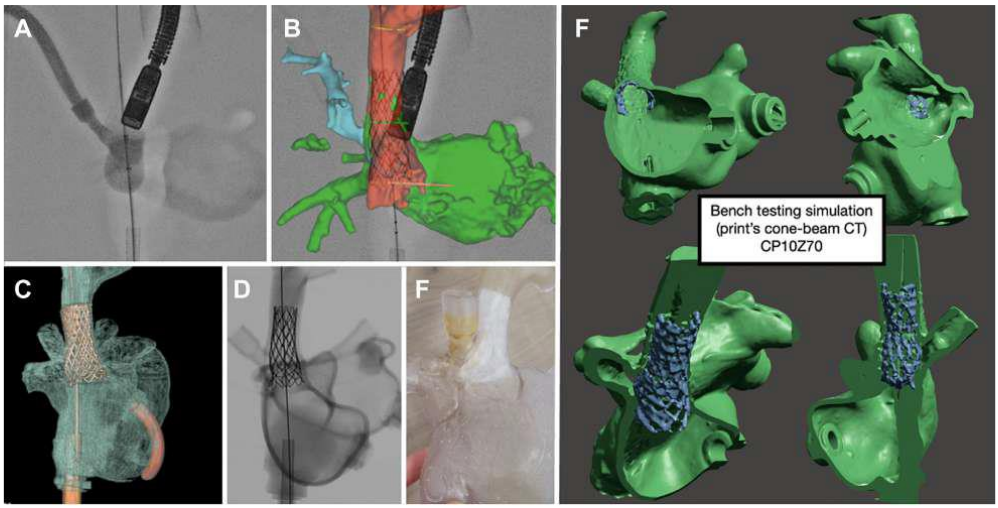

In vitro simulation with bench testing of the procedure using a 3D-printed model (same patient as in Figure 2). The model was connected to a perfused system allowing hands-on simulation testing. (A) Balloon interrogation. (B, C, and F) 3D CT fusion/reconstruction. (D) X-ray fluoroscopic images. (E) 3D model macroscopic aspect following 7-cm 10-zig covered CP stent deployment. Abbreviations as in Figure 3.

puncture. A venovenous guidewire circuit using an 0.035-inch Amplatz Extra Stiff wire (Cook Medical) is established from the right femoral vein to the RIJV.

Balloon interrogation of the SVC is performed using a large, compliant balloon inflated in the anticipated stent landing zone until TEE confirms abolition of the shunt. A 24- or 34-mm Amplatzer sizing balloon (St. Jude Medical); a 16- to 30-mm large, 6-cm long AltoSa-XL PTA balloon (AndraTec GmbH); or a PTS-X balloon (NuMED) are usually used, choosing at least a 2- to 4-mm larger balloon than the SVC diameter on cross-sectional imaging. During balloon inflation, SVC flow occlusion is confirmed by an SVC angiogram through the RIJV, whereas RUPV patency is checked using color Doppler interrogation by TEE, RUPV venography from the pigtail catheter, and simultaneous RUPV and LA pressure measurements. An SVC balloon interrogation test is an essential step to confirm procedural suitability. An aliasing on the color Doppler, a gradient increase on continuous Doppler of RUPV, or an increase in pulmonary venous pressures during balloon interrogation reflect a high risk of potential obstruction of RUPV flow while implanting the stent. There is no agreed-on cutoff value, but an RUPV/LA gradient up to 3 mm Hg is generally accepted. In case of a greater obstruction during SVC ballooning, the operator may choose to either abort the procedure or proceed to stent implantation using pulmonary venous protection by placing a "protective" balloon in the pulmonary vein during implantation of the SVC stent. The aim of this technique is to prevent excessive stent bulging into the pulmonary vein.

After SVC balloon interrogation, a long, covered stent is implanted in the SVC-RA junction to close the defect and redirect the RUPV flow into the LA. The azygous vein is usually occluded by the covered stent implantation without clinical consequences. Covered stent implantation is the cornerstone of the procedure. Unlike stenting in other CHD interventions, stent implantation in the setting of SVD is more complex because of the following inherent features of the defect: 1) the upper part of the stent needs to be deployed in the SVC, which is distensible, without a targeted stenotic landing zone to anchor the device; and 2) the caudal part of the stent needs to be flared up to 3 times the stent diameter in the SVC in order to occlude the defect and redirect the pulmonary venous flow, leading to an often unpredictable degree of stent. Hence, the ideal stent

FIGURE 5 Transcatheter Sinus Venosus Defect correction

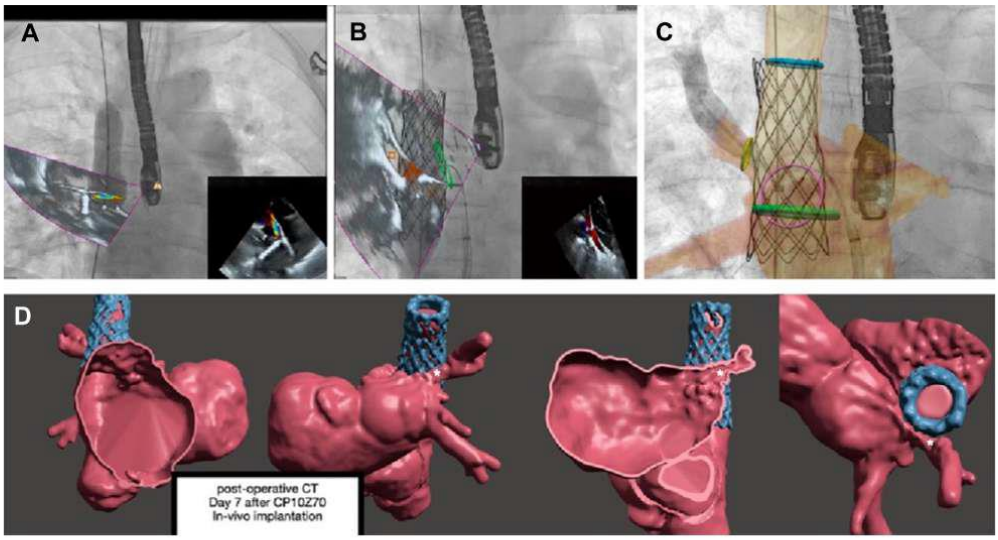

In vivo implantation of a 7-cm 10-zig covered CP stent (same patient as in Figures 2 and 3). (A to C) Multimodal fusion imaging guidance (A and B, transesophageal echocardiography fusion and C, computed tomography fusion) showing right upper pulmonary vein (RUPV) patency during (A) balloon interrogation and (B and C) after stent deployment. (D) 3D reconstruction of CT scan at postoperative day 7 showing good stent positioning (blue) and RUPV patency (white asterisk). Abbreviations as in Figure 3.

for transcatheter SVD correction must be long enough (up to 11 cm) and expandable to large diameters (up to 35 mm) without tearing the covering and with acceptable foreshortening. Based on these requirement specifications, 2 balloon-expandable stents are most used in transcatheter SVD correction: the 10-zig covered Cheatham-platinum (CP) stent (NuMED Inc) and the Optimus XXL covered stent (AndraTec GmbH). The main characteristics of these stents are summarized in Table 2. The 10-zig covered CP stent is available in lengths of 5.0, 5.5, and 6.0 cm, which are suitable for use in percutaneous SVD correction.[29] The stent was initially available in customizable versions up to 110 mm in length and up to a 34-mm diameter. However, only 50- and 60-mm stents subsequently received the Conformité Européene mark and Food and Drug Administration approval, and the longer versions are currently unavailable in many countries even though most SVD cases require stents longer than 60 mm.[29] The Optimus XXL covered stent has been widely used in various indications in patients with CHD, such as prestenting for percutaneous pulmonary valve implantation and aortic coarctation.[30] A covered 99-mm-long Optimus stent has been developed specifically for SVD correction. Other customizable stent lengths are in development. The stent is mounted on a Gemini Balloon (AndraTec GmbH),

TABLE 2 Characteristics of the 2 Mostly Used Stents for Transcatheter SVD Closure

	10-Zig Covered Cheatham-Platinum Stent[a]	Optimus XXL Covered Stent[b]
Stent type	Balloon-expandable, nonpremounted stent	Balloon-expandable, nonpremounted stent
Stent design	10-zig pattern	15-zig pattern, hybrid cell design
Material	Platinum-iridium/PTFE	Cobalt-chromium/PTFE
Covering	PTFE covering (glued to the struts at each end)	End-free sandwich PTFE covering (thermally bonded to all the struts of the stent)
Balloon	BIB balloon[a]	Gemini balloon[b]
Sheath	16-F to 20-F	14-F
Expansion range	26-30 mm	22-28 mm
Length (licensed for use in SVD closure)	50, 55, 60 mm	48, 57, 99 mm
Percentage shortening at 28-mm diameter	28	21

[a]NuMED Inc. [b]AndraTec GmbH.
BIB = balloon-in-balloon; PTFE = polytetrafluoroethylene; SVD = sinus venosus defect.

TABLE 3 Procedural Characteristics in Large Single-Center or Multicenter Series of Transcatheter Closure of Sinus Venosus Defect

First Author, Year	Number of Center(s)	N	Age, (y)	Stent Used	Additional Stent	PV Balloon Protection	Additional Procedure	Success Rate
Hansen et al, 2020[2]	1	25	45 (33-54)	10-zig covered CP stent	13 (54.2)	4 (16.0)	PFO closure (n = 1)	25 (100)
Sivakumar et al, 2020[32]	1	24	30 (6-56)	Various stent types, including covered CP, covered Optimus, and AndraStent XXL	9 (37.5)	4 (16.7)	PFO closure (n = 1)	24 (100)
Rosenthal et al, 2021[29]	12	75	45 (11-76)	10-zig covered CP stent	32 (42.7)	17 (22.7)	PFO or secundum ASD closure (n = 2) Pacemaker leads through the stent (n = 2 with pre-existing pacemaker indication)	75 (100)
Hejazi et al, 2022[33]	1	14	35.5 (5.8-54)	8- or 10-zig covered CP stent	7 (50.0)	Unknown	None	14 (100)

Values are median (minimum-maximum) or n (%) unless otherwise indicated.
ASD = atrial septal defect; CP = Cheatham-platinum; PFO = patent foramen ovale; PV = pulmonary vein.

which has a design and features similar to the balloon-in-balloon catheter.

The usual method of stent deployment with a balloon-expandable stent is to manually crimp the covered stent on a long and large balloon with an outer diameter at the expected diameter of the stent on the SVC. To prevent stent migration, the diameter of the stent is oversized by 2 to 4 mm with respect to the SVC. A length of positioning in the SVC above the abnormally connected pulmonary vein of at least 2 cm is expected to provide sufficient stent stability. The stent is advanced from the right femoral vein through a large sheath. The stent is deployed in 2 steps using the balloon-in-balloon inflation process. The stability of the stent is assessed. Postdilation can be performed at the upper part to further stabilize the stent. In case of stent instability, a second bare-metal stent can be implanted to anchor the covered stent. Then, after assessing the free flow of the pulmonary vein to the left atrium, postdilation of the lower part of the stent is performed with a larger balloon until any residual shunting is noted on TEE. Patients receive aspirin for 6 months, with some operators using concomitant clopidogrel for 2 months.[2] Clinical evaluation, a 12-lead electrocardiogram, and transthoracic echocardiography are performed at 3, 6, and 12 months after the procedure. A CT scan should be performed at 2 to 3 months to assess the stent position and confirm unobstructed pulmonary venous drainage. A cardiac magnetic resonance scan could be performed at 1 year to assess right heart remodeling and to investigate potential residual shunting.[26] Subsequently, annual clinical follow-up is recommended.

RESULTS AND COMPLICATIONS

Background. Abdullah et al[1] first reported on their experience in 2013 and later published a case series of 4 patients aged 7 to 23 years old whose SVD was successfully closed using a covered CP stent. Garg et al[19] described successful closure of SVD in a 35-year-old patient using a 12 mm × 61 mm Advanta V12 covered stent (Getinge) in the SVC. Crystal et al[31] used 3 telescoping self-expanding stent grafts in a 23-year-old woman. Thakkar et al[23] illustrated the utility of comprehensive preprocedural planning and simulation in facilitating the transcatheter closure of SVD using a self-expanding stent graft. The approach was subsequently modified by the CHD group at St Thomas' Hospital who described a reproducible and effective method for the evaluation and transcatheter closure of SVD with PAPVD. At their program, all patients 16 years of age and older referred with SVD and PAPVD are evaluated for both surgical and transcatheter closure.[2,20,21,26]

Worldwide experience. Since the first description of percutaneous SVD correction, several case series have been published in the literature.[2,29,32,33] These reports are summarized in **Tables 3 and 4** and Supplemental Table 1. These procedures mainly used a covered CP stent, but the use of other balloon-expandable stents (ie, covered Advanta V12,[19] AndraStent [AndraMed GmbH],[32] Optimus-CVS [AndraTec],[32,34,35] BeGraft [Bentley InnoMed],[36,37] and long G-ARMOR [Numed Inc][38]) and self-expandable stents has been reported.[23,31,39] Small residual flow may disappear over time as the enlarged RA remodels to a smaller size that allows the caudal edge of the SVD to come up to the covered stent.[40]

TABLE 4 Outcomes in a Large Single-Center or Multicenter Series of Transcatheter Closure of Sinus Venosus Defect

		Procedural Complications				Follow-Up		
First Author, Year	N	Major Complications	Stent Migration	PV Obstruction	Other Life-Threatening Complication(s)	Follow-Up Duration (mo)	> Trivial Residual Shunt	Late Reintervention or Late Complication
Hansen, 2020[2]	25	2 (8.0)	1 (4.0)[a]	0 (0)	1 (4.0) Tamponade[a]	16.8 (9.6-20.4)	1 (4.0)	None described
Sivakumar, 2020[32]	24	4 (16.7)	3 (12.5)[a,b]	0 (0)	1 (4.2) Left innominate vein occlusion[b]	20 (3-54)	0 (0)	None described
Rosenthal et al, 2021[29]	75	4 (5.3)	2 (2.7)[a]	1 (1.3)[a]	1 (1.3) Tamponade[a]	21.6 (2-61.2)	5 (7)	None described
Hejazi et al, 2022[33]	14	0 (0)	0 (0)	0 (0)	0 (0)	16.5 (0.5-31.5)	0 (0)	None described

Values are n (%) or median (minimum-maximum) unless otherwise indicated. Major complications defined as stent migration, PV obstruction, and/or other life-threatening complication. [a]Transcatheter management. [b]Surgical management.
PV = pulmonary vein.

Significant residual shunting at the caudal end of the SVC stent necessitated the consideration of implanting an additional, overlapping covered stent. Occasionally, shunt closure was achieved with implanting an atrial septal occluder.[1] Compared to classic surgical complications, sinus node dysfunction has not been reported. Longer follow-up is warranted to ensure durable patency of the covered SVC stents. The reported rate of major procedural complication varies between 0% and 4% in large single-center or multicenter series[2,29,32,33] but that has declined with the growing experience and enhanced safety.

Stent instability or migration. The stent stability is determined by the length of the stent deployed within the SVC. Firm apposition of an adequate length of stent is required to prevent stent instability or migration, especially when flaring the bottom end to achieve complete closure. Stent instability is associated with a shorter segment apposed to the SVC, which is defined as the distance between the cranial stent end to the beginning of the flared segment.[2] When stent apposition is short and felt to be insufficient to provide secure anchoring, an additional overlapping bare-metal stent is deployed in the upper segment of the SVC below the innominate vein to overlap the cranial portion of the covered stent.[2,26] The longer the initial stent is, the less likelihood of needing an additional anchoring stent. In earlier reports, several telescoping stents were used to correct the defect.[19,21,31] In some patients, a landing zone bare-metal stent was placed in the SVC followed by the 10-zig covered CP stent, and then the top end was sandwiched with a third bare-metal stent.[29] Because longer stents have been made available, a second stent is less likely to be required. In an international series of 75 patients treated with the 10-zig covered CP stent, the requirement for additional stents decreased from 62% of the 29 patients who had a 6.0-cm 10-zig covered CP stent to 23% of the 22 patients who received a 7.5- to 8.0-cm 10-zig covered CP stent; the unique patient who had an initial 11.0-cm 10-zig covered CP stent did not require a second stent.[29] In a preliminary experience with the use of the 100-mm 15-zig covered Optimus-CVS XXL stent, 3 of 6 patients required an additional bare-metal anchoring stent, including 1 case of stent stabilization after its migration to the right atrium.[35]

Technical modifications have been proposed to address potential migration of the stent. Suture connection of interdigitating covered CP stents has been reported in a 38-year-old man with SVD with PAPVC and persistent left-sided SVC to the coronary sinus. A 6-cm 10-zig covered CP stent and a 5-cm 10-zig covered CP stent were overlapped and secured together by a 0-silk suture.[41] Stent migration toward the RA has been reported, either during flaring of the caudal portion of the stent or shortly after the procedure, before discharge. Periprocedural migration can be stabilized by deployment of an anchoring stent from the jugular vein that holds and fixes the caudally embolized stent,[35] whereas early postprocedural embolization may require surgical removal and simultaneous repair of the defect.[26,29] Hejazi et al[33] reported the temporary suture-holding technique in 14 patients allowing for precise stent placement by a surgical suture that is looped around the strut of the stent; the stent-balloon assembly is then advanced from the RIJV to the RA by pushing on the stent and pulling the balloon from the RFV into the RIJV sheath (**Figure 6**). A small vascular balloon is inflated to partially expand the stent in the SVC, and the stent position can be readjusted to have enough stent

FIGURE 6 Ex Vivo Images Describing Temporary Suture-Holding Technique

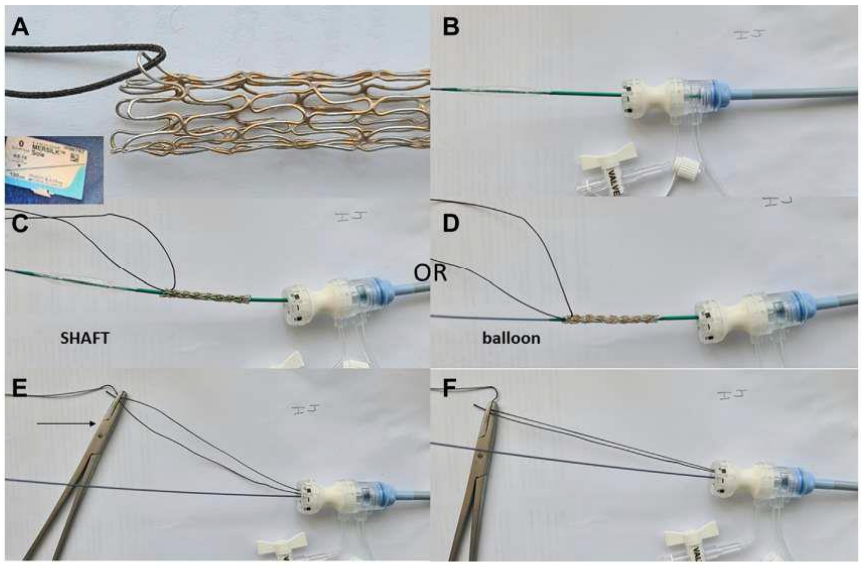

(A) A surgical suture (MERSILK KS-75 [Ethicon], straight needle, 100-cm long, size 0) was inserted through 1 of the superior vena cava stent struts. For better understanding, a noncovered stent is depicted. Of note, the suture is just sliding/looping around the strut of the stent. There is no knot. (B) A picture demonstrating a vascular balloon (12 mm × 6 cm, Mustang [Boston Scientific]) inserted retrogradely over the wire rail and exteriorized through the right internal jugular vein (RIJV) sheath. (C and D) The chosen stent held by the suture is crimped over the (C) balloon or (D) its shaft. (E and F) The stent-balloon assembly is advanced from the RIJV to the right atrium by pushing on the stent and pulling the balloon from the right femoral vein into the RIJV Dryseal (GORE). The 2 extremities of the suture are held by a needle holder.

length in the SVC for good anchoring along with its caudal end below the inferior rim of the SVD. The small balloon is then removed while holding the stent in position with the suture and replaced by a larger balloon equal to the SVC diameter.[33] To our knowledge, very late stent migration has not been reported.

Pulmonary vein stenosis/occlusion. RUPV occlusion is uncommon because the pulmonary venous flow is pretested during balloon interrogation of the SVC. Such an occurrence can be resolved by inflation of a noncompliant balloon in the RUPV and reverse remodeling of the SVC stent. However, in 1 patient of the international series, the protective balloon in the RUPV deflated during SVC stent deployment, leading to RUPV compression by the stent. Deployment of an additional stent to seal the lower end of the defect further compressed the vein with a significant reduction in RUPV flow at the end of the procedure. The patient was treated with a video-assisted upper lobectomy 5 months later because of hemoptysis associated with RUPV occlusion.[29]

FUTURE DIRECTIONS

A decade after the first reported cases of transcatheter SVD closure, the procedure remains a purview of a few specialized centers worldwide.[29] However, the closure technique has evolved, and >80% of superior SVDs are amenable to percutaneous closure in contemporary practice.[25] A growing number of series reported high technical success and low complication rates, suggesting that the technique can be scaled to the wider community of CHD interventionalists. Open questions remain about the long-term durability and the possibility of late complications, the minimal acceptable age and/or weight to safely perform the procedure, and the feasibility of serial dilation of the

TABLE 5 Future Directions

Main unmet needs
Development of dedicated materials
Development of modified safety techniques
Growing experience of interventionists engaged in such programs
Classification of anatomical variations in SVD to guide transcatheter feasibility and procedural planning
Main unanswered questions
What is the right place of transcatheter SVD closure vs surgery?
What is the long-term outcome of transcatheter SVD closure?
What is the extent of cardiac remodeling after transcatheter SVD closure?
Is there a minimal age or weight to safely proceed with transcatheter closure?
Cost analysis of transcatheter vs surgical closure of SVD

SVD = sinus venosus defect.

SVC stent to match pediatric patients' growth until adulthood. Table 5 summarizes the main unmet needs and unanswered questions regarding percutaneous SVD closure.

CONCLUSIONS

Transcatheter closure of SVD with PAPVD has emerged as a feasible alternative to surgery in carefully selected patients. Careful patient selection based on advanced multimodality imaging is paramount to maximize the success rate and the safety of the procedure. Modified safety techniques have been proposed to further streamline the procedure and avoid complications. Although early and medium-term results are promising, longer follow-up studies are warranted to determine the role of this innovative procedure in the routine management of patients with SVD.

ACKNOWLEDGMENTS The authors thank GCS HUGO, AVIESAN, and FHU PRECICARE.

FUNDING SUPPORT AND AUTHOR DISCLOSURES

This work was supported by the French Federation of Cardiology (to Dr Hascoet) and the French Society of Cardiology (to Dr Batteux). Dr Baruteau is supported by the French Government as part of the "Investments of the future" program managed by the National Research Agency (grant reference ANR-16-IDEX-0007). All other authors have reported that they have no relationships relevant to the contents of this paper to disclose.

ADDRESS FOR CORRESPONDENCE: Dr Alban-Elouen Baruteau, Département Médico-chirurgical de Cardiologie Pédiatrique et Congénitale, Centre Hospitalier Universitaire de Nantes, 7 Quai Moncousu, 44093 Nantes Cedex 01, France. E-mail: albanelouen.baruteau@chu-nantes.fr.

REFERENCES

1. Abdullah HAM, Alsalkhi HA, Khalid KA. Transcatheter closure of sinus venosus defect with anomalous pulmonary venous drainage: innovative technique with long-term follow-up. *Catheter Cardiovasc Interv*. 2020;95:743-747.

2. Hansen JH, Duong P, Jivanji SGM, et al. Transcatheter correction of superior sinus venosus defects as an alternative to surgical treatment. *J Am Coll Cardiol*. 2020;75:1266-1278.

3. Liu Y, Chen S, Zühlke L, et al. Global birth prevalence of congenital heart defects 1970-2017: updated systematic review and meta-analysis of 260 studies. *Int J Epidemiol*. 2019;48:455-463.

4. Brida M, Chessa M, Celermajer D, et al. Atrial septal defect in adulthood: a new paradigm for congenital heart disease. *Eur Heart J*. 2022;43:2660-2671.

5. Geva T, Martins JD, Wald RM. Atrial septal defects. *Lancet*. 2014;383(9932):1921-1932.

6. Relan J, Gupta SK, Rajagopal R, et al. Clarifying the anatomy of the superior sinus venosus defect. *Heart*. 2022;108:689-694.

7. Chowdhury UK, Anderson RH, Pandey NN, et al. A reappraisal of the sinus venosus defect. *Eur J Cardiothorac Surg*. 2022;61:1211-1222.

8. Naqvi N, McCarthy KP, Ho SY. Anatomy of the atrial septum and interatrial communications. *J Thorac Dis*. 2018;10(suppl 24):S2837-S2847.

9. Baumgartner H, De Backer J, Babu-Narayan SV, et al. 2020 ESC guidelines for the management of adult congenital heart disease. *Eur Heart J*. 2021;42:563-645.

10. Stout KK, Daniels CJ, Aboulhosn JA, et al. 2018 AHA/ACC Guideline for the Management of Adults With Congenital Heart Disease: a report of the American College of Cardiology/American Heart Association Task Force on Clinical Practice Guidelines. *J Am Coll Cardiol*. 2019;73:e81-e192.

11. Attenhofer Jost CH, Connolly HM, Danielson GK, et al. Sinus venosus defect: long-term postoperative outcome for 115 patients. *Circulation*. 2005;112:1953-1958.

12. Iyer AP, Somanrema K, Pathak S, Manjunath PY, Pradhan S, Krishnan S. Comparative study of single- and double-patch techniques for sinus venosus defect with partial anomalous pulmonary venous connection. *J Thorac Cardiovasc Surg*. 2007;133:656-659.

13. Stewart RD, Bailliard F, Kelle AM, Backer CL, Young L, Mavroudis C. Evolving surgical strategy for sinus venosus defect: effect on sinus node function and late venous obstruction. *Ann Thorac Surg*. 2007;84:1651-1655.

14. Ait-Ali L, Ravaglioli A, Festa P, et al. The different surgical impact of the superior cavoatrial incision in children and adults. *Cardiol Young*. 2021;31:751-755.

15. Liava'a M, Kalfa D. Surgical closure of atrial septal defects. *J Thorac Dis*. 2018;10:S2931-S2939.

16. Said SM, Burkhart HM, Dearani JA, et al. Outcome of caval division techniques for partial anomalous pulmonary venous connections to the superior vena cava. *Ann Thorac Surg*. 2011;92:980-984.

17. Lin H, Yan J, Wang Q, et al. Outcomes of the Warden procedure for partial anomalous pulmonary venous drainage. *Pediatr Cardiol*. 2020;41:134-140.

18. Okonta KE, Sanusi M. Superior sinus venosus defect: overview of surgical options. *Open J Thorac Surg*. 2013;3:114-122.

19. Garg G, Tyagi H, Radha AS. Transcatheter closure of sinus venosus defect with anomalous drainage of right upper pulmonary vein into superior vena cava-an innovative technique. *Catheter Cardiovasc Interv*. 2014;84:473-477.

20. Velasco Forte MN, Byrne N, Valverde I, et al. Interventional correction of sinus venosus defect and partial anomalous pulmonary venous drainage: procedural planning using 3D printed models. *J Am Coll Cardiol Img*. 2018;11:275-278.

21. Riahi M, Velasco Forte MN, Byrne N, et al. Early experience of transcatheter correction of superior sinus venosus defect with partial anomalous

pulmonary venous drainage. *EuroIntervention*. 2018;14:868-876.

22. Batteux C, Azarine A, Karsenty C, et al. Sinus venosus ASDs: imaging and percutaneous closure. *Curr Cardiol Rep*. 2021;23:138.

23. Thakkar AN, Chinnadurai P, Breinholt JP, Lin CH. Transcatheter closure of a sinus venosus defect using 3D printing and image fusion guidance. *Catheter Cardiovasc Interv*. 2018;92:353-357.

24. Butera G, Sturla F, Pluchinotta FR, Caimi A, Carminati M. Holographic augmented reality and 3D printing for advanced planning of sinus venosus ASD/partial anomalous pulmonary venous return percutaneous management. *J Am Coll Cardiol Intv*. 2019;12:1389-1391.

25. Brancato F, Stephenson N, Rosenthal E, et al. Transcatheter versus surgical treatment for isolated superior sinus venosus atrial septal defect. *Catheter Cardiovasc Interv*. 2023;101:1098-1107.

26. Baruteau AE, Jones MI, Butera G, Qureshi SA, Rosenthal E. Transcatheter correction of sinus venosus defect with partial anomalous pulmonary venous drainage: the procedure of choice in selected patients? *Arch Cardiovasc Dis*. 2020;113:92-95.

27. Batteux C, Meliani A, Brenot P, Hascoet S. Multimodality fusion imaging to guide percutaneous sinus venosus defect closure. *Eur Heart J*. 2020;41:4444-4445.

28. Alkhouli M, Campsey DM, Higgins L, Badhwar V, Diab A, Sengupta PP. Transcatheter closure of a sinus venosus defect via transhepatic access. *J Am Coll Cardiol Intv*. 2018;11:e113-e115.

29. Rosenthal E, Qureshi SA, Jones M, et al. Correction of sinus venosus defects with the 10 zig covered Cheatham-platinum stent - an international registry. *Catheter Cardiovasc Interv*. 2021;98:128-136.

30. Haddad RN, Hascoet S, Karsenty C, et al. Multicentre experience with Optimus balloon-expandable cobalt-chromium stents in congenital heart disease interventions. *Open Heart*. 2023;10:e002157.

31. Crystal MA, Vincent JA, Gray WA. The wedding cake solution: a percutaneous solution of a form fruste superior sinus venosus defect. *Catheter Cardiovasc Interv*. 2015;86:1204-1210.

32. Sivakumar K, Qureshi S, Pavithran S, Vaidyanathan S, Rajendran M. Simple diagnostic tools may guide transcatheter closure of superior sinus venosus defects without advanced imaging techniques. *Circ Cardiovasc Interv*. 2020;13:e009833.

33. Hejazi Y, Hijazi ZM, Saloos HA, Ibrahim H, Mann GS, Boudjemline Y. Novel technique for transcatheter closure of sinus venosus defect: the temporary suture-holding technique. *Catheter Cardiovasc Interv*. 2022;100:1068-1077.

34. Haddad RN, Bonnet D, Gewillig M, Malekzadeh-Milani S. Modified safety techniques for transcatheter repair of superior sinus venosus defects with partial anomalous pulmonary venous drainage using a 100-mm Optimus CVS covered XXL stent. *Catheter Cardiovasc Interv*. 2022;99:1558-1562.

35. Batteux C, Ciobotaru V, Bouvaist H, Kempny A, Fraisse A, Hascoet S. Multicenter experience of transcatheter correction of superior sinus venosus defect using the covered Optimus XXL stent. *Rev Esp Cardiol (Engl Ed)*. 2023;76(3):199-201.

36. Pascual-Tejerina V, Sánchez-Recalde Á, Cantador JR, López EC, Gómez-Ciriza G, Gutiérrez-Larraya F. Transcatheter repair of superior sinus venosus defect with partial anomalous pulmonary venous drainage with the chimney double stent technique. *Rev Esp Cardiol (Engl Ed)*. 2019;72:1088-1090.

37. Alizade E, Keskin B, Kılıçgedik A, Imanov E. Percutaneous closure of the superior sinus venosus defect associated with a partial pulmonary anomalous venous drainage. *Acta Cardiol*. 2022;25:1-4.

38. Morgan GJ, Zablah J. A new FDA approved stent for congenital heart disease: first-in-man experiences with G-ARMOR™. *Catheter Cardiovasc Interv*. 2022;100:1261-1266.

39. Yalamanchi R, Sivaprakasam MC, Janke RVR, Chandrasekharan K, Sadhasivam VS, Showkathali R. Unanticipated complication of transcatheter closure of superior sinus venosus defect. *J Cardiol Cases*. 2021;25:99-102.

40. Sivakumar K. How to do it? Transcatheter closure of superior sinus venosus defects. *Ann Pediatr Cardiol*. 2022;15:169-174.

41. Tan W, Levi D, Perens G, Aboulhosn J. Suture connection of overlapping covered CP stents for transcatheter treatment of sinus venosus defect with anomalous pulmonary venous connection. *Catheter Cardiovasc Interv*. 2022;100:399-403.

KEY WORDS 3-dimensional technology, congenital heart disease, multimodal fusion imaging, sinus venosus defect, transcatheter closure

APPENDIX For a supplemental video and table, please see the online version of this paper.

Première correction percutanée de CIA sinus venosus en France

Ce travail de thèse a été débuté en mars 2020, grâce à l'impulsion donnée par la première correction percutanée française de CIA sinus venosus, publiée dans European Heart Journal (case report ci-dessous)[27] réalisée par notre équipe à l'Hôpital Marie Lannelongue.

La patiente de 71 ans était référée pour CIA sinus venosus avec hypertension artérielle pulmonaire modérée multifactorielle.

Récusée de la chirurgie en raison de multiples comorbidités (âge, hypertension pulmonaire, obésité), la patiente a été antérieurement traitée par voie endovasculaire pour cœur pulmonaire chronique post-embolique (angioplastie des artères lobaires). Une prise en charge percutanée de sa cardiopathie congénitale a été discutée en réunion pluridisciplinaire car le cathétérisme hémodynamique post-dilatation des artères pulmonaires retrouvait une persistance d'hypertension pulmonaire (PAP moyenne 33 mmHg) en rapport avec un shunt gauche droit significatif (QP/QS 2), chez une patiente symptomatique.

La stratégie percutanée, alternative à l'abstention thérapeutique, a été décidée sur la base de la première série publiée par une équipe anglaise.

L'analyse préopératoire de faisabilité a été effectuée à partir du scanner injecté, via un modèle 3D imprimé en SLS. L'effet de la correction a été simulée directement à la main par implantation directe du stent dans le modèle imprimé. Le stent nu avait été artisanalement recouvert par une membrane de PTFE suturée permettant son effet barrière. Visuellement, le résultat semblait satisfaisant et la technique procédurale était préparée en amont : rail rigide fémoro-jugulaire, ponction transseptale de sécurité pour mise en place d'un guide dans la veine pulmonaire anormale au cas où l'inflation du stent engendrerait une sténose de la tunnélisation.

L'intervention était effectuée sous anesthésie générale et par guidage renforcé par la fusion d'image multimodale via les logiciels Vesselnavigator (fusion scanner + scopie) et Echonavigator (fusion ETO + scopie) (Philips Healthcare, Andover, UK). L'intervention a été un succès avec une bonne stabilité du stent, l'absence de shunt résiduel et l'absence d'occlusion des veines tunnélisées. La patiente a pu sortir de l'hôpital au 2è jour postopératoire.

CASE REPORT 1 : multimodality fusion imaging to guide sinus venosus atrial septal defect closure (publié dans European Heart Journal)

C Batteux, A Meliani, P Brenot, S Hascoet

Référence bibliographique 27

CARDIOVASCULAR FLASHLIGHT

doi:10.1093/eurheartj/ehaa292

Multimodality fusion imaging to guide percutaneous sinus venosus atrial septal defect closure

Clément Batteux*, Alia Meliani, Philippe Brenot, and Sébastien Hascoet

Department of Congenital Heart Diseases, Centre de Référence Cardiopathies Congénitales Complexes M3C, Hôpital Marie Lannelongue, Groupe Hospitalier Paris Saint Joseph, Université Paris-Sud, 133 avenue de la résistance, 92350 Le Plessis Robinson, France

* Corresponding author. Tel: + (33) 140942545, Email: batteuxcl3ment@gmail.com

A 76-year-old woman with NYHA-WHO III dyspnoea was referred for chronic thrombo-embolic pulmonary hypertension. A sinus venosus atrial septal defect (ASD) with partial anomalous pulmonary vein return (PAPVR) was also diagnosed. Preoperative cardiac computed tomography (CT) was used to build an STL model to assess the feasibility of the recently developed percutaneous ASD closure technique. We created a printed 3D cardiac model to simulate stenting of the superior vena cava that would close the defect and redirect the PAPVR to the left atrium (*Panel A*).

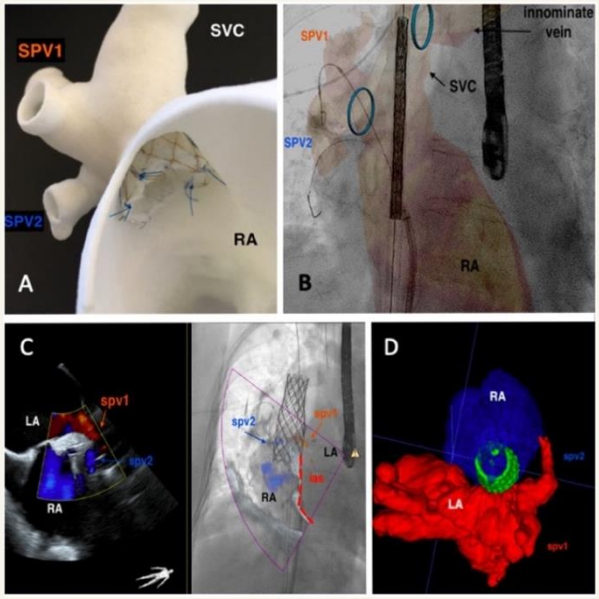

During the procedure, the STL model extracted from CT data was merged with fluoroscopy. This fusion modality was useful for continuously checking the position of the innominate vein and PAPVR during the ballooning test and stent deployment (*Panel B*, Supplementary material online, *Videos S1–S3*). Another fusion procedure was conducted to combine real-time 3D transoesophageal echocardiography (TOE) and fluoroscopy. This fusion modality was particularly useful for monitoring PAPVR flow in colour Doppler on the fluoroscopy screen during stent deployment. Indeed, avoiding obstruction of the redirection pathway to the left atrium was the main concern (*Panel C*, Supplementary material online, *Videos S4 and S5*). The procedure was successful. The absence of residual leakage or pulmonary vein obstruction was confirmed by CT and 3D STL modelling (*Panel D*) before discharge. In this challenging case, multimodality and fusion imaging improved real-time 3D understanding and guidance of a complex percutaneous treatment for congenital heart disease.

(*Panel A*) Front view of the printed model: covered stent positioned within the superior vena cava, simulating the procedure (3dheartmodeling.com®). (*Panel B*) Front view of the CT scan and fluoroscopy fusion between during stent positioning, using Vesselnavigator® software (Philips Healthcare, Andover, UK). Blue circles are positioned on the CT scan view at the opening of the pulmonary veins into the superior vena cava and at the junction between the innominate vein and superior vena cava. (*Panel C*) View of the fusion between transoesophageal echocardiography (TOE) and fluoroscopy after stent deployment, using 3D echonavigator® software (Philips Healthcare, Andover, UK). Colour Doppler shows unobstructed flow through the pulmonary veins and left atrium. (*Panel D*) Top-down view of the post-procedure 3D colour model based on CT data. Confirmation of unobstructed flow through the pulmonary veins to the left atrium. IAS, inter-atrial septum; IPV, inferior pulmonary vein; LA, left atrium; RA, right atrium; SPV 1 & 2, superior (1) and inferior (2) contingents of anomalous pulmonary veins; SVC: superior vena cava.

Acknowledgement: Pr Alain Fraisse, Royal Brompton Hospital and Harefield NHS Foundation Trust, UK (proctoring support), Dr Vlad Ciobotaru ,Clinique Franciscains, Nimes, France (3D printing support) and Dr Meriem Kara (Hôpital Marie Lannelongue).

Funding: Grant from the non-profit organization Association pour la Recherche et le Developpement en Radiologie Interventionnelle (ARDRI).

Supplementary material is available at *European Heart Journal* online.

PROBLÉMATIQUES

Encouragée par le succès de ce premier cas français, l'équipe de cathétérisme des cardiopathies congénitales de l'Hôpital Marie Lannelongue a souhaité développer cette nouvelle technique thérapeutique.

Ce projet de développement a été soutenu par l'ensemble du pôle de cardiopathie congénitale de l'hôpital, incluant les médecins cardiologues et cardiopédiatres, les chirurgiens et le pôle d'anesthésie réanimation. Elle a également reçu un soutien intentionnel de la part de la direction générale et de la pharmacie pour l'utilisation de matériel médical peu ou pas remboursé, dans le cadre du projet d'innovation.

Dès le début du projet, plusieurs prérequis et problématiques ont été identifiées dans le cadre global du lancement d'un programme d'innovation thérapeutique concernant la correction percutanée des CIA sinus venosus :

-s'assurer de la sécurité de cette nouvelle intervention en ce qui concerne la technique procédurale elle-même, les matériaux utilisés, l'adaptation du corps humain à long terme vis-à-vis de l'action thérapeutique effectuée.

-s'assurer de la faisabilité de l'intervention par la sélection stricte des patients candidats d'un point de vue clinique, morphométrique, et anatomique

-évaluer l'efficacité de la nouvelle technique en comparaison au gold standard chirurgical.

-envisager un élargissement de sélection des patients candidats en respectant les trois points sus-cités, dans une optique de démocratisation de la procédure.

-optimiser la préparation préopératoire des interventions par le biais de la simulation pour diminuer le risque d'effets indésirables et augmenter le taux de succès.

-optimiser l'intervention elle-même pour diminuer le risque d'effets indésirables et augmenter le taux de succès.

-s'assurer d'un suivi régulier des patients opérés selon une surveillance standardisée efficace.

-articuler la prise en charge pré et post opératoire de patients venant de toute la France avec la participation active des médecins correspondants.

-diffuser nos pratiques clés sur le sujet afin d'élargir le nombre de centres experts souhaitant participer à ce nouveau programme innovant, dans le respect des prérequis et problématiques détaillés ci-dessus.

OBJECTIFS DE LA THÈSE

Cette thèse avait pour objectifs d'améliorer la connaissance et la prise en charge des CIA sinus venosus grâce à la technologie 3D et ses applications, à la lueur de la nouvelle technique endovasculaire de correction, développée récemment.

Pour cela, ce travail a été articulé autour de 3 axes principaux, interconnectés tout au long de ce projet.

Le premier axe consistait en l'amélioration de la compréhension anatomique de cette cardiopathie singulière, après modélisation tridimensionnelle standardisée, via la prise en compte, la description et la mesure des composants anatomiques clés la définissant.

Le second axe reposait sur la mise en place d'un programme global de simulation préopératoire de la correction percutanée, afin d'en évaluer sa faisabilité, ses challenges, et ses risques, de manière individualisée et ciblée pour chaque patient candidat.

Le troisième axe consistait en l'application clinique en France de la nouvelle technique de correction percutanée, par la mise en place et la conduite d'une étude prospective comparative à l'échelon national, après une phase de recherche et développement en lien avec l'industrie.

MATERIEL ET METHODE

I. Modélisation 3D d'une cardiopathie congénitale

Tout au long de cette thèse, la modélisation 3D des CIA sinus venosus était effectuée de manière standardisée selon la méthode suivante.

1. Co-encadrement Master 2

Mika Gkogkou (Anatomie 2D des CIA sinus venosus) Anatvenosus : Variabilité anatomique des communications inter atriales sinus Venosus : apport de la modélisation tridimensionnelle. Bourse de master 2 recherche de la Fédération Française de Cardiologie 2021 (20 000 euros)

2. Recueil des patients et sélection des scanners

Les patients de la cohorte rétrospective provenaient de la base historique de l'Hôpital Marie Lannelongue opérés en chirurgie à cœur ouvert entre 2008 et 2020. Seuls les patients ayant eu un scanner exploitable ont pu être modélisés en 3 dimensions et donc inclus.

Les patients de la cohorte prospective provenaient des patients référés par nos correspondants partenaires pour prise en charge soit percutanée soit chirurgicale à partir de 2020. Les scanners pouvaient avoir été faits soit dans la région d'origine, soit à l'Hôpital Marie Lannelongue. Les scanners retenus devaient être injectés, et d'assez bonne qualité avec une prise de contraste homogène sur un temps tardif afin de bien visualiser les retours veineux pulmonaires et la communication entre les deux oreillettes. Certains patients provenaient de centres internationaux nous ayant sollicité pour une modélisation 3D et un avis spécialisé en rapport avec un projet de correction percutanée.

3. Extraction des images DICOM

Les séquences tomodensitométriques de bonne qualité étaient extraites, quand disponibles, depuis le logiciel PACS Carestream de l'hôpital.

Parfois, les données étaient transmises par les correspondants, soit par CD envoyé par voie postale, soit par wetransfer®, soit via la plateforme ROFIM®, permettant un chargement direct dans les logiciels de modélisation ci-après.

4. Segmentation semi-automatique (logiciel ITK-snap)

ITK-SNAP[113] est un logiciel participatif gratuit en open-access qui propose une segmentation semi-automatique utilisant des méthodes de contours actifs, ainsi que des délimitations manuelles et une navigation dans les images. En plus de ces fonctions principales, ITK-SNAP offre de nombreux utilitaires supplémentaires. Parmi les capacités essentielles d'ITK-SNAP, on trouve :

- Curseur lié pour une navigation 3D fluide
- Segmentation manuelle dans trois plans orthogonaux simultanément
- Une interface graphique moderne
- Support de nombreux formats d'image 3D, y compris NIfTI et DICOM
- Support de la visualisation et de la segmentation simultanées de plusieurs images
- Support d'images couleur, multi-canaux et 3D+temps
- Capacités d'enregistrement d'images manuelles et automatiques
- Interpolation de segmentation entre les coupes
- Outil de coupe 3D pour un post-traitement rapide des résultats de segmentation
- Accès à des algorithmes avancés via le service de segmentation distribué (DSS)
- Documentation complète avec tutoriels et vidéos

Fidèle à sa vision originale, le design d'ITK-SNAP se concentre spécifiquement sur le problème de la segmentation d'image, en minimisant les fonctionnalités superflues ou non liées. Le design met également l'accent sur l'interaction et la facilité d'utilisation, la majorité des efforts de développement étant consacrée à l'interface utilisateur.

Après sélection de la région d'intérêt (appelée ROI pour *region of interest*) où se trouve les composants anatomiques de la malformation à modéliser, l'image dans les 3 plans de l'espace est binarisée sur le plan de son intensité lumineuse liée à la présence de produit de contraste. L'ajustement manuel du contraste lumineux est possible en modifiant le seuillage de l'intensité (tresholding) de telle sorte que les composants anatomiques de la malformation puissent ressortir et les composants inutiles s'effacer.

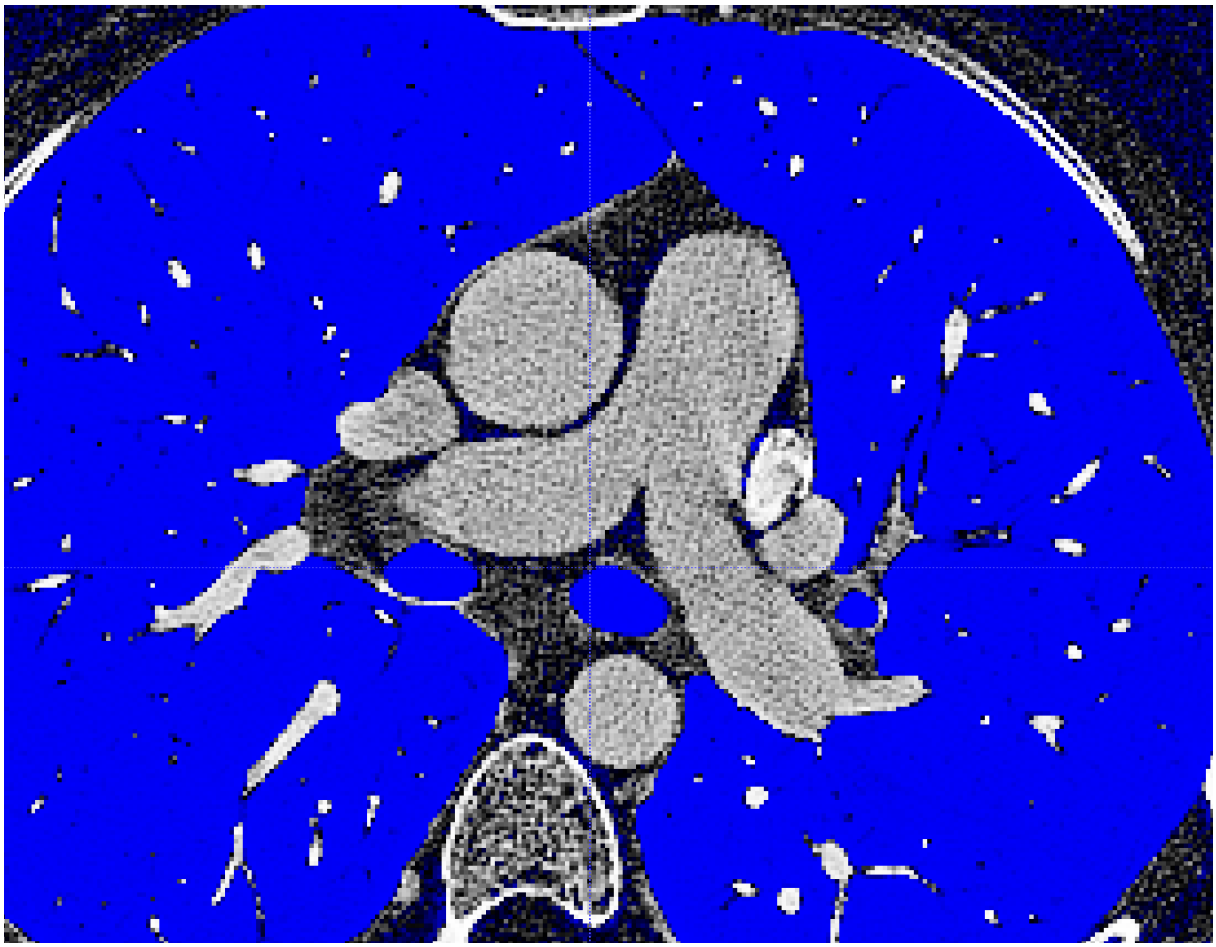

Figure 38 : sélection de la ROI (region of interest)

Modification manuelle de l'intensité lumineuse et du contraste permettant d'individualiser les structures anatomiques d'intérêt et lancer le processus de segmentation.

L'étape suivante consiste, après individualisation des composants anatomiques souhaités, à positionner des bulles de propagation à l'intérieur des composants anatomiques.

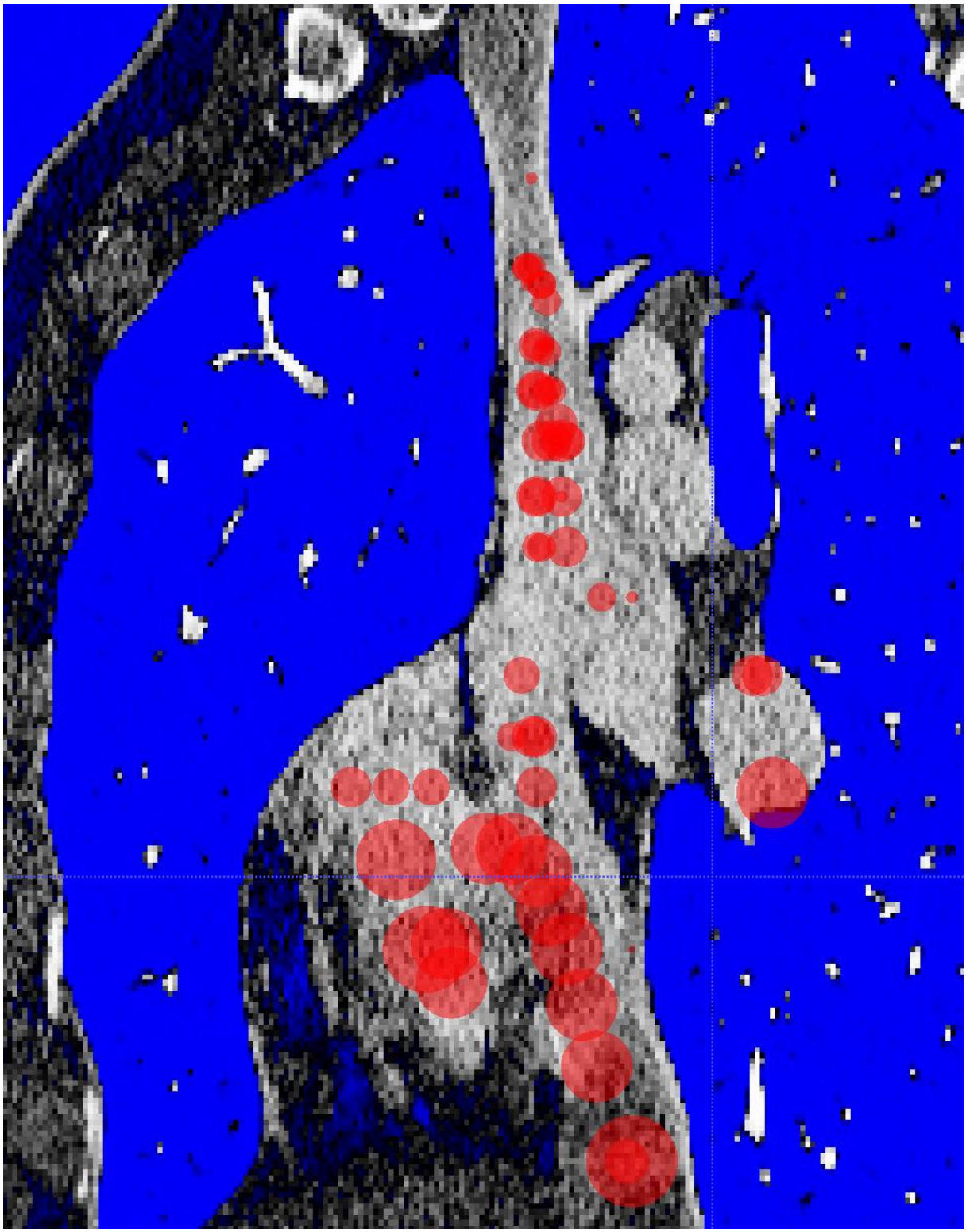

Figure 39 : : dépôt de bulles de propagation dans les régions anatomiques souhaitées avant d'autoriser leur propagation.

Plus la bulle est grosse plus elle va se propager rapidement. Plus le contraste lumineux est important, plus la segmentation sera véloce.

Après acceptation de l'opérateur, les bulles peuvent ainsi de propager de proche en proche jusqu'à ce qu'elles soient arrêtées par une modification de contraste lumineux. Cette opération peut être répétée à souhait, permettant de reconstruire les structures anatomiques de manière séquentielle.

Figure 40 : remplissage des structures d'intérêt par propagation.

Utilisation de la segmentation semi-automatique via la méthode de contours actifs (ITK-snap software).

La caractérisation anatomique 3D finalement obtenue peut alors être exportée sous format STL correspondant à un nuage de voxels connectés les uns les autres.

Ce STL global pourra alors être transféré vers un autre logiciel de post-traitement[114, 115], permettant lui d'améliorer la visualisation et d'affiner l'analyse et les mesures anatomiques souhaitées.

5. Post-traitement (logiciel Meshmixer)

A ce stade, le modèle 3D consiste donc en un nuage de voxels inter-connectés. Il correspond basiquement au sang à l'intérieur des structures étudiées et c'est donc un volume plein.

Pour dessiner les structures anatomiques d'intérêt structures, il faut alors, après lissage préalable du modèle, définir artificiellement une couche externe fine (comprise le plus souvent entre 0.6 et 0.8 mm). Le logiciel va donc créer la couche externe au sang selon l'épaisseur choisie, et l'on obtiendra ainsi un volume 3D creux correspondant à la malformation anatomique, artificiellement « vidée » de son sang.

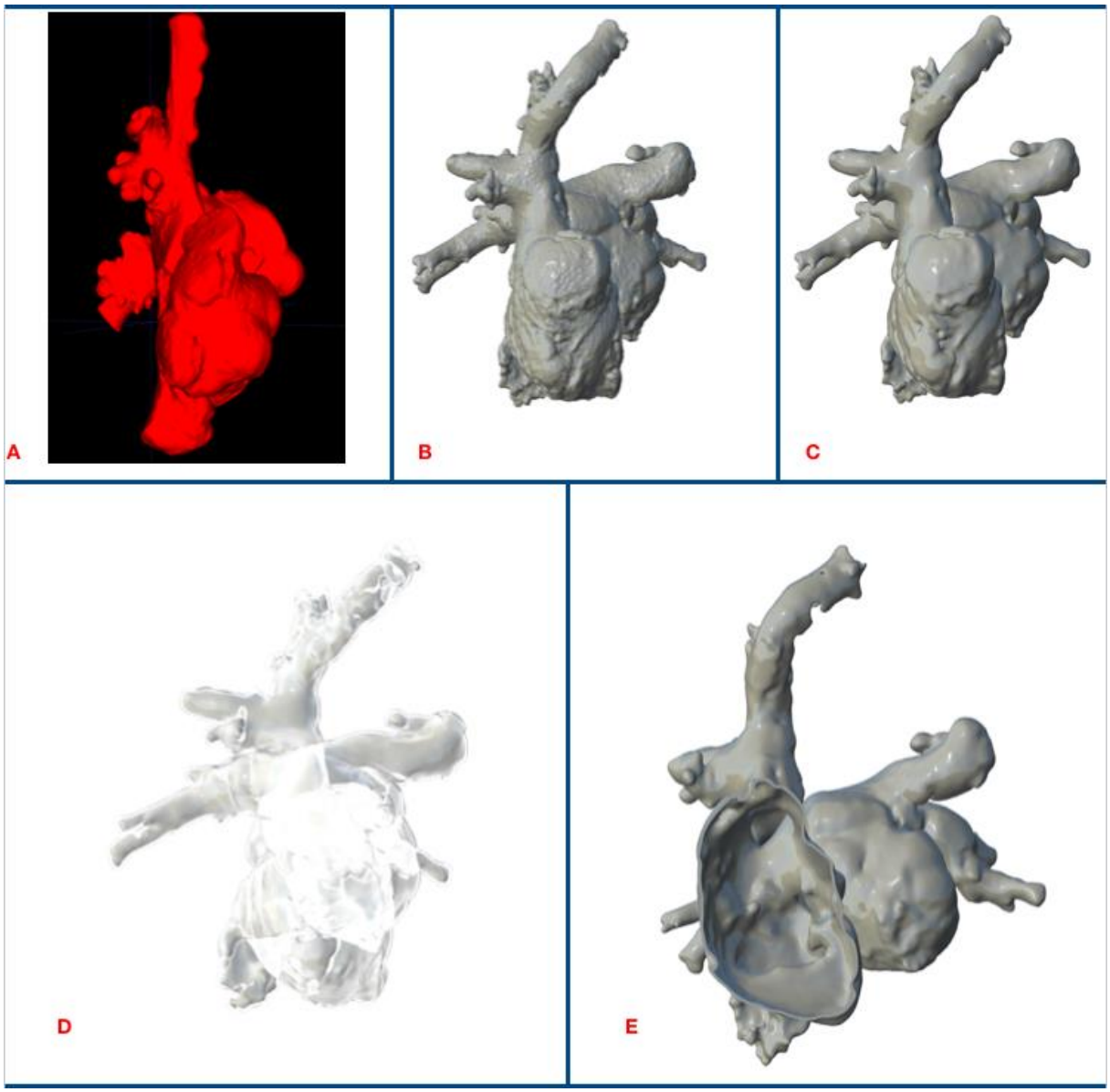

Figure 41 : Post-traitement d'un modèle 3D de CIA sinus venosus.

A : volume 3D obtenu après propagation en fonction du contraste lumineux (segmentation semi-automatique, ITK-snap software). B : STL brut obtenu (Meshmixer software). C : STL traité après polissage externe afin d'obtenir un meilleur rendu sans modifier l'anatomie propre. D : création d'une couche externe artificielle de 0.7 mm permettant de supprimer l'intérieur du modèle en ne gardant que sa néo-coque. E : résultat final du modèle 3D après post-traitement permettant la navigation et les mesures internes.

A partir de ce modèle, l'opérateur pourra naviguer à loisir à l'intérieur de la malformation pour en analyser les structures d'intérêts, les différents rapports entre ces structures et il pourra également effectuer des mesures 3D standardisées.

II. Développement d'un banc d'essai

Le développement d'un banc d'essai en cardiologie nécessite plusieurs étapes et prérequis permettant la reproductibilité artificielle d'une intervention sur modèle imprimé.

1. Coopérations

Le projet du banc d'essai a été pensé et appliqué avec l'étroite coopération de plusieurs intervenants d'horizons variés, qui s'est avérée aussi fructueuse qu'indispensable.

-**Vlad Ciobotaru**, co-doctorant dans l'école doctorale IFTA au sein de l'hôpital Marie Lannelongue où nous avons partagé la même unité de recherche (U999).

Médecin cardiologue et spécialisé en impression 3D adaptée à la cardiologie interventionnelle, ce dernier a par son sens de l'innovation et sa passion, participé grandement à la naissance et au développement du banc d'essai jusqu'à sa standardisation. La coopération entre sa société 3DHeartmodeling et le département de recherche clinique de l'hôpital Marie Lannelongue, a permis la progression du banc d'essai en termes de matériaux, techniques de branchement, fonctionnalité, et applicabilité.

- **Grégoire Albenque** étudiant en master 2 (Optimisation du banc d'essai pour simulation des corrections percutanées de CIA sinus venosus. Bourse 2022 master 2 recherche de la Fédération Française de Cardiologie, 20 000 euros)

-Étudiants ingénieurs, en stage à l'hôpital, rattachés au projet du banc d'essai.

-Roxane Nguyen-Quemper de l'école CY Tech a pu travailler sur la modélisation 3D de la cuve en plexiglas nécessaire au développement du banc d'essai.

-Antoine Bourgoin et Jean Louis Dupin de l'IFSBM (institut de formation supérieure biomédicale) ont pu au cours de leur stage travailler sur un cahier des charges relatif à la mise en place du banc d'essai.

-William Arditi de Centrasupelec a participé précieusement au développement du banc d'essai. Il a pu pendant son stage réfléchir et proposer un projet de cuve transparente permettant d'accueillir un banc d'essai pour réaliser l'intervention souhaitée. Il a accompagné les premières sessions de simulation in-vitro et permis l'amélioration constante du programme au cours de sa présence.

Tous ces stagiaires avec une grande motivation et un grand intérêt pour le projet ont été accueillis à l'hôpital Marie Lannelongue grâce au travail et l'accompagnement du Service d'innovation et d'études précliniques du groupe hospitalier Paris Saint-Joseph.

2. Adaptation et recherche du meilleur matériau de printing

Les multiples techniques d'impression 3D et matériau disponibles rendent les possibilités (et les difficultés) nombreuses pour aboutir au modèle de simulation souhaité. En cardiologie interventionnelle, le modèle imprimé sur lequel travaille l'opérateur doit répondre à plusieurs caractéristiques indispensables à la bonne conduite de l'intervention in-vitro.

Le modèle doit être solide et ainsi résister aux différentes conditions de charge imposées (charges internes quand le modèle est perfusé, charges externes quand le modèle est manipulé et connecté).

Le modèle doit être radio-transparent afin que l'intervention se déroule sous contrôle de la scopie dans les mêmes conditions qu'en salle de cathétérisme, sans contrôle artificiel possible de la vue.

Il doit être également écho-transparent pour permettre le guidage par échographie trans-oesophagienne, comme dans les conditions du réel.

Il doit aussi être flexible et présenter une distensibilité se rapprochant d'un tissu cardiaque vivant.

Enfin, il doit être résistant à l'eau, afin d'être utilisé de manière immergée, prérequis indispensable aux interventions endovasculaire, qui-plus-est guidées par échographie.

L'obtention du matériau idéal passe donc par des étapes de test de qualité, nombreuses, et séquencées de manière standardisées selon le prérequis détaillés ci-dessus.

De la qualité et consistance du matériau dépendra également la qualité d'impression et donc la précision du support de travail permettant de mener à bien la simulation sur banc d'essai.

Figure 42 : différents matériaux testés pour l'impressoin des modèles 3D de CIA sinus venosus.

Figure 42 : Gauche haut de la table : SLA, bas de la table : polyjet. Droite : modèle en SLS avec implantation manuelle d'un stent nu.

3. Recherche et développement du support pour banc d'essai

Le support du banc d'essai est une cuve remplie d'eau qui permet l'accueil du modèle imprimé en 3D et sa connexion éventuelle. La cuve doit être la moins gênante possible, que ce soit concernant l'intervention technique de l'opérateur pendant la simulation, mais également en termes de connectivité entre le modèle et l'extérieur.

Elle doit donc être, en plus d'une solidité et étanchéité sans faille, totalement radio-transparente afin de ne pas gêner la fluoroscopie. Elle doit assimiler des composants permettant de connecter le modèle à la cuve elle-même, mais également de le connecter à l'extérieur de la cuve, permettant d'effectuer les manœuvres liées à la simulation (montée de guide, montée de ballon, montée de stent, interposition d'une sonde d'échographie, système de raccord pour réalisation d'angiographies).

Un travail préalable d'ingénierie est donc indispensable pour intégrer toutes les fonctions souhaitées du banc d'essai en passant par l'interface qu'est la cuve entre l'extérieur (zone technique de contrôle et geste opératoire) et l'intérieur du modèle (zone opératoire proprement dite).

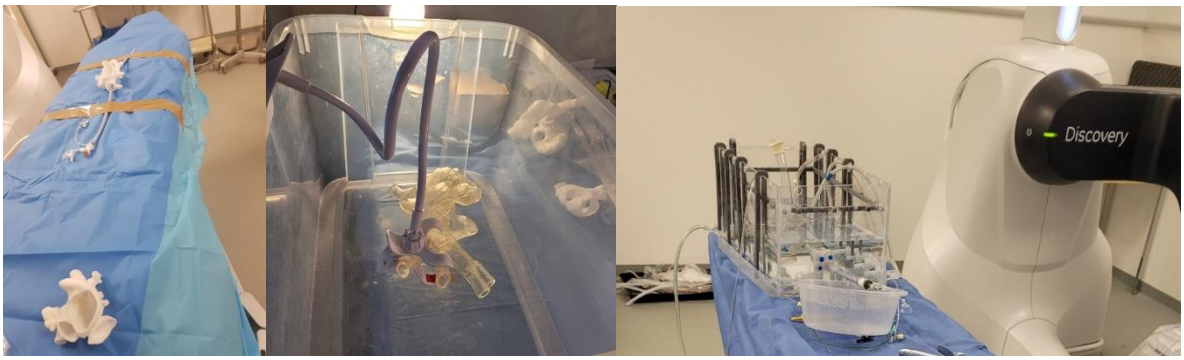

Figure 43 : progression du banc d'essai en terme de support pour le modèle imprimé.

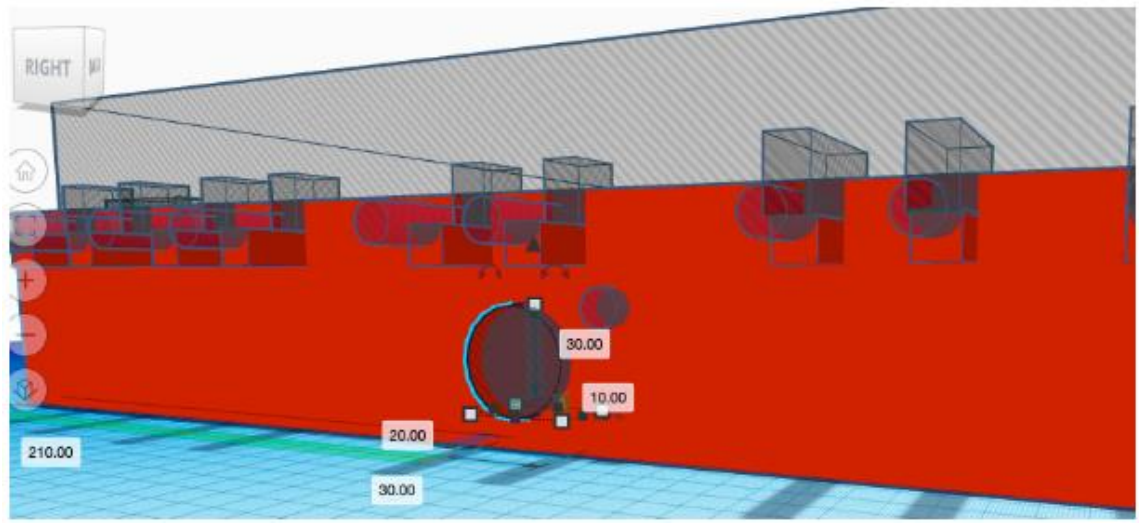

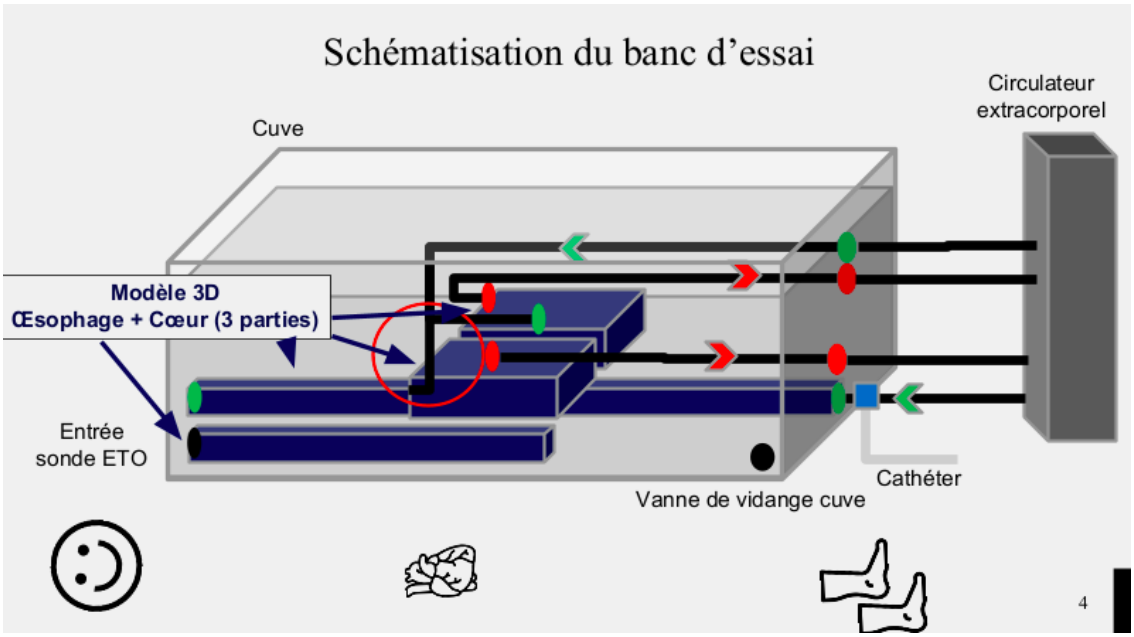

Figure 44 : conceptualisation et modélisation d'une cuve et sa connectique pour acceuil du modèle imprimé et simulation de la procédure interventionnelle

Travail des stagiaires CY tech et CentraleSupélec.

Développement d'un banc d'essai - Cahier des Charges					
Exigences			Solution privilégiée		
Ensemble	Critère	Pré-requis	Alternatives envisagées	Solution retenue	Barrières potentielles
Modèle	Faisabilité - Mode d'impression	Modèle 3D physiquement réalisable			
	Faisabilité - Coût financier	Coût raisonnable	Alginate>Collagène>HPF+	10$ contre 2000$	
	Faisabilité - Délais de livraison	Les plus courts possibles			
	Flexibilité / Dilatabilité	Exigences relativement peu contraignantes, légère flexibilité / élasticité du matériau	HPF+>Alginate>Collagène		
	Etanchéité	Etanchéité complète exigée			
	Connectabilité avec les appareils de mesure	Doit permettre l'introduction d'appareils de mesure (manomètre, etc.)			
	Connectabilité avec le dispositif de raccord à l'appareil de circulation extracorporel	Connexion rapide et facile au reste du dispositif			
	Réutilisabilité	Non dégradable face aux agents de nettoyage standards			contre-indications nettoyage
Module de visualisation par imagerie	Angle de vue	Doit représenter la vue obtenue par échographie trans-oesophagienne			
	Radio-opacité	Très faible radio-opacité			
	Dimensions (diamètre)	Diamètre suffisant pour permettre le passage de la sonde (1.5cm de diamètre)			
	Proximité avec le modèle	Le module doit être proche du modèle pour reproduire au mieux les conditions de visualisation réelle du cœur par ETO			
	Réutilisabilité	Non dégradable face aux agents de nettoyage standards			
Fluide	Coût	Coût minimal	Eau + Silicate de Sodium ou	3 euros le kg	
	Fabrication	Commandable facilement ou faisabilité maison à privilégier	Eau + alcool polyvinylique	30 euros le kg	
	Délais de livraison	Les plus courts possibles			
	Viscosité	Viscosité similaire au sang			
	Radio-opacité	Faible radio-opacité			
Cuve	Etanchéité	Etanchéité totale de l'ensemble	Plexiglas et valves unidirectionnelles		
	Ports de connexion entrée-sortie	Orifices entrées-sorties (pour le circuit extracorporel et le remplissage/vidage de la cuve)			
	Support pour modèle et module de visualisation	Support empêchant la rotation/le déplacement du cœur par rapport au module de visualition			
	Radio-opacité	Très peu radio-opaque pour assurer une bonne visualtion par échographie	Plexiglas ok		

Figure 45 : cahier des charges pour le développement d'un banc d'essai complet

Travail des stagiaires IFSBM

4. Perfusion du modèle

Comme dans les procédures de cathétérisme interventionnel in-vivo, le cœur reste perfusé pendant les interventions, à la différence de la chirurgie à cœur ouvert où le cœur est arrêté et vidé de son sang. Cela implique donc l'apport au modèle d'une perfusion continue à débit contrôlé, en prenant en compte l'inflow (arrivée de la perfusion du modèle) et l'outflow (sortie de la perfusion du modèle) ainsi que la spécificité de la circulation cardiaque en parallèle.

Pour la simulation de la correction percutanée des CIA sinus venosus, la zone d'intérêt de la perfusion se situe à droite entre les veines caves (inflow) et la valve tricuspide (outflow) et à gauche entre les veines pulmonaires (inflow) et la valve mitrale (outflow). Le reste de la circulation (ventricules, AP, Aorte) peut être artificiellement négligé.

Le mode de perfusion du modèle peut alors s'envisager par connexion externalisée comme dans la circulation extracorporelle, ou de manière internalisée en s'appropriant l'eau de la cuve comme tampon entre l'exterieur et l'intérieur du modèle.

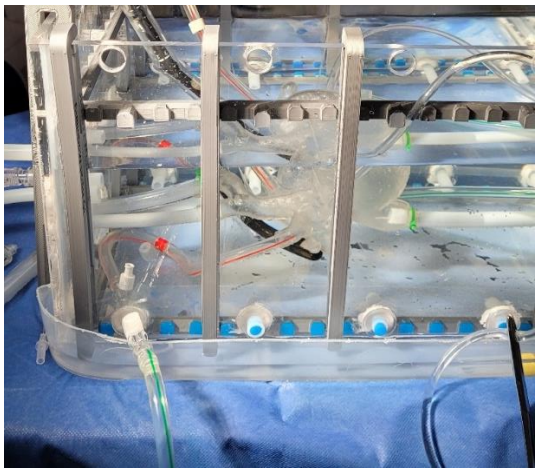

Figure 46 : amélioration des connectiques du modèle imprimé

5. Outils permettant de se rapprocher des conditions in vivo

Les outils nécessaires à la réalisation d'une intervention sur banc d'essai sont les mêmes que ceux utilisés dans la vraie vie et la construction du banc de simulation a été guidée par cet objectif clé.

L'introduction des cathéters, ballons et stents doit se faire selon les mêmes modalités qu'en condition réelle.

L'angiographie apparait indispensable car aide à se repérer à l'intérieur du modèle transparent, et permet le contrôle de certains points interventionnels techniques précis (test d'occlusion, calibration).

Le guidage par échographie trans-oesophagienne, comme dans la correction percutanée in vivo, est indispensable. Aussi, le modèle doit être echo-transparent, le fluide de la cuve doit conduire sans écho les ultrasons, et la sonde doit suivre au mieux le trajet de l'œsophage du patient, afin que les repères et constatations échographiques soient les mêmes au cours de la simulation que lors de l'échographie réalisée sur le patient réel.

La fusion d'image entre le scanner et la fluoroscopie ainsi qu'entre l'échographie et la fluoroscopie, vrai avantage en salle de cathétérisme pendant les interventions, doit être également disponible sur le banc d'essai, aussi bien pour optimiser la préparation et la conduite de l'intervention, que pour former les médecins non-initiés à cette nouvelle intervention.

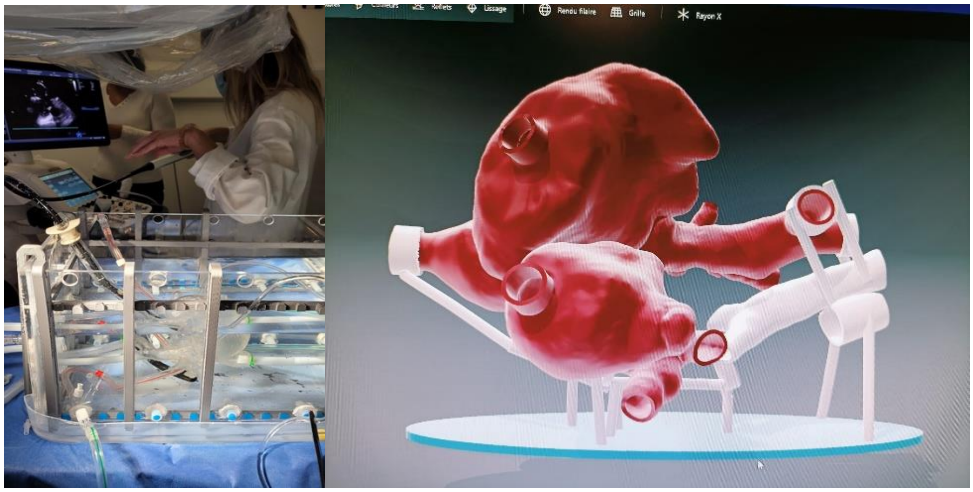

Figure 47 : création d'un support anatomique de sonde d'ETO

Rapprochement vers les conditions in vivo avec création d'un support anatomique permettant de recréer le trajet anatomique de la sonde d'échographie trans-oesophagienne propre au patient étudié.

6. Contrôle des résultats

Le contrôle du résultat de l'intervention sur banc d'essai est indispensable pour en évaluer rétrospectivement les process effectués, les forces et faiblesses intrinsèques du banc d'essai, ainsi que les résultats propres de l'intervention testée.

Pour cela, plusieurs méthodes de contrôles étaient imaginées.

-contrôle angiographique ou colorimétrique (observation du passage libre d'un flux redirigé, indemne de sténose, constatation de l'absence et de la persistance de shunt résiduel après correction.

-contrôle tomodensitométrique par Cone-Beam du modèle après l'intervention, permettant une analyse précise, fine et mesurable des actions effectuées sur le modèle. Cela permettait aussi d'envisager l'analyse précise du comportement du modèle et des stents utilisés pendant la simulation.

La salle de cathétérisme expérimentale de l'Hôpital Marie Lannelongue utilisée pour la simulation sur banc d'essai (General Electrics) permet la recherche et le développement technique relatif à tous les points décrits ci-dessus, afin d'obtenir un banc d'essai le plus complet possible, et fidèle au déroulement de l'intervention percutanée étudiée.

III. De la demande compassionnelle à l'étude prospective

1. Demande compassionnelle

Les premiers cas français de correction percutanée de CIA sinus venosus ont été effectués après demande compassionnelle à l'agence nationale de santé du médicament (ANSM), concernant l'utilisation de stents couverts n'ayant pas soit l'AMM soit le marquage CE pour le type d'intervention proposée.

En effet, les stents nécessaires à la correction percutanée des CIA sinus venosus sont des stents couverts de longue taille et de diamètres variables.

Les deux principales marques disponibles en France étaient et sont toujours aujourd'hui

-les CP10Z stent de la marque Numed, ayant le marquage CE pour une longueur allant jusqu'à 60 mm, mais n'ayant pas l'AMM pour les implantations intracardiaques. Les stents de + grande longueur (70 et 80 mm) n'ayant eux pas le marquage CE et étant produits sur demande.

-les stents Optimus de la marque Andratec, ayant l'AMM et le marquage CE pour leur longueur allant jusqu'à 57mm ; les stents de 80 et 100 mm n'ayant ni marquage CE ni AMM.

La modélisation et simulation virtuelle et sur banc d'essai a montré au cours de cette thèse que la longueur de stent nécessaire est souvent bien plus important que celle des stents ayant le marquage CE et l'AMM, c'est pourquoi des demandes compassionnelles étaient initialement réalisées.

Ces demandes compassionnelles ont concerné les patients non éligibles à la chirurgie car présentant des comorbidités trop importantes.

Un dossier fourni comportant des éléments cliniques, d'imagerie, et de simulation devait être présenté à l'ANSM de manière individualisée pour chaque cas, afin de justifier l'utilisation de ces stents spécifiques. A cette contrainte médico-administrative nécessaire s'ajoutait une contrainte pharmaceutique liée à la demande spécifique de financement par la pharmacie lié au matériel non remboursé. Les délais observés

entre la demande compassionnelle, l'accord des autorités, puis la réception des stents pour réaliser les interventions, étaient également conséquents[117, 118].

2. Projet d'étude prospective

D'un consensus commun entre les parties prenantes du projet au sein de l'Hôpital Marie Lannelongue et nos homologues de l'agence nationale de santé du médicament, il a été décidé d'évoluer depuis les demandes compassionnelles individuelle (qui devenaient fréquentes, donc non exceptionnelles !) vers un projet d'étude clinique prospective, dont les objectifs envisagés étaient multiples :

-s'affranchir d'une demande individuelle et donc d'un travail médico-administratif conséquent, ainsi que des délais engendrés avant la prise en charge réelle des patients.

-élargir le projet de correction percutané des CIA sinus venosus à l'échelon national via la participation de centres volontaires experts en cardiopathies congénitales complexes.

-regrouper les analyses de dossiers des patients candidats dans une réunion de concertation pluridisciplinaire.

-optimiser et faciliter la surveillance de cette nouvelle intervention par la création d'un protocole de suivi standardisé.

-faciliter la surveillance externe de cette nouvelle intervention par un organisme externe de contrôle, indispensable à la conduite d'une étude prospective.

C'est dans ce contexte que l'étude Optivenosus a vu le jour en France en 2022.

3. Sécurité et suivi

La centralisation par réunion de concertation pluridisciplinaire des dossiers des patients candidats, leur sélection rigoureuse, la conduite des corrections percutanée dans des centres experts autorisés et supervisés, ainsi que la surveillance postopératoire par protocole standardisé devraient permettre d'évaluer cette nouvelle technique interventionnelle avec des éléments sérieux et robustes.

La comparaison de la nouvelle technique avec le traitement chirurgical de référence devrait pouvoir également optimiser la sélection des patients vers l'une ou l'autre des possibilités thérapeutiques, basée sur des critères anatomiques, cliniques et thérapeutiques standardisés.

RESULTATS

I. Anatomie des CIA sinus venosus

ARTICLE ORIGINAL 1 : ANATVENOSUS

New Anatomical Classification to Plan Transcatheter Sinus Venosus Defect Correction Based on 3D Models

Clément **Batteux**, MD, MHSc, PhD candidate[1, 2, 3*], Efthymia **Gkogkou**, MD, MHSc [4], Grégoire **Albenque**, MD, MHSc, PhD candidate[1, 2, 3], Jean Noel **Andarelli**, MD[1], Vlad **Ciobotaru,** MD, MHSc, PhD candidate[2, 3, 5], Régine **Roussin**, MD[1] Sébastien **Hascoet**, MD, PhD, FESC[1, 2, 3]

Circulation: Cardiovascular Imaging
Manuscript Submission and Peer Review System

URL: https://circimaging-submit.aha-journals.org/

Manuscript Number: CIRCCVIM/2024/017912

Title: New Anatomical Classification to Plan Transcatheter Sinus Venosus Defect Correction Based on 3D Models

Authors:
clément batteux (Marie Lannelongue Hospital)
Efthymia Gkogkou (Centre Hospitalier Universitaire Sainte-Justine (4))
Grégoire Albenque (Department of congenital cardiac surgery and congenital cardiac diseases, Marie Lannelongue Hospital)
Jean-Noel Andarelli (hôpital Marie Lannelongue (1))
Vlad Ciobotaru (cabinet Dr Ciobotaru)
Régine Roussin (hôpital Marie Lannelongue (1))
Sebastien Hascoet (Hopital Marie Lannelongue)

New Anatomical Classification to Plan Transcatheter Sinus Venosus Defect Correction Based on 3D Models

Clément **Batteux**, MD, MHSc, PhD candidate[1, 2, 3*], Efthymia **Gkogkou**, MD, MHSc[4], Grégoire **Albenque**, MD, MHSc, PhD candidate[1, 2, 3], Jean Noel **Andarelli**, MD[1], Vlad **Ciobotaru,** MD, MHSc, PhD candidate[2, 3, 5], Régine **Roussin**, MD[1] Sébastien **Hascoet**, MD, PhD, FESC[1, 2, 3]

[1] Filière des cardiopathies congénitales enfant adultes, hôpital Marie Lannelongue, centre constitutif du réseau maladies rares malformations cardiaques congénitales complexes - M3C, les Hôpitaux Saint Joseph et Marie Lannelongue, 133 avenue de la résistance, 92350 Le Plessis Robinson, France.

[2] Faculté de Médecine Kremlin-Bicêtre, Université Paris-Saclay, France.

[3] Université Paris-Saclay, INSERM, UMR_S 999, Hypertension Pulmonaire : Physiopathologie and Innovation Thérapeutique (HPPIT), AP-HP, Hôpital Bicêtre, Hôpital Marie Lannelongue (Groupe Hospitalier Paris Saint Joseph), ERN-LUNG, Le Plessis-Robinson, France

[4] Cardiologie pédiatrique et congénitale, Centre Hospitalier Universitaire Sainte-Justine, 3175 chemin de la Côte-Sainte-Catherine, Montréal, QC H3T 1C5, Canada

[5] Cardiologie, Hôpital des Franciscaines 3 rue Jean Bouin, 30000 Nîmes, France

Short title : Classification of Sinus Venosus Defect

[*]Corresponding author : Clément Batteux, batteuxcl3ment@gmail.com, cardiopathies congénitales enfant adultes, hôpital Marie Lannelongue, Hôpital Marie Lannelongue, 133 avenue de la résistance, 92350 Le Plessis Robinson, France. Orcid 0001-6270-6154.

Total word count : 6089

Background: Superior sinus venosus defect (SVD) is a complex congenital heart disease (CHD) with a wide spectrum of anatomical variations. The innovative procedure of transcatheter SVD correction (TCSVD) is feasible in selected cases, highlighting the need for a detailed morphological understanding. This study aims to provide an anatomical classification of SVD using 3D models.
Methods: CT scans with superior SVD were 3D-modeled using semi-automatic segmentation. Key parameters such as superior vena cava (SVC) size, SVC overriding, caudal defect extension, and the size/orientation of anomalous pulmonary vein return (APVR) were analyzed in this single center cohort study.
Results: A total of 197 patients with superior SVD were studied. SVC overriding was absent in 38% of cases, and >50% in 7%. A single anomalous pulmonary vein ostium was identified in 52%, while additional ostia were observed in 48%. Among children >12 years, 83% had a SVC diameter larger than 14 mm (first quartile of adult population). SVD were classified in two types: Fenestration (30%) and Cavo-atrial (70%), based on overriding degree and defect extension. Associated lesions included left superior vena cava (15%) and ostium secundum atrial septal defect (8%).
Conclusion: 3D segmentation of a large cohort of SVD provides a new accurate and simplified anatomical description and classification, enabling tailored strategies for TCSVD.

Key words
Congenital heart disease, Sinus Venosus Defect, Anatomy, Three-Dimension, Segmentation, Transcatheter therapy.

Clinical Perspective
We present a new 3D models-based anatomical classification of sinus venosus defects, which enhances our understanding of this complex congenital heart disease. This detailed anatomical framework can facilitate a standardized description of this complex condition among cardiologists and interventionists, allowing a practical feasibility screening for transcatheter correction based on a preoperative patient-tailored planning. Ultimately, this study could improve success rate and outcomes of transcatheter correction of sinus venosus defects.

Non-standard Abbreviations and Acronyms

APVR : abnormal pulmonary vein return
ASD : atrial septal defect
CAJ : cavo-atrial junction
Cardiac CT : cardiac computed tomography
DICOM : digital imaging and communications in medicine
IV : innominate vein
LA : left atrium
LSVC : left superior vena cava
PFO : patent foramen ovale
RA : right atrium
STL : standard tesselation language
SVC superior vena cava
SVD : sinus venosus defect
TCSVD : transcatheter correction of sinus venosus defects
3D : three dimension

Introduction

The anatomy of sinus venosus defects (SVDs) is a multifaceted and often debated [1-3] subject, primarily due to the complexities surrounding its embryological origins. First described by Peacock[4] in 1858, this malformation is characterized by a high defect communicating left and right atrial chambers, outside the region of the oval fossa, specifically posteriorly and superiorly to it[5]. The distinguishing feature for diagnosing SVD lies in the integrity of the oval fossa, which allows differentiation from other types of inter- atrial communications[6, 7]. This defect is associated with abnormal pulmonary venous return (APVR) from the right lung to the superior vena cava (SVC) or the cavo-atrial junction (CAJ), leading to what is termed a "double" left-to-right shunt. This shunt occurs not only through the defect itself but also via the APVR connecting to right circulation. It is crucial to understand that a SVD is not an atrial septal defect (ASD) but represents a distinct malformation with unique anatomical implications. Anatomical descriptions reveal considerable variability, including the

SVC shape and dimension, the number of pulmonary veins involved, the characterization, size and orientation of the defect, the term of overriding of the SVC, and the potential associated presence of a left superior vena cava (LSVC) [8]. Chowdhury and al[9] (2022) have introduced several concepts to describe the malformation based on detailed imaging studies, including axial, sagittal, and modified orthogonal scan sections. They suggest a standardized approach to measuring overriding, zone of implantation of the abnormal pulmonary veins, and caudal extension of the defect.

Transcatheter correction of sinus venosus defect (TCSVD) is a recent endovascular approach that involves placing a covered stent from the SVC to the right atrium (RA) [10-12]. The goal is to isolate the caval flow from the anomalous pulmonary vein return (APVR) and simultaneously close the defect at the posterior part of the stent. The success of TCSVD depends on addressing three key challenges, which are directly influenced by anatomical features:
-The covered stent must be securely anchored in the SVC to prevent embolization.
-The stent must redirect the APVR to the left atrium (LA) at its posterior part while ensuring good patency.
-The covered stent must eliminate the double shunt, both at the APVR level and, if present, at the defect site.
In light of advancements in transcatheter correction of SVD (TCSVD), there is a growing need to optimize anatomical description which is critical given the individual variability observed in anatomic presentations. Recent advancements in imaging technology and 3D modeling have significantly improved our understanding of the complex anatomy associated with SVD, facilitating better intervention strategies by tailoring TCSVD to each anatomic specifies[13-16]. While TCSVD is primarily considered for adults, the feasibility of these interventions in children populations is also a source of debate[17, 18]. This raises important questions regarding the timing of intervention and the growth dynamics of the SVC in younger patients.

This study aimed to provide a detailed description and to set a practical classification of superior SVD based on analysis from 3D models, enhancing the understanding of their anatomical features and implications.

Secondary objectives were to analyze feasibility of TCSVD depending on anatomic specific features and to study dimensions related to patient growth in order to evaluate possible age cut-offs for the selection of candidates for TCSVD.
By addressing these objectives, the article seeks to contribute to the refinement of diagnostic and therapeutic strategies in the management of this clinical condition.

METHOD

Data Collection

Beginning in 2020, we included patients referred with a SVD who underwent a cardiac CT scan for anatomical assessment prior to surgical or transcatheter repair. For patients referred before 2020, data collection was conducted retrospectively, while those referred thereafter were assessed prospectively. DICOM images were extracted from PACS Carestream® following patient anonymization.

3D Modeling via Semi-Automatic Segmentation

The extracted DICOM images were imported into ITK-SNAP® software to facilitate 3D modeling of the malformation through a semi-automatic segmentation process. ITK-SNAP® is an open-source software that employs the active contouring method for segmentation[19]. After selecting the most suitable CT sequence and adjusting the contrast intensity, segmentation was carried out by a trained congenital physician to isolate and characterize the malformation in three dimensions. The resulting segmentation was saved in STL format, generating a mesh of voxels.
For subsequent post-segmentation processing, the STL file was transferred to Meshmixer ® software, which enables refinement and enhancement of the STL model to improve its visual and analytical quality for 3D analysis[20]. Figure 1.

Anatomic analysis

-Pulmonary Vein Ostia analysis

We opted to focus on ostia of right pulmonary veins rather than the exact number of veins. In instances where two veins drain into the LA, RA, or SVC via a single ostium, we considered this as one ostium rather than two distinct veins. Figure 2.

-Main and Additional Pulmonary Vein Ostia

As observations always reveal a principal ostium in spatial correspondence to the the communication zone, we designated this ostium as the main anomalous pulmonary

vein ostium, with any supplementary ostium observed higher up or below, classified as additional anomalous pulmonary vein ostia. Figure 2.

-SVC Overriding

SVC overriding was assessed by visualizing the 3D model of the malformation from within, after artificially sectioning the SVC at its midpoint along the axis of the azygos vein. By extending the SVC caudally, we estimated SVC overriding through the LA, categorizing it as absent, <50%, 50%, or >50%, as applicable. Figure 3.

-Caudal Extension of the Defect

Navigation through the 3D model enabled a more precise definition of the caudal extension of the defect. We first identified the lower boundary of the communication zone (considered as the defect) between the right and left chambers. Then, a plane cut was then made at the superior level of the CAJ. When the defect boundary point was at the same level as the CAJ point, caudal extension was zero. When the defect point was below or above the CAJ point, caudal extension was assessed and measured positive or negative respectively. Figure 4.

Measurements

Demographic data, including age, weight, height at the time of CT scan, and gender, were collected. Associated lesions, such as LSVC and atrial septal defect/patent foramen ovale (ASD/PFO), were documented.

Based on the anatomical analysis outlined above, several parameters related to the SVD 3D model were quantified :

-SVC overriding was classified as absent, <50%, 50%, or >50%.

-Caudal extension was quantified in millimeters and categorized as negative, absent, or positive.

-The dimensions of the main pulmonary vein ostium were measured (both maximum and minimum diameters) (Figure 2), and its angulated connection relative to the SVC or CAJ was evaluated in degrees across two axis (frontal and axial). Figure 5A and 5B.

This analysis was also performed for any additional pulmonary vein ostia if present.

-Several distances were measured to precise the relationships between the SVC, the anomalous pulmonary vein ostia, and the communication between the left and right chambers:

- Maximum SVC diameters (in millimeters) measured at 4 different levels: the innominate vein, the upper anomalous pulmonary vein ostium (if any), the main anomalous pulmonary ostium and at CAJ (Figure 5C).
- Distance (in millimeters) between the upper anomalous pulmonary vein ostium and the level of the innominate vein (Figure 5D).
- Distance (in millimeters) between the upper anomalous pulmonary vein ostium and the lower edge of the communication between the two atrial chambers (Figure 5D).

Theses distances were studied in the global cohort and in the adult population.

Diameters of the SVC depending on LSVC presence or absence were reported, as well as evolution of right SVC diameter with age.

Virtual simulation

Meshmixer software® was used to virtually implant a covered stent onto the 3D models SVD. Virtual TCSVD were performed on different anatomical types, and the dimensions of the stent to be implanted were adjusted to meet the three key endpoints of the procedure: patency of the anomalous pulmonary vein ostia, stent stability, and suppression of the shunt.

Statistical Analysis

Distances were recorded in millimeters and angles in degrees.
Continuous variables were described using medians, and interquartile ranges (Q1-Q3) when the normality was not verified by a Shapiro-wilk test.
Qualitative variables were described with percentages.
Statistical analysis were performed using “R” ® statistic software with Wilcoxon test for p value and quadratic square-racked equation for growing analysis.

Ethical statement

This study protocol received approval from a local ethics committee (IRB 00012157).

RESULTS

From May 2020 to September 2024, 197 superior SVD patients with available and interpretable preoperative cardiac CT were included, allowing to proceed on 3D modeling.

General results

Demographic data and 3D analysis are described in table 1.

3D measurements are described in table 2.

Table 3 shows the right SVC diameter if LSVC associated or not: a difference in right SVC diameters was observed at all the levels tested except in the CAJ.

Growing of the SVC

Figure 6 shows the evolution of the SVC diameter growth with age at different levels in global cohort and if LSVC is absent or present

Table 4 shows the repartition in % of children between 12 and 18 years-old having SVC diameters and lengths superior to the first interquartile range (Q1) and superior to the median of adult population.

Anatomic patterns and classification

2 main patterns emerged from the 3D analysis performed on our cohort, depending on the SVC over-riding and the caudal extension.

-Fenestration type (Figure 7)

First pattern concerned SVD where nor over-riding nor caudal extension was noticed. This anatomic type was found in 30% of cases and was considered as a fenestration type because not related to the cavo-atrial junction but just to the SVC.

A maximal tolerance of 10 mm caudal extension was accorded to refer a 3D anatomy to this pattern at condition that over-riding was absent. Different subtypes were established regarding the position and shape of the fenestration in the SVC (anterior, lateral, antero-lateral, bridge).

-Cavo-atrial type (Figure 8)

Second pattern concerned SVD where a significant caudal extension and an over-riding of SVC was noticed.

This anatomic type was found in 57% of cases.

We noticed 13% of grey types where over-riding was found without caudal extension (5.5%) or when caudal extension was found without over-riding (7.5%)

We assumed to address these grey types as cavo-atrial type, that extend its proportion to 70% of the cohort.

Classification

Figure 9 represents the classification we established to describe SVD anatomy with practical considerations.

Three parameters were taken into account: overriding, caudal extension, and the number of abnormal ostia involved.

When one main PV ostium was observed, subtype was single, and when additional PV ostia were observed, subtype was florid.

The distribution of our cohort according to this classification is also provided.

Florid subtype was found in 47% of cases with fenestration and 35% of cases with cavo-atrial type

LVSC was observed in 17% of fenestration cases and 14.5% of cavo-atrial cases.

Virtual Simulation (Figure 10)

In the **fenestration type**, APVR ostia is above the CAJ wich is typically a flairing zone (for shunt abolition and eventually for stent impaction). Patency of the anomalous pulmonary vein ostium to the LA seemed to be not a concern in this case, as the ostium is located above the CAJ, where the stent is typically over-inflated (flairing zone). With no SVC overriding present, the stability of the device could rely on double-point impaction: one at the superior aspect (innominate level) and another at the inferior part if straight enough (cavo-atrial level). In this mind, the distance between the upper APVR ostia and innominate vein (anchoring zone), as well as the diameter of the cavo-atrial junction (flaring zone), were key factors in ensuring good stent stability and complete shunt suppression.

In the **cavo-atrial type**, the main APVR ostium is positioned relatively low, at the same level as CAJ. Consequently, the patency of the APVR after rerouting largely depends on the degree of flaring of the stent at this level. A careful balance between flaring and maintaining APVR patency at the same level, must be achieved, which may sometimes require protection of the APVR from the left side following trans-septal puncture. In the absence of high additional ostia, stent stability was not a significant concern for cavo-atrial types.

DISCUSSION

Anatomical Concepts

This study, motivated by insights from 3D modeling of the variable anatomies associated with SVD, aims to introduce new concepts and refine those previously described[9]. The work has been conducted in light of recent advancements in transcatheter therapies and is intended to be pragmatic in its approach[21].

-APVR ostia

Given the considerable variability in right lung drainage in the general population[22], and particularly in patients with SVD[8, 23], we have chosen to focus on the ostia of the right pulmonary veins, rather than the precise number of veins involved. The concept of the "main pulmonary vein ostia" simplifies the understanding and the description of the variability in anomalous pulmonary venous return (APVR) associated with SVD.

-what is the defect?

The characterization of the defect of superior SVD remains a subject of debate[6,8,9], as its appearance can vary depending on the viewpoint. It may be visualized as a hole, or more commonly, as a conical volume, influenced by its relation to the main anomalous ostium, the caudal extension, and the degree of SVC overriding. For example, what is termed a defect in a fenestration type may appear as a hole, while in a cavo-atrial type, it may present as a large conical volume. We argue that the defect itself should not be considered a primary parameter in SVD evaluation but rather a consequence of the aforementioned anatomical factors.

In this context, we chose to assess the distance from the upper APVR ostia to the lower margin of the communication between the two atrial chambers, to define the shunting zone, rather than attempting to define the defect itself.

-caudal extension of the defect

Our definition of caudal extension is based on 3D analysis of the cavo-atrial junction, which cannot be accurately assessed in orthogonal views due to the variable orientation of the SVC as it enters the RA. We arbitrarily chose to focus on a plane cut at the superior aspect of the CAJ, as it appeared to be the most reproducible. In this context, we allowed a 10mm extension for fenestration type given that the oblique orientation of the SVC leads to an fake caudal extension of the defect. The

lower aspect of the CAJ was thus not chosen because it was often not determinable accurately.

-Over-riding of the SVC

The concept of overriding, previously described[9] using a comparable method of tetralogy of Fallot assessment involved a virtually planar extending of the interatrial septum to determine the degree of SVC overriding with the LA. We modified this method by virtually prolonging the SVC in 3D, after cutting the SVC at the level of the azygos vein, which is almost perpendicular to the SVC. This modification revealed a larger proportion of “no overriding” cases compared to previous studies. As shown in previous publications, we maintain that overriding is not a mandatory criterion for characterizing the defect.

Need for Classification

Our goal was to propose a classification for superior SVD, as their descriptions and therapeutic implications often vary significantly among practitioners. This classification aims to standardize the anatomical language used to describe SVD, facilitating communication and allowing for more precise targeting of therapeutic strategies. By defining key points such as overriding, caudal extension, and the number of pulmonary vein ostia, we hope to address the specific challenges posed by each individual anatomy[24].

Implications for TCSVD

Single Types

-Single Fenestration Type: This type involves a high unique communication zone between the two atrial chambers corresponding to the main pulmonary vein ostia. Since the cavo-atrial region is not involved, pulmonary vein protection is not typically required in the initial approach. The stent implantation strategy should focus on: Ensuring good stent impaction at the innominate vein region to prevent device embolization (the distance between the pulmonary vein ostia and the innominate vein should be evaluated to ensure it is sufficient).Achieving good stent impaction at the CAJ (below the APVR ostia) to avoid residual shunting.

A "8" shape of the stent is often expected in TCSVD procedures regarding this type.

-*Single Cavo-Atrial Type*: This type is frequently encountered, with the cavo-atrial junction involved and the APVR ostium positioned relatively low. For TCSVD, stent stability is not generally an issue if the distance between the APVR and the innominate vein is adequate. However, there is a risk of residual shunting, which must be balanced with the potential for pulmonary vein occlusion, as stent flaring at the caudal part may cause PV occlusion to reduce the shunt.

Florid Types

When an additional pulmonary vein ostium is involved in the malformation, its position relative to the main pulmonary vein ostium is critical. If the additional ostium is below the main ostium, it generally does not pose a significant concern for TCSVD as rerouting the main pulmonary vein will also reroute the additional vein. However, if the additional ostium is above the main, special caution is required. A strategy of either balloon protection or allowing the vein to remain in the SVC channel must be carefully considered. Precise study using 4D flow MRI with selective QP:QS analysis can help determine the best approach based on the expected haemodynamic role for the additional upper vein.

LSVC+

As we demonstrated, when a LSVC is present, the right SVC diameter is much smaller at its upper portion than at the cavo-atrial level.
In such cases, a highly conformable stent should be used for TCSVD, as it will need to be impacted at the narrower upper portion of the SVC while expanding at the wider base to avoid residual shunting.

Perspectives

Building a significant 3D database of superior SVD, we aim to perform virtual TCSVD procedures on digital twins, testing different devices to assess the challenges and feasibility of treatment[25]. This will help determine the expected success rates of various devices based on each type of defect classification.
Regarding patient selection for TCSVD[18, 21, 24], we suggest that the minimum age for considering this procedure should likely be envisaged around 12 years, as our findings show that SVC growth stabilizes in diameter and length around this age.

The Optivenosus study is an ongoing nationwide prospective study in France (NCT 05865119) that compares surgical and transcatheter approaches for the correction of superior SVD. This study incorporates 3D modeling, classification, and virtual simulation based on SVD 3D models to guide patient referral to either the transcatheter or surgical treatment group. Initial results from the first phase of the study, which recently concluded, are expected to be published soon.

Limitation

One limitation of this study is that 3D modeling using semi-automatic segmentation is time-consuming and not widely available. Additionally, these tools require expertise in congenital heart disease to be used effectively. On the other hand, 2D analysis or automatic segmentations process can appears to lack sufficient accuracy and to be not fully adapted to clinical practice.

Conclusion

Superior SVD encompass a wide anatomical spectrum and cannot be described in a single way. Our study provides new insights into the anatomy and classification of SVD, utilizing 3D modeling from a large cohort of patients. This approach aims to standardize the description and understanding of this complex condition, ultimately improving patient selection and tailoring strategies for transcatheter therapy.

Aknowledgements

Philippe Aldebert, Gilles Bosser, Hélène Bouvaist, Ivan Bouzguenda, Vlad Ciobotaru, Nicolas Combes, Claire Dauphin, Géraud Delessalle, Fanny Dion, Phuoc Duong, Alain Fraisse, Nikolaus Haas, Roland Hénaine, Ali Houeijeh, Lucile Houyel, André Jakob, Clément Karsenty, Magalie Ladouceur, Jean-Paul Lethor, Jelena Radojevic, Tobias Rutz, Manuel Santos, Domenico Sirico.

Sources of funding

No sources of funding used for this publication

Disclosures

Sebastien Hascoet, proctoring support for Abbott vascular, Edwards Lifesciences and Venus Medtech.

The other authors declare they have no conflict of interests.

References

1. Van Praagh S, Carrera ME, Sanders SP, Mayer JE, Van Praagh R. Sinus venosus defects: unroofing of the right pulmonary veins--anatomic and echocardiographic findings and surgical treatment. Am Heart J. 1994 Aug;128(2):365-79.
2. Lewis F J, Taufic M, Vacro R L, Niazi S. The surgical anatomy of atrial septal defects: experiences with repair under direct vision. Ann Surg 1955;142:401-17.
3. Ross D N. The sinus venosus type of atrial septal defect. Guy's Hospital Report 1956;105:376-81.
4. Peacock TB. Malformations dependent on arrest of development at an early period of fetal life. In: Peacock TB, ed. Malformations of the human heart. London: John Churchill, 1858:24-5.
5. Shaner RF. The high defect in the atrial septum. Can Med Assoc J 1958;78:688-9.
6. Anderson RH, Ettedgui JA, Devine WA. Sinus venosus defect. Am Heart J. 1995 Jun;129(6):1229-32. doi: 10.1016/0002-8703(95)90423-9. PMID: 7754966.
7. al Zaghal AM, Li J, Anderson RH, Lincoln C, Shore D, Rigby ML. Anatomical criteria for the diagnosis of sinus venosus defects. Heart. 1997 Sep;78(3):298-304. doi: 10.1136/hrt.78.3.298. PMID: 9391294.
8. Relan J, Gupta SK, Rajagopal R, Ramakrishnan S, Gulati GS, Kothari SS, Saxena A, Sharma S, Rajashekar P, Anderson RH. Clarifying the anatomy of the superior sinus venosus defect. Heart. 2022 May;108(9):689-694. doi: 10.1136/heartjnl-2021-319334.
9. Chowdhury UK, Anderson RH, Pandey NN, Sharma S, Sankhyan LK, George N, Goja S, Arvind B. A reappraisal of the sinus venosus defect. Eur J Cardiothorac Surg. 2022 May 27;61(6):1211-1222. doi: 10.1093/ejcts/ezab556. PMID: 35090016.
10. Abdullah HAM, Alsalkhi HA, Khalid KA. Transcatheter closure of sinus venosus atrial septal defect with anomalous pulmonary venous drainage: Innovative technique with long-term follow-up. Catheter Cardiovasc Interv.

2020 Mar 1;95(4):743-747. doi: 10.1002/ccd.28364. Epub 2019 Jun 14. PMID: 31197932.

11. Garg G, Tyagi H, Radha AS. Transcatheter closure of sinus venosus atrial septal defect with anomalous drainage of right upper pulmonary vein into superior vena cava--an innovative technique. Catheter Cardiovasc Interv. 2014 Sep 1;84(3):473-7. doi: 10.1002/ccd.25502. Epub 2014 Apr 23. PMID: 24753393.
12. Hansen JH, Duong P, Jivanji SGM, Jones M, Kabir S, Butera G, Qureshi SA, Rosenthal E. Transcatheter Correction of Superior Sinus Venosus Atrial Septal Defects as an Alternative to Surgical Treatment. J Am Coll Cardiol. 2020 Mar 24;75(11):1266-1278. doi: 10.1016/j.jacc.2019.12.070. PMID: 32192652.
13. Batteux C, Azarine A, Karsenty C, Petit J, Ciobotaru V, Brenot P, Hascoet S. Sinus Venosus ASDs: Imaging and Percutaneous Closure. Curr Cardiol Rep.
14. Batteux C, Meliani A, Brenot P, Hascoet S. Multimodality fusion imaging to guide percutaneous sinus venosus atrial septal defect closure. Eur Heart J 2020.
15. Stephenson N, Rosenthal E, Jones M, Deng S, Wheeler G, Pushparajah K, Schnabel JA, Simpson JM. Virtual Reality for Preprocedure Planning of Covered Stent Correction of Superior Sinus Venosus Atrial Septal Defects. Circ Cardiovasc Interv. 2024 Nov 5:e013964. doi: 10.1161/CIRCINTERVENTIONS.123.013964. Epub ahead of print. PMID: 39498563; PMCID: PMC7616809.
16. Rosenthal E, Qureshi SA, Jones M, Butera G, Sivakumar K, Boudjemline Y, Hijazi ZM, Almaskary S, Ponder RD, Salem MM, Walsh K, Kenny D, Hascoet S, Berman DP, Thomson J, Vettukattil JJ, Zahn EM. Correction of sinus venosus atrial septal defects with the 10 zig covered Cheatham-platinum stent - An international registry. Catheter Cardiovasc Interv. 2021 Jul 1;98(1):128-136. doi: 10.1002/ccd.29750. Epub 2021 May 7. PMID: 33909945.
17. El-Andari R, Moolla M, John K, Slingerland A, Campbell S, Nagendran J, Hong Y, Mathew A. Outcomes Following Surgical Repair of Sinus Venosus Atrial Septal Defects: A Systematic Review and Meta-Analysis. J Am Heart Assoc. 2024 Jun 18;13(12):e033686. doi: 10.1161/JAHA.123.033686. Epub 2024 Jun 14. PMID: 38874063; PMCID: PMC11255747.

18. Sagar P, Sivakumar K, Thejaswi P, Rajendran M. Transcatheter Covered Stent Exclusion of Superior Sinus Venosus Defects. J Am Coll Cardiol. 2024 Jun 4;83(22):2179-2192. doi: 10.1016/j.jacc.2024.03.417. PMID: 38811095.
19. Paul A. Yushkevich, Joseph Piven, Heather Cody Hazlett, Rachel Gimpel Smith, Sean Ho, James C. Gee, and Guido Gerig. User-guided 3D active contour segmentation of anatomical structures: Significantly improved efficiency and reliability. Neuroimage 2006 Jul 1;31(3):1116-28.
20. Butera G, Sturla F, Pluchinotta FR, Caimi A, Carminati M. Holographic Augmented Reality and 3D Printing for Advanced Planning of Sinus Venosus ASD/Partial Anomalous Pulmonary Venous Return Percutaneous Management. JACC Cardiovasc Interv. 2019 Jul 22;12(14):1389-1391. doi: 10.1016/j.jcin.2019.03.020. Epub 2019 May 15. PMID: 31103542.
21. Sivakumar K. How to do it? Transcatheter correction of superior sinus venosus defects. Ann Pediatr Cardiol. 2022 Mar-Apr;15(2):169-174. doi: 10.4103/apc.apc_92_21. Epub 2022 Aug 19. PMID: 36246755; PMCID: PMC9564414.
22. Anselmino M, Blandino A, Beninati S, Rovera C, Boffano C, Belletti M, Caponi D, Scaglione M, Cesarani F, Gaita F. Morphologic analysis of left atrial anatomy by magnetic resonance angiography in patients with atrial fibrillation: a large single center experience. J Cardiovasc Electrophysiol. 2011 Jan;22(1):1-7. doi: 10.1111/j.1540-8167.2010.01853.x. PMID: 20662985.
23. Ng LY, Nolke L, James A, Grant B, Franklin O, Redmond JM, McGuinness J, Walsh K, McMahon CJ. Multimodality imaging in delineation of complex sinus venosus defects and treatment outcomes over the last decade. Cardiol Young. 2022 Jul;32(7):1112-1120. doi: 10.1017/S1047951121003851. Epub 2021 Sep 15. PMID: 34521491.
24. Callahan R, Gillespie MJ. Transcatheter Superior Sinus Venosus Defect Closure: Experience Increases Patient Eligibility. J Am Coll Cardiol. 2024 Jun 4;83(22):2193-2195. doi: 10.1016/j.jacc.2024.04.017. PMID: 38811096.
25. Tandon A, Burkhardt BEU, Batsis M, Zellers TM, Velasco Forte MN, Valverde I, McMahan RP, Guleserian KJ, Greil GF, Hussain T. Sinus Venosus Defects: Anatomic Variants and Transcatheter Closure Feasibility Using Virtual Reality Planning. JACC Cardiovasc Imaging. 2019 May;12(5):921-924. doi: 10.1016/j.jcmg.2018.10.013. Epub 2018 Dec 12. PMID: 30553676.

Tables

Demography (n = 197)	
Age at CT (year) Median (range), SD	43 (17-62), 0.9 to 86.5
Female/Male (%)	55/45
Tall (cm) Median (range), SD	163 (153 - 172), 54 to 190
Height (kg) Median (range), SD	64 (48-75), 9 to 121
Associated lesions, n (%)	*42 (21)*
LSVC	30 (15)
ASD/PFO	16 (8)
Over-riding, n (%)	197 (100)
OR -	75 (38)
<50%	94 (48)
50%	14 (7)
>50%	14 (7)
Caudal extension, n (%)	197 (100)
Positive	137 (70)
No	30 (15)
Negative	30 (15)
subgroup >18 yo, mm (range)	
n = 143	
Positive	12.5 (7- 16)
No, n (%)	n = 21 (15)
Negative	7.5 (12 -4)
Number of total RPV ostia (% of patients)	2 (4%); 3 (55%); 4 (35%), 5 (5%); 6 (1%)
Additional abnormal vein ostia, %	
0	52%
1	43% (supra 47%; infra 53%)
2	5% (supra + infra 66%; supra + supra 34%)

Table 1 : Population and 3D parameters
Range represents the 1st and the 3rd quartil (Q1 and Q3).

	All (n = 197)	*Subgroup >18 yo (n = 143)*
SVC* max diameter, mm (Q1-Q3)		
at IV †	16 (13 - 18)	*17 (14-18)*
at upper abnormal ostia	17 (15-19)	*18 (16-20)*
at main abnormal ostia	19 (16-25)	*20 (18-23)*
at cavo-atrial junction	27 (23-31)	*28.5 (25-32)*
Distance upper APVR - IV‡ mm (Q1-Q3)	29 (20-38)	33 (25-41)
Distance upper APVR – defect mm (Q1-Q3)	38 (30-51)	42 (33-53)
Abnormal pulmonary vein ostia	**Main pulmonary vein ostia (n = 196)**	
Max diameter, mm (Q1-Q3)	19 (15.5 - 23.5)	
Min diamer, mm (Q1-Q3)	12 (9 - 15)	
Frontal orientation, degree (Q1-Q3) SD	15 (5 - 25) 0 to 355	
Axial orientation, degree (Q1-Q3) SD	15 (5 - 25) 0 to 355	
clockwise, hour time (Q1-Q3) SD	9:30 (9 - 10) 6 to 12	
	1 additional pulmonary vein ostia (n = 84)	
Supra/Infra (%)	47/53	
Max diameter, mm (Q1-Q3)	10 (7 - 12)	
Min diameter, mm (Q1-Q3)	8 (6 - 10)	
Frontal orientation, degree (Q1-Q3) SD	40 (25 - 70) 0 to 355	
Axial orientation, degree (Q1-Q3) SD	60 30 - 85) 0 to 355	
clockwise, hour time (Q1-Q3) SD	10:30 (10 - 11:30) 6:30 to 14	
	2 additional pulmonary veins ostia (n = 10)	
Supra + supra (%)	34%	
Supra+ infra (%)	66%	
Infra + infra (%)	0%	
Max diameter, mm (Q1-Q3e)	7.5 (7 - 8)	
Min diamer, mm (Q1-Q3)	6.4 (6 - 6.75)	
Frontal orientation, degree (Q1-Q3) SD	280 (35 - 300) 20 to 330	
Axial orientation, degree (Q1-Q3) SD	270 (70 - 330) 0 to 355	
clockwise, hour time (Q1-Q3) SD	10 (9 - 11) 8 to 11:30	

Table 2 : 3D measurements
* Superior vena cava, † Innominate Vein, ‡ distance between innominate vein and upper abnormal pulmonary vein return.
Degrees angulation is explained in Figure 5A/B.

SVC * max diameter mm (Q1-Q3)	>18 yo (LSVC +) ‡	>18 yo (LSVC -)	p value
at IV †	*13 (11-14)*	*17 (15-19)*	*p<0.001*
at upper abnormal ostia	*14 (12-16)*	*18 (16-20)*	*p = 0.005*
at main abnormal ostia	*15 (14-17.75)*	*20 (19-23)*	*p <0.001*
at cavo-atrial junction	*27 (23-28.5)*	*29 (25-33)*	*p = 0.052*

Table 3: Right SVC diameter if LSVC associated or not.
*Superior vena cava, † Innominate vein, ‡ left superior vena cava

Adults (n = 143)	Q1 (mm)	Median (mm)
SVC* diameter		
at IV †	14	17
at upper abnormal ostia	16	18
at main abnormal ostia	18	20
at cavo-atrial junction	25	28.5
Distance upper APVR-IV ‡	25	33
Distance upper APVR-defect	33	42
Children 12-18 yo (n = 12)	**>/= Q1 (mm)**	**>/= Median (mm)**
SVC diameter, %		
at IV	83	42
at upper abnormal ostia	50	50
at main abnormal ostia	92	58
at cavo-atrial junction	75	58
Distance upper APVR-IV, %	83	42
Distance upper APVR-defect, %	92	33
Distance upper APVR-IV > 20 mm, %	92	

Table 4 : repartition in % of children between 12 and 18 years-old having SVC diameters and lengths superior to the first interquartile range (Q1) and superior to the median of adult population.
*Superior vena cava, † Innominate vein, ‡ distance between innominate vein and upper abnormal pulmonary vein return

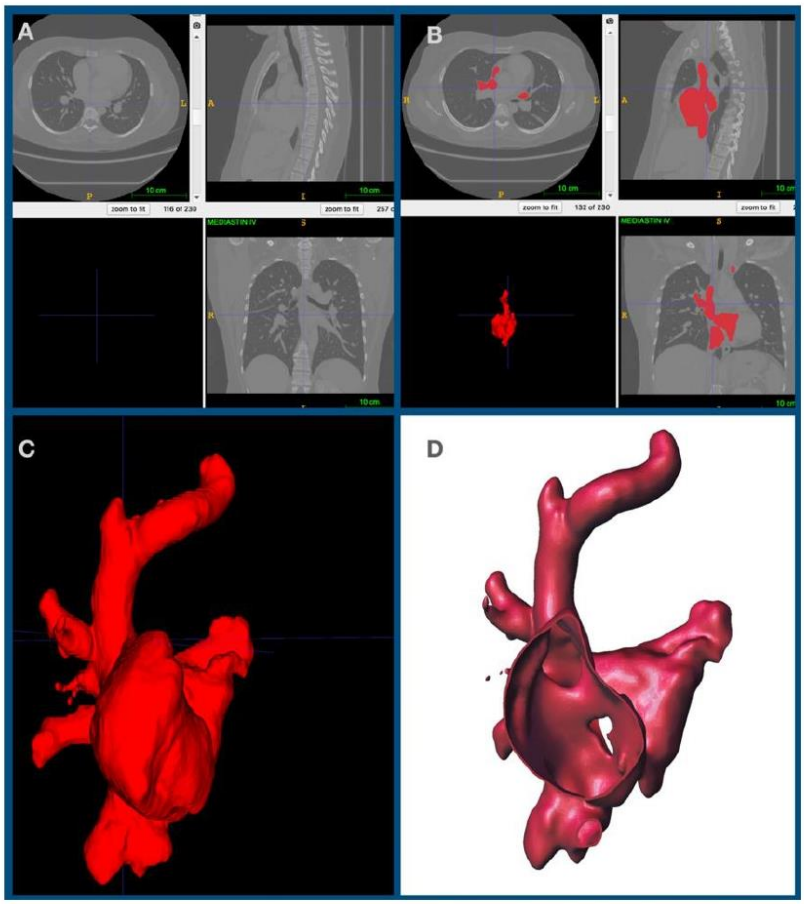

Figure 1: 3D modeling of SVD with semi-automatic segmentation using Itk-snap® and Meshmixer® softwares

A: Original images in the 3 orthogonal plans (axial, sagittal, frontal).

B: Semi-automatic segmentation using active contouring method on ITK-snap® software.

C: Result of semi-automatic segmentation on ITK-snap® allowing the save as a STL model. Note that the 3D model is full, representing the blood inside the anatomic structure.

D: Result of post-processing treatment on Meshmixer®, after polishing and creation of an external 0.7 mm shell, permitting the obtention of an empty model. This process allows 3D navigation and 3D measurements.

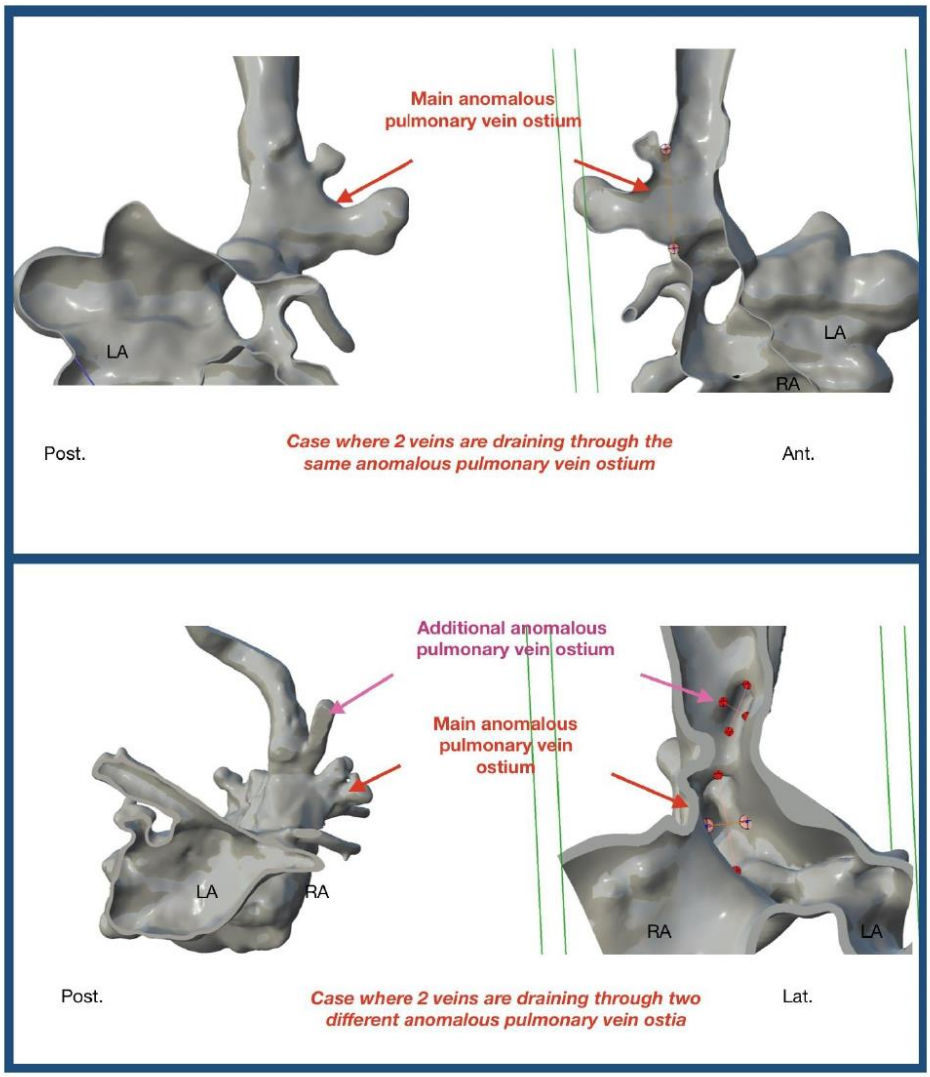

Figure 2: Pulmonary vein ostia analysis and measurements

Exemple of 2 distincts APVR configuration (LA : left atrium, RA : right atrium)

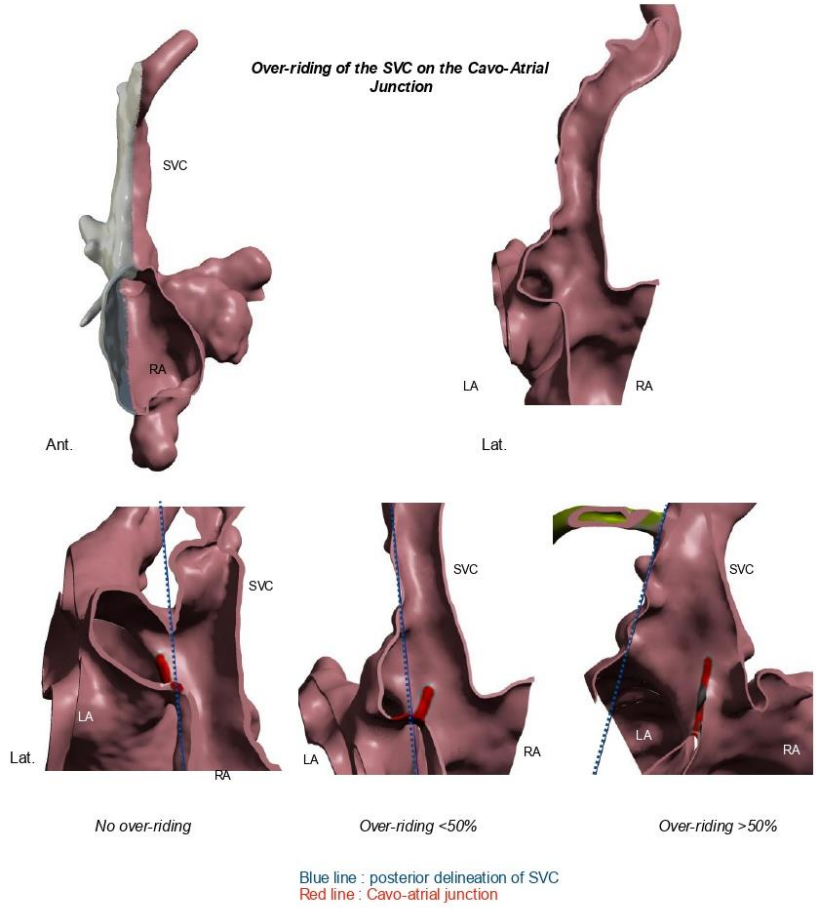

Figure 3 : Over-riding analysis process (SVC : superior vena cava, RA : right atrium, LA : left atrium)

A plan cutt is done vertically to the SVC in frontal view, passing through the azygos vein axis (up-left image)

Analysis of the over-riding is then performed from right lateral view (up-right image) by marking the cavo-atrial junction (red line) and delineating the posterior side of the superior vena cava.

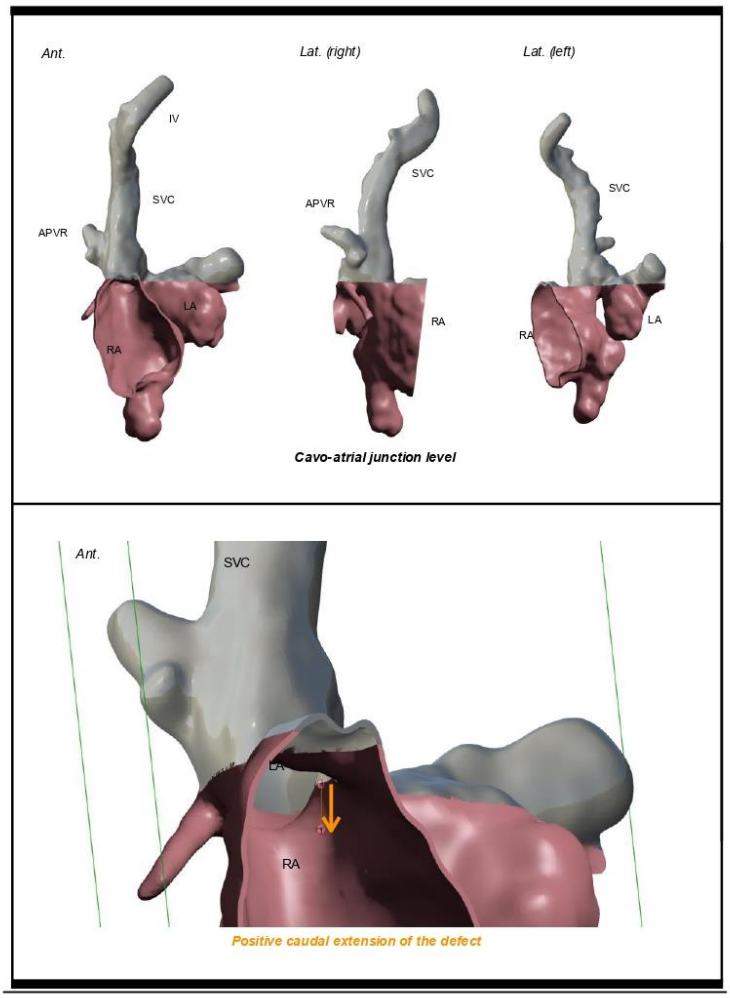

Figure 4: Caudal extension analysis process (IV : innominate vein, APVR : abnormal pulmonary vein return, SVC : superior vena cava, RA: right atrium, LA : left atrium)
A plan cutt is made horizontally to the SVC at the superior level of the cavo-atrial junction.
Caudal extension is evaluated from inside RA view, by measuring the distance between the superior level of the cavo-atrial junction and the upper margin of the defect between RA and LA.
Measurement in millimeters is noted positive if the margin of the defect is below CAJ, and negative if margin of the defect above the CAJ.

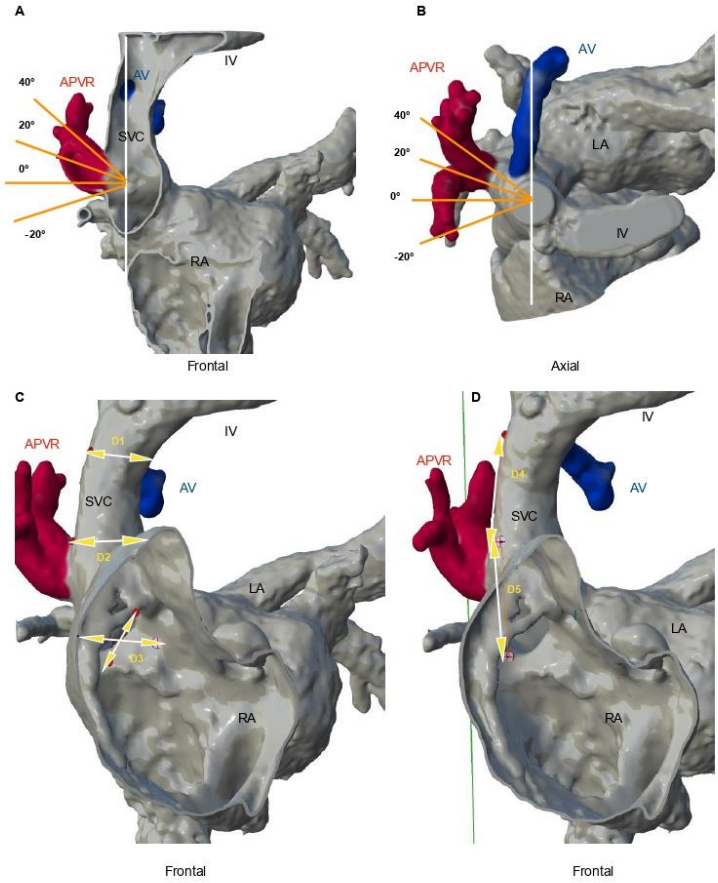

Figure 5 : 3D measurements

RA and LA : right and left atria, IV : innominate vein, AV : azygos vein, SVC : superior vena cava, APVR : abnormal pulmonary vein return.

A and B: Angulated connection (in degree) of abnormal pulmonary vein ostia with superior vena cava or cavo-atrial junction in frontal (A) and axial (B) view.

C: Maximum SVC diameters (in millimeters) measured at different levels: the innominate vein (D1), the upper anomalous pulmonary vein ostium (if any), the main anomalous pulmonary ostium (D2) and at cavo-atrial junction (D3).

D : Distance (in millimeters) between the upper anomalous pulmonary vein ostium and the level of the innominate vein (D4) and distance (in millimeters) between the upper anomalous pulmonary vein ostium and the lower edge of the communication between the two atrial chambers (D5).

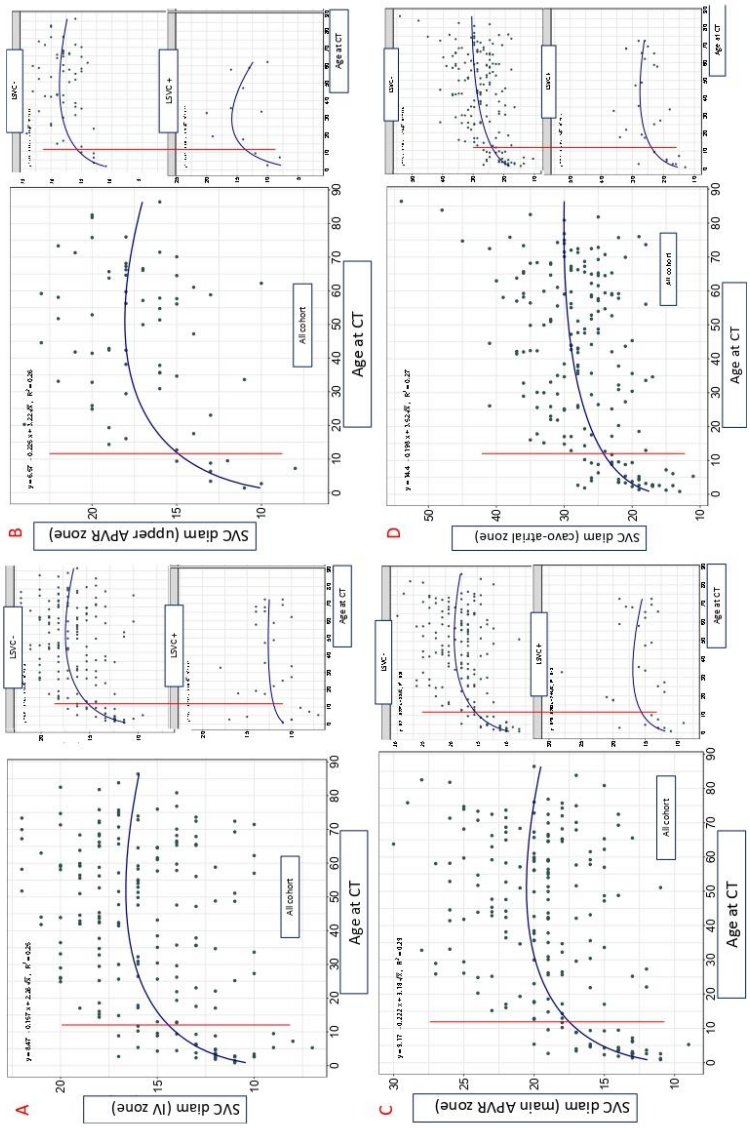

Figure 6 : repartition of SVC diameter (millimeters) at different level in the global population and if LSVC is present or absent, depending on age using quadratic square-racked equation.

Panel A : innominate vein level, panel B upper APVR level, panel C : main APVR level, panel D : cavo-atrial junction level. A red line is put at the age 12 in all panels.

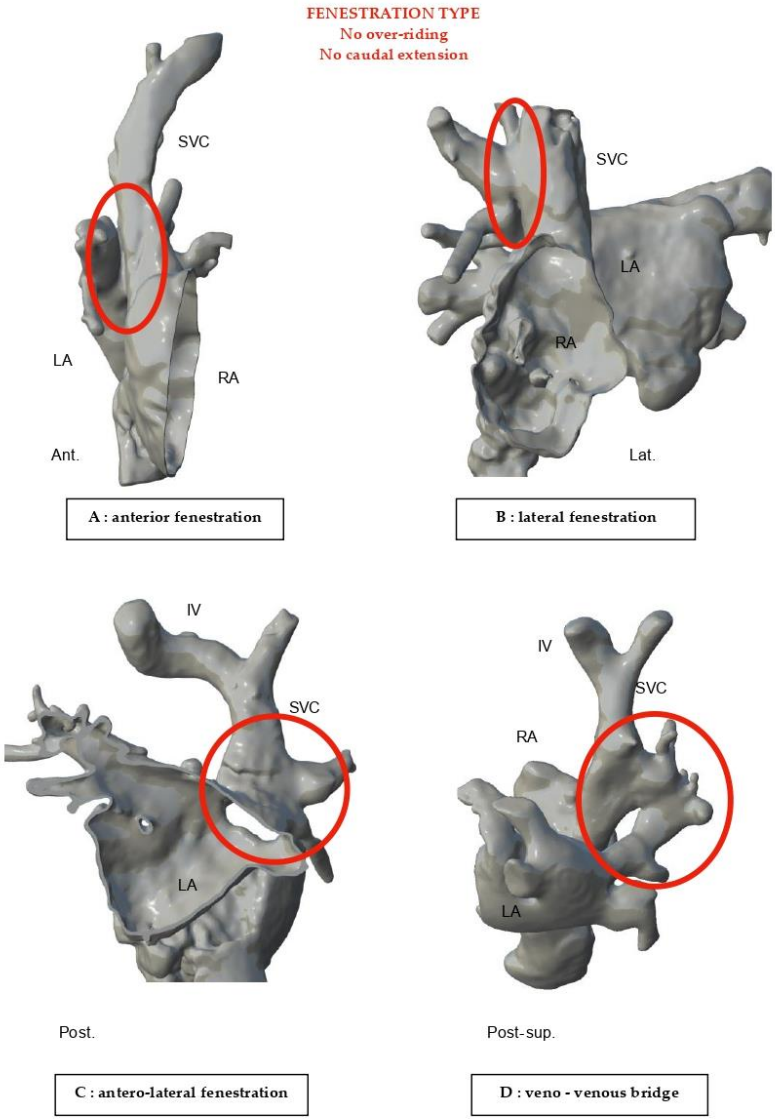

Figure 7: Fenestration type

RA: right atrium, LA : left atrium, SVC : superior vena cava, IV : innominate vein

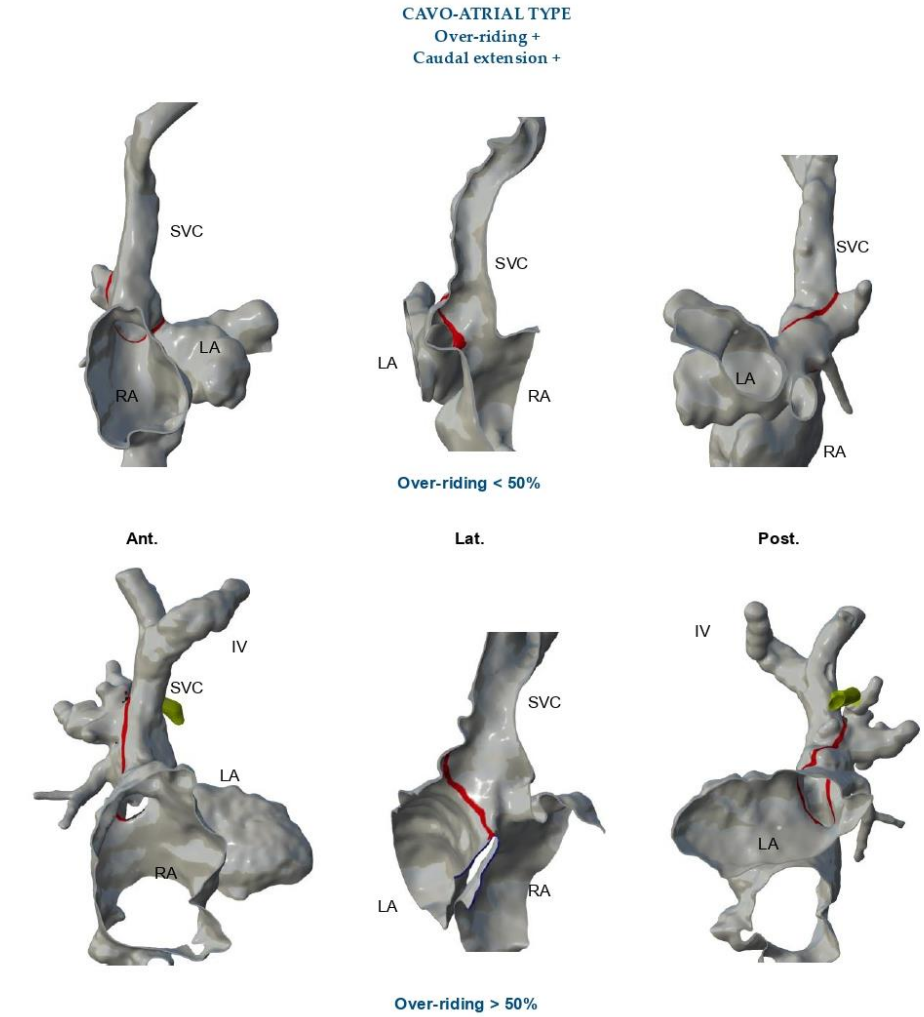

Figure 8: Cavo-atrial type

RA: right atrium, LA : left atrium, SVC : superior vena cava, IV : innominate vein

Red line : delineation of the communication zone depending on degree of over-riding.

Green vein (if any): azygos vein.

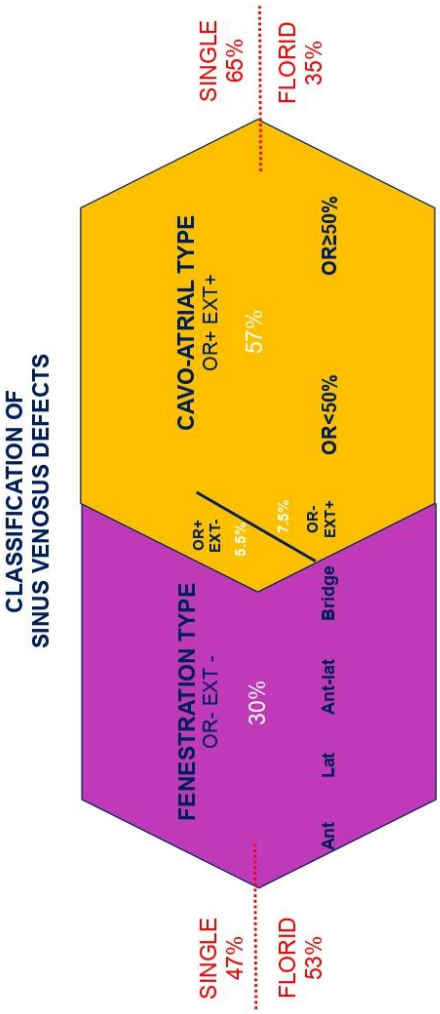

Figure 9: Classification of sinus venosus defects (OR : over-riding, EXT : caudal extension, single : one single main abnormal ostia, florid : presence of additional abnormal ostia).

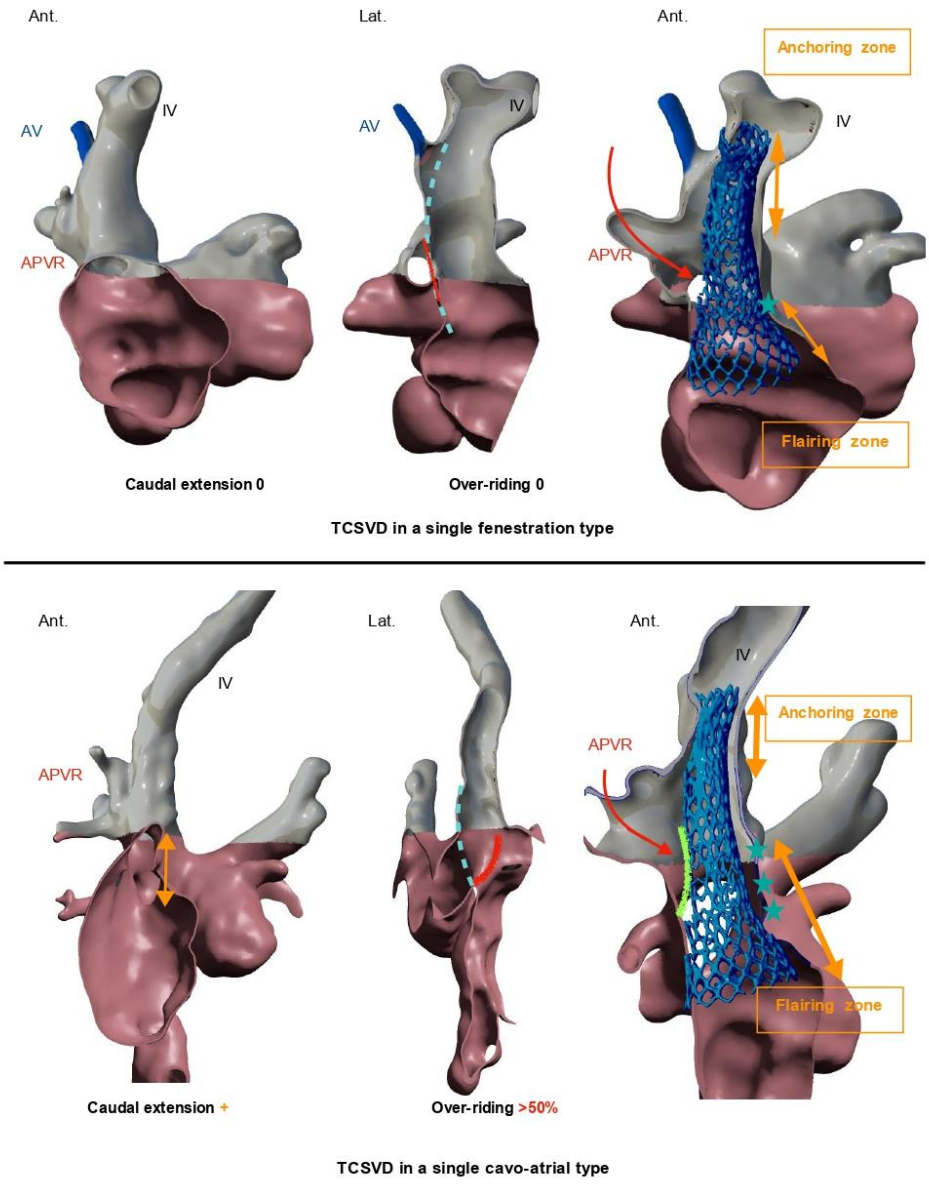

Figure 10 : virtual simulation depending on anatomical type

Implantation of an Optimus XXL® covered stent (Andratec) previously reconstructed.

Blue dotted line : superior vena cava delineation. Red line : cavo-atrial junction. Red arrow : APVR pathway to the LA after stent placement. Green star : possible shunting zone. Green line : possible obstruction zone for APVR ostia channel to LA.

II. Développement d'un programme de simulation de correction transcutannée des CIA Sinus Venosus

ARTICLE ORIGINAL 2 : SIMUVENOSUS

Transcatheter correction of sinus venosus defect : results of simulation program (en cours de review dans Canadian Journal of Cardiology)

Canadian Journal of Cardiology

TRANSCATHETER CORRECTION OF SINUS VENOSUS DEFECT:RESULTS OF A SIMULATION PROGRAM

--Manuscript Draft--

Manuscript Number:	
Article Type:	Original Research Basic
Corresponding Author:	Clément Batteux, MD Marie-Lannelongue Hospital Le Plessis Robinson, FRANCE
First Author:	Clément Batteux, MD
Order of Authors:	Clément Batteux, MD
	Vlad Ciobotaru, MD
	Slimane Idir
	Delphine Chevalier
	Hélène Beaussier
	Régine Roussin, MD
	Benoit Decante
	Océane Hache
	Florence Lecerf
	Clément Karsenty, MD, PhD
	Nicolas Combes, MD
	Antoine Agathon
	Grégoire Albenque, MD
	Sébastien Hascoet, MD, PhD
Abstract:	Introduction Transcatheter correction of sinus venosus defect (TC-SVD) with covered stent is a new therapeutic option. Its success rely on achieving complete shunt occlusion, free re-routed pulmonary vein patency, and device stability. We sought to develop a multimodality simulation program to enhance safety and efficiency of TC-SVD. Methods For each patient referred, a 3D heart model was produced from cardiac computed tomography. A stent tailored to anatomical parameters was virtually implanted on the digital twin. 3D heart model was printed for each patient. Printing material evolved with the aim to mimic heart tissue characteristics with echogenicity and radio-transparency. The 3D heart model was plugged in a perfused bench test to perform individualized hands-on simulation training (HOST) and stent implantation using a similar method compared to clinical practice. Results From March 2020 to January 2023, 15 patients had TC-SVD with previous virtual simulation, of whom 10 patients had also HOST on the 3D printed heart model. At the end of the study period, the bench-test fulfilled the several expectations. It allowed a TC-SVD HOST in condition close to reality, guided by transesophageal echocardiography, fluoroscopy and fusion imaging between CT-scan and fluoroscopy. The steps included balloon testing in the superior vena cava, pulmonary veins protection with a balloon when necessary and stent implantation in the superior vena

	cava. In all 15 patients was achieved a successful clinical procedure with results close to in-vitro testing Conclusion A multimodality simulation program contributed to excellent outcomes of TC-SVD in a preliminary new therapeutic program.
Suggested Reviewers:	alain fraisse A.Fraisse@rbht.nhs.uk specialist on congenital heart diseases and sinus venosus transcatheter therapy
	eric rosenthal Eric.Rosenthal@gstt.nhs.uk specialist /KOL on sinus venosus defect and congenital heart disease
	damien kenny damien_kenny@icloud.com specialist on congenital heart disease Cath intervention and sinus venosus
	gareth morgan drgarethjmorgan@gmail.com specialist on congenital heart disease and device development and research
	pablo tome pablo.tome@me.com specialist in SVD correction and device research and development

TRANSCATHETER CORRECTION OF SINUS VENOSUS DEFECT: RESULTS OF A SIMULATION PROGRAM

Clément **Batteux** MD, PhD student[1,2]; Vlad **Ciobotaru** MD, PhD student[2,3]; Slimane **idir**[1] ; Delphine **Chevalier**[1]; Hélène **Beaussier**[1] Pharm D; Régine **Roussin**[1] MD; Benoit **Decante**[1]; Océane **Hache**[1]; Florence **Lecerf**[1]; Clement **Karsenty**, MD, PhD[4]; Nicolas **Combes**, MD[4]; Antoine **Agathon**[1]; Grégoire **Albenque** MD, MSc[1]; Sébastien **Hascoet** MD, PhD, FESC[1,2].

1. Hôpital Marie Lannelongue, centre de référence réseau maladies rares M3C cardiopathies congénitales complexes, Faculté de médecine Paris-Saclay, Université Paris-Saclay, 133 avenue de la résistance, 92350 Le Plessis Robinson, France
2. INSERM UMR-S 999, Université Paris-Saclay, 92350 Le Plessis Robinson, France
3. Clinique Franciscaine, CHU Nîmes, 3DHeartmodeling, Nîmes, France
4. Chu Toulouse, Clinique Pasteur, 31000 Toulouse, France

Corresponding author : Clément Batteux (cbatteux@ghpsj.fr)

Disclosures

Sebastien Hascoet, proctoring support for Abbott vascular, Edwards Lifesciences and Venus Medtech.
The other authors declare they have no conflict of interests.

Funding

Association le Coeur dans la main

Association pour la recherche et le développement en radiologie interventionnelle

Fédération française de cardiologie

Fondation hospital saint joseph

Aknowledgements : William Arditi, Roxane Nguyen-Quemper, IMT mines Alès, Centrale Supelec school, Andreas Kohl, Pierre Landreau, Mika Gkogkou.

Structured abstract

Introduction

Transcatheter correction of sinus venosus defect (TC-SVD) with covered stent is a new therapeutic option. Its success rely on achieving complete shunt occlusion, free re-routed pulmonary vein patency, and device stability. We sought to develop a multimodality simulation program to enhance safety and efficiency of TC-SVD.

Methods

For each patient referred, a 3D heart model was produced from cardiac computed tomography. A stent tailored to anatomical parameters was virtually implanted on the digital twin. 3D heart model was printed for each patient. Printing material evolved with the aim to mimic heart tissue characteristics with echogenicity and radio-transparency. The 3D heart model was plugged in a perfused bench test to perform individualized hands-on simulation training (HOST) and stent implantation using a similar method compared to clinical practice.

Results

From March 2020 to January 2023, 15 patients had TC-SVD with previous virtual simulation, of whom 10 patients had also HOST on the 3D printed heart model. At the end of the study period, the bench-test fulfilled the several expectations. It allowed a TC-SVD HOST in condition close to reality, guided by transesophageal echocardiography, fluoroscopy and fusion imaging between CT-scan and fluoroscopy. The steps included balloon testing in the superior vena cava, pulmonary veins protection with a balloon when necessary and stent implantation in the superior vena cava. In all 15 patients was achieved a successful clinical procedure with results close to in-vitro testing

Conclusion

A multimodality simulation program contributed to excellent outcomes of TC-SVD in a preliminary new therapeutic program.

Key-words

Sinus venosus, transcatheter therapy, interventional cardiology, virtual simulation, 3D printing, hands-on simulation training, congenital heart disease.

MeSH terms

Congenital heart disease, 3D printing, Sinus venosus.

ABBREVIATIONS

APVR: anomalous pulmonary vein return

HOST: hands-on simulation training

LA : left atrium

RA : right atrium

SVD : sinus venosus defect

TC-SVD : Transcatheter correction of sinus venosus defect

INTRODUCTION

Sinus venosus defect (SVD) is a rare congenital heart disease characterized by an inter-atrial shunt located at the superior cavo-atrial junction. This condition is frequently associated with an abnormal pulmonary vein return (APVR) of one or more components of the right pulmonary veins into the superior vena cava (SVC) [1-3]. The chronic left-to-right shunt associated with SVD can lead to significant complications, including pulmonary hypertension and supraventricular arrhythmias, thereby necessitating timely intervention. Surgical repair remains the gold standard treatment option for preventing these adverse outcomes [4].

In recent years, transcatheter correction of sinus venosus defect (TC-SVD) has emerged as a promising alternative therapeutic strategy for selected patients who are at increased risk for surgical intervention [5]. The TC-SVD procedure involves the placement of a covered stent extending from the SVC into the right atrium (RA) to effectively halt the shunting mechanism and redirect the flow from the abnormal pulmonary vein to the left atrium (LA). The success of this procedure is critically dependent on the patient's anatomical features, which must be conducive to stable stent implantation. This includes avoiding occlusion of the abnormal pulmonary vein return while also preventing residual shunting. Moreover, the stent utilized must be appropriately sized and shaped to accommodate the SVC, making precise sizing, positioning, and configuration vital for the success of the procedure [6, 7].

Currently, there are no commercially available devices specifically labeled for TC-SVD. The commonly employed devices, such as the 10-Zig covered Cheatham-platinum stent (CP10Z stent, Numed) [8] and the covered OPTIMUS XXL stent (Andratec) [9], do not have European certification, and their usage typically relies on compassionate approval from national health authorities. These devices are designed to offer sufficient length, conformability, and variability in diameter to adapt to the unique anatomical considerations of each patient. A thorough three-dimensional (3D) understanding of these anatomical characteristics is essential for assessing the feasibility of TC-SVD [10, 11].

Advancements in 3D heart modeling and bench-testing have emerged as invaluable pre-procedural tools [12] for planning complex transcatheter cardiac interventions. These interventions encompass a range of procedures, including left atrial appendage closure [13], paravalvular leakage closure [14], and pulmonary valve implantation [15], among others. The advantages of adopting a 3D modeling approach and utilizing hands-on simulation training (HOST) in interventional cardiology are numerous. These include the optimization of the learning curve for practitioners, assessment of procedural feasibility, anticipation of potential complications, and contributions to research and development of innovative devices [16-18]. Moreover, health authorities, surgical teams, and patients have expressed a strong interest in a simulation program designed to validate the feasibility of TC-SVD prior to actual procedures.

Despite some existing cases where 3D printing has been applied in the planning of TC-SVD, a standardized simulation that closely mimics reality has yet to be fully developed [19-21]. The primary objective of this study was to develop, validate, and establish a comprehensive TC-SVD simulation program, integrating numerical twins and HOST utilizing 3D printed models.

METHODS

1. Study Design and Ethical Considerations

A prospective single-center cohort study was designed to include all patients undergoing transcatheter SVD correction. The study protocol received approval from a local ethics

committee (IRB 00012157). The detailed step-by-step TC-SVD simulation program is illustrated in Figure 1. Once the simulation program was completed, the data were analyzed in a multidisciplinary meeting to refine the in-vivo TC-SVD strategy as necessary.

2. 3D Reconstruction and Virtual Simulation

For each patient, Digital Imaging and Communication in Medicine (DICOM) images were extracted from cardiac computed tomography (CT). The heart was segmented, and a 3D heart model was created in standard tessellation language (STL) format using dedicated segmentation software (itksnap.org). ITK-SNAP® is an open-source collaborative software that provides semi-automatic segmentation through active contour methods, in addition to manual delineation and image navigation[22-24]. The 3D heart model was subsequently imported into Meshmixer® software (Autodesk, San Francisco, USA) to generate a digital twin in 3D mesh coordinates, facilitating precise measurements and navigation [20, 22]. Various anatomical parameters were assessed, including SVC dimensions, the degree of overriding, left SVC associations, and the number and positioning of APVR components.

Additionally, 3D models of covered stents were derived from CT scans of patients who had previously undergone transcatheter SVD correction (Figure 2). The stent that best fit the heart model was then virtually implanted on the digital twin to simulate the procedure. Manual adjustments were made to align the stent with the SVC wall and redirect the APVR to the LA. Expected stent stability, patency of the APVR to the LA, and the risk of residual shunting were carefully evaluated to estimate the feasibility of the procedure, and stent dimensions were recorded (Figure 3).

3. 3D Printing

Technical specifications for the 3D printed model were provided to a partner specializing in 3D printing within cardiology (3DHeart Modeling, Caissargues, France) [25]. Collaborative research and development efforts between the medical team and the printing company were undertaken to ensure that the printed material mimicked the deformability and solidity of human cardiac tissue to support stent implantation. The model needed to be

easily integrated into bench testing, waterproof, and possess sufficient radiotransparency and echogenicity to accurately simulate the procedure under realistic conditions.

4. Bench Test and HOST

A dedicated bench test was developed to facilitate the seamless integration of the 3D printed model with a water pump, which simulated blood circulation. The pump was connected to both the SVC and the APVR, allowing for the assessment of flow dynamics in the right and left sides of the heart following stent implantation. Imaging guidance during the bench tests aimed to replicate the imaging modalities used in the catheterization laboratory, incorporating fluoroscopy, trans-oesophageal echography, and fusion imaging techniques between fluoroscopy and cardiac CT. HOST was conducted in a catheterization laboratory dedicated to clinical research.The bench test was designed to allow for a step-by-step simulation of TC-SVD, including compliant balloon testing, semi-compliant balloon testing, and stent implantation, as previously reported [26, 27]. Connections were established to facilitate the implantation of a stiff guidewire through the femoral and jugular veins (femoro-jugular rail). The use of a vascular angioplasty balloon to maintain patency of the APVR pathway was also incorporated if necessary. Angiographic and colorimetric tests were performed post-stent implantation to verify pulmonary vein patency and shunt occlusion. Colorimetric injections of iodinated contrast were used to visually confirm the patency of the APVR and the suppression of left-to-right shunting (supplementary material). A cone-beam CT (CBCT) of the 3D printed model post-stent implantation was performed to generate a comprehensive model for further assessment of the feasibility and efficacy of the in-vitro procedure.

5. In-Vivo TC-SVD Correction

The procedures were performed using a methodology similar to previously reported techniques [26, 27]. Briefly, procedures were conducted under general anesthesia with multimodal imaging guidance, including trans-oesophageal echography and fusion imaging between echocardiography and fluoroscopy (Echonavigator, Philips, Netherlands) and between CT scans and fluoroscopy (Vesselnavigator, Philips, Netherlands) [28, 29]. The initial phase of the procedure involved balloon testing in the SVC[30,31] to evaluate distensibility by

inflating a compliant balloon at its upper level, establishing the target diameter for the stent. A semi-compliant balloon was then inflated in the SVC at the APVR level, corresponding to the predicted stent diameter, to assess the risk of pulmonary vein obstruction. If deemed necessary, a transseptal puncture was performed, and a vascular angioplasty balloon was placed in the pulmonary vein to the left atrium.

The second phase of the procedure involved positioning and inflating a balloon-expandable covered stent in the SVC. An additional post-inflation was generally performed at the inferior section of the stent to secure it to the cavo-atrial junction and prevent residual shunting [30, 31].

RESULTS

1. **Population Characteristics**

Between March 2020 and January 2023, a total of 15 patients (12 women, 3 men) underwent TC-SVD at our institution. The median age was 59 years (range: 18 to 75). Of these, ten patients were deemed unsuitable for SVD surgery due to comorbidities identified during multidisciplinary meetings: 7 patients were being treated for pulmonary hypertension, 4 had heart failure, 2 were classified as obese with a body mass index exceeding 30, and 6 were over 70 years old. The remaining 5 patients were free from significant comorbidities, and TC-SVD correction was indicated following a comprehensive multidisciplinary discussion informed by the simulation program. All 15 patients underwent virtual simulation on the digital model, with 10 patients receiving additional HOST on the 3D printed models.

2. **Virtual Navigation and Simulation on digital twin**

All patients presented with SVD and APVR within the SVC, each displaying distinct anatomical features (Figure 4). One patient (6%) exhibited a left SVC. Eleven patients had a single APVR component (74%), while two patients had two components, and two had three components (13%). Notably, SVC overriding was observed in six patients, demonstrating varying degrees (<50% n = 3; >50% n = 6. Six patients had veno-venous bridge without over-rirding (40%). The length of the SVC ranged from 49 mm to 85 mm, with a median of 65 mm.

TC-SVD was deemed feasible for all cases following stent implantation in the digital twin. Six cases required APVR protection, and mild residual shunts were anticipated in another six patients based on simulated outcomes. Stent ideal final length ranged from 60 to 95 mm (median 77 mm).

3. **3D Printed Model and Bench Tools**

a. Bench Test Development

Table 1 outlines the progressive improvements made to the simulation bench program over a 34-month timeline. During this period, HOST was successfully conducted on ten different 3D printed models. Optivenosus section relies on the ongoing actual TC-SVD program in France, supported by the final bench's version. The first case's simulation program included 3D reconstruction, virtual simulation and 3D printing with a thermo-poly-urethan model. A custom made covered CP stent was manually inserted inside the 3D model to confirm the procedure feasibility[6].

b. **Printing Material and Technique**

The first 3 models were printed with thermo-poly-urethane (TPU) using selective laser sintering (SLS) technic with a 100 000 euros printer. Polymer cost was 300 euros per model, impression time was 12 hours and deconditioning time was 12 hours. Despite a good solidity and an easy print, radiotransparency and echogenicity were not optimal with this material.
The following 2 models were printed with polyjet on a 70 000 euros printer. Polymer cost was 600 euros per model, impression time was 10 hours and deconditioning time was 5 hours. This material was transparent to the eyes and didn't produced artefact on CBCT but revealed to be fragile when water-immerged and not fully echogenic.
Last models were printed with stereolithography (SLA) on a 24 000 euros printer. Polymer cost was 450 euros per model, impression time was 18 hours and post-printing treatment time was 6 hours. Best balance between solidity, echogenicity and water-resistancy was found with this printed material. Figure 5.

In addition to material cost, human-time and expertise regarding conception, production, and reliability-check of the printed models were found to be additional key-factors.

c. **Immersion and Circulation**

The first stent was manually positioned on the 3D printed model (Figure 6a). Subsequently, the next 9 models were plugged on the bench test and stents were implanted under fluoroscopy guidance (General Electric, Boston, USA).Models were initially perfused with an extracorporeal pump to simulate blood circulation (Figure 6b), and in the last models, the circulation system was miniaturized using portative pumps as those used in domestical aquarium (*Cokdez®*).The printed model was immerged and perfused into the sealed tank full of water. It was externally connected by two "venous accesses" represented by DrySeal 20 french sheaths in right jugular vein and right femoral vein. Left heart circulation consisted in right pulmonary veins inflow and mitral annulus outflow. Right heart circulation consisted in an innominate vein inflow and a tricuspid annulus outflow (Figure 6c).

d. **Multimodal Guidance**

Trans-oesophageal echography served as guidance modality for TCSVD procedures[30]. The 3D printed models were continually updated to permit stable and accurate probe positioning during testing, thereby enhancing accuracy and efficiency following patient oesophagus anatomy(Figure 7). Fusion imaging guidance (HeartVision software, General Electric, Boston, USA)[28, 29] further improved guidance accuracy during stent placement and deployment (Figure 8).

e. **Step-by-Step TC-SVD**

Each step of the TC-SVD procedure was effectively simulated during HOST. 5 of 10 patients were assessed at risk for APVR occlusion requiring PV balloon protection, confirming the virtual simulation findings.

After stent implantation, a tiny to moderate residual shunt was observed in 4 patients and no PV occlusion was observed.

TC-SVD correction was demonstrated as feasible il all patients during HOST.

(Figures 9 and 10).

f. **In-Vitro TCSVD Results and Retro-Validation**

The results of the TC-SVD procedures were validated using colorimetric control and post-HOST CBCT analysis (Figure 11 and supplementary material). Retro-validation procedures compared the 3D models constructed from pre-procedural CT data and the post-bench testing CBCT outputs (Figure 12).

4. **Preliminary Outcomes**

All the 15 patients had successful TCSVD[6, 16,20] during the study period. Main stents implanted were CP10Z (Numed) in 10 cases (60 mm : n= 2; 70 mm : n=3; 80 mm : n= 4; 85 mm : n=1), Optimus XXL 100 mm (Andratec) in 4 cases, and Begraft 58 mm (Bentley) in one case.

All the procedures were conducted with the presence of the printed model in the cath-lab to be manipulated and live-observed including by the echo-interventionist during guidance.

In all patients was achieved a technical success with discharge at day 2. No major adverse events or surgical conversions or re-interventions were encountered.

In 5 cases, an additional bare metal stent was implanted in the SVC at the top of the first stent with partial overlapping, to reinforce stent stability.

APVR patency to left atrium was achieved in all cases.

APVR protection was used in 7 cases (85% reliability from numerical twin prediction and 83% reliability from bench test prediction)

Residual tiny to mild shunting was notified in 5 cases (57% reliability from numerical twin prediction, 66% reliability from bench test prediction) (table 1).

After a median follow up of 35 months ranging from 23 to 47 months, all the patients had improvement in their clinical condition, underscoring the efficacy and safety of the TC-SVD approach.

DISCUSSION

Interventional cardiology has witnessed significant advancements in technology and equipment, enhancing the treatment of cardiovascular diseases. As these interventions

become more sophisticated, the importance of rigorous bench testing for the development and evaluation of interventional devices cannot be overstated [32]. The standardization of our simulation program represents, to our knowledge, the first comprehensive achievement in the TCSVD approach.

The infinite anatomical variation of the sinus venosus defect and the various strategic approaches for TCSVD align well with the design and implementation of this program.

Hansen and his team[19] described in 2020 a preliminary draft of a simulation program for TCSVD, which was based on cross-sectional imaging, virtual simulation, stent implantation in an inert 3D printed model, followed by visual and imaging inspection of the results. We aimed to advance virtual simulation and realistic bench testing for the reasons outlined above.

1. Benefits of Bench Testing

Bench testing allowed the simulation of diverse clinical scenarios, including challenging anatomical features and different TCSVD strategies. This realistic testing environment enables a more accurate assessment of how TCSVD procedures could be performed and how devices perform in various situations, enhancing predictability in real-world applications.

A. Simple Cases

For simple TCSVD cases, where stent implantation appears straightforward, the simulation provided valuable insights into decision-making, helping to avoid trans-septal puncture and pulmonary protection from the left atrium. In some in vivo cases, we were able to proceed confidently without trans-septal puncture or pulmonary vein protection, significantly reducing procedural time and simplifying techniques. This allowed us to focus on critical aspects during the procedure, such as stent positioning and post-inflation to minimize potential residual shunting.

B. Complex Cases

For complex cases, pulmonary veins needing rerouting must be protected from the left atrium due to the risk of obstruction during stent inflation. Challenges include adapting stent shapes to different anatomical areas. At the upper level of impaction, the device must

provide stability to avoid embolization and must be circumferentially impacted with good radial force and minimal recoil. At the mid-level of impaction, the device must show sufficient conformability and smoothness to allow for local deformation provided by the protective balloon. At the lower level (cavo-atrial junction and right atrium), the device must be conformable and dilatable to avoid residual shunting around the stent. Identifying specific challenges and selecting appropriate devices are crucial steps in tailoring the TCSVD to match each individual's unique anatomy.

C. Other Valuable Insights

Some cases initially deemed unsuitable for TCSVD due to anatomical barriers were ultimately found to be feasible after bench testing. Conversely, some complex cases were deemed unsuitable based on simulation findings and were recommended for surgical repair. We provided HOST training for complex cases and less experienced practitioners, receiving positive feedback. Additionally, the use of transesophageal echography during bench testing improved the learning curve for interventionists, familiarizing them with key echo images and for echo-interventionists helping them develop precise guidance techniques tailored to each case.

D. Device Research and Development

Bench testing has yielded significant insights into device research and development. By exposing devices to physiological conditions and stress testing, we have identified potential weaknesses, material fatigue, and design flaws that could compromise safety and efficacy in real-world applications. Under fluoroscopy, we conducted various stent tests, measuring target diameters, burst pressures, lengths, conformability, and foreshortening. Understanding foreshortening through testing is crucial, as underestimating it could result in devices becoming shorter than anticipated, potentially causing the inferior part to “jump” over the defect, leading to significant bidirectional shunting. Bench testing serves as a critical component of quality assurance, ensuring interventional devices meet high safety standards before clinical use. Our research and development efforts led to the creation of a stent specifically tailored for TCSVD, with design requirements including sufficient length, excellent conformability, minimal foreshortening, and proper gripping of the SVC for stability. The second generation of the Optimus XXL stent (80 and 100 mm) was developed

with a 20 mm superior uncovered section to better anchor to the SVC wall. Newly tailored devices are emerging, significantly enhancing the feasibility of TCSVD by overcoming anatomical barriers, such as the JoveVB stent [33] and G-Armor stent [34].

E. Benefits of Fusion Imaging Guidance for TCSVD

The advantages of using fusion imaging guidance for TCSVD interventions can be summarized in two major points. These benefits have been evaluated through both bench testing and in vivo interventions 6,35. Visualization: The 3D model generated from cardiac CT is projected onto the intervention screen and merged with fluoroscopic images, enhancing visual capabilities and providing a comprehensive view of the malformation for all participants. This combined visualization improves understanding and allows for more accurate assessment throughout the intervention. Planning: Anatomical landmarks and planning markers, such as lines, rings, and distances, can be added to the 3D model, facilitating precise device placement, which is crucial for successful intervention. This can enhance confidence and efficiency, potentially speeding up the procedure.

F. Benefits of Cone Beam CT Before and After HOST

By systematically performing pre- and post-HOST CBCT on printed models, we have been able to retro-validate our virtual segmentation, print accuracy, and stability. Analyzing post-HOST CTs has provided insights regarding TCSVD, such as understanding where residual shunting is expected, allowing us to focus on these concerns during in vivo sessions.

2. Prospective Optivenosus Study

As TCSVD is emerging and devices used for TCSVD do not yet have CE marking, the French regulatory health body (ANSM) mandated stringent testing protocols to ensure the safety and effectiveness of new devices for TCSVD. The simulation program achievement detailed in this paper allowed us to validate it as a preoperative requirement for the Optivenosus study (NCT 05865119), which began in January 2023. This prospective comparative cohort study allows for the implantation of Optimus XXL covered stents of 80 and 100 mm lengths before potential CE marking acceptance. The Optivenosus study relies on strict preoperative patient selection criteria for TCSVD, including clinical, anatomical, and bench criteria. By providing comprehensive data on device behavior under various conditions, manufacturers

and physicians can expedite the regulatory approval process, ultimately bringing new technologies to patients more efficiently. Since the beginning of the Optivenosus study, 30 additional patients referred for TCSVD have benefited from the simulation program and subsequent in vivo procedures.

3. Limitations

A. Technical Aspects

While we successfully used a distensible yet robust material in our bench testing, uncertainty remains regarding how closely this material mimics human tissue in terms of distensibility. This uncertainty is compounded by the natural variability in human tissue distensibility, influenced by age and load conditions. Observations from the cath lab reveal that caval and atrial tissues tend to become thinner, more fragile, and more distensible in older patients. Consequently, the potential instability of the device and the degree of residual shunting at the cavo-atrial junction after stent implantation sometimes remain uncertain following bench testing, presenting an area for further investigation.

B. Cost of Bench Testing and Grant Dependence

The cost and availability of devices have been significant limitations in our bench testing. Stents used for TCSVD are expensive, and while some have been generously provided, financial constraints meant not all stents were covered. As a result, we could not assess overall results for cases involving bare-metal stents, particularly regarding residual shunting risks. Nonetheless, post-stent implantation CBCT analysis proved valuable for outcome assessment. Bench testing could potentially reduce costs for companies by providing critical insights into how design modifications affect performance, allowing engineers to refine prototypes before initiating costly clinical trials. A major limitation often cited is the overall cost and sustainability of a simulation program, which requires substantial funding. Financial support is essential until governments recognize it as a reimbursable complementary examination. Potential solutions for continued operation include renting the simulation program or offering it to physicians seeking to enhance their skills or focus on specific cases.

CONCLUSION

TCSVD has become a valuable alternative to surgical repair in adults. Like any new percutaneous intervention, it must be prepared, safe, and efficient. We achieved a comprehensive simulation program to address safety and efficiency endpoints by anticipating, planning, and adapting strategies to tailor the procedure to each patient. This innovative process allows interventionists to prepare for TCSVD procedures finely, addressing specific anatomical challenges.

What is known about this topic?

TC-SVD is a new and challenging procedure where success relies on anatomical features. 3D reconstruction and planning are sometimes used to optimize the success rate of in vivo interventions.

What does this study add?

We established the first comprehensive simulation program for transcatheter correction of sinus venosus defect (TC-SVD), allowing us to approach the intervention under near-realistic conditions using both a digital twin and a perfused printed model. This program has proven valuable for training interventionists and echo-interventionists, enabling customized procedures tailored to patients, anticipating challenges in real-life scenarios, and contributing to the development of new devices specifically designed for this intervention.

References

1) al Zaghal AM, Li J, Anderson RH, Lincoln C, Shore D, Rigby ML. Anatomical criteria for the diagnosis of sinus venosus defects. Heart. 1997 Sep;78(3):298-304. doi: 10.1136/hrt.78.3.298. PMID: 9391294; PMCID: PMC484934.
2) Van Praagh S, Carrera ME, Sanders SP, Mayer JE, Van Praagh R. Sinus venosus defects: unroofing of the right pulmonary veins--anatomic and echocardiographic findings and surgical treatment. Am Heart J. 1994 Aug;128(2):365-79. doi: 10.1016/0002-8703(94)90491-x. PMID: 8037105.
3) Li J, Al Zaghal AM, Anderson RH. The nature of the superior sinus venosus defect. Clin Anat. 1998;11(5):349-52. doi: 10.1002/(SICI)1098-2353(1998)11:5<349::AID-CA11>3.0.CO;2-J. PMID: 9725582.
4) V. Muroke, M. Jalanko, J. Haukka, V. Anttila, T. Pätilä, J. Sinisalo, Long-term outcome after surgical correction of sinus venosus defect in a nationwide register-based cohort study., Int J Cardiol. (2023) 131433.
5) Abdullah HAM, Alsalkhi HA, Khalid KA. Transcatheter closure of sinus venosus atrial septal defect with anomalous pulmonary venous drainage: Innovative technique with

long-term follow-up. Catheter Cardiovasc Interv. 2020 Mar 1;95(4):743-747. doi: 10.1002/ccd.28364.
6) Batteux C, Meliani A, Brenot P, Hascoet S. Multimodality fusion imaging to guide percutaneous sinus venosus atrial septal defect closure. Eur Heart J. 2020 Dec 7;41(46):4444-4445. doi: 10.1093/eurheartj/ehaa292. PMID: 32428931.
7) Riahi M, Velasco Forte MN, et al. Early experience of transcatheter correction of superior sinus venosus atrial septal defect with partial anomalous pulmonary venous drainage. EuroIntervention. 2018 Oct 20;14(8):868-876.
8) Rosenthal E, Qureshi SA, Jones M, et al. Correction of sinus venosus atrial septal defects with the 10 zig covered Cheatham-platinum stent - An international registry. Catheter Cardiovasc Interv. 2021 Jul 1;98(1):128-136. doi: 10.1002/ccd.29750. Epub 2021 May 7. PMID: 33909945.
9) Batteux C, Ciobotaru V, Bouvaist H, Kempny A, Fraisse A, Hascoet S. Multicenter experience of transcatheter correction of superior sinus venosus defect using the covered Optimus XXL stent. Rev Esp Cardiol (Engl Ed). 2023 Mar;76(3):199-201. English, Spanish. doi: 10.1016/j.rec.2022.08.004. Epub 2022 Aug 30. PMID: 36055641.
10) Batteux C, Azarine A, Karsenty C, et al. Sinus Venosus ASDs: Imaging and Percutaneous Closure. Curr Cardiol Rep. 2021 Aug 19;23(10):138. doi: 10.1007/s11886-021-01571-7. PMID: 34410510.
11) Baruteau AE, Hascoet S, Malekzadeh-Milani S, et al. Transcatheter Closure of Superior Sinus Venosus Defects. JACC Cardiovasc Interv. 2023 Nov 13;16(21):2587-2599. doi: 10.1016/j.jcin.2023.07.024. Epub 2023 Oct 18. PMID: 37855807.
12) Abudayyeh I, Gordon B, Ansari MM, Jutzy K, Stoletniy L, Hilliard A. A practical guide to cardiovascular 3D printing in clinical practice: Overview and examples. J Interv Cardiol. 2018 Jun;31(3):375-383. doi: 10.1111/joic.12446. Epub 2017 Sep 25. PMID: 28948646.
13) Ciobotaru V, Combes N, Martin CA, et al. Left atrial appendage occlusion simulation based on three-dimensional printing: new insights into outcome and technique. EuroIntervention. 2018 Jun 20;14(2):176-184. doi: 10.4244/EIJ-D-17-00970. PMID: 29537376.
14) Ciobotaru V, Tadros VX, Batistella M, et al. 3D-Printing to Plan Complex Transcatheter Paravalvular Leaks Closure. J Clin Med. 2022 Aug 15;11(16):4758. doi: 10.3390/jcm11164758. PMID: 36012997; PMCID: PMC9410469.
15) Odemis E, Aka İB, Ali MHA, Gumus T, Pekkan K. Optimizing percutaneous pulmonary valve implantation with patient-specific 3D-printed pulmonary artery models and hemodynamic assessment. Front Cardiovasc Med. 2024 Jan 8;10:1331206. doi: 10.3389/fcvm.2023.1331206. PMID: 38259310; PMCID: PMC10800937.
16) Jivanji SGM, Qureshi SA, Rosenthal E. Novel use of a 3D printed heart model to guide simultaneous percutaneous repair of severe pulmonary regurgitation and right ventricular outflow tract aneurysm. Cardiol Young. 2019 Apr;29(4):534-537. doi: 10.1017/S1047951119000106. Epub 2019 Apr 10. PMID: 30968796.
17) Asif A, Shearn AI, Turner MS, et al. Assessment of post-infarct ventricular septal defects through 3D printing and statistical shape analysis. J 3D Print Med. 2023 Mar;7(1):3DP3. doi: 10.2217/3dp-2022-0012. Epub 2023 Jan 18. PMID: 36911812; PMCID: PMC9990116
18) Batteux C, Haidar MA, Bonnet D. 3D-Printed Models for Surgical Planning in Complex Congenital Heart Diseases: A Systematic Review. Front Pediatr. 2019 Feb 11;7:23. doi: 10.3389/fped.2019.00023. PMID: 30805324; PMCID: PMC6378296.

19) Hansen JH, Duong P, Jivanji SGM, et al. Transcatheter Correction of Superior Sinus Venosus Atrial Septal Defects as an Alternative to Surgical Treatment. J Am Coll Cardiol. 2020 Mar 24;75(11):1266-1278. doi: 10.1016/j.jacc.2019.12.070. PMID: 32192652.
20) Batteux C, Ciobotaru V, Arditi W, et al. Transcatheter correction of sinus venosus defect in a patient with a challenging anatomical configuration: From bench testing to clinical success. Catheter Cardiovasc Interv. 2023 Dec;102(7):1265-1270. doi: 10.1002/ccd.30898. Epub 2023 Nov 17. PMID: 37975208.
21) Butera G, Sturla F, Pluchinotta FR, Caimi A, Carminati M. Holographic Augmented Reality and 3D Printing for Advanced Planning of Sinus Venosus ASD/Partial Anomalous Pulmonary Venous Return Percutaneous Management. JACC Cardiovasc Interv. 2019 Jul 22;12(14):1389-1391. doi: 10.1016/j.jcin.2019.03.020. Epub 2019 May 15. PMID: 31103542.
22) Batteux C, Abakka S, Gaudin R, Vouhé P, Raisky O, Bonnet D. Three-dimensional geometry of coronary arteries after arterial switch operation for transposition of the great arteries and late coronary events. J Thorac Cardiovasc Surg. 2021 Apr;161(4):1396-1404. doi: 10.1016/j.jtcvs.2020.06.036. Epub 2020 Jun 29. PMID: 32713644.
23) Paul A. Yushkevich, Joseph Piven, Heather Cody Hazlett, Rachel Gimpel Smith, Sean Ho, James C. Gee, and Guido Gerig. User-guided 3D active contour segmentation of anatomical structures: Significantly improved efficiency and reliability. *Neuroimage* 2006 Jul 1;31(3):1116-28.
24) Codari M, Papini GDE, Melazzini L, et al. Does Tetralogy of Fallot affect brain aging? A proof-of-concept study. PLoS One. 2018 Aug 21;13(8):e0202496. doi: 10.1371/journal.pone.0202496. PMID: 30130369; PMCID: PMC6103512.
25) Ciobotaru V, Tadros VX, Martin CA, Hascoet S. Complex transcatheter left atrial appendage closure using a tailored trans-jugular approach simulated by 3D printing: a case report. Eur Heart J Case Rep. 2022 Jul 27;6(8):ytac304. doi: 10.1093/ehjcr/ytac304. PMID: 35965604; PMCID: PMC9366637.
26) Brancato F, Stephenson N, Rosenthal E, et al. Transcatheter versus surgical treatment for isolated superior sinus venosus atrial septal defect. Catheter Cardiovasc Interv. 2023 May;101(6):1098-1107. doi: 10.1002/ccd.30650. Epub 2023 Apr 1. PMID: 37002948.
27) Sivakumar K, Qureshi S, Pavithran S, Vaidyanathan S, Rajendran M. Simple Diagnostic Tools May Guide Transcatheter Closure of Superior Sinus Venosus Defects Without Advanced Imaging Techniques. Circ Cardiovasc Interv. 2020 Dec;13(12):e009833. doi: 10.1161/CIRCINTERVENTIONS.120.009833. Epub 2020 Nov 25. PMID: 33233933.
28) Heugen R. VesselNavigator by Philips. Eur Heart J. 2015 Oct 1;36(37):2483. PMID: 26709406.
29) Vento V, Soler R, Fabre D, et al. Optimizing imaging and reducing radiation exposure during complex aortic endovascular procedures. J Cardiovasc Surg (Torino). 2019 Feb;60(1):41-53. doi: 10.23736/S0021-9509.18.10673-2. Epub 2018 Aug 28. PMID: 30160093.
30) Kabir SR, Simpson JM, Jones MI, Butera G, Qureshi SA, Rosenthal E. TEE Guidance During Transcatheter Treatment of Superior SVASDs With PAPVD. JACC Cardiovasc Imaging. 2022 Jan;15(1):160-167. doi: 10.1016/j.jcmg.2020.11.010. Epub 2021 Jan 13. PMID: 33454255.
31) Baruteau AE, Jones MI, Butera G, Qureshi SA, Rosenthal E. Transcatheter correction of sinus venosus atrial septal defect with partial anomalous pulmonary venous drainage:

The procedure of choice in selected patients? Arch Cardiovasc Dis. 2020 Feb;113(2):92-95. doi: 10.1016/j.acvd.2019.09.014. Epub 2020 Feb 11. PMID: 32057661.
32) Hascoët S, Roussin R, Batteux C. Treatment of sinus venosus defect: Time to tune. Int J Cardiol. 2024 Mar 15;399:131630. doi: 10.1016/j.ijcard.2023.131630. Epub 2023 Dec 2. PMID: 38048883.
33) J. Vettukattil, A. Subramanian, A. Barthur, J. Mahimarangaiah, Transcatheter closure of sinus venosus defect: First-in-human implant of a dedicated self-expanding VB stent system, Catheterization and Cardiovascular Interventions. (2023).
34) Morgan GJ, Zablah J. A new FDA approved stent for congenital heart disease: First-in-man experiences with G-ARMOR™. Catheter Cardiovasc Interv. 2022 Dec;100(7):1261-1266. doi: 10.1002/ccd.30447. Epub 2022 Nov 2. PMID: 36321626.
35) Halaby R, Vidula MK, Gillespie MJ, Herrmann HC, Chen T. Multimodality Imaging for Procedural Planning and Guidance of Percutaneous Sinus Venosus Defect Closure. JACC Cardiovasc Interv. 2022 Aug 22;15(16):e187-e188. doi: 10.1016/j.jcin.2022.06.025. Epub 2022 Jul 27. PMID: 35907748.

Table 1: Improvement of the simulation bench program with ten HOST on printed models.

SLS: Selective Laser Sintering.

PJ: PolyJet.

SLA: Stereolithography.

TSP: Trans-septal Puncture.

BiB: Balloon in Balloon.

Figure Captions

Figure 1: Overview of the TC-SVD simulation program.

Figure 2: Virtual Device Bank for TC-SVD.

Figure 3: Virtual simulation of TC-SVD using Meshmixer (Autodesk).

- **Red structures:** Abnormal pulmonary vein to re-route.
- **Blue stent:** Optimus XXL 100mm after flaring of the caudal part.
- **Arrow:** Channel space for APVR routing to the LA.

Figure 4: 3D modeling of SVD using ITK-snap software: large anatomic spectrum.

- **A:** SVD + left superior vena cava (blue).
- **B:** SVD “veno-venous bridge”: APVR and ASD at the same level (arrow), treated as one entity.

- **C:** SVD with 2 abnormal pulmonary veins connected to the SVC (arrows).
- **D:** SVD with 3 abnormal pulmonary veins connected to the SVC (arrows).
- **Legend:** RA - right atrium, LA - left atrium.

Figure 5: 3D printing step by step (3D Heart Modeling Company).

Figure 6: Tools improvements for bench testing.

- **A:** Emerged model for fluoroscopic guidance.
- **B:** Submerged model with external ECMO pump.
- **C:** Submerged model with internal pumps; separation of left and right circulation.

Figure 7: TOE probe anatomic support study for accurate TOE guidance.

- **a:** 3D study and creation of probe support.
- **b:** 3D print of adaptable TOE probe support for each case.
- **c:** Bench test results.

Figure 8 (Central illustration) : Fusion imaging guidance during bench test (HeartVision, General Electric).

- Preoperative 3D anatomy reconstructed in color, merged with fluoroscopy.
- Graduated pigtail inserted for procedural measurements.
- **Note:** Protective balloon in upper pulmonary vein during stent impaction.
- **Landmarks:**
    - Yellow circle: cavo-atrial junction level.
    - Orange circles: innominate vein and upper APVR level.
    - Blue and red circles: 2 APVR ostia.

Figure 9: Balloon testing & stent implantation during bench test.

- **A:** TCSVD situation without PV stenosis risk.
    1. Semi-compliant balloon shows contrast stagnation on SVC upper level (blue arrows), indicating target diameter reached; angiogram shows free pathway to LA (red arrow).
    2. Measurements for balloon and stent selection.

3. Stent implantation confirmed free PV channeling (red arrow) without residual shunting.

- **B:** TCSVD situation with PV stenosis risk.
    1. Semi-compliant balloon shows contrast stagnation, indicating high PV stenosis risk.
    2. Decision to protect pulmonary vein neo-channel during stent deployment.
    3. Post-dilation of stent's caudal part to avoid residual shunting.

Figure 10: TOE guidance during bench test.

Figure 11: Post-implantation CBCT analysis and colorimetric control.

A: Axial analysis of stent diameters; neo-channel patency verified.

B: Longitudinal analysis of stent conformability and expected shortening.

C: Colorimetric control assesses PV pathway and shunt suppression; residual shunt noted.

Figure 12: Concordance and accuracy of 3D printed model with numerical data from native CT.

3D model identical in anatomy and dimensions for virtual and bench simulations.

Stent implantation confirmed need for pulmonary vein protection in both cases.

Supplementary material

Video 1 : colorimetric injection during benchtest control the absence of residual shunt and the APVR patency

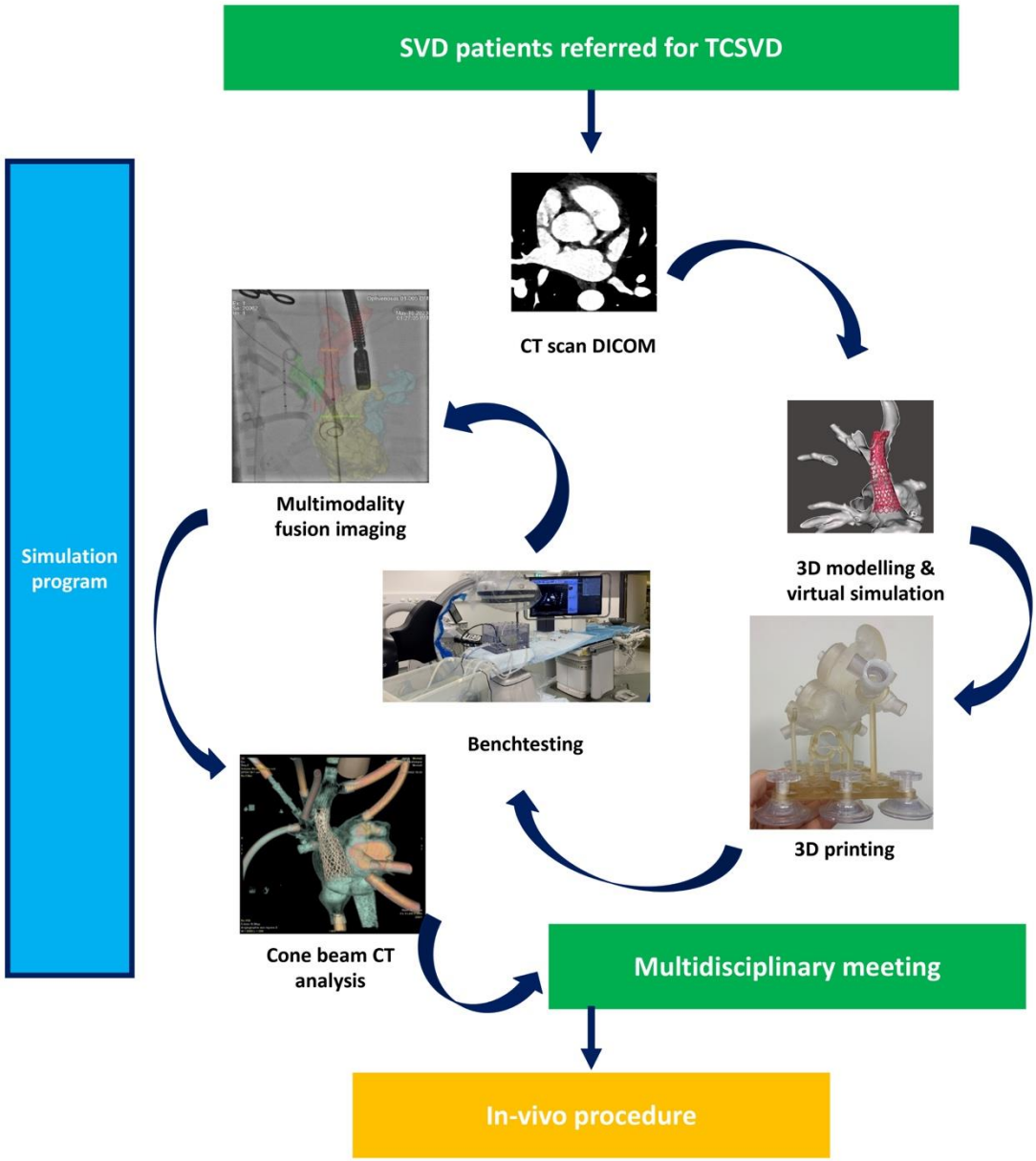

Central illustration (Figure 1)

table 1

Click here to access/download;

Cases / Benchtools	1	3	4	5	6	8	9	10	14	15	OPTIVENOSUS
3D printed model											
SLS/PJ/SLA	SLS	SLS	SLS	SLS/PJ	SLS/PJ	SLA	SLA	SLA	SLA	SLA	SLA
Radio-transparent	X	X	X	X	X	V	V	V	V	V	V
Echogenic	X	X	X	X	X	V	V	V	V	V	V
Model perfusion											
Static water	X	V	V	V							
Mono-circulation	X	X	X	X	V	V	V	V	V		
Left-right separated circulation (external)	X	X	X	X	X	X	X	X	X	V	
Left-right separated circulation (in-tank)	X	X	X	X	X	X	X	X	X	X	V
Guidance											
Visual control	V	V	V	V	V	V	V	V	V	V	V
Fluoroscopy	X	V	V	V	V	V	V	V	V	V	V
TOE	X	X	X	X	X	V	V	V	V	V	V
TOE integrated support	X	X	X	X	X	X	X	X	X	X	V
Cardiac CT fusion	X	X	X	X	X	X	V	V	V	V	V
Cone beam control	NO	V	V	V	V	V	V	V	V	V	V
In vitro procedure											
Stent type and size	Bare CP*	CP10Z60	CP10Z60	OPT80	CP10Z70	CP10Z70	OPT99	OPT99	CP10Z70	OPT80	OPTIVENOSUS
In vivo procedure											
TSP	YES	YES	YES	YES	YES	NO	NO	YES	YES	YES	OPTIVENOSUS
PV protection	NO	NO	YES	YES	NO	NO	NO	NO	YES	YES	OPTIVENOSUS
BiB	28x60	22x60	20x60	20x80	24x80	20x80	22x80	22x80	22x55	22x70	OPTIVENOSUS
Stent	CP10Z80	CP10Z60	OPT 58	CP10Z80	CP10Z85	CP10270	OPT99	OPT99	CP10Z70	OPT99	OPTIVENOSUS
Additional stent	NO	NO	YES	YES	NO	YES	NO	YES	NO	YES	OPTIVENOSUS
Stability	V	V	V	V	V	V	V	V	V	X	OPTIVENOSUS
Shunt	NO	Tiny	NO	NO	NO	NO	NO	NO	Tiny	mild	OPTIVENOSUS
PV patency	V	V	V	V	V	V	V	V	V	V	OPTIVENOSUS

Table 1 : Improvement of the simulation bench program with ten HOST on printed-models.

Figure 2

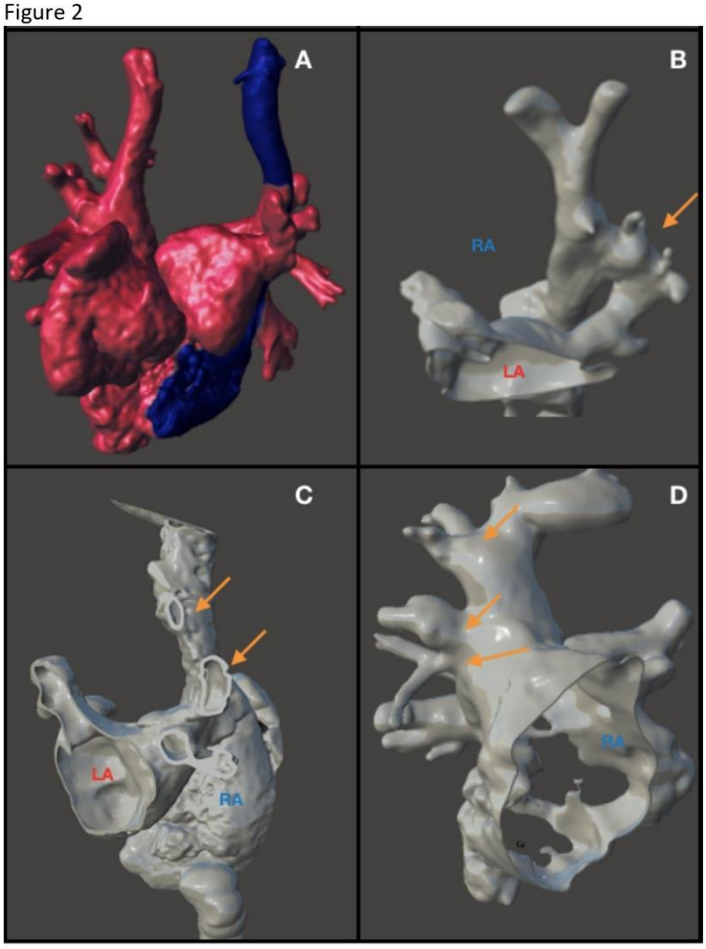

Figure 3

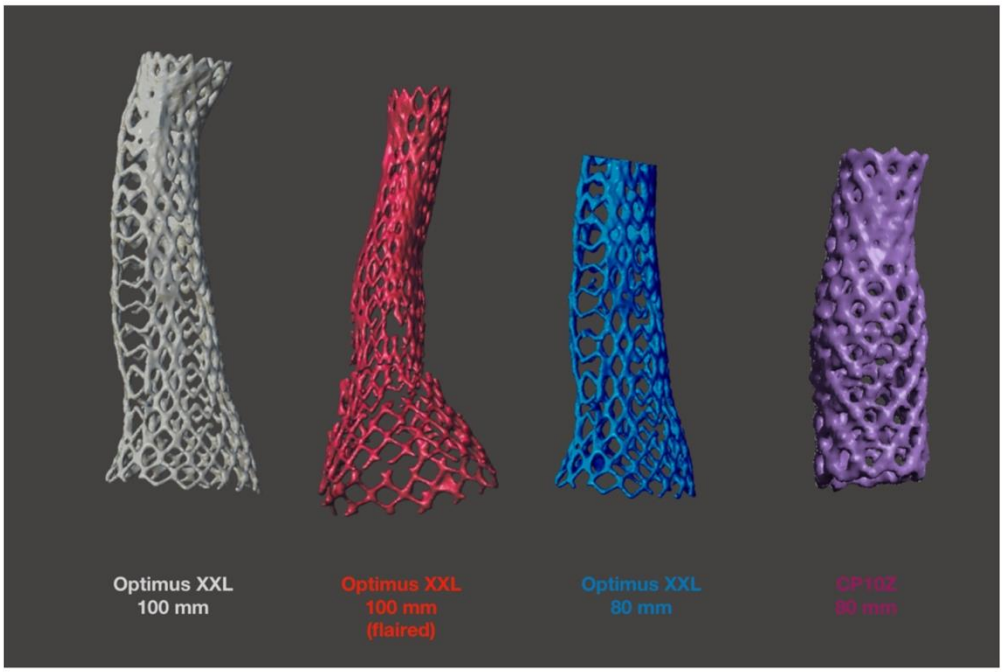
Optimus XXL
100 mm
Optimus XXL
100 mm
(flaired)
Optimus XXL
80 mm
CP10Z
80 mm

Figure 4

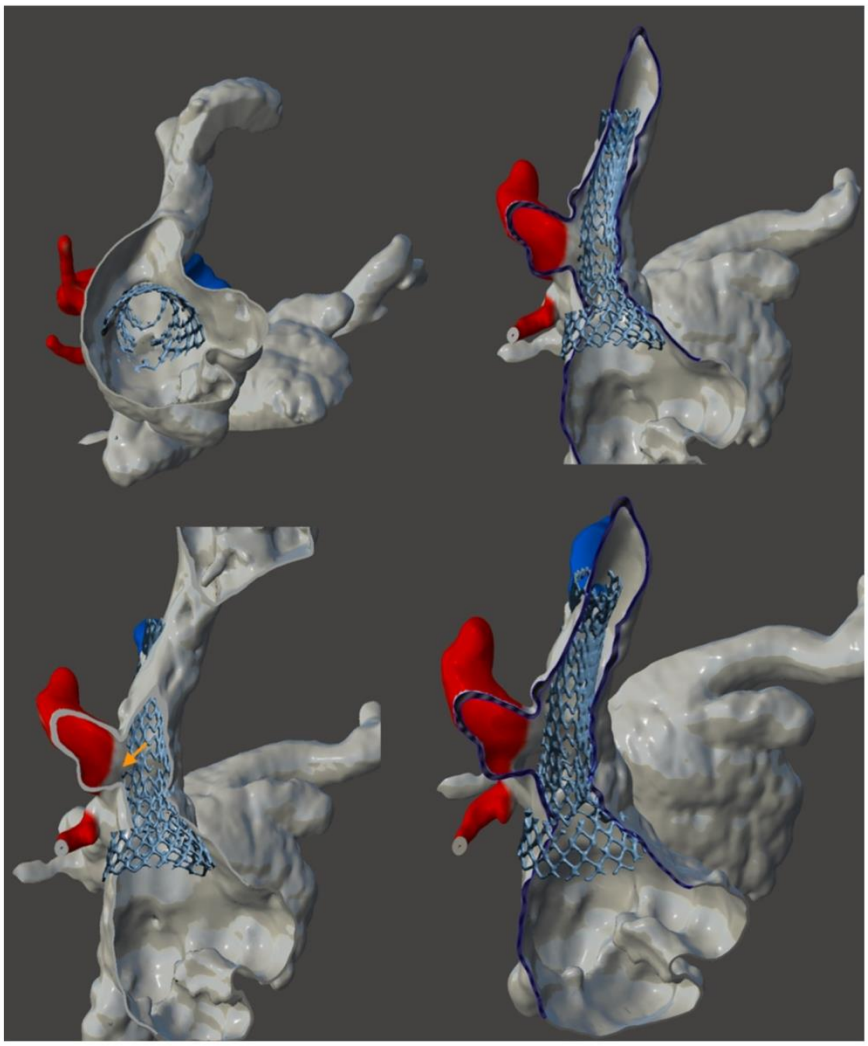

Figure 5

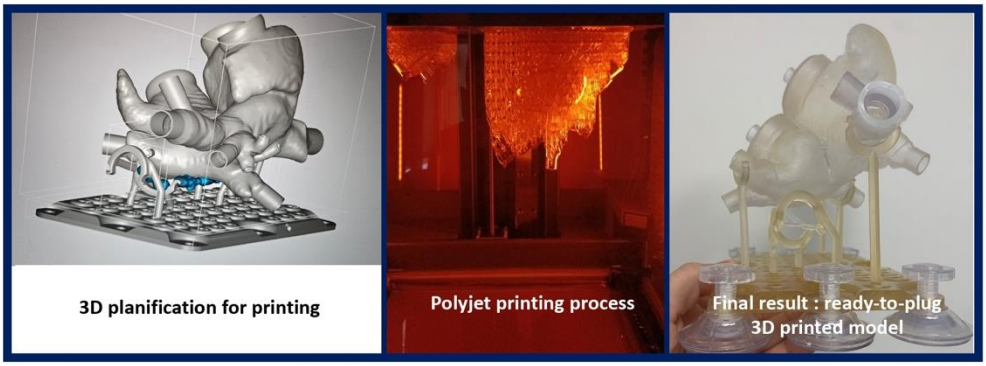

Figure 6

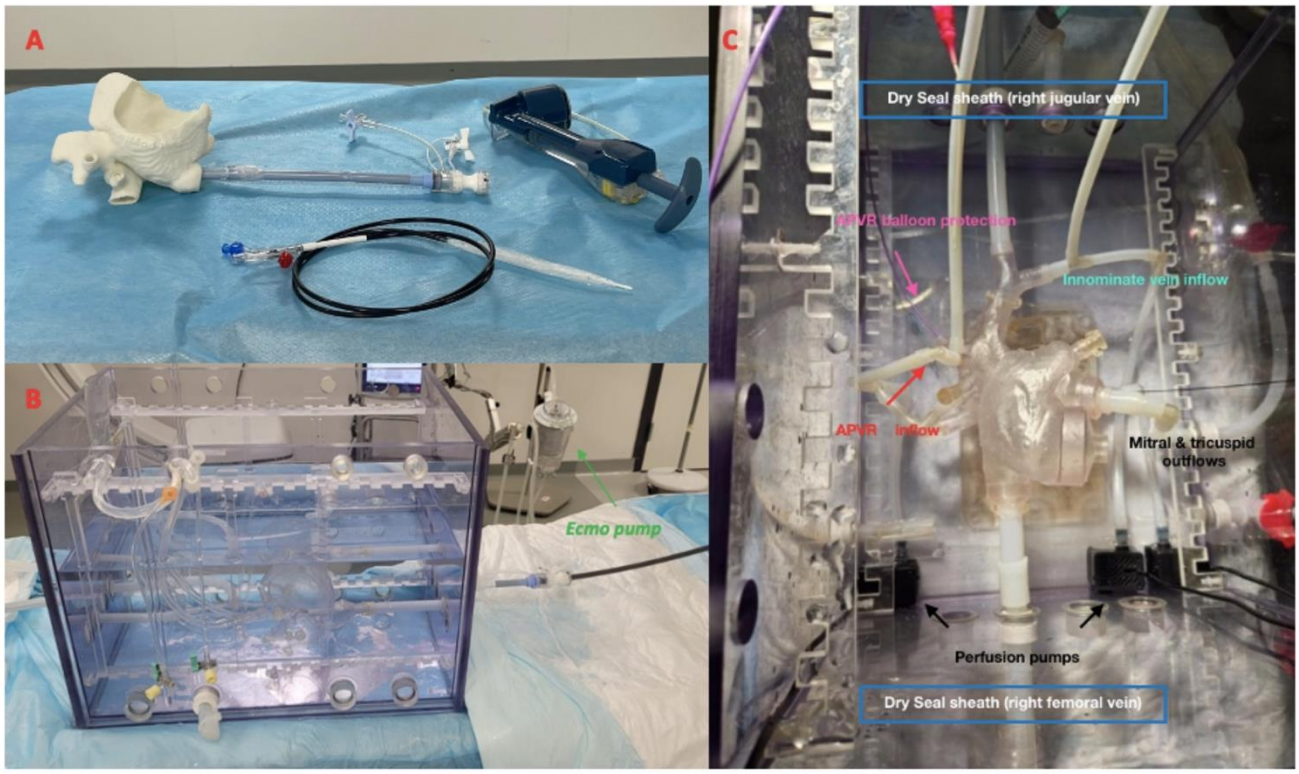

Figure 7

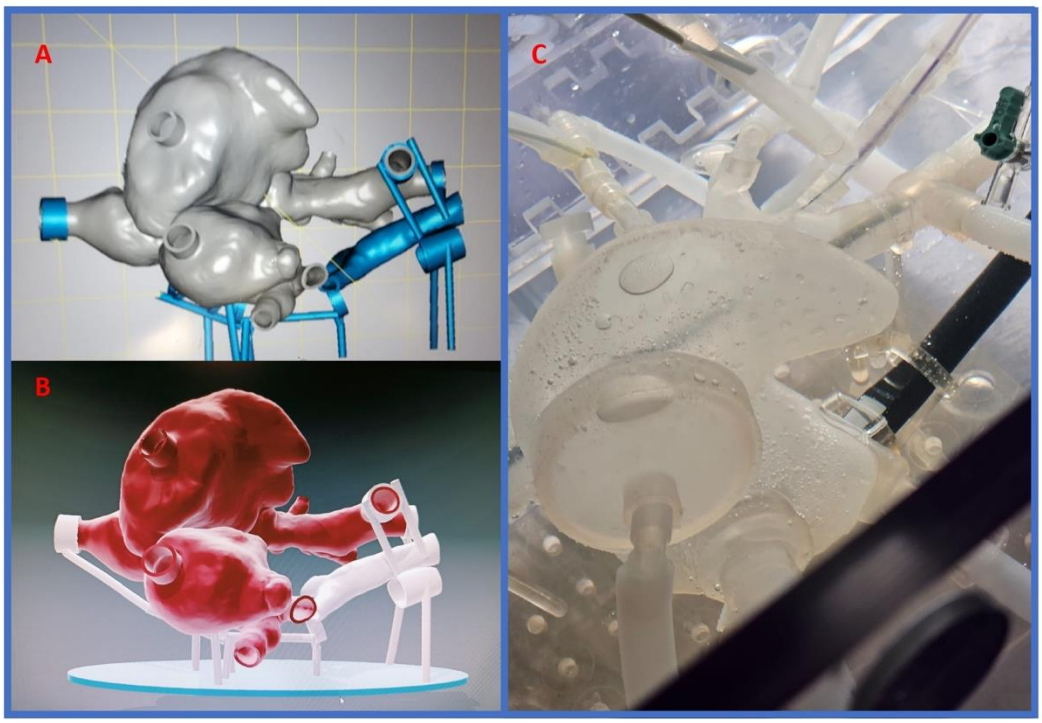

Figure 8

Figure 9

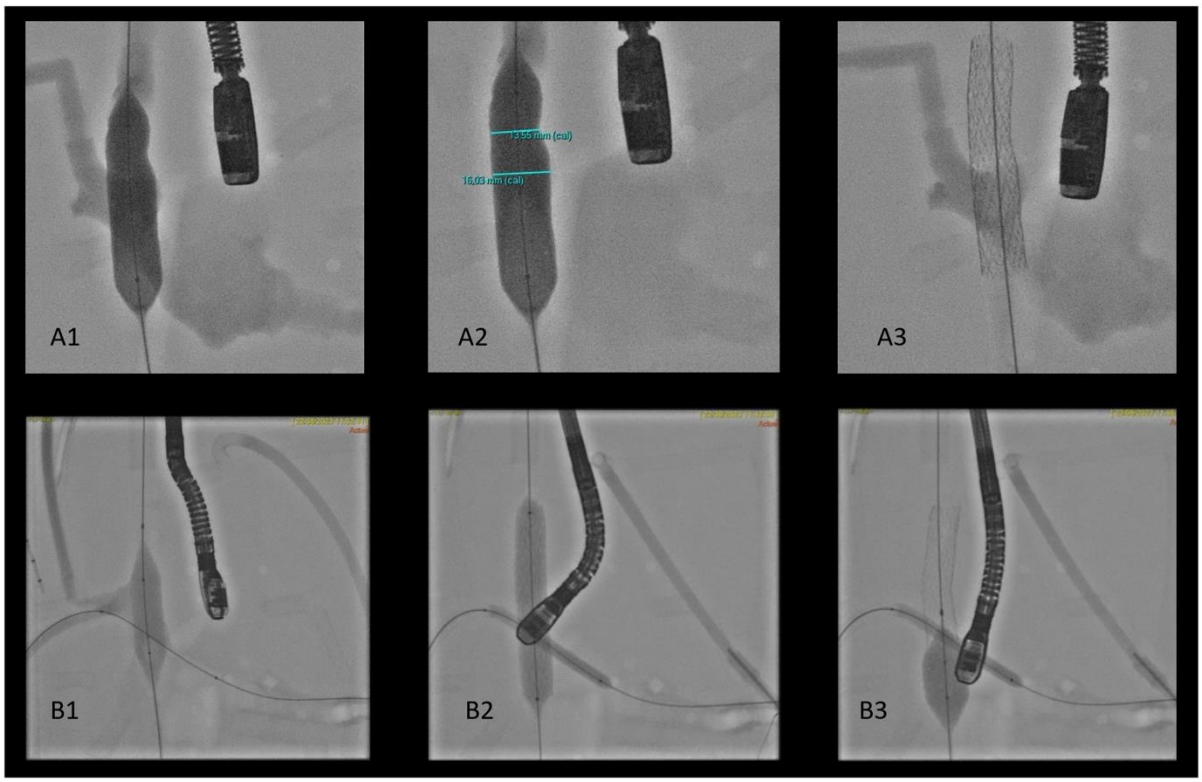

Figure 10

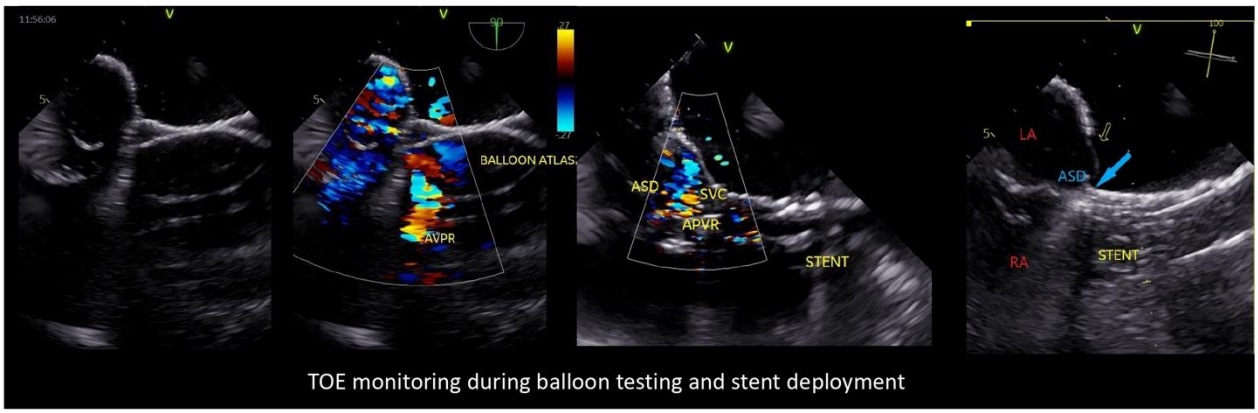

Figure 11

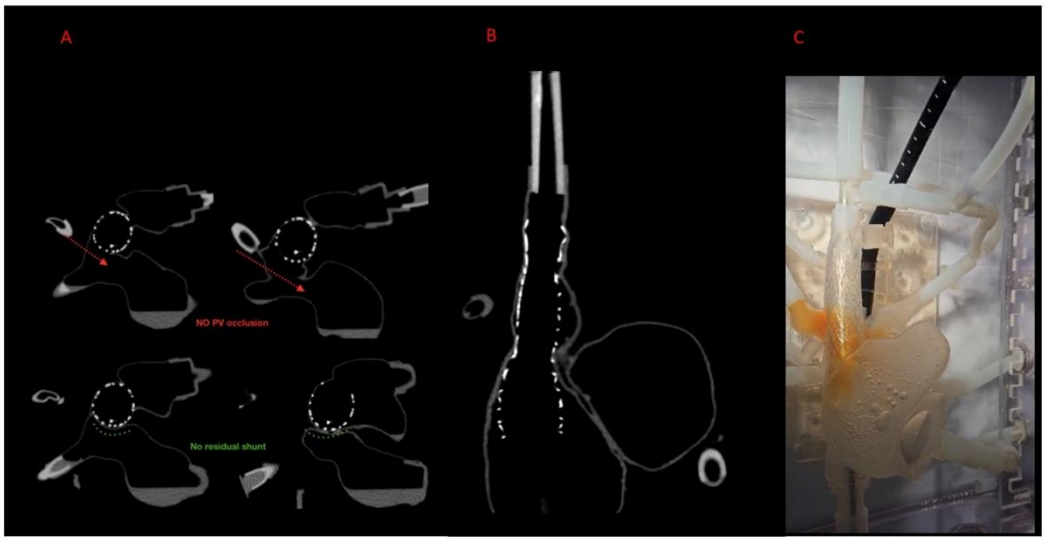

Figure 12

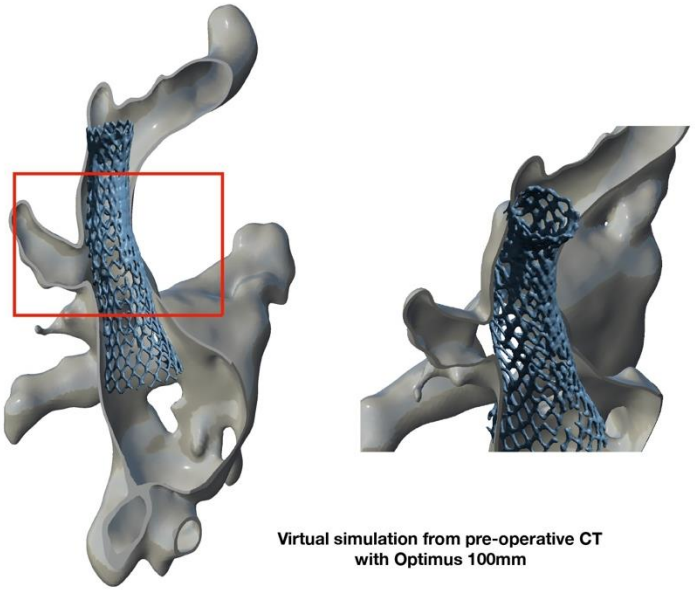

Virtual simulation from pre-operative CT
with Optimus 100mm

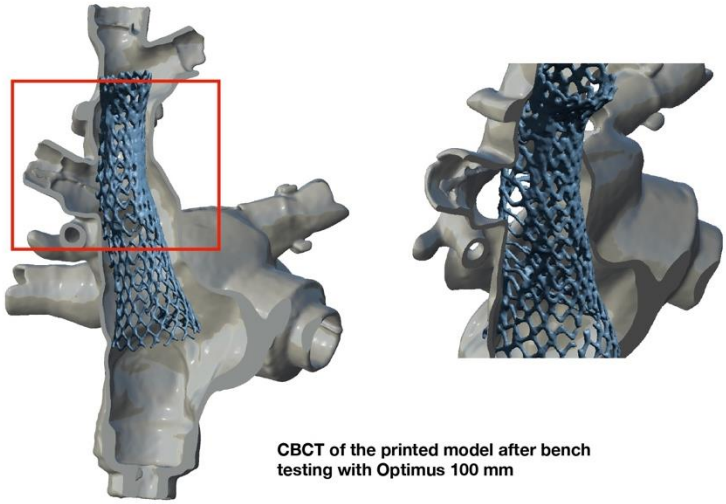

CBCT of the printed model after bench
testing with Optimus 100 mm

Figure 48 : photo d'équipe après session de simulation sur banc d'essai.

De gauche à droite : Antoine Agathon, Clément Batteux, Roxane Nguyen-Quemper, Daphné Madec, Asma Tajouri, Pierre Alexandre Fontanges, Jied Laribi, Sébastien Hascoet, Vlad Ciobotaru, William Arditi, Pierre Landreau.

III. Recherche et développement en lien avec l'industrie

Les premiers stents utilisés pour cette procédure en France étaient les stent CP10Z (Numed, USA) d'une longueur de 60 à 80 mm. Pour des longueurs supérieures à 60 mm, une fabrication à la demande était proposée par la société, après obtention d'un accord préalable d'utilisation compassionnelle auprès de l'agence de santé du médicament, en l'absence de marquage CE et d'AMM[27].

Rapidement, notre choix s'est donc orienté vers l'utilisation d'un autre stent, le stent OPTIMUS XXL (Andratec) dont le design nous semblait approprié aux corrections percutanées, et dont la fabrication sur mesure était plus rapide, probablement en raison de la proximité géographique de cette société basée en Allemagne et de la dévotion de son CEO, Andreas Kohl, très impliqué dans ce projet[116, 117].

Par ailleurs, ces stents avaient déjà le marquage CE pour des longueurs moindres[118].

Le design de ce stent nous a séduit en raison de son processus de fabrication spécifique et des propriétés biomécaniques qui en découlent :
-un design des mailles en « S » permettant de limiter le raccourcissement durant son déploiement.
-des extrémités courbes, facilitant un ancrage non traumatique.
-une fabrication à partir d'un tube unique initial, permettant d'éviter la distorsion voir la rupture.
-un polissage électrolytique du métal réduisant la corrosion et la thrombogénicité
-une membrane de couverture en PTFE (polytetrafluoroethylene) appliquée à la face interne et externe du stent par compression mécanique et non chimique.
-une proportion de métal Cobalt-Chrome moindre que les autres stents du marché.

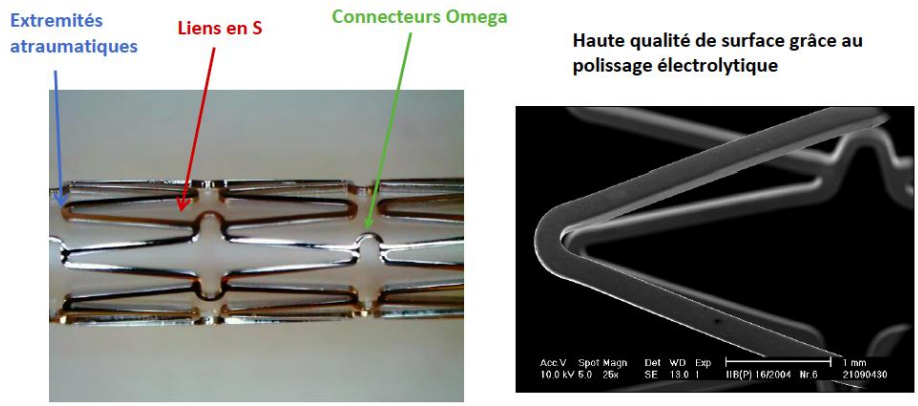

Figure 49 : design de fabrication du stent Optimus (Andratec)

En effet, les mailles du stent ne sont pas toutes jointives, ce qui lui confère une conformabilité plus importante, paramètre clé pour la correction percutanée des CIA sinus venosus, où le stent doit être modelé de manière adaptée à certaines zone d'ancrage dans la veine cave supérieure, et parfois sur-dilaté pour corriger des shunts résiduels, au niveau de la jonction cavo-atriale.
Sa composition en alliage de Cobalt-Chrome permet également une force radiale interessante et nécessaire.

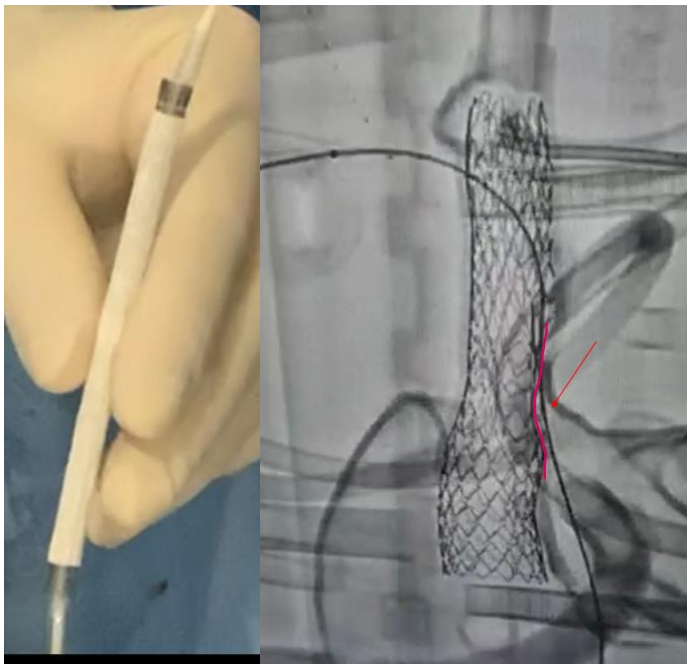

Le raccourcissement n'est pas trop important puisqu'il mesure 90 mm déployé pour 100 mm serti.
Il apparait conformable car on voit qu'il a bien été déformé par le ballon de protection coronaire (résultat souhaité pour éviter de créer une sténose)

Cette caractéristique est également recherchée lorsqu'on procède au flairing de la partie inférieure du stent pour supprimer le shunt résiduel.

Figure 50 : Mise en place d'un stent Optimus XXL 100 mm couvert sur banc d'essai.

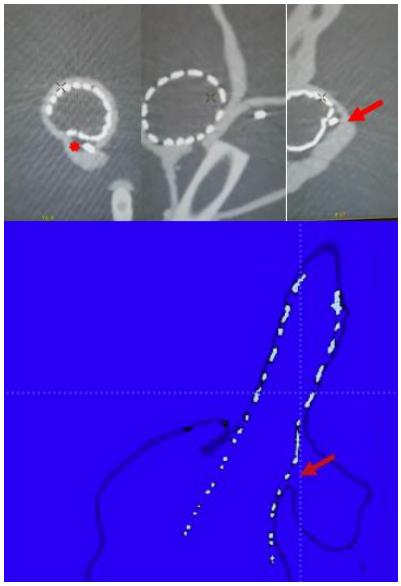

La conformabilité souhaitée du stent est bien visible en coupe axiale sur le cone beam.

Il peut avoir une forme ronde, ovalaire, voir concave sur la zone de protection du ballon (étoile)

Il est moulé par le ballon de protection pour laisser un chenal perméable après dégonflage du ballon de protection (flèches)

Figure 51 : : analyse du cone-beam post implantation

Initialement, les stents proposés par ANDRATEC étaient totalement couverts d'une longueur de 80, 85, 90 ou 100 mm.

Figure 52 : : photo du stent Optimus 100 mm XXL Andratec (quasi) totalement couvert.

Grâce à une coopération constante entre notre équipe interventionnelle et la société ANDRATEC, coopération ayant lieu aussi bien en pré-procédure (en salle de cathétérisme expérimentale), qu'au cours de l'intervention (en salle de cathétérisme in-vivo) mais enfin également au cours de débriefing et brainstorming, nous avons imaginé ensemble la seconde génération de stents dédiés à la correction percutanée des CIA sinus venosus.

Ces stents ont vu leur gamme de longueur simplifiée à 80 ou 100 mm après constatation que l'utilisation de tailles intermédiaires était souvent superflue, ce qui a permi de simplifier les processus de fabrication et probablement d'en réduire les couts.

La couverture du stent a été modifiée en laissant une partie découverte du stent à sa partie supérieure, allant de 15 à 20 mm en fonction de la longueur totale du stent. Cette propriété de stent nu à la partie supérieure du stent devait permettre un meilleur ancrage dans la veine cave supérieure du stent à sa partie crâniale, par absence totale d'interposition de matériel entre le ballon d'inflation, les mailles du stent et le tissu cave. Cela devait réduire encore le risque d'embolisation du stent par glissement vers l'oreillette droite, complication très redoutée car menant le plus souvent à une intervention chirurgicale urgente afin d'extraire le stent ayant embolisé.

La nouvelle gamme de stent a pu être testée spécifiquement au cours de sessions sur banc d'essai expérimental.

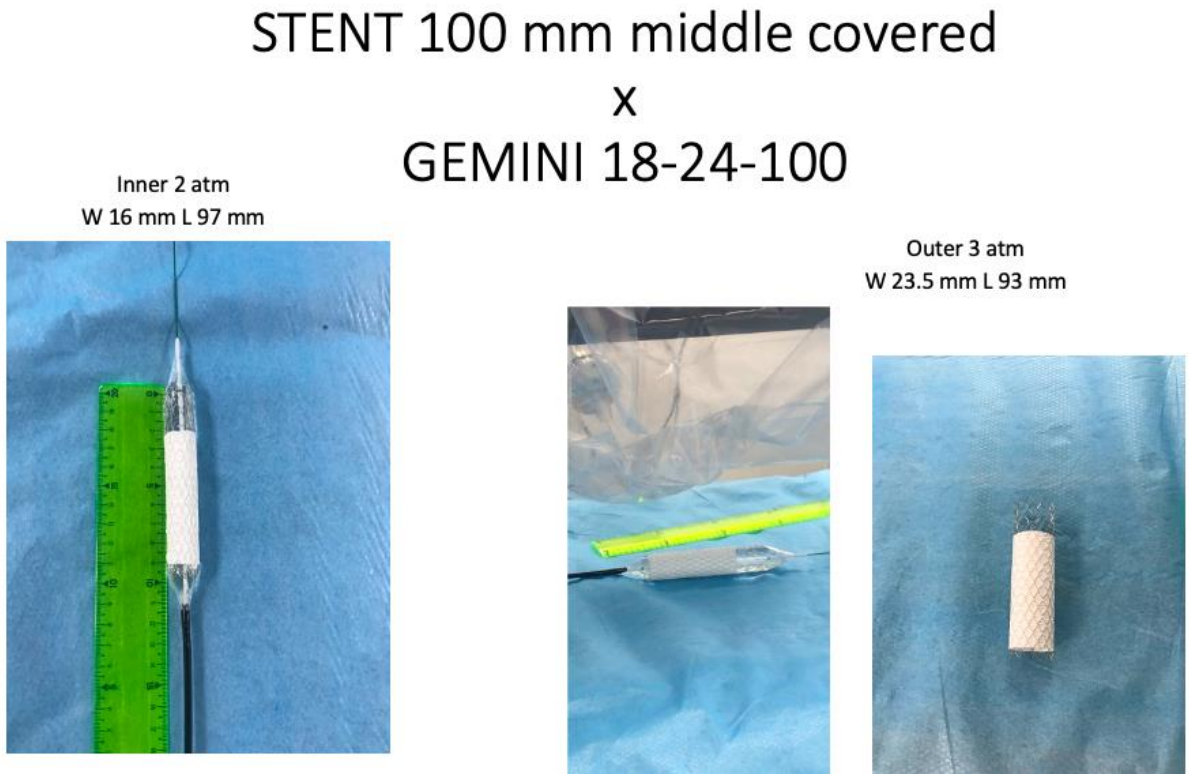

Figure 53 : test du matériel en salle de cathétérisme expérimental.

Stent Optimus 100 mm XXL partiellement couvert, ballon Gemini 18 x 24 x 100. Mesures de diamètre et de raccourcissement pour des inflations progressivement croissantes. A droite : aspect du stent totalement ouvert.

Différentes mesures étaient effectuées concernant les ballons d'inflation fournis également par ANDRATEC, le comportement des stents en fonction du diamètre d'inflation choisi, leur propriétés biomécaniques (conformabilité, le degré de recoil, raccourcissement) et leur solidité au cours des inflations à des diamètres extrêmes.

			STENT 100 XXL MC		
			Diameter (mm)		Lenght (mm)
Gemini 20-26-100	inner	manuel			
		1 atm			
		2 atm	18,5		95
		3 atm			
	Outer	manuel			
		1 atm			
		2 atm			
		3 atm	25,5 bottom	26.5 top	84

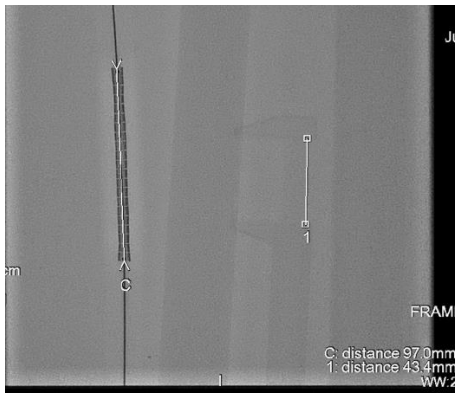

Figure 54 : Gauche : analyse précise en salle de cathétérisme des mesures de diamètre et raccourcissement progressivement croissants en fonction des pressions adressées au ballon d'inflation. Droite : mesure par fluoroscopie avant inflation

Ces analyses brutes fournies aux autorités de santé ont permis le démarrage de l'étude Optivenosus autorisant l'utilisation standardisée de ces stents non marqués CE, chez des patients sélectionnés, afin d'en évaluer les performances dans la vraie vie.

LETTER TO THE EDITOR 1: multicenter experience of transcatheter correction of superior sinus venosus defect using the covered stent Optimus XXL (publiée dans Revista Espanola de Cardiologia en 2023)

Référence bibliographique 117

C Batteux, V Ciobotaru, H Bouvaist, A Kempny, A Fraisse, S Hascoet

Multicenter experience of transcatheter correction of superior sinus venosus defect using the covered Optimus XXL stent

Experiencia multicéntrica en la corrección transcatéter del defecto del seno venoso superior con el* stent *Optimus XXL recubierto

To the Editor,

Superior sinus venosus defect (SVD) is a rare congenital heart disease accounting for 5% to 10% of all cases of atrial septal defect.Transcatheter correction of SVD using covered Cheatham-Platinum stents (NuMED, United States) has emerged as an alternative to open-heart surgery.[1–3] The 50- and 60-mm long stents subsequently received Conformite Europeenne marking and Food and Drug Administration approval. However, the anatomical configuration of SVD often requires a stent longer than 60 mm, which are currently unavailable in many countries.[3] The Optimus XXL stent (AndraTec GmbH, Germany) is a nonpremounted, balloon-expandable, cobalt-chrome, extra large stent, used for endovascular stenting of aortic coarctation or for right ventricle outflow tract stenting.[4] A covered 99-mm long version was specifically developed for SVD correction, as recently reported in one case.[5]

We report a multicenter case serie of 6 additional consecutive cases achieved in 3 centers in 2 countries between November 2021 and March 2022 in adults aged 26 to 72 years. The study design was approved by an ethics committee (GERM, IRB00012157). Informed consent was obtained from the patients.

Patient and procedural characteristics are reported in table 1. All patients complained of dyspnea and had significant left-to-right

Table 1
Description of patients' characteristics, procedural data and outcomes.

Patient	1	2	3	4	5	6
Age	43	26	42	60	49	72
Symptoms	Dyspnea	Dyspnea	Dyspnea, pulmonary hypertension	Dyspnea, atrial fibrillation	Dyspnea	Dyspnea, pulmonary hypertension
Ratio of pulmonary to systemic output		2.5	2.2			2.9
Mean pulmonary artery pressure, mmHg	19	12	38			29
Pulmonary vascular resistance, Wood Unit			5.1			2
High anomalous pulmonary venous return	No	Yes	Yes	Yes	Yes	No
Preprocedural planning	Virtual simulation 3-dimensional printed model hands-on simulation testing	Virtual simulation 3-dimensional printed model hands-on simulation testing	Virtual simulation 3-dimensional printed model hands-on simulation testing	Virtual simulation	Virtual simulation	Virtual simulation 3-dimensional printed model hands-on simulation testing
Pulmonary vein management	No transseptal puncture	Transseptal puncture, no balloon protection	Transseptal puncture, balloon protection	Transseptal puncture, balloon protection	Transseptal puncture, balloon protection	Transseptal puncture, balloon protection
Stent delivery balloon	Covered Optimus 99 XXL Balloon-in-Balloon 22 mm x 80 mm	Covered Optimus 99 XXL Balloon-in-Balloon 22 mm x 80 mm	Covered Optimus 99 XXL Balloon-in-Balloon 18 mm x 80 mm	Covered Optimus 99 XXL Gemini 30 mm x 100mm	Covered Optimus 99 XXL Gemini 30 mm x 100 mm	Covered Optimus 99 XXL Balloon-in-Balloon 22 mm x 70 mm
Additional stent	No	Bare Optimus XL at the upper end	No	No	Bare Cheatham Platinium stent at the upper end	Bare Optimus XL at the upper end
Stent stability	Yes	Yes	Yes	Yes	Yes	Migration to the right atrium - stent stabilized using an additional stent in the superior vena cava
Pulmonary vein obstruction	No	No	No	Pulmonary vein obstruction of the upper right component resolved by dilation and reverse remodelling of the stent	No	No
Periprocedural complication	No	No	No	No	No	Obstruction of right ventricle inflow, with right to left shunt through a foramen ovale - resolved by covered stent strut opening by balloon dilation
Residual shunt	Tiny, nonsignificant	No	No	Moderate	No	Minor
Follow-up	9 mo - clinical success	9 mo - clinical success	6 mo - clinical success	5 mo - remaining dyspnea and moderate residual shunting	4 mo - clinical success	2 mo - remaining dyspnea, residual minor bidirectional shunting

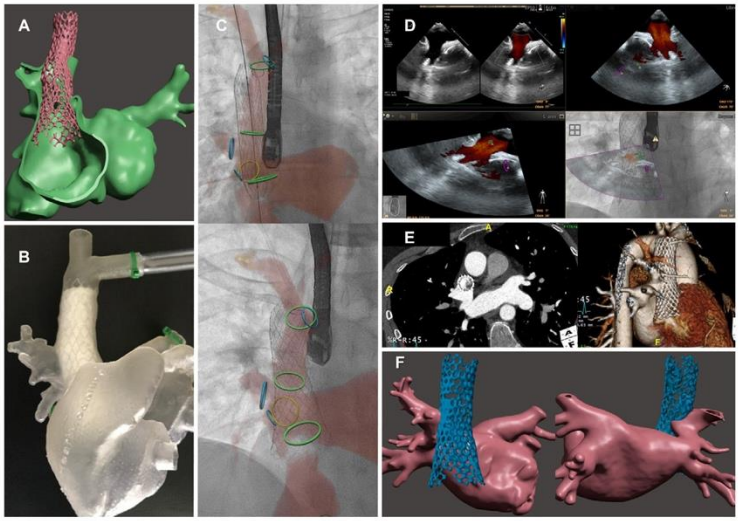

Figure 1. Clinical case 1. A 43-year-old man with SVD. A: computer simulation of Optimus stent implantation. B: hands-on simulation testing. C: stent implantation under fusion imaging guidance. D: color Doppler flow showing a widely patent pulmonary vein channel toward the left atrium. E and F: cardiac tomography confirms excellent position of the stent, complete occlusion of the SVD and widely patent pulmonary vein channel.

shunt. High opening of the anomalous pulmonary venous return in the superior vena cava (SVC) was idenfied in 4 cases. Procedural feasibility was tested on virtual simulation in all patients and hands-on simulation training in 4 (figure 1).[6] To define the best treatment option, a multidisciplinary team including heart surgeons assessed the imaging and simulation processes. Transcatheter correction was considered as an alternative to surgery in all patients. As previously described,[1–3,6] all procedures were performed under general anesthesia and transesophageal echocardiography guidance. Multimodal fusion imaging was applied in 5 patients (figure 1). A venous femoro-jugular rail was used. Transseptal access was employed to establish an anomalous pulmonary venous return pathway in 5 patients, with balloon inflation simultaneous to Optimus stent deployment in 4.

In 2 patients, a single size (outer/inner balloon of 30/14-mm diameter and 100-mm length) Gemini balloon-in-balloon was used to implant the stent (AndraTec GmbH, Germany). The maximum diameter of this ballon was larger than the SVC diameter. In 4 patients, the single size 100-mm length Gemini balloon was not chosen given a too large diameter and other 20 to 30 mm shorter balloon-in-balloon stents were used (NuMED, United States), with an outer balloon diameter between 18 to 22 mm to match the diameter of the SVC (figure 1). This setting required additional inflations of the extremities of the stent that were not fully expanded by the smaller balloons. A second uncovered stent was implanted at the upper part of the stent in 3 patients to provide additional anchoring to the SVC.

In 4 patients, we achieved technical and clinical success. One procedure was marked by pulmonary vein obstruction reversed by pulmonary vein balloon dilation but leading to residual shunting and persistant dyspnea. One of the 4 patients in whom a shorter balloon-in-balloon was used was complicated by displacement of the stent toward the right atrium. The stent was subsequently anchored in the SVC using another uncovered stent and struts of the Optimus stent had to be opened to restore flow toward the right ventricle. In this patient, a modified suture control technique may have been useful to secure the stent position before full stent deployment and impaction on SVC was obtained.[5] Outcome was favorable. Unadequate diameter or length of the balloon-in-balloon contributed to these 2 complications.

Transcatheter correction of a SVD using a covered Optimus XXL 99-mm stent was feasible in all 6 patients. The strengths of the Optimus stent are its adequate length and high comformability. This allows deep and stable implantation in the SVC, whereas its good flexibility allows optimal flaring of the the proximal part of the end of the stent to achieve complete shunt closure. When the area of stent implantation in the SVC is too short, the stent may migrate, as observed in 1 patient. A modification of the Optimus stent with a longer uncovered part at the upper end was performed to address this issue and strengthen the anchoring in the SVC. Currently available Gemini balloons with multiple balloon sizes will also optimize stent implantation.

To conclude, the Optimus covered, 99 mm-long, Optimus XXL stent allows successful transcatheter SVD. Further experience and a wider range of stent/balloons are needed.

FUNDING

Marie Lannelongue Department of Research and Innovation, 3D Heart Modeling Co (Caissargues, France), the nonprofit organisation *Le coeur dans la main*, a grant of the *Federation Francaise de Cardiologie* and a *Bourse Hélène de Marsan* grant from the French Society of Cardiology

AUTHORS' CONTRIBUTIONS

C. Batteux, and V. Ciobotaru participated in the study design and preclinical testing. C. Batteux, V. Ciobotaru, H. Bouvaist,

A. Kempny, A. Fraisse and S. Hascoet participated in the clinical cases and data collection. S. Hascoet and A. Fraisse drafted the manuscript. All authors critically revised the manuscript.

CONFLICTS OF INTEREST

S. Hascoet has received proctoring and consultant fees from Abbott and a research grant from Edwards lifesciences. A. Fraisse has received proctoring and consultant fees from Abbott and Occlutech. A. Kempny, H. Bouvaist, C. Batteux and V. Ciobotaru have no disclosures.

Acknowledgment

We thank A. Wolfe, M. Gatzoulis, P. Brenot, W. Arditi, J. Radojevic, B. Decante, W. Li, F. Lecerf, C. Lacerda, G. Albenque, L. Aubrege, H. Beaussier and F. Rémy for their contribution to this work.

Clement Batteux,[a,b] Vlad Ciobotaru,[a,c] Hélène Bouvaist,[d] Aleksander Kempny,[e] Alain Fraisse,[e] and Sebastien Hascoet[a,b,e,*]

[a]*Hopital Marie Lannelongue, centre de reference reseau maladies rares M3C, Groupe Hospitalier Paris Saint Joseph, Universite Paris-Saclay, BME Lab, Le Plessis-Robinson, France*
[b]*Institut national de la santé et de la recherche médicale (INSERM), Unite Mixte de Recherche UMR S-999, Universite Paris-Saclay, Le Plessis-Robinson, France*
[c]*Clinique Franciscaines, 3Dheartmodeling, Nîmes, France*
[d]*Centre Hospitalier Universitaire de Grenoble, France*
[e]*Royal Brompton Hospital, London, United Kingdom*

* Corresponding author.
E-mail address: s.hascoet@ghpsj.fr (S. Hascoet).

Available online 30 August 2022

REFERENCES

1. Batteux C, Meliani A, Brenot P, Hascoet S. Multimodality fusion imaging to guide percutaneous sinus venosus atrial septal defect closure. *Eur Heart J.* 2020;41:4444–4445.
2. Hansen JH, Duong P, Jivanji SGM, et al. Transcatheter Correction of Superior Sinus Venosus Atrial Septal Defects as an Alternative to Surgical Treatment. *J Am Coll Cardiol.* 2020;75:1266–1278.
3. Rosenthal E, Qureshi SA, Jones M, et al. Correction of sinus venosus atrial septal defects with the 10 zig covered Cheatham-platinum stent – An international registry. *Catheter Cardiovasc Interv.* 2021;98:128–136.
4. Morgan GJ, Ciuffreda M, Spadoni I, DeGiovanni J. Optimus covered stent: Advanced covered stent technology for complex congenital heart disease. *Congenit Heart Dis.* 2018;13:458–462.
5. Haddad RN, Bonnet D, Gewillig M, Malekzadeh-Milani S. Modified safety techniques for transcatheter repair of superior sinus venosus defects with partial anomalous pulmonary venous drainage using a 100-mm Optimus-CVS covered XXL stent. *Catheter Cardiovasc Interv.* 2022;99:1558–1562.
6. Batteux C, Azarine A, Karsenty C, et al. Sinus Venosus ASDs: Imaging and Percutaneous Closure. *Curr Cardiol Rep.* 2021;23:138.

https://doi.org/10.1016/j.rec.2022.08.004
1885-5857/

CASE REPORT 2 : Transcatheter correction of sinus venosus defect in a patient with a challenging anatomical configuration : from benchtesting to clinical success.

Référence bibliographique 116
C Batteux, V Ciobotaru, W Arditi, B Decante, C Karsenty, N Combes, S Hascoet

Received: 17 January 2022 | Revised: 4 April 2023 | Accepted: 22 October 2023
DOI: 10.1002/ccd.30898

CASE REPORT

WILEY

Transcatheter correction of sinus venosus defect in a patient with a challenging anatomical configuration: From bench testing to clinical success

Clement Batteux MD, PhD student[1,2] | Vlad Ciobotaru MD, PhD student[2,3,4] | William Arditi MEng[5] | Benoit Decante MSc[1] | Clement Karsenty MD, PhD[6] | Nicolas Combes MD, MSc[1,7] | Sebastien Hascoet MD, PhD[1,2]

[1]Department of congenital heart diseases, Marie Lannelongue Hospital, M3C network, Groupe Hospitalier Paris Saint Joseph, School of Medicine, Paris-Saclay University, Marie Lannelongue Hospital, Plessis-Robinson, France, France

[2]UMR-S 999, INSERM, Plessis-Robinson, France, France

[3]Department of cardiology, Centre Hospitalier Universitaire de Nîmes, Nîmes, France, France

[4]Department of cardiology, Clinique Franciscaines, Nîmes, France, France

[5]Department of biomedical engineering, CentraleSupélec, Paris-Saclay University, Gif-sur-Yvette, France, France

[6]Department of pediatric cardiology, Hôpital des Enfants, M3C network, CHU Toulouse, Toulouse, France, France

[7]Department of cardiology, Clinique Pasteur, Toulouse, France, France

Correspondence
Sebastien Hascoet, Hopital Marie Lannelongue, 133 Avenue de la résistance, 92350 Le Plessis-Robinson, France.
Email: s.hascoet@ghpsj.fr

Funding information
Le coeur dans la main; Federation Francaise de Cardiologie; Fondation Hopital Saint Joseph; Bourse Hélène de Marsan, Société Francaise de Cardiologie, Grant/Award Number: 2020

Abstract

We report successful transcatheter correction of a sinus venosus defect in a 72-year-old woman with anomalous pulmonary venous return in a challenging anatomical configuration. The procedure was facilitated by hands-on simulation training on a newly developed, perfused, 3D-printed model.

KEYWORDS
3D printing, catheterization, complex congenital heart disease, hands on simulation training, sinus venosus defect, stent

1 | INTRODUCTION

Transcatheter correction of sinus venosus defect (SVD) has emerged as an alternative to open-heart surgery when the anatomic configuration is suitable.[1] A long, wide, covered stent is implanted into the superior vena cava (SVC) to channel the anomalous pulmonary venous return (APVR) to the left atrium at the posterior part of the stent and to occlude the shunt between the two atria.[1,2] The three main challenges consist in achieving complete shunt occlusion, maintaining APVR patency, and achieving stable stent implantation.[1] The procedure benefits from multimodality imaging.[2,3] We report successful transcatheter SVD correction in a 72-year-old patient with APVR in a challenging anatomical configuration. The procedure was facilitated by simulation on a newly developed, perfused, 3D-printed model.

2 | CLINICAL CASE

SVD was diagnosed in a 72-year-old woman with dyspnoea. She had substantial right-heart overload (Qp/Qs = 1.8) and mild pulmonary hypertension (mean pulmonary artery pressure = 26 mmHg on a diagnostic catheterization). Cardiac CT showed two right upper pulmonary veins (PV) draining in a superior vena cava (SVC) measuring 20 mm in diameter above (Figure 1). The most upper component (PV1) of the APVR measured 9 mm in diameter and opened posteriorly in the SVC 21 mm below the level of the inominate vein and 19 mm above the opening of the second upper PV (PV2) measuring 9 × 18 mm diameter. The distance between PV1 and the inferior rim of the sinus venosus defect was 61 mm. Figure 2A shows the relationship between the two components of the APVR and the SVC.

After multidisciplinary discussion including surgeons and in accordance with the patient's wishes, transcatheter correction was considered instead of surgery or medical follow-up. Informed signed consent was obtained and data were included in a prospective local registry (IRB00012157). Given the expected risk of right superior PV occlusion associated with the challenging anatomy, we used a step-by-step simulation program that included 3D modeling, virtual simulation, 3D printing, and hands-on simulation training (HOST) to assess procedure feasibility.[3]

2.1 | Virtual simulation

A 3D stereolithography (STL) model of the heart was segmented using cardiac CT DICOM (Meshmixer, 3Dmatics; Autodesk) software. The APVR had two components of which one opened into the SVC at a particularly distal site (PV1).

A STL of a covered stent was produced from a previous clinical procedure and merged with the SVD STL to simulate the procedure. The results did not rule out feasibility of transcatheter correction but confirmed the high risk of superior PV obstruction (Figure 2A and Video S1).

2.2 | 3D printing and HOST

We printed a 3D model of the SVD (3D Heart Modeling). Material was developed to produce similar echogenicity, radiotransparency, and distensibility to those of cardiovascular tissue (Figure 2B).

The 3D-printed model was fixed in a container filled with radiotransparent and echogenic liquid and plugged to a pump-driven circuit to simulate the procedure in a catheterization laboratory, with close-to-reality conditions including transesophageal echocardiography (TEE), fluoroscopy, and angiography (Figure 2B and Video S2).

The first step consisted in inflation of a compliant balloon (Amplatz sizing balloon n°34; Abbott) to assess distensibility and stretched diameter of the SVC. The SVC diameter above the PV1 was

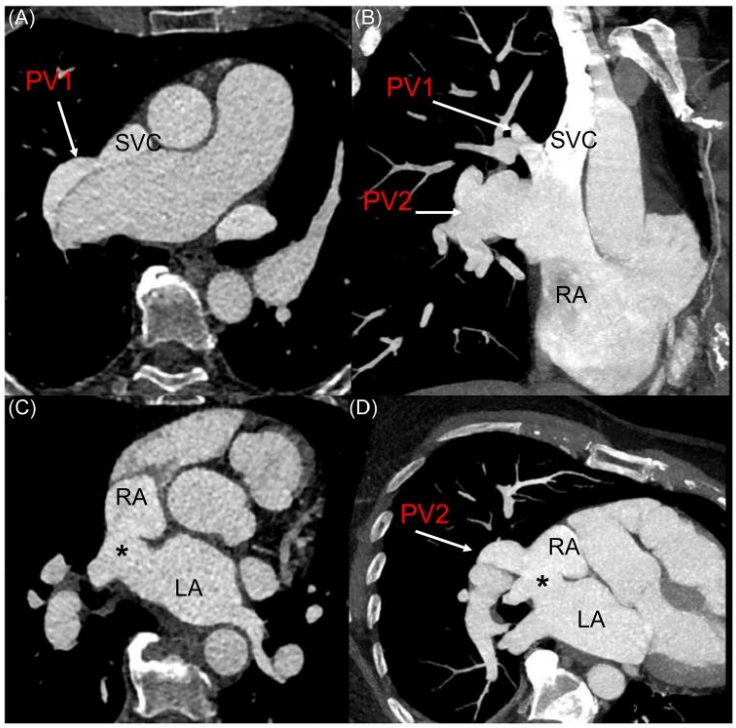

FIGURE 1 Sinus venosus defect (*). White arrows indicate the anomalous pulmonary venous return with two segmental right superior pulmonary veins (PV1 and PV2) opening into the superior vena cava (SVC). LA, left atrium; RA, right atrium. (A) transversal view at the level of PV1 abutment in the SVC. (B) Frontal view showing PV1 and PV2 abutment in the SVC. (C) Transversal view showing the sinus venosus defect. (D) Oblique view showing the sinus venosus defect and PV2 abutment in the SVC. [Color figure can be viewed at wileyonlinelibrary.com]

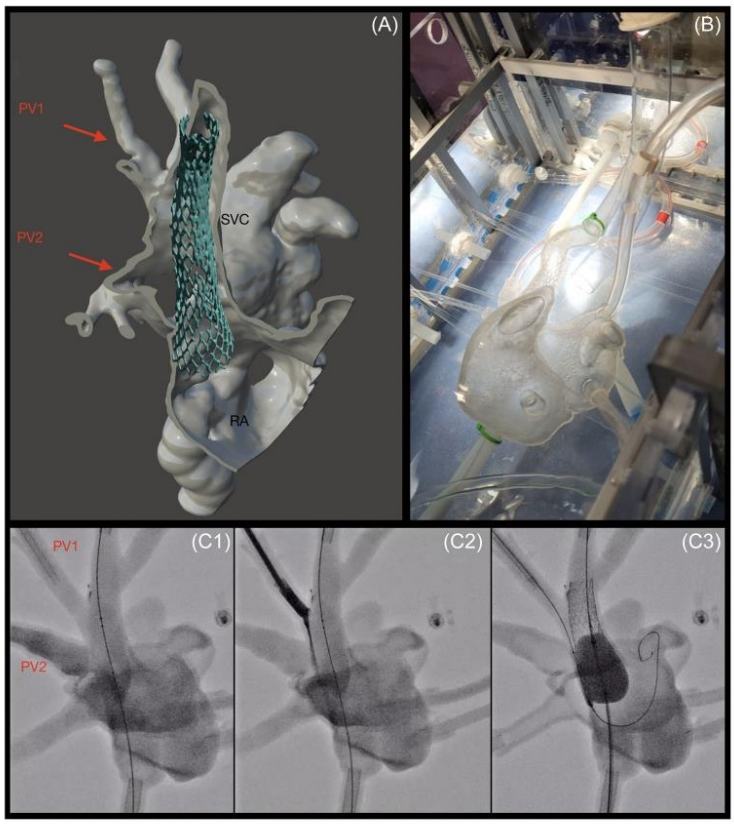

FIGURE 2 (A) 3D reconstruction of the atria and sinus venosus defect with a virtual simulation of stent implantation. The right superior pulmonary veins (PV1 and PV2) were rerouted to the left atrium (LA) with a tiny channel and the possibility of PV1 getting occluded. RA, right atrium; SVC, superior vena cava. (B) Photo of the 3D-printed model and container. (C1, C2, C3) Fluoroscopy of the 3D-printed model during procedure simulation. (C1) Angiography in the lower component of the anomalous pulmonary venous return (PV2) during balloon sizing using a noncompliant balloon. The PV2 is channeled to the left atrium without osbtruction and without residual left to right shunt. (C2) Angiography in the upper component of the APVR (PV1) during balloon sizing using a noncompliant balloon. PV1 has a thin streak of contrast draining toward LA. This did not give a confident guarantee that this vein would stay patent during the actual procedure. It indicated that a noncompliant high-pressure balloon was required in PV1 for its protection during stent deployment in the SVC as it was done on the model. (C3) Flairing of the lower part of the stent implanted in the superior vena cava of the printed model. [Color figure can be viewed at wileyonlinelibrary.com]

measured at 20 mm. A bulge of the compliant balloon obstructed the PV1. Then a noncompliant balloon at the expected diameter of the stent (Atlas 22 mm in diameter; BARD Peripheral Vascular Inc.) was inflated in the SVC. PV2 pathway to the left atrium was large (Figure 2.C1) and PV1 remained patent but with a very narrow channel to the left atrium (Figure 2.C2). Feasibility of the transcatheter SVD correction was not ruled out but based on this observation, protecting the PV1 channel with inflation of a vascular ballon was decided. A 80-mm long stent was deployed in the SVC, with simulatenous inflation of a 9-mm in diameter balloon posteriorly in the PV1 toward the left atrium (Figure 2.C3). The stent was stable and properly positioned. The lower end of the stent was flared (Figure 2.C3). Cone-beam CT (Figure 3A,B), dissection (Figure 3C,D reconstruction of the 3D stented model (Figure 3D) confirmed the good stent position and PV patency.

2.3 | Transcatheter procedure

General anesthesia and TEE guidance were used. Preprocedural CT was merged with fluoroscopy (GE Healthcare). A venous femoro-jugular rail was achieved using a 0.035 inch stiff wire (jugular vein

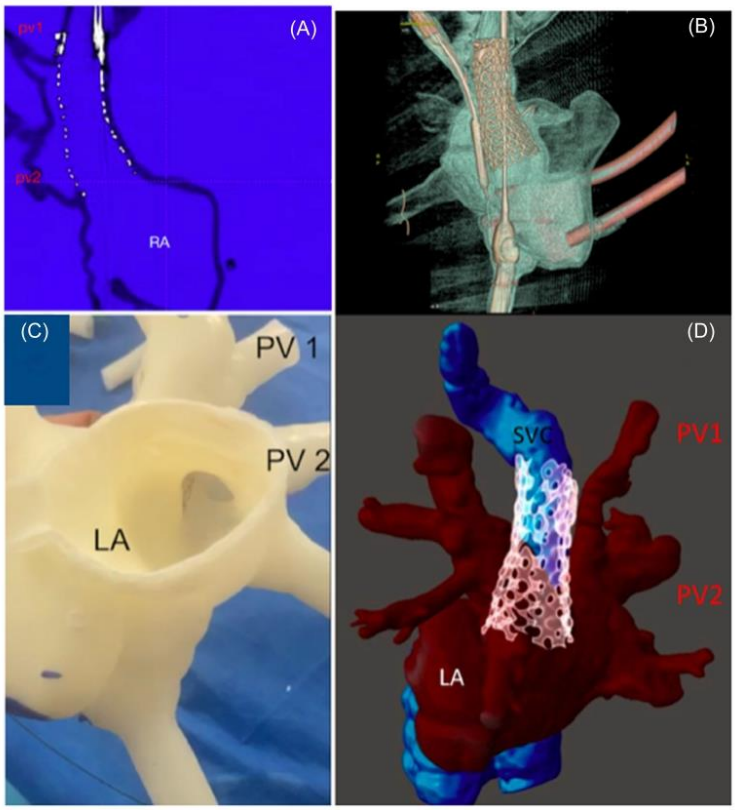

FIGURE 3 (A, B) Cone-beam tomography. (A) 2D frontal view of the cone-beam CT of the stented model with the patency of PV1. (B) 3D reconstruction of the printed model with the stent and a balloon inflated in the pulmonary vein. (C) Dissection of the 3D model. (D) Cardiac tomography of the model with the stent. The 3D reconstruction shows the patent channel from the right upper pulmonary vein to the left atrium. 2D, two-dimensional. [Color figure can be viewed at wileyonlinelibrary.com]

access: 6 Fr; right femoral vein 20 Fr). The atrial septum was punctured from the controlateral femoral vein (8.5 Fr), and a 0.035 inch guidewire was inserted from the left atrium into the right superior PV. PV, SVC, right and left atrial pressures were equal at 10 mmHg at the beginning of the procedure, reflecting the large nonrestrictive sinus venosus defect.

Compliant-balloon inflation in the SVC obstructed the superior anomalous PV. Inflation of a noncompliant balloon to the SVC diameter measured above the APVR left a patent posterior channel from this PV to the left atrium (Figure 4A,B).

A customized 85-mm-long, 10Z CP stent was mounted on a customized 24-mm-large, 80-mm-long BIB balloon (NuMed) and advanced to the SVC in a 20 Fr, 65 cm long Dry-Seal sheath (W.L. Gore & Associates, Inc.). An Armada balloon (Abbott) 9 mm in diameter and 80 mm in length was inflated in the superior PV toward the left atrium to prevent vein obstruction after stent inflation (Video S3). The stent was stable and well positioned. The lower end was flared under TEE guidance to occlude any residual shunting (Figure 4C,D). All steps of the procedure replicated the simulation. At the end of the procedure, upper PV1 pressure and left atrial pressures were equal to 18 mmHg reflecting absence of PV stenosis. SVC and right atrium pressures were equal to 9 mmHg suggesting the lack of significant residual shunt (Figure 4E,F).

Cardiac CT before discharge confirmed the effective stent positioning without shunting and with patent PVs (Figure 5 and Video S4). The 3D final stent position was consistent with the CT of the 3D-printed model after HOST (Figure 3D). The patient experienced no adverse events and heart function was improved. She was discharged on Day 3 under single antiplatelet therapy. After 6 months of follow-up, functional status was improved. PV remains patent on CT scan. No residual shunt was observed on echocardiography. Follow-up remains uneventful at 2 years after the procedure.

3 | DISCUSSION

The first transcatheter SVD corecction procedure was reported in 2013.[4] In recent years, many centres have adopted this technique with 75 procedures reported in 12 centres in 2021.[1] The growing experience has confirmed the feasibility and effectiveness of this procedure in carefully selected cases and with specifically developed equipment.[1,5] Growing experience has also identified risks, including stent migration and pulmonary vein occlusion.[1]

To facilitate assessment of the feasibility of this type of procedure, a three-dimensional understanding of the anatomical relationships of the APVR is essential. Most centres have used 3D-printed models of candidate patients before embarking on this procedure.[2,3,5,6] Favourable shapes have been identified with APVR close to the atria and in a posterior position, with a correctly sized SVD, neither too small to avoid restriction nor too large to avoid residual shunt. In these favorable cases, simulation on a 3D-printed model is no longer necessary. In the case presented here, the anatomical configuration, that is not unusual, was initially considered not favorable for transcatheter correction because of a high and lateral abutment in the SVC of a APVR component. In this configuration, the risk was either an occlusion of the PV if the stent was implanted high, or an instability of the stent and the persistence of an partial APVR if the stent was implanted below the level of the upper PV. Finally, using HOST on a 3D printed model, we were able to achieve complete correction of the SVD by protecting this PV with a balloon as suggested by Hansen and coll.[5]

Multiple types of 3D printed models have beed developed. The particularity of the 3D model used is that it is radiolucent, echogenic, and perfused with a pump to reproduce the conditions of the procedure. The flexibility and distensibility of the printing material was studied to approach that of the SVC. The contribution of the HOST, in this case, was the anticipation of the risk of occlusion of the right superior PV but the feasibility of PV protection by a ballon allowing its channelling along the stent to the left atrium. The second information was an anticipation of the anatomical relationships, for example, distance of the area to be covered, upper target diameter of the stent, to tailor the choice of the stent and balloon, specifically ordered for this procedure. Limitations are the cost of the model and the time required for 3D reconstruction, printing, and simulation. In addition, only a bare stent was provided for HOST while a covered stent was used in vivo. Nevertheless, in this challenging clinical case, we are convinced of the contribution of the HOST to the clinical success.

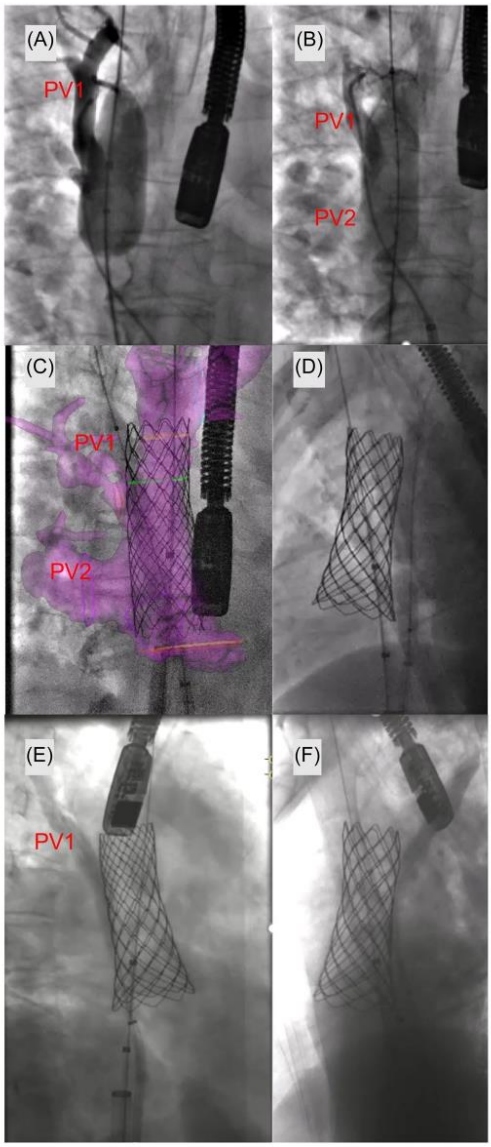

FIGURE 4 Transcatheter correction of the sinus venosus defect. (A) Compliant balloon sizing of the superior vena cava (Amplatz sizing balloon 34 mm). Obstruction of the upper component of the anomalous pulmonary venous return is observed (PV1). (B) Inflation of a noncompliant 24 mm in diameter Atlas balloon. Flow from the PV1 to PV2 and left atrium is observed. (C) Fusion of preprocedural CT and fluoroscopy. A covered CP10Z85 stent was deployed in the superior vena cava with protection of the right superior pulmonary vein by a 8 cm-long Armada balloon. (D) Stent deployment, left oblique anterior view. (E, F) Final stent position and angiography in the right superior pulmonary vein showing the patent channel to the left atrium. No significant residual shunting is seen. [Color figure can be viewed at wileyonlinelibrary.com]

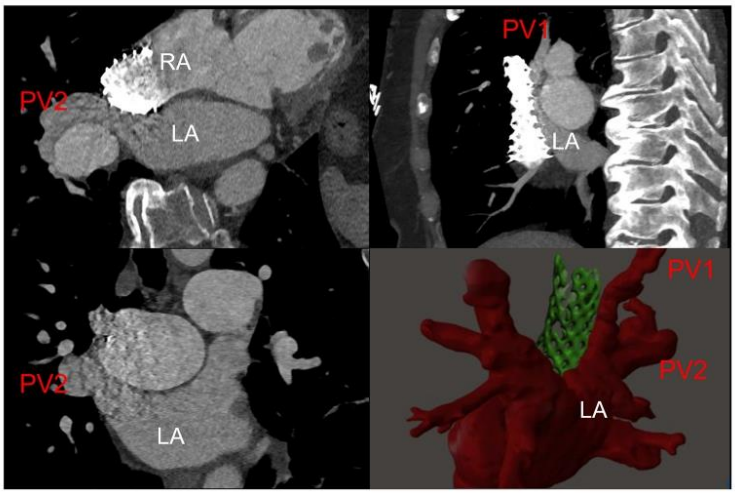

FIGURE 5 Multiplanar reformatted image of cardiac tomography postprocedure. The pulmonay veins are channeled to the left atrium without obstruction. [Color figure can be viewed at wileyonlinelibrary.com]

4 | CONCLUSION

Transcatheter correction of SVD proved feasible in a patient with a challenging anatomical configuration. HOST can be a useful and reliable tool for preparing the procedure, assessing its feasibility, the risk of PV obstruction, and for determining tailored stent and balloon mensurations.

ACKNOWLEDGMENTS

The authors would like to thank Antoinette Wolfe, Frederic Remy, and Roxane Nguyen Quemper for their contribution to this work. Marie Lannelongue Department of Research and Innovation, 3D Heart Modeling Co. (Caissargues, France), a grant from Federation Francaise de Cardiologie and a *Bourse Hélène de Marsan* grant from the French Society of Cardiology.

CONFLICTS OF INTEREST STATEMENT

Sebastien Hascoet: proctoring activity and consultant fees for Abbott and Edwards lifesciences. Clement Batteux, Vlad Ciobotaru, William Arditi, Benoit Decante, Clement Karsenty, Nicolas Combes: None.

ORCID

Clement Batteux http://orcid.org/0000-0001-6270-6154
Vlad Ciobotaru http://orcid.org/0000-0002-8964-2493
William Arditi http://orcid.org/0000-0002-8523-4492
Benoit Decante http://orcid.org/0000-0003-1642-7589
Clement Karsenty http://orcid.org/0000-0002-3303-5854
Nicolas Combes http://orcid.org/0000-0002-5238-7791
Sebastien Hascoet http://orcid.org/0000-0002-8695-0503

REFERENCES

1. Rosenthal E, Qureshi SA, Jones M, et al. Correction of sinus venosus atrial septal defects with the 10 zig covered cheatham-platinum stent—an international registry. *Catheter Cardiovasc Interv*. 2021;98(1):128-136.
2. Batteux C, Meliani A, Brenot P, Hascoet S. Multimodality fusion imaging to guide percutaneous sinus venosus atrial septal defect closure. *Eur Heart J*. 2020;41(46):4444-4445.
3. Batteux C, Azarine A, Karsenty C, et al. Sinus venosus ASDs: imaging and percutaneous closure. *Curr Cardiol Rep*. 2021;23(10):138.
4. Garg G, Tyagi H, Radha AS. Transcatheter closure of sinus venosus atrial septal defect with anomalous drainage of right upper pulmonary vein into superior vena cava—an innovative technique. *Catheter Cardiovasc Interv*. 2014;84(3):473-477.
5. Hansen JH, Duong P, Jivanji SGM, et al. Transcatheter correction of superior sinus venosus atrial septal defects as an alternative to surgical treatment. *JACC*. 2020;75(11):1266-1278.
6. Butera G, Sturla F, Pluchinotta FR, Caimi A, Carminati M. Holographic augmented reality and 3D printing for advanced planning of sinus venosus ASD/partial anomalous pulmonary venous return percutaneous management. *JACC Cardiovasc Interv*. 2019;12(14):1389-1391.

SUPPORTING INFORMATION

Additional supporting information can be found online in the Supporting Information section at the end of this article.

How to cite this article: Batteux C, Ciobotaru V, Arditi W, et al. Transcatheter correction of sinus venosus defect in a patient with a challenging anatomical configuration: from bench testing to clinical success. *Catheter Cardiovasc Interv*. 2023;102:1265-1270. doi:10.1002/ccd.30898

IV. Étude prospective nationale OPTIVENOSUS

1. Historique

4 stents OPTIMUS XXL ont été implantés avant le début de l'étude après accord de la demande compassionnelle transmise à l'ANSM, à partir de novembre 2021.
3 cas étaient faits à l'Hôpital Marie Lannelongue et le 4e cas était fait à l'hôpital universitaire de Grenoble[117].
Les 4 interventions se sont parfaitement déroulées et les patients sont sortis d'hospitalisation au deuxième jour post-opératoire.
Les 4 interventions avaient été préalablement simulés sur écran et sur banc d'essai permettant de vérifier un comportement du stent adéquat. Les procédures in-vivo ont ensuite répondu aux attentes concernant le stent utilisé.
A la date d'écriture de cette thèse, tous les patients se portent bien, sont améliorés cliniquement par la correction percutanée, sans complication notée.

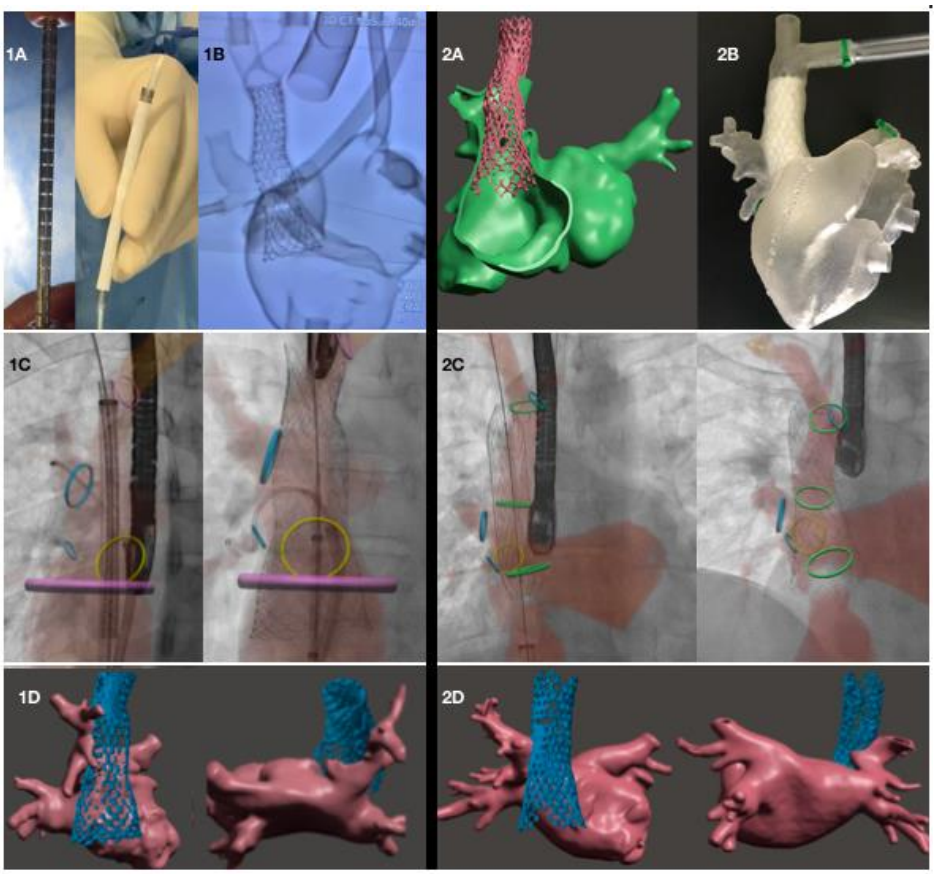

1. Benchtesting with non-sterile device
2. Pre-procedural virtual and in-vitro implantation of the device
3. Case in real life
4. Comparison between post-stent implantation on the patient (right) and on the 3D printed model (right).

Figure 55 : one of the first described use of Optimus XXL 99mm for SVD percutaneous correction

Batteux C & al. Multicenter experience of transcatheter correction of superior sinus venosus defect using the covered Optimus XXL stent. Rev Esp Cardiol 2023.

2. Création du Logo

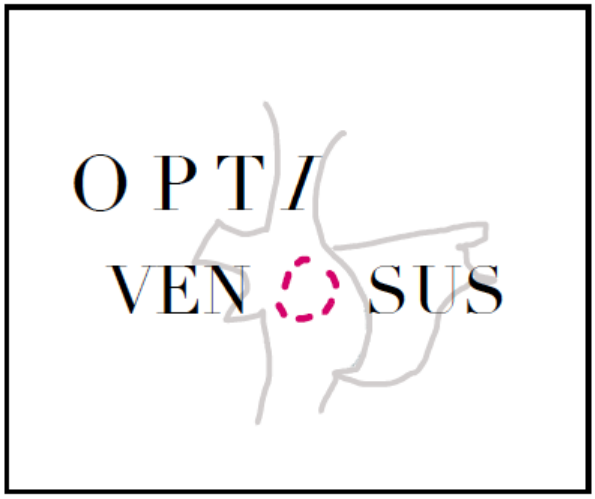

Figure 56 : logo officiel Optivenosus

La participation en tant qu'investigateur pour l'Hôpital Marie Lannelongue à cette étude, ainsi que la fonction de membre du Corelab d'imagerie, m'a poussé à m'investir dans la création d'un logo spécifique de cette étude, reprenant le nom de l'étude et des visuels clés concernant l'anatomie des CIA sinus venosus.

3. Partenaires et soutient financier

La Fondation Hôpital Saint Joseph est l'organisme principal ayant soutenu sur le plan institutionnel et financier l'étude Optivenosus.
D'autres financements ont été apportés au projet par l'intermédiaire des différentes bourses détaillées ci-dessous :
-2024 : Bourse de recherche industrielle Optivenosus 2 (Andratec) : 180 000€
-2023 : Bourse de recherche Optivenosus (Filiale de Cardiologie Pédiatrique et Congénitale de la Société Française de Cardiologie) : 50 000€
-2023 : Bourse de recherche industrielle Optivenosus (Andratec) : 180 000€
-2023 : Bourse appel à projet recherche Optivenosus (association de patients Association Nationale Cardiaques Congénitaux : 10 000€
-2023 : Bourse de recherche industrielle Optivenosus (3DHeart modeling) : 70 000€
-2022 : Bourse appel à projet en équipes Optivenosus (Fédération Française de Cardiologie) : 50 000€

-2022 : Bourse appel à projet recherche Optivenosus (Filière maladies rares - maladies cardiaques héréditaires Cardiogen) : 10 000€

-2022 : Bourse appel à projet recherche Optivenosus (association de patients Petits Cœurs de Beurre) : 3000€

4. Design de l'étude

Titre : Sécurité et Efficacité du traitement percutané par stent couvert en comparaison avec le traitement chirurgical chez les patients ayant une Communication Inter Atriale (CIA) de type *sinus venosus* / OPTIVENOSUS

N°ID-RCB : 2022-A01507-36

12 centres français médico-chirurgicaux- réseau Cardiopathie Congénitale Complexe (M3C)

Investigateur coordonnateur	Dr Sébastien HASCOËT, Hôpital Marie Lannelongue
Coordinateur	Pr Alban BARUTEAU, CHU Nantes

Objectif principal

Évaluation de la sécurité et de l'efficacité de la correction par cathétérisme de la CIA-SV à l'aide de stents couverts OPTIMUS déployés avec le ballon GEMINI en comparaison au traitement chirurgical de référence.

Critère principal :

A 6 mois, critère net associant efficacité de la correction de la CIA-SV définie par l'occlusion complète du shunt ET l'absence d'événement majeur lié à l'intervention (décès ou, dans le cas de la correction de la CIA-SV par voie percutanée, décision de conversion chirurgicale).

En l'absence de différence entre les deux groupes sur ce critère de jugement primaire, seront testés de manière hiérarchique :

- Critère d'efficacité : réduction du volume télédiastolique du ventricule droit (si l'IRM n'est pas possible – Réduction de la Surface télédiastolique du ventricule droit à l'échocardiographie)
- Critère de sécurité : défini par l'absence de ré-intervention percutanée ou chirurgicale, ou d'un accident vasculaire cérébral ou d'un trouble du rythme de la conduction nécessitant la pose d'un stimulateur cardiaque.

Critères secondaires

Après la correction trans-cathéter d'une CIA-SV à l'aide d'un stent couvert OPTIMUS ou après la correction chirurgicale, évaluation à 1 mois et 6 mois, 12 mois et 24 mois de la sécurité et de l'efficacité sur des critères additionnels. Évaluation de la sécurité jusqu'à 5 ans après l'intervention dans les 2 groupes.

Population concernée

Tous les patients de + de 12 ans adressés pour correction de CIA sinus venosus pris en charge dans les centres médico-chirurgicaux du réseau MC3 (malformation cardiaque congénitale complexe)
Partie 1 : Chirurgie considérée en 1ère intention pour tous les patients.
Cathétérisme envisagé pour patient majeur inéligible à la chirurgie sur décision de la RCP et ayant une forme anatomique favorable.
Partie 2 : chirurgie considérée en 1ère intention pour tous les patients.
Cathétérisme envisagé pour les patients majeurs inéligibles à la chirurgie (sur décision de la RCP) et ayant une forme anatomique favorable OU **patient majeur éligible à la chirurgie mais ayant une forme anatomique très favorable pour la prise en charge percutanée**.
3 critères techniques étudiés pour faisabilité de la prise en charge percutanée : stabilité attendue du stent, absence de risque d'obstruction des veines pulmonaires, absence de risque de shunt résiduel.
Analyse statistique en 2 temps
-analyse descriptive des 30 patients inclus dans le groupe cathétérisme.
-analyse comparative entre les deux groupes, menée sur le critère de jugement principal.
L'étude sur le critère de jugement principal est une étude de cohorte prospective comparative. Elle sera donc rapportée sur la base des critères du STROBE Statement (Strengthening the Reporting of Observational Studies in Epidemiology).
S'agissant d'une étude comparative, on se rapprochera le plus possible de la méthodologie de reporting d'une étude randomisée. L'analyse principale sera menée en intention de traiter.
Les résultats seront présentés sous forme de moyenne ± un écart type si le paramètre suit une distribution normale et médiane [écart interquartile] si la distribution n'est pas normale pour les paramètres quantitatifs. Pour les paramètres qualitatifs, les résultats seront présentés sous la forme de nombres (proportions).
Il n'est pas envisagé de technique de remplacement des données manquantes. Le principe de l'analyse se fera selon le principe d'un essai de différence. Par définition (maladie rare) la puissance de l'étude sera faible. C'est pourquoi tous les paramètres seront présentés avec leurs intervalles de confiance à 95%. Bien que cela ne soit pas recommandé, la puissance de la comparaison sera calculée *a posteriori* sur le critère de jugement principal.
Calendrier
Partie 1 : Début des inclusions : 12/05/2023
Fin des inclusions groupe endovasculaire : Inclusion du 30e patient groupe stent avec procédure endovasculaire effectivement réalisée.
Suivi des patients : 5 ans
Analyse des données de la partie 1 sur le critère de jugement principal : 2025
Partie 2 : Début des inclusions : septembre 2024.
Fin des inclusions du groupe endovasculaire : inclusion du 60e patient avec procédure endovasculaire effectivement réalisée.

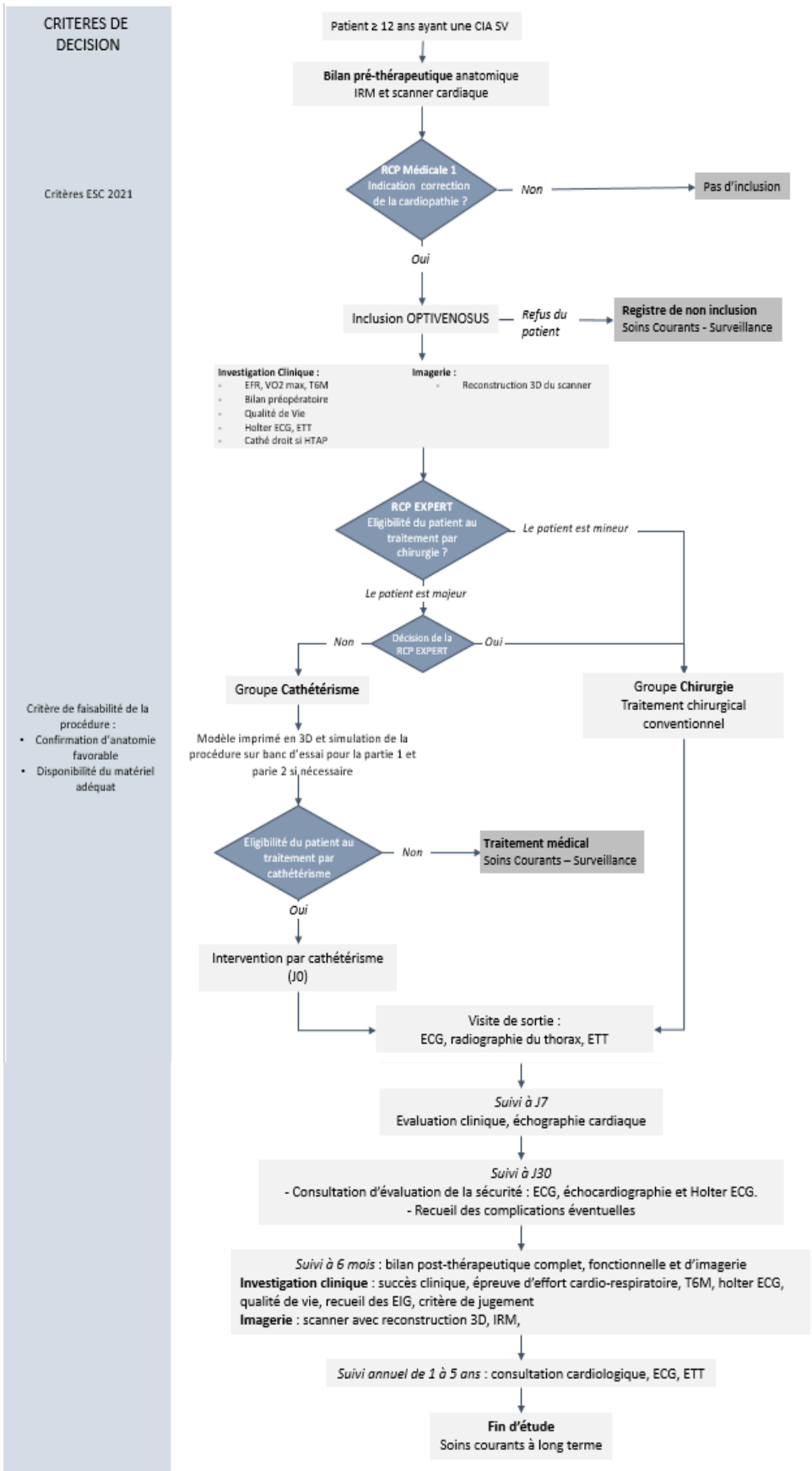

Figure 57 : flow chart initial de l'étude Optivenosus avec critères d'inclusion et d'exclusion ainsi que le protocole de suivi des patients

5. RCP nationales et eCRF

L'étude Optivenosus est basée sur la décision collégiale d'éligibilité des patients vis-à-vis des deux techniques opératoires analysées, à savoir la chirurgie (qui reste aujourd'hui le gold standard) et la correction percutanée.

Les décisions d'inclure les patients dans l'un des deux bras thérapeutiques est prise en réunion de concertation pluridisciplinaire, ayant lieu de manière mensuelle.

Ces RCP sont effectuées via la plateforme ROFIM qui permet le partage sécurisé d'informations médicales ainsi que de données d'imagerie. Au cours d'une visioconférence, les praticiens concernés peuvent ainsi partager leur point de vue sur chaque cas, aboutissant à une recommandation de prise en charge.

Les participants, sont de manière obligatoire, un médecin du centre investigateur, un chirurgien cardiaque congénitaliste et un cathétériseur interventionnel spécialisé en cardiopathie congénitale ayant l'expérience des correction percutanées de CIA sinus venosus. La présence du médecin référent du patient est souhaitée, et médecins des différents centres participants à l'étude sont systématiquement invités.

Classiquement, la RCP débute par une présentation clinique du patient, de son histoire de la maladie, de ses antécédents, comorbidités et traitements éventuels.

L'imagerie du patient est ensuite analysée en coupe (ETT, scanner, IRM) puis en 3D dimensions après modélisation 3D de la cardiopathie par le doctorant concerné par ce travail de thèse.

Une simulation virtuelle de la correction percutanée sur jumeau numérique projetée sur écran est ensuite proposée afin d'en évaluer sa faisabilité, ses challenges et ses risques.

La décision d'orienter le patient vers un des deux bras thérapeutique, unanime, est ensuite colligée sur une fiche de RCP prévue à cet effet. Parallèlement, le eCRF est complété en amont et au cours de la RCP, et aura pour vocation a être complété après l'intervention et durant le suivi postopératoire du patient.

Ci-joint, quelques extraits du eCRF créé et édité par notre équipe, permettant le suivi standardisé du patient inclus dans l'étude, depuis la phase préopératoire décisionnelle jusqu'au suivi postopératoire de 5 ans minimum.

Ce eCRF est édité via la plateforme RedCap et permet aux médecins investigateurs ainsi qu'aux attachés de recherche clinique des différents centres participants, de

colliger et suivre les évènements éventuels et le suivi de leur patient après l'intervention.

Cardiac MRI

Cardiac MRI performed	○ No ○ Yes
If not, reason	_____
Date	_____
LEFT :	
Left ventricular ejection fraction (%)	_____
If left ventricular ejection fraction not available :	☐ Not available
Indexed LV end-diastolic volume (ml/m2)	_____
If indexed LV end-diastolic volume not available	☐ Not available
Indexed LV end-telesystolic volume (ml/m2)	_____
If indexed LV end-telesystolic volume not available :	☐ Not available
RIGHT :	
Right ventricular ejection fraction (%)	_____
If right ventricular ejection fraction not available	☐ Not available
Indexed RV end-telediastolic volume (ml/m2)	_____
If indexed RV end-telediastolic volume not available	☐ Not available
Indexed RV end-telesystolic volume (ml/m2)	_____
If indexed RV end-telesystolic volume not available	☐ Not available
Right atrial surface (cm²)	_____
If right atrial surface not available	☐ Not available
Qp/Qs	_____

Right catheterization

Catheterization performed	○ No ○ Yes
If no, reason :	_____
Date	_____
Pressures :	
APVR (mmHg)	_____
If APVR not available	☐ Not available
SVC (mmHg)	_____
If SVC not available	☐ Not available
LA (mmHg)	_____
If LA not available	☐ Not available
Capillary (mmHg)	_____
If capillary not available	☐ Not available
RA (mmHg)	_____
If RA not available	☐ Not available
PA (mmHg)	_____
If PA not available	☐ Not available
Sat VI (%)	_____
If Sat VI not available	☐ Not available
Sat PA (%)	_____
If Sat PA not available	☐ Not available

Center Of Origin Opinion Regarding SVD Percutaneous Correction

/!\ Once this data has been completed, no further change will be possible /!\

	No	Yes	Not available
Cardiac anatomy appearing to be suitable for percutaneous treatment	○	○	○
_ Risk of APVR compression	○	○	○
_ Risk of residual shunt	○	○	○
_ Risk of stent instability	○	○	○
_ 2nd anchoring stent may be required	○	○	○
_ Possible need for transseptal	○	○	○
_ PV protection possibly necessary	○	○	○

Stent length estimation - length (mm) _____

Stent size estimation - delivering balloon target diameter (mm) _____

Estimated flairing at the inferior part of the stent (mm) _____

If estimated flairing at the inferior part of the stent not available : ☐ Not available

Estimated complexity of the transcathether procedure
○ Green (straightforward)
○ Orange (feasible but challenging)
○ Red (not feasible or highly challenging)
○ Not available

3D CT Virtual Simulation (CORELAB Scanner)

	No	Yes	Not available
Cardiac anatomy appearing to be suitable for percutaneous treatment	○	○	○
_ Risk of APVR compression	○	○	○
_ Risk of residual shunt	○	○	○
_ Risk of stent instability	○	○	○
_ 2nd anchoring stent may be required	○	○	○
_ Possible need for transseptal	○	○	○
_ PV protection possibly necessary	○	○	○

Stent length estimation - length (mm) _____

Stent size estimation - delivering target balloon diameter (mm) _____

Estimated flairing at the inferior part of the stent (mm) _____

If estimated flairing at the inferior part of the stent not available : ☐ Not available

Estimated complexity of the transcathether procedure :
○ Green (straightforward)
○ Orange (feasible but challenging)
○ Red (not feasible or highly challenging)
○ Not available

Bench Test

	No	Yes	Not available
Cardiac anatomy appearing to be suitable for percutaneous treatment	○	○	○
_ Risk of APVR compression	○	○	○
_ Risk of residual shunt	○	○	○
_ Risk of stent instability	○	○	○
_ 2nd anchoring stent may be required	○	○	○
_ Possible need for transseptal	○	○	○
_ PV protection possibly necessary	○	○	○

Stent length estimation - length (mm)	_____
Stent size estimation - delivering target balloon diameter (mm)	_____
Estimated flairing at the inferior part of the stent (mm)	_____
If estimated flairing at the inferior part of the stent not available :	☐ Not available
Estimated complexity of the transcathether procedure :	○ Green (straightforward) ○ Orange (feasible but challenging) ○ Red (not feasible or highly challenging) ○ Not available

Results	
Stent in position	○ No ○ Yes ○ Not available
APVR obstruction	○ No ○ Yes ○ Not available
If APVR obstruction, specify :	○ Absent ○ Mild ○ Moderate ○ Severe
Residual shunt	○ No ○ Yes ○ Not available
If residual shunt, specify :	○ Absent ○ Mild ○ Moderate ○ Severe
Cardiac surgical conversion	○ No ○ Yes ○ Not available
If cardiac surgery conversion, specify the reason	_____
Other emergency surgery performed	○ No ○ Yes ○ Not available
If other emergency surgery, specify the reason	_____

12-01-2024 21:18 projectredcap.org REDCap

6. Accompagnement des centres dans la prise en charge

L'étude Optivenosus est multicentrique est permet aux centres experts dans la prise en charge des cardiopathies congénitales, au sein du réseau M3C, de réaliser les interventions de correction percutanée dans leur centre. Si besoin, un accompagnement médico-technique leur est proposé pour les premiers cas, permettant ainsi d'opérer les patients candidats dans des conditions de sécurité et d'expertise optimisées.

Ci après, la liste des centres participants à l'étude Optivenosus.

Centre 1 : Hôpital Marie-Lannelongue
Centre 2 : CHU Nantes
Centre 3 : CHU Toulouse
Centre 4 : CHU Lille
Centre 5 : CHU Bordeaux
Centre 6 : CHU Lyon

Centre 7 : CHU Marseille
Centre 8 : CHU Clermont-Ferrand
Centre 9 : HEGP Paris
Centre 10 : CHU Necker APHP Paris
Centre 11 : CHU Tours
Centre 12 : Clinique Pasteur, Toulouse
Centre 13 : CHU Grenoble

STUDY DESIGN : Safety and Efficacy of Transcatheter Correction of Sinus Venosus Defect Using 70-100 mm Long Partially PTFE-Covered Optimus-CVS® XXL Stents Compared to Surgery: The OPTIVENOSUS Study Design

Clément Batteux, MD, MHSc, PhD candidate[1, 2, 3], Vlad Ciobotaru, MD, MHSc, PhD candidate[2, 3, 4], Raymond N. Haddad, MD, MHSc, PhD candidate[1, 2, 3, 5], Ali Houeijeh, MD, PhD[6], Clément Karsenty, MD, PhD[7], Ivan Bouzguenda, MD[8], Régine Roussin, MD[1], Nicolas Combes, MD, MHSc[1, 9], Mohamed Bakloul, MD[10], Philippe Aldebert, MD[11], Marien Lenoir, MD[11], Fanny Dion, MD[12], Bruno Lefort, MD, PhD[12], Gilles Bosser, MD, PhD[13], Damien Bonnet, MD, PhD[14], Alain Fraisse, MD, PhD[15], Hélène Bouvaist, MD[16], Jurgen Hoerer, MD, PhD[17], Pamela Moceri, MD, PhD[18], Claire Dauphin, MD[19], Jelena Radojevic, MD[1, 20], Jean-Benoit Thambo, MD, PhD[21], Florence Lecerf, MHSc[5], Oceane Hache[5], Delphine Chevalier, PharmD[5], Hélène Beaussier, PharmD, PhD[5], Laure Aubrège, ME, PharmD[5], Arshid Azarine, MD, MHSc, PhD candidate[3, 22], Benoit Decante, MHSc[3, 5], Gilles Chatellier, MD, PhD[5], Magalie Ladouceur[22], MD, PhD[1, 23], Alban-Elouen Baruteau, MD, PhD[24], Roland Hénaine, MD, PhD[10], Grégoire Albenque, MD, MHSc, PhD candidate[1, 2, 3], Sébastien Hascoët, MD, PhD, FESC[1, 2, 3, 5*]

[1] Filière des cardiopathies congénitales enfant adultes, hôpital Marie Lannelongue, centre constitutif du réseau maladies rares malformations cardiaques congénitales complexes - M3C, les Hôpitaux Saint Joseph et Marie Lannelongue, 133 avenue de la résistance, 92350 Le Plessis Robinson, France.
[2] Faculté de Médecine Kremlin-Bicêtre, Université Paris-Saclay, France.
[3] Université Paris-Saclay, INSERM, UMR_S 999, Hypertension Pulmonaire : Physiopathologie and Innovation Thérapeutique (HPPIT), AP-HP, Hôpital Bicêtre, Hôpital Marie Lannelongue (Groupe Hospitalier Paris Saint Joseph), ERN-LUNG, Le Plessis-Robinson, France
[4] Cardiologie, Clinique Les Franciscaines, 3DHeartModeling, Nîmes, France
[5] Direction de la Recherche et de l'Innovation Médicale, MALIC, Hôpitaux saint Joseph Marie Lannelongue, 133 Avenue de la Résistance, 92350 Le Plessis Robinson, France.
[6] Service de cardiologie pédiatrique, centre de compétence du réseau maladies rares malformations cardiaques congénitales complexes - M3C, Centre Hospitalier Universitaire de Lille, 2 Av. Oscar Lambret, 59000 Lille, France
[7] Service de cardiologie pédiatrique, centre de compétence du réseau maladies rares malformations cardiaques congénitales complexes- M3C, Hôpital des enfants, CHU Toulouse, 330 avenue de Grande Bretagne, 31300 Toulouse, France
[8] Cabinet Intercard, Hôpital Privé de la Louvière, bâtiment Vendôme, 20 rue Ballon, 59800 Lille, France
[9] Service de cardiologie, Clinique Pasteur, 31000 Toulouse, France
[10] Département Médico-Chirurgical de Cardiologie Congénitale du Fœtus, de l'Enfant et de l'Adulte, centre de compétence du réseau maladies rares malformations cardiaques congénitales complexes - M3C, Hôpital Louis Pradel, Hospices civils Lyon, 59 boulevard Pinel, 69500 Bron, France

[11] Service de cardiologie pédiatrique , centre de compétence du réseau maladies rares malformations cardiaques congénitales complexes - M3C, Hôpital Timone, Assistance Publique des Hôpitaux de Marseille, 278 rue Saint-Pierre, 13385 Marseille, France
[12] Service de cardiologie pédiatrique, centre de compétence du réseau maladies rares malformations cardiaques congénitales complexes - M3C, CHU Tours, France
[13] Service de cardiologie congénitale et pédiatrique, centre de compétence du réseau maladies rares malformations cardiaques congénitales complexes - M3C, CHU Nancy, France
[14] Centre de Référence Malformations Cardiaques Congénitales Complexes - M3C, Hôpital Universitaire Necker-Enfants malades, Assistance Publique-Hôpitaux de Paris (AP-HP), Paris, France.
[15] Royal Brompton & Harefield Hospitals, Guys & St Thomas's NHS Trust and National Heart and Lung Institute, Imperial College, Sydney Street, London, SW3 6NP, United Kingdom
[16] Service de cardiologie, centre de compétence du réseau maladies rares malformations cardiaques congénitales complexes - M3C, CHU Grenoble Alpes, Grenoble, France
[17] Department of Congenital Heart Disease and Pediatric Cardiology, German Heart Centre Munich, Technical University of Munich, Munich, Germany
[18] Service de Cardiologie, centre de compétence du réseau maladies rares malformations cardiaques congénitales complexes - M3C, CHU Nice, France
[19] Service de cardiologie pédiatrique, centre de compétence du réseau maladies rares malformations cardiaques congénitales complexes - M3C, CHU Clermont-Ferrand, France
[20] Cabinet de cardiologie foetale pediatrique et congenitale, 2 rue François Epailly - Maison Médicale des 2 Rives, Clinique Rhena, 67000 Strasbourg, France
[21] Service de cardiologie pédiatrique, centre constitutif du réseau maladies rares malformations cardiaques congénitales complexes - M3C, CHU Bordeaux, IHU LIRYC, Electrophysiology and Heart Modeling Institute, CRCTB, INSERM U1045, Pessac, France.
[22] Service de radiologie, les hôpitaux Saint-Joseph et Marie Lannelongue, 133 avenue de la résistance, 92350 Le Plessis Robinson, France.
[23] Service de cardiologie, Hôpitaux Universitaires de Genève, Rue Gabrielle-Perret-Gentil 4, 1205 Genève, Suisse
[24] Service de cardiologie pédiatrique, centre de compétence du réseau maladies rares malformations cardiaques congénitales complexes - M3C, Centre Hospitalier Universitaire de Nantes, 1 Pl. Alexis-Ricordeau, 44093 Nantes, France
*Corresponding Author:
Dr Sébastien HASCOËT, MD, PhD, FESC
Department of Pediatric and Adult Congenital Heart Diseases
Hôpital Marie Lannelongue, Groupe Hospitalier Paris Saint-Joseph
133 avenue de la Résistance 92350 Le Plessis-Robinson, France
Email: s.hascoet@ghpsj.fr; Tel.: +33 140 942 800

Acknowlegments
We would like to thank (by alphabetical order) Antoine Agathon; Pascal Amedro, MD, PhD; Denis Angoulvant, MD, PhD; Elise Barre, MD; Emre Belli, MD; Hizia Benkerrou; Aurélie Blondeau; Elisabeth Castanier-Martel; Clémence Charlon; Philippe Charron, MD, PhD; Anne Chauvire Drouard; Olivier Chavanon, MD; Sarah Cohen, MD, PhD; Fatoumata Coulibaly; Claire Delcourte; Stephane Dequand; Charlotte Denis, MD; Jean-Marc El Arid, Ali Fekraoui, Lalie Fellahi; Sylvie Di Filippo, MD, PhD, Olivia Domanski, MD; Clémence Escoffier; Virginie Fouilloux, MD, PhD; Claire Galoin-Bertail, MD; Francois Godart, MD, PhD; Juliette Goutner; Emilie Grezes; Sophie Guiti Malekzadeh Milani, MD; Slimane Idir, Francis Juthier, MD, PhD; Fabien Labombarda, MD, PhD; Daniela Laux, MD; Marien

Lenoir, MD; Mohamed Ly, MD; Amélie Maack; Gaelle Marguin; Marie-Paule Masseron; Djedjiga Naudin Anne Moulin-Zinsch, MD; Laura Olivares; Caroline Ovaert, MD, PhD; Claire Paradis; Jérôme Petit, MD; Olivier Raisky, MD, PhD; Guillaume Reverdito, MD; Hichem Sakhi, MD; Catherine Sportouch, MD; Imène Triaki; Jérôme Troncy; Olivier Vahdat, MD for their support.

ABSTRACT

Background: Transcatheter correction of sinus venosus defect (SVD) provides a less invasive alternative to open-heart surgery. This study evaluates the safety and efficacy of 70 to 100mm partially PTFE-covered balloon-expandable Optimus-CVS® XXL stents (AndraTec, Germany), specifically designed for SVD repair, compared to surgical intervention.

Methods: OPTIVENOSUS study is a French nationwide, multicenter, prospective comparative cohort study of patients with indications for SVD correction (May 2023 – Feb 2031). The study comprises two parts, with a comprehensive shift in patient assignment to the catheter group. Part 1 will enroll 30 adult patients (>18 years) deemed ineligible for surgery by a multidisciplinary team, who will undergo feasibility assessment for catheter correction, including virtual simulations and three-dimensional-printed bench testing. Part 2 will add 30 adult patients with favorable anatomy, considered directly for stent therapy, while 3D-printed bench testing will be reserved for complex cases. Surgical patients (≥12 years) will be continuously enrolled throughout the study, with no enrolment cap. All patients will receive standardized follow-up for up to 5 years.

Results: Primary endpoint is a 6-month composite measure of safety and efficacy, defined by trivial or absent residual shunt and the absence of major adverse events (death or surgical conversion). If no significant difference is found, efficacy (end-diastolic right ventricular volume reduction) and safety (absence of re-intervention, stroke, pacemaker implantation, or severe arrhythmia) will be further evaluated using hierarchical analysis.

Conclusion: OPTIVENOSUS study evaluates the safety and effectiveness of transcatheter SVD correction with Optimus-CVS® XXL stents versus surgery.

Clinicaltrial.gov Identifier: NCT05865119

Keywords: catheterization, congenital heart disease, covered stent, sinus venosus defect.

List of abbreviations: 3D: three-dimensional; ASD: atrial septal defect; CHD: congenital heart disease; Co-Cr: cobalt-chromium; CT: cardiac tomography; ITT: Intention-to-Treat; MRI: myocardial resonance imaging; PARPVR: partial anomalous right pulmonary venous return; PTFE: Polytetrafluoroethylene; RV: right ventricular; RVEDV: right ventricular end-diastolic volume; SVD: sinus venosus defect; SVC: superior vena cava.

Graphical Abstract

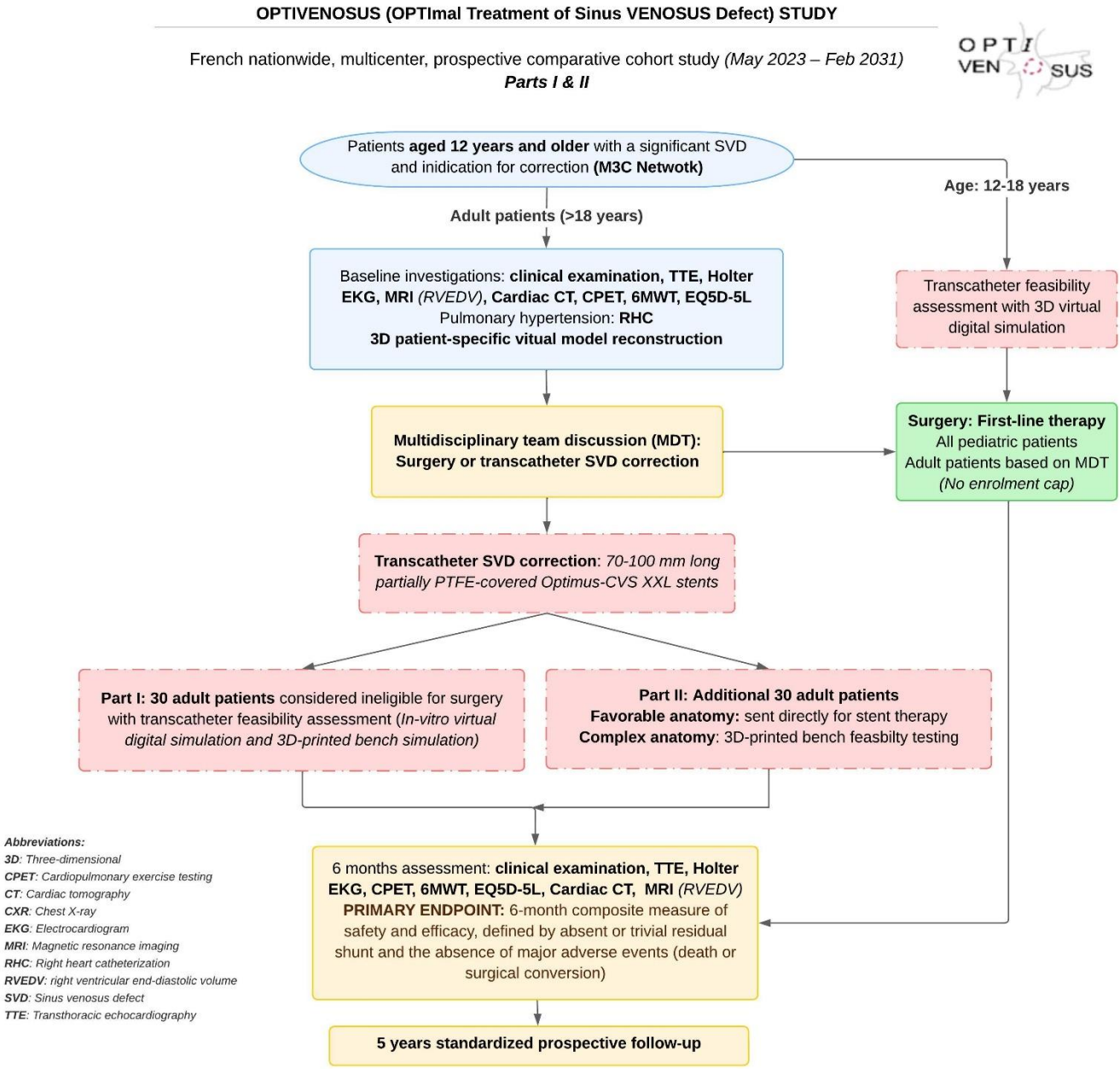

INTRODUCTION

Superior sinus venosus defect (SVD) is a complex congenital heart defect (CHD) characterized by an interatrial shunt caused by the absence of a common wall between the superior vena cava (SVC) and the right pulmonary veins [1, 2]. This defect and the partial anomalous right pulmonary venous return (PARPVR) into the SVC, create a left-to-right shunt that results in right heart volume overload, dilation of the right heart chambers, and pulmonary congestion. If left untreated, SVD can lead to severe long-term complications such as stroke, supraventricular arrhythmias, pulmonary hypertension, and heart failure [3]. Intervention is essential to correct the defect and prevent these adverse outcomes, particularly when significant right heart volume overload is present [4].

Historically, SVD correction has been performed exclusively through open-heart surgery, where normal blood flow is restored by redirecting the anomalous pulmonary venous return

through the interatrial communication into the left atrium [5–13]. However, this traditional approach is associated with potential complications such as stenosis of the SVC or pulmonary veins, residual shunting, scar-related re-entrant atrial tachycardia, and sinoatrial node dysfunction. In response to these challenges, an alternative technique has been developed that involves the implantation of a long PTFE-covered stent from the SVC to the right atrium. This method redirects the anomalous pulmonary venous flow into the left atrium and occludes its connection with the right atrium [14, 15]. First introduced in 2009 [2], this innovative approach was applied in France in 2020 [16]. While preliminary results are promising, they remain limited by variations in stent choice, along with guidance and implantation techniques across centers, necessitating further investigation to fully assess the long-term benefits [13, 17–33].

The selection and deployment of stents for transcatheter SVD correction are influenced by several factors, including the diameter of the SVC and the number and configuration of anomalous pulmonary veins. For many cases, stents longer than 70 mm are required [17]. Certain manufacturers, such as NuMED (United States), have developed extended stents specifically for SVD correction. Notably, the feasibility and safety of transcatheter SVD correction using CP10Z stents have been demonstrated in an international multicenter study [17]. However, these stents currently lack European certification for lengths greater than 60 mm, which are often necessary [17]. Moreover, issues such as stent embolization, innominate vein occlusion, and endoleak due to tears in the fragile covering polytetrafluoroethylene (PTFE) membrane have been documented [17, 34-36]. In contrast, the efficacy of 70-100 mm long, partially PTFE-covered Optimus-CVS XXL balloon-expandable cobalt-chromium (Co-Cr) stents (AndraTec, Germany), designed specifically for this procedure, has yet to be conclusively established, although preliminary reports suggest their feasibility [18, 25].

The primary objective of this study is to evaluate the efficacy of transcatheter SVD correction using Optimus-CVS XXL stent technologies in comparison to conventional surgical approaches. To address this, a nationwide multicenter prospective interventional cohort study was designed, the protocol for which is outlined below.

METHODS

Study aim

To evaluate the safety and efficacy of transcatheter treatment for SVD in patients aged over 18 years old using 70-100 mm long, partially PTFE-covered Optimus-CVS XXL balloon-expandable Co-Cr stents, implanted with AltoSA-XL GEMINI dual balloon catheters, in comparison to surgical intervention.

Study design and patient assignment

The OPTIVENOSUS (OPTImal Treatment of Sinus VENOSUS Defect) study is a French nationwide, multicenter, prospective comparative open cohort study of patients aged 12 and older with indications for SVD correction.

The study's flowchart is presented in Fig. 1. The study will be conducted in two parts, during which only adult patients over 18 years of age will be eligible for the transcatheter option. Pediatric patients aged 12 to 18 years will undergo in-vitro virtual digital simulations to assess the feasibility of transcatheter correction in children; however, surgical intervention will remain their exclusive treatment option throughout both phases of the study.

Part 1 will enroll 30 patients in the stent group to assess feasibility, followed by Part 2, which will include 30 additional patients in the same group with a comprehensive shift in patient assignment to the catheter group (described below). Patients referred for surgery will be continuously enrolled throughout the study period without a cap on the number until the last transcatheter procedure is completed. In Part 1, surgery will serve as the first-line approach for all patients. Adult patients (over 18 years) deemed ineligible for surgery—based on a

multidisciplinary team evaluation—will undergo a feasibility assessment for transcatheter SVD correction. This assessment will include virtual simulations and in-vitro bench testing using personalized three-dimensional (3D)-printed models [37]. Surgical ineligibility will be determined by factors such as advanced age (over 60 years), comorbidities (e.g., coronary artery disease, obesity, diabetes, lung disease, renal failure, or antithrombotic therapy), or specific anatomical considerations. Additionally, patients with a history of SVD-related complications (e.g., arrhythmia, heart failure, or pulmonary hypertension) and challenging anatomical features (e.g., a high connection of the PARPVR in the SVC) will undergo comprehensive evaluation.

In Part 2, surgery will remain the primary treatment strategy for all patients. However, adult patients with highly favorable anatomical features may be considered for catheterization if they meet three specific criteria: (1) sufficient stent stability, defined as more than 2 cm between the upper edge of the PARPVR and the lower edge of the innominate vein; (2) no risk of pulmonary vein obstruction during virtual simulation; and (3) the anticipated absence of a residual shunt. Virtual numerical simulations on digital twins will enhance anatomical assessments for all patients in this phase, while 3D-printed bench testing will be reserved for cases with complex anatomy. Complex anatomy is defined as multiple right pulmonary veins draining into the SVC, at least one right superior pulmonary vein located within 2 cm of the innominate vein, a cavo-atrial junction exceeding 30 mm in diameter, or a risk of pulmonary venous obstruction during virtual simulation.

Research and ethical standards

The study will adhere to Strengthening the Reporting of Observational Studies in Epidemiology (STROBE) guidelines. All procedures associated with this study adhere to Good Clinical Practice (GCP) guidelines and comply with the ethical standards outlined in the 1964 Declaration of Helsinki and its subsequent amendments. The study protocol has received approval from an independent Ethics Committee, known as the "Comité de Protection des Personnes" (2022-A01507-36), and is authorized by the national agency for drug and medical device safety, the "Agence Nationale de Sécurité du Médicament et des Dispositifs Médicaux." Additionally, the study is registered on ClinicalTrials.gov under the identifier NCT05865119. Permission has been obtained from AndraTec to use and acknowledge their products. Written informed consent will be secured from all participants aged 18 and older. For participants aged 12 to 18, the study requires non-opposition from their parents or legal guardians regarding data processing before inclusion. All participants must consent to be followed throughout the study period and must be affiliated with a French or European Union healthcare system.

Study funding

Marie-Lannelongue Hospital serves as the study promoter, while Fondation Saint Joseph Hospital is the primary sponsor of the OPTIVENOSUS study. Additional research funding has been secured from the French Society of Cardiology (Filiale de Cardiologie Pediatrique et Congénitale de la Société Française de Cardiologie), the French Federation of Cardiology (Fédération Française de Cardiologie), CARDIOGEN (filière nationale de santé maladies cardiaques héréditaires ou rares), the CRC-3F and the patient organizations "Association Nationale des Cardiaques Congénitaux", "Le cœur dans la main" and "Association Petit Coeur de Beurre." Medical devices for the study have been provided by AndraTec and 3D-printed models have been provided by 3DHeartModeling.

Study population

Participants over 12 years old with SVD requiring correction within the M3C network will be enrolled over two years. The indication for SVD correction will be based on the criteria outlined in the 2020 European Society of Cardiology (ESC) guidelines. This includes both symptomatic and asymptomatic individuals who exhibit significant right ventricular (RV)

volume overload or have a history of ischemic stroke attributed to paradoxical embolism [4]. RV volume overload will be defined as a right ventricular end-diastolic volume (RVEDV) exceeding 112 mL/m² for women and 121 mL/m² for men, as assessed by magnetic resonance imaging (MRI) [38]. Exclusion criteria will include patients under legal guardianship or curatorship, individuals deprived of liberty, those under judicial protection, pregnant or breastfeeding women, and patients currently enrolled in another interventional research protocol.

Patient recruitment

Participants will be recruited through the French Network for Complex Congenital Heart Diseases (M3C network). A total of 11 centers within the M3C network, which specialize in managing complex CHDs, have agreed to participate in this study. Throughout the country, 24 investigators—including pediatric cardiologists, adult congenital cardiologists, and pediatric cardiac surgeons—will oversee patient recruitment. Each site will be managed by a local principal investigator, supported by co-investigators, a research nurse or fellow, and a clinical research assistant. All team members are trained in Good Clinical Practice and are well acquainted with the study protocol. Each center will be responsible for recruiting participants and conducting scheduled follow-up visits.

Screening of eligible participants will involve a range of diagnostic modalities, including transthoracic echocardiography, MRI, cardiac computed tomography (CT) scans, Holter ECG monitoring, cardiopulmonary exercise tests, six-minute walking distance assessments, and EQ5D-5L quality of life questionnaires [39]. Utilizing data from CT scans, a digital twin will be created through 3D reconstruction of the heart and veins, allowing for virtual simulation of transcatheter SVD correction. Pre-operative assessments will include spirometry and carotid ultrasound. Patients at risk for coronary artery disease will undergo coronary CT scans and/or coronary angiography. Additionally, patients with suspected pulmonary hypertension will have right heart catheterization to calculate pulmonary vascular resistance using the Fick method and to assess the degree of left-to-right shunting, which will inform the indication for shunt correction. Indications for SVD correction in these patients will be validated through a multidisciplinary meeting that includes pulmonologists from the reference center for pulmonary hypertension management at Kremlin-Bicetre Hospital (Pulmotension network). A national multidisciplinary online meeting will convene monthly on the secure ROFIM platform to evaluate eligibility for study participation and the appropriateness of various therapeutic options.

Study devices

The Optimus-CVS® XXL is a PTFE-covered, balloon-expandable, non-premounted vascular stent. Made from high-density Co-Cr alloy (MP35N) using precision laser-cut technology, it features a 4.2 mm inner diameter and the patented hybrid-cell "Crown" design, comprising 15 rounded Zig segments connected by Omega-Flex links, with a strut thickness of 0.22 mm and segment length of 4.8 mm [40]. It incorporates a sandwich covering with thermally bonded inner and outer Nano-PTFE layers and an end-free design, leaving half a row of bare-metal cells at both extremities [41, 42]. CE-approved as a Class IIb medical device, it is available in 9 standard lengths (13, 18, 23, 28, 33, 38, 43, 48, and 57 mm) with an IFU-defined functional expansion range of 22 to 28 mm, requiring a minimal crimping platform size of 13 Fr and a recommended introducer sheath size of 17 Fr.

To address the specific requirements of the study procedure, custom lengths of 70 mm, 80 mm, 90 mm, and 100 mm have been developed, designated by model references ATCV-70XXL, ATCV-80XXL, ATCV-90XXL, and ATCV-100XXL. The covering design was refined for each model, incorporating a 2 cm uncovered cranial section (Fig. 2).

Stent deployment will be achieved using the AltoSa-XL-Gemini® PTA over-the-wire dual balloon catheter (0.035-inch guidewire compatible) by AndraTec (Fig. 2) [42], available in

four outer diameter sizes—24 mm (18 mm inner balloon), 26 mm (20 mm inner balloon), 28 mm (22 mm inner balloon), and 30 mm (24 mm inner balloon)—with lengths of 70, 80, 90, and 100 mm and a catheter shaft size of 14 Fr.
Other devices used during the procedure include the Exeter Retrieval Snare, AltoSa-XL PTA balloon catheter, AltoSa-SFT Tacking Balloon Catheter, and guidewires such as the Lokum "Amplatz-Type", Lokum "L-Quest", and Lokum "L-Quest-Mini", all manufactured by AndraTec.

STUDY INTERVENTIONS AND PLANNING

Surgical correction

Surgical repairs will be conducted at participating centers following established protocols. The choice of SVD correction technique, whether single patch, double patch, or Warden procedure, will be left to the discretion of the operating team. Surgical procedures will be performed either through a sternotomy approach or via video-thoracoscopy.

3D patient-specific virtual model

Cardiac CT scan sequences will be selected, anonymized, and extracted in DICOM format. These DICOM images will then be imported into semi-automatic segmentation software (ITK-SNAP), utilizing active contour segmentation **(Fig. 3A)**. Initially, the region of interest (ROI) will be selected, and the image contrast will be adjusted to enhance delineation between the anatomical region and the background. Propagation bubbles will be applied to the anatomical region to be modeled, initiating local propagation that follows the light intensity and stops at contrast boundaries, resulting in an anatomical filling of the structures of interest. This filling will be exported as a voxel cloud in STL format and processed in Meshmixer for smoothing and polishing. A 0.7 mm outer shell will be added to represent blood within the structures. Finally, after removing the initial filling, a definitive hollow anatomical structure will be created **(Fig. 3B-D)**.

In-vitro virtual digital simulation

For virtual simulation of transcatheter correction of SVD, a stent library will be developed, featuring various models that can be modified in length and diameter to accurately match the anatomical model. The shape and dimensions of the implanted stent will be analyzed to verify the efficacy and safety of the correction, ensuring the absence of residual shunt and pulmonary vein stenosis.

In-vitro 3D-printed bench simulation

From the STL model, a 3D printed physical model will be created using stereolithography (SLA) printing technology (3DHeartModeling, Nimes, France) resulting in a flexible, distensible, radio-transparent, and ultrasound-transparent structure for each patient. This model will be perfused on a test bench, allowing the in-vitro execution of the procedure under conditions that closely mimic real-life scenarios, utilizing tools such as fluoroscopic guidance, transesophageal echocardiography, and multimodal image fusion **(Fig. 3E)**. The test bench simulation will facilitate a step-by-step execution of the procedure, helping to identify specific challenges related to the patient's anatomy. Results will be monitored using cone-beam CT scans of the model with the stent, along with angiographic and colorimetric tests. Overall, the integration of 3D modeling, virtual simulation, and physical simulation will provide comprehensive preparation for the intervention, enabling the identification of potential challenges and risks associated with transcatheter correction for each patient.

Transcatheter correction

Transcatheter correction of SVD will be performed at each participating center under the supervision of a physician experienced in this procedure. All interventions will be performed under general anesthesia, guided by digital fluoroscopy and transesophageal echocardiography. Before the procedure, antibiotic prophylaxis and intravenous heparin will

be administered. Standardized procedural steps will be followed, including the creation of a jugular-femoral venovenous wire rail, as well as trans-septal puncture and pulmonary vein protection when indicated.
The procedure will start with SVC angiography, including pressure and angiographic measurements. Next, the SVC distensibility will be assessed using a compliant balloon, either PTS-X (NuMED) or AMPLATZER Sizing Balloon II (Abbott). The stent diameter will usually be 4 mm larger than the diameter of the SVC above the PAPVR during the balloon test. Before stent implantation, a semi-compliant AltoSa-XL balloon of the same diameter will be used to reevaluate the risk of pulmonary vein obstruction. Subsequently, a correctly sized partially covered Optimus-CVS XXL stent will be manually mounted on an AltoSA-XL GEMINI dual balloon catheter, ensuring both components are of the same length. This assembly will be introduced through a 20 Fr Gore DrySeal delivery sheath via the right femoral vein. Stent placement will be guided by simultaneous transesophageal imaging, as well as imaging fusion between CT scan and fluoroscopy, complemented by angiography from the right internal jugular vein and right upper pulmonary vein.
Post-dilation of the stent may be performed to ensure proper anchoring within the SVC and to eliminate any residual shunting at the lower end. If a risk of vein obstruction is identified, pulmonary vein protection will be implemented by inflating a small balloon in the pulmonary vein, extending into the left atrium, to maintain patency. Following stent deployment and post-dilation, if stent instability or residual shunt through the bare part of the stent is suspected, additional bare-metal or covered stents of shorter lengths may be implanted, as necessary. Final assessments will include angiograms of the SVC and right upper pulmonary veins, pressure measurements in the right upper pulmonary vein, left atrium, and right atrium, as well as transesophageal echocardiography to evaluate residual shunting and exclude pulmonary venous obstruction **(Fig. 4).**

Follow-up

Following surgical or transcatheter SVD correction, the follow-up process will be consistent for both approaches. Patients will have a follow-up outpatient consultation with transthoracic ultrasound within the first two weeks and again one month after the procedure to assess immediate outcomes and ensure procedural safety. A CT scan will be performed at six months post-procedure to evaluate the anatomical outcomes of both endovascular and surgical corrections. At the six-month mark, a comprehensive clinical evaluation will be conducted, including transthoracic echocardiography, MRI, cardiac CT scans, Holter ECG monitoring, cardiopulmonary exercise tests, six-minute walking distance assessments, and EQ5D-5L quality of life questionnaires. Any adverse events occurring during this period will be meticulously documented and analyzed by an independent monitoring and adjudication committee. Subsequently, patients will continue their follow-up with clinical examinations, echocardiography, and ECGs at one year, followed by annual visits for up to five years within the study framework, ending in February 2031.

Study endpoints

The study's primary endpoint will be a 6-month composite measure combining the effectiveness of SVD correction, defined by trivial or absent residual shunt, and the absence of major intervention-related adverse events (death or, in the case of transcatheter SVD correction, conversion to surgery).
If no significant difference is found between the two groups on this primary endpoint, hierarchical testing will be conducted for the following secondary endpoints: effectiveness (RVEDV reduction, or, if MRI is not possible, RV end-diastolic surface area reduction on echocardiography) and safety (defined by the absence of transcatheter or surgical re-intervention, stroke, or conduction-related arrhythmias requiring pacemaker implantation).

Secondary endpoints include safety and technical success at 1 month, defined by the procedural success rate for correction of abnormal pulmonary venous return and shunt occlusion. The incidence of each of the following complications will be assessed: ECMO, dialysis, stroke, arrhythmias requiring medical or electrical intervention, and severe conduction disorders requiring pacemaker implantation. Additional measures include the length of initial hospitalization, duration of stay in intensive care, and duration of mechanical ventilation, as well as any other adverse events during the procedure, hospitalization, and up to 30 days post-procedure. The occurrence of re-hospitalization or extended initial hospitalization due to a serious adverse event related to the procedure will also be monitored. Efficacy at 6 months will include changes in baseline quality of life, dyspnoea evaluated by the NYHA score, results from the 6-minute walk test, maximal VO2, RVEDV by MRI, and RV end-diastolic area by echocardiography. Additionally, the presence and grade of residual shunt will be assessed by echocardiography and MRI (grade 0 to 4), as well as SVC patency and pulmonary venous return using multimodal imaging techniques.
Safety at 6 months will be evaluated by the rate of unplanned re-admissions related to the cardiac condition and the incidence of complications associated with the heart disease and its therapeutic management. At 12 and 24 months, safety will be reassessed with the same criteria as the primary endpoint at 6 months. Safety at 3, 4, and 5 years will focus on the collection of major complications related to the heart condition and its treatment.

Data collection and management

Data will be collected at each center using browser-based electronic data capture (EDC) software (REDCap). Online observation forms will be accessible to participating sites. Each subject will receive a unique identification code, and all collected data will be confidential and coded. A secure correspondence table linking the identification code to each participant's name will be maintained by the principal investigator at each site, in a file with restricted access. The centralized data will be entered into a coded database managed by the promoter. Access to study-related files will be limited to participants and the promoter's clinical research department. Data processing and statistical analysis will be conducted at the promoter's site.

Statistical analysis

The analysis will be conducted following the review and locking of the database, utilizing R software® (R Core Team, 2021, Vienna, Austria). All enrolled subjects will contribute to characterizing the study population's baseline characteristics. Statistical analysis will be conducted in two phases: first, a descriptive analysis of the 60 patients included in the stent group will be performed, followed by a comparative analysis of the primary endpoint. Baseline variables will be reported as mean ± standard deviation for normally distributed data and as median [interquartile range] for non-normally distributed data. The statistical analysis populations will include the Intention-to-Treat (ITT) Population, analyzed within their treatment arm; the Per-Protocol Population, comprising ITT patients without protocol deviations; and the Safety Population, including all patients intended for stent placement. Analyses will compare proportions using the chi-square test or Fisher's exact test, means with the Student's t-test or Wilcoxon test, and adjusted means based on baseline values using ANCOVA. The 6-month endpoint incidence will be analyzed using time-to-event models, including Kaplan-Meier curves and Cox proportional hazards models, with results presented as estimated proportions and 95% confidence intervals. Risk comparisons will be expressed as hazard ratios with corresponding 95% confidence intervals. Due to the rarity of occurrences, all parameters will include 95% confidence intervals. Statistical tests will be conducted with an alpha risk of 5%, defining p-values ≤ 0.05 as statistically significant. A descriptive analysis of demographic, anatomical, procedural, and follow-up data will also be reported for the cohort of pediatric patients who underwent the surgical procedure. No imputation of missing values is planned, but if missing values become significant—affecting

primary endpoints or causing imbalances between groups—imputation methods may be considered, with justifications provided in the statistical analysis plan.

EXPECTED RESULTS AND DISCUSSION

The primary strength of the OPTIVENOSUS study lies in its prospective design, comparing the efficacy of transcatheter SVD correction to established surgical methods. The innovative use of digital twin simulation tools allows for a personalized approach for each patient, providing pre-procedural analysis to anticipate therapeutic choices and technical considerations. Simulations are performed both virtually and on 3D-printed bench models, enabling procedure simulations under conditions closely resembling real-life scenarios. Despite ongoing debates [32, 33], previous studies have demonstrated that simulation on 3D-printed models significantly enhances the success rate of complex cardiovascular interventions like transcatheter SVD correction [15, 19, 23, 28, 38–42].

While a randomized controlled trial would ideally demonstrate superiority, such an approach was deemed impractical due to significant limitations. Many patients with SVD are not eligible for both treatment options due to anatomical factors or comorbidities like pulmonary hypertension, which complicate surgical procedures. Moreover, randomized trials in cardiac surgery often face patient resistance, especially in rare conditions like SVD, limiting participant recruitment. As a result, the study adopts a pragmatic approach with an open cohort design, analyzing all patients over 12 years old with SVD, regardless of their treatment choice. All participants will undergo the same pre- and post-intervention investigations and follow-up. On the other hand, the use of varying surgical techniques could potentially influence the outcomes and will require careful evaluation during the analysis. Additionally, cases deemed ineligible for transcatheter correction may present greater complexity during surgical intervention.

This study uses a modified version of the balloon-expandable, partially PTFE-covered Optimus-CVS XXL stent, which has previously shown efficacy in treating various congenital heart lesions [40–42, 48, 49]. The modified stent, designed specifically for transcatheter SVD correction, features a longer covered section extending up to 10 cm, with an uncovered 2 cm segment to facilitate secure anchoring in the SVC and potentially preserve a small accessory vein draining high in the SVC.

The OPTIVENOSUS study will prospectively evaluate the safety and efficacy of transcatheter treatment for SVD in patients aged over 18 years old using 70-100 mm long, partially PTFE-covered Optimus-CVS XXL balloon-expandable Co-Cr stents, implanted with AltoSA-XL GEMINI dual balloon catheters, in comparison to conventional open-heart surgery [13, 50]. Based on the findings from the OPTIVENOSUS study, the therapeutic algorithm for managing SVD could be further optimized and refined.

Conclusions

We expect the transcatheter treatment using Optimus-CVS XXL stents to deliver results comparable to surgery in terms of the primary endpoint while offering faster recovery and improved quality of life. These outcomes could support the development of transcatheter treatment as a faster, minimally invasive alternative to surgery. The success of this study will also contribute to validating dedicated equipment, particularly as European regulatory standards tighten.

References

1. Van Praagh S, Carrera ME, Sanders SP, Mayer JE, Van Praagh R. Sinus venosus defects: Unroofing of the right pulmonary veins—Anatomic and echocardiographic findings and surgical treatment. *Am Heart J* 1994;128:365–79. https://doi.org/10.1016/0002-8703(94)90491-X.
2. Butts RJ, Crean AM, Hlavacek AM, Spicer DE, Cook AC, Oechslin EN, et al. Veno-venous bridges: the forerunners of the sinus venosus defect. *Cardiol Young* 2011;21:623–30. https://doi.org/10.1017/S1047951111000710.
3. Tajouri A, Batteux C, Ly R, Houyel L, Hascoet S. Inferior sinus venosus defect and anomalous hepatic venous return to the coronary sinus leading to Eisenmenger syndrome. *Cardiol Young* 2022. https://doi.org/10.1017/S1047951122001354.
4. Baumgartner H, De Backer J, Babu-Narayan SV, Budts W, Chessa M, Diller GP, et al. 2020 ESC Guidelines for the management of adult congenital heart disease. *Eur Heart J* 2021;42:563–645. https://doi.org/10.1093/eurheartj/ehaa554.
5. Muroke V, Jalanko M, Haukka J, Anttila V, Pätilä T, Sinisalo J. Long-term outcome after surgical correction of sinus venosus defect in a nationwide register-based cohort study. *Int J Cardiol* 2023:131433. https://doi.org/10.1016/j.ijcard.2023.131433.
6. Okonta KE, Sanusi M. Superior sinus venosus atrial septal defect: Overview of surgical options. *Open J Thoracic Surg* 2013;3:114–22. https://doi.org/10.4236/ojts.2013.34024.
7. Lin H, Yan J, Wang Q, Li S, Sun H, Zhang Y, et al. Outcomes of the Warden Procedure for Partial Anomalous Pulmonary Venous Drainage. *Pediatr Cardiol* 2020;41:134–40. https://doi.org/10.1007/s00246-019-02235-8.
8. Said SM, Burkhart HM, Dearani JA, Eidem B, Stensrud P, Phillips SD, et al. The outcome of caval division techniques for partial anomalous pulmonary venous connections to the superior vena cava. *Ann Thorac Surg* 2011;92:980–5. https://doi.org/10.1016/j.athoracsur.2011.04.110.
9. Ait-Ali L, Ravaglioli A, Festa P, Tamburrini A, Marrone C, Cuman M, et al. The different surgical impact of the superior cavoatrial incision in children and adults. *Cardiol Young* 2021;31:751–5. https://doi.org/10.1017/S1047951120004540.
10. Stewart RD, Bailliard F, Kelle AM, Backer CL, Young L, Mavroudis C. Evolving surgical strategy for sinus venosus atrial septal defect: Effect on sinus node function and late

venous obstruction. *Ann Thorac Surg* 2007;84:1651–5. https://doi.org/10.1016/j.athoracsur.2007.04.130.

11. Iyer AP, Somanrema K, Pathak S, Manjunath PY, Pradhan S, Krishnan S. Comparative study of single- and double-patch techniques for sinus venosus atrial septal defect with partial anomalous pulmonary venous connection. *J Thorac Cardiovasc Surg* 2007;133:656–9. https://doi.org/10.1016/j.jtcvs.2006.08.076.
12. Attenhofer Jost CH, Connolly HM, Danielson GK, Bailey KR, Schaff HV, Shen WK, et al. Sinus venosus atrial septal defect: Long-term postoperative outcome for 115 patients. *Circulation* 2005;112:1953–8. https://doi.org/10.1161/CIRCULATIONAHA.104.493775.
13. Brancato F, Stephenson N, Rosenthal E, Hansen JH, Jones MI, Qureshi S, et al. Transcatheter versus surgical treatment for isolated superior sinus venosus atrial septal defect. *Catheter Cardiovasc Interv* 2023;101:1098–107. https://doi.org/10.1002/ccd.30650.
14. Baruteau AE, Jones MI, Butera G, Qureshi SA, Rosenthal E. Transcatheter correction of sinus venosus atrial septal defect with partial anomalous pulmonary venous drainage: The procedure of choice in selected patients? *Arch Cardiovasc Dis* 2020;113. https://doi.org/10.1016/j.acvd.2019.09.014.
15. Baruteau A-E, Hascoet S, Malekzadeh-Milani S, Batteux C, Karsenty C, Ciobotaru V, et al. Transcatheter closure of superior sinus venosus defects. *JACC Cardiovasc Interv* 2023. https://doi.org/10.1016/j.jcin.2023.07.024.
16. Batteux C, Meliani A, Brenot P, Hascoet S. Multimodality fusion imaging to guide percutaneous sinus venosus atrial septal defect closure. *Eur Heart J* 2020;41. https://doi.org/10.1093/eurheartj/ehaa292.
17. Rosenthal E, Qureshi SA, Jones M, Butera G, Sivakumar K, Boudjemline Y, et al. Correction of sinus venosus atrial septal defects with the 10 zig covered Cheatham-Platinum stent: An international registry. *Catheter Cardiovasc Interv* 2021;98. https://doi.org/10.1002/ccd.29750.
18. Batteux C, Ciobotaru V, Bouvaist H, Kempny A, Fraisse A, Hascoet S. Multicenter experience of transcatheter correction of superior sinus venosus defect using the covered Optimus XXL stent. *Rev Esp Cardiol (Engl Ed)* 2023;76:199–201. https://doi.org/10.1016/j.rec.2022.08.004.

19. Batteux C, Ciobotaru V, Arditi W, Decante B, Karsenty C, Combes N, et al. Transcatheter correction of sinus venosus defect in a patient with a challenging anatomical configuration: From bench testing to clinical success. *Catheter Cardiovasc Interv* 2023;102:1265–70. https://doi.org/10.1002/ccd.30898.
20. Hansen JH, Duong P, Jivanji SGM, Jones M, Kabir S, Butera G, et al. Transcatheter correction of superior sinus venosus atrial septal defects as an alternative to surgical treatment. *J Am Coll Cardiol* 2020;75. https://doi.org/10.1016/j.jacc.2019.12.070.
21. Riahi M, Forte MNV, Byrne N, Hermuzi A, Jones M, Baruteau AE, et al. Early experience of transcatheter correction of superior sinus venosus atrial septal defect with partial anomalous pulmonary venous drainage. *EuroIntervention* 2018;14. https://doi.org/10.4244/EIJ-D-18-00304.
22. Garg G, Tyagi H, Radha AS. Transcatheter closure of sinus venosus atrial septal defect with anomalous drainage of right upper pulmonary vein into superior vena cava: An innovative technique. *Catheter Cardiovasc Interv* 2014;84:473–7. https://doi.org/10.1002/ccd.25502.
23. Butera G, Sturla F, Pluchinotta FR, Caimi A, Carminati M. Holographic augmented reality and 3D printing for advanced planning of sinus venosus ASD/partial anomalous pulmonary venous return percutaneous management. *JACC Cardiovasc Interv* 2019;12:1389–91. https://doi.org/10.1016/J.JCIN.2019.03.020.
24. Vettukattil J, Subramanian A, Barthur A, Mahimarangaiah J. Transcatheter closure of sinus venosus defect: First-in-human implant of a dedicated self-expanding VB stent system. *Catheter Cardiovasc Interv* 2023. https://doi.org/10.1002/ccd.30814.
25. Haddad RN, Bonnet D, Gewillig M, Malekzadeh-Milani S. Modified safety techniques for transcatheter repair of superior sinus venosus defects with partial anomalous pulmonary venous drainage using a 100-mm Optimus-CVS® covered XXL stent. *Catheter Cardiovasc Interv* 2022. https://doi.org/10.1002/ccd.30136.
26. Gertz ZM, Strife BJ, Shah PR, Parris K, Grizzard JD. CT angiography for planning of percutaneous closure of a sinus venosus atrial septal defect using a covered stent. *J Cardiovasc Comput Tomogr* 2018;12:174–5. https://doi.org/10.1016/j.jcct.2017.09.007.
27. Sivakumar K, Qureshi S, Pavithran S, Vaidyanathan S, Rajendran M. Simple diagnostic tools may guide transcatheter closure of superior sinus venosus defects without advanced

imaging techniques. *Circ Cardiovasc Interv* 2020. https://doi.org/10.1161/CIRCINTERVENTIONS.120.009833.

28. Thakkar AN, Chinnadurai P, Breinholt JP, Lin CH. Transcatheter closure of a sinus venosus atrial septal defect using 3D printing and image fusion guidance. *Catheter Cardiovasc Interv* 2018;92:353–7. https://doi.org/10.1002/ccd.27645.
29. Crystal MA, Vincent JA, Gray WA. The wedding cake solution: A percutaneous correction of a form fruste superior sinus venosus atrial septal defect. *Catheter Cardiovasc Interv* 2015;86:1204–10. https://doi.org/10.1002/ccd.26031.
30. Abdullah HAM, Alsalkhi HA, Khalid KA. Transcatheter closure of sinus venosus atrial septal defect with anomalous pulmonary venous drainage: Innovative technique with long-term follow-up. *Catheter Cardiovasc Interv* 2020;95:743–7. https://doi.org/10.1002/ccd.28364.
31. Hejazi Y, Hijazi ZM, Saloos HA, Ibrahim H, Mann GS, Boudjemline Y. Novel technique for transcatheter closure of sinus venosus atrial septal defect: The temporary suture-holding technique. Catheter Cardiovasc Interv. 2022; 100(6):1068-1077. https://doi.org/10.1002/ccd.30415
32. Thejaswi P, Sagar P, Sivakumar K. Zero-contrast transcatheter closure of sinus venosus defect in advanced renal failure. Ann Pediatr Cardiol. 2024; 17(2):141-145. doi: 10.4103/apc.apc_29_24. https://doi.org/10.4103/apc.apc_29_24
33. Sagar P, Sivakumar K, Thejaswi P, Rajendran M. Transcatheter Covered Stent Exclusion of Superior Sinus Venosus Defects. J Am Coll Cardiol. 2024; 83(22):2179-2192. https://doi.org/10.1016/j.jacc.2024.03.417
34. Qureshi F, Sivakumar K, Sagar P. Endoleak in covered CP stent causes procedural failure during transcatheter closure of sinus venosus defects. *Catheter Cardiovasc Interv* 2023. https://doi.org/10.1002/ccd.30942.
35. Sagar P, Sivakumar K. Different mechanisms for persistent and residual left-to-right shunt after transcatheter sinus venosus defect closure and their management. Ann Pediatr Cardiol. 2024; 17(1):45-51. https://doi.org/10.4103/apc.apc_190_23
36. Sivakumar K, Sagar P, Thejaswi P, Ramaswamy R, Chandrasekaran R. Innominate vein occlusion by the fabric of covered stent during transcatheter closure of sinus venosus defects - Causes, management, and outcome. Ann Pediatr Cardiol. 2024;17(1):59-63. https://doi.org/10.4103/apc.apc_186_23

37. Batteux C, Azarine A, Karsenty C, Petit J, Ciobotaru V, Brenot P, et al. Sinus venosus ASDs: Imaging and percutaneous closure. *Curr Cardiol Rep* 2021;23. https://doi.org/10.1007/s11886-021-01571-7.
38. Petersen SE, Khanji MY, Plein S, Lancellotti P, Bucciarelli-Ducci C. European Association of Cardiovascular Imaging expert consensus paper: A comprehensive review of cardiovascular magnetic resonance normal values of cardiac chamber size and aortic root in adults and recommendations for grading severity. *Eur Heart J Cardiovasc Imaging* 2019;20:1321–31. https://doi.org/10.1093/ehjci/jez232.
39. Nordenfelt P, Dawson S, Wahlgren CF, Lindfors A, Mallbris L, Björkander J. Quantifying the burden of disease and perceived health state in patients with hereditary angioedema in Sweden. Allergy Asthma Proc. 2014; 35(2):185-90. https://doi.org/10.2500/aap.2014.35.3738
40. Haddad RN, Hascoet S, Karsenty C, Houeijeh A, Baruteau A-E, Ovaert C, et al. Multicentre experience with Optimus balloon-expandable cobalt–chromium stents in congenital heart disease interventions. *Open Heart* 2023;10:e002157. https://doi.org/10.1136/openhrt-2022-002157.
41. Haddad RN, Bonnet D, Malekzadeh-Milani S. Transcatheter closure of extracardiac Fontan conduit fenestration using new promising materials. J Card Surg. 2021; 36(11):4381-4385. https://doi.org/10.1111/jocs.15916
42. Haddad RN, Bonnet D, Alsac JM, Malekzadeh-Milani S. Promising PTFE-coating technology of Optimus-CVS™ stents: The new player for congenital heart disease interventions. Int J Cardiol Congenit Heart Dis. 2022;7:100323. https://doi.org/10.1016/j.ijcchd.2022.100323
43. Ciobotaru V, Tadros V-X, Martin CA, Hascoet S. Complex transcatheter left atrial appendage closure using a tailored trans-jugular approach simulated by 3D printing: A case report. *Eur Heart J Case Rep* 2022;6. https://doi.org/10.1093/ehjcr/ytac304.
44. Ciobotaru V, Tadros V-X, Batistella M, Maupas E, Gallet R, Decante B, et al. 3D printing to plan complex transcatheter paravalvular leaks closure. *J Clin Med* 2022;11:4758. https://doi.org/10.3390/jcm11164758.
45. Houeijeh A, Petit J, Isorni MA, Sigal-Cinqualbre A, Batteux C, Karsenty C, et al. 3D modeling and printing in large native right ventricle outflow tract to plan complex percutaneous pulmonary valve implantation. *Int J Cardiol Congenit Heart Dis* 2021;4. https://doi.org/10.1016/j.ijcchd.2021.100161.

46. Ciobotaru V, Combes N, Martin CA, Marijon E, Maupas E, Bortone A, et al. Left atrial appendage occlusion simulation based on three-dimensional printing: New insights into outcome and technique. *EuroIntervention* 2018;14:176–84. https://doi.org/10.4244/EIJ-D-17-00970.
47. Hascoet S, Smolka G, Bagate F, Guihaire J, Potier A, Hadeed K, et al. Multimodality imaging guidance for percutaneous paravalvular leak closure: Insights from the multi-centre FFPP register. *Arch Cardiovasc Dis* 2018;111:421–31. https://doi.org/10.1016/j.acvd.2018.05.001.
48. Morgan GJ, Ciuffreda M, Spadoni I, DeGiovanni J. Optimus covered stent: Advanced covered stent technology for complex congenital heart disease. *Congenit Heart Dis* 2018;13. https://doi.org/10.1111/chd.12596.
49. Haddad RN, Eicken A, Adel Hassan A, Gendera K, Kasem M, Georgiev S. Proof of concept: A new solution for low-profile transcatheter implantation of Optimus-L stents in small children. *Can J Cardiol* 2024;40:77–86. https://doi.org/10.1016/j.cjca.2023.09.015.
50. Hascoët S, Roussin R, Batteux C. Treatment of sinus venosus defect: Time to tune. *Int J Cardiol* 2023:131630. https://doi.org/10.1016/j.ijcard.2023.131630.

Figures Legend

Fig. 1
Study flowchart

Fig. 2
A 100 mm partially PTFE-covered Optimus-CVS® XXL stent (A) manually mounted onto an AltoSa-XL-Gemini® PTA over-the-wire dual balloon catheter (B, C).

Fig. 3
Creation of a 3D patient-specific hollow model from CT scan sequences (A–D) for virtual digital simulation and in-vitro 3D-printed bench simulation (E).

Fig.4
Fluoroscopic images of transcatheter correction of SVD using a 100 mm partially PTFE-covered Optimus-CVS® XXL stent (A–F).

Figures

Fig. 1

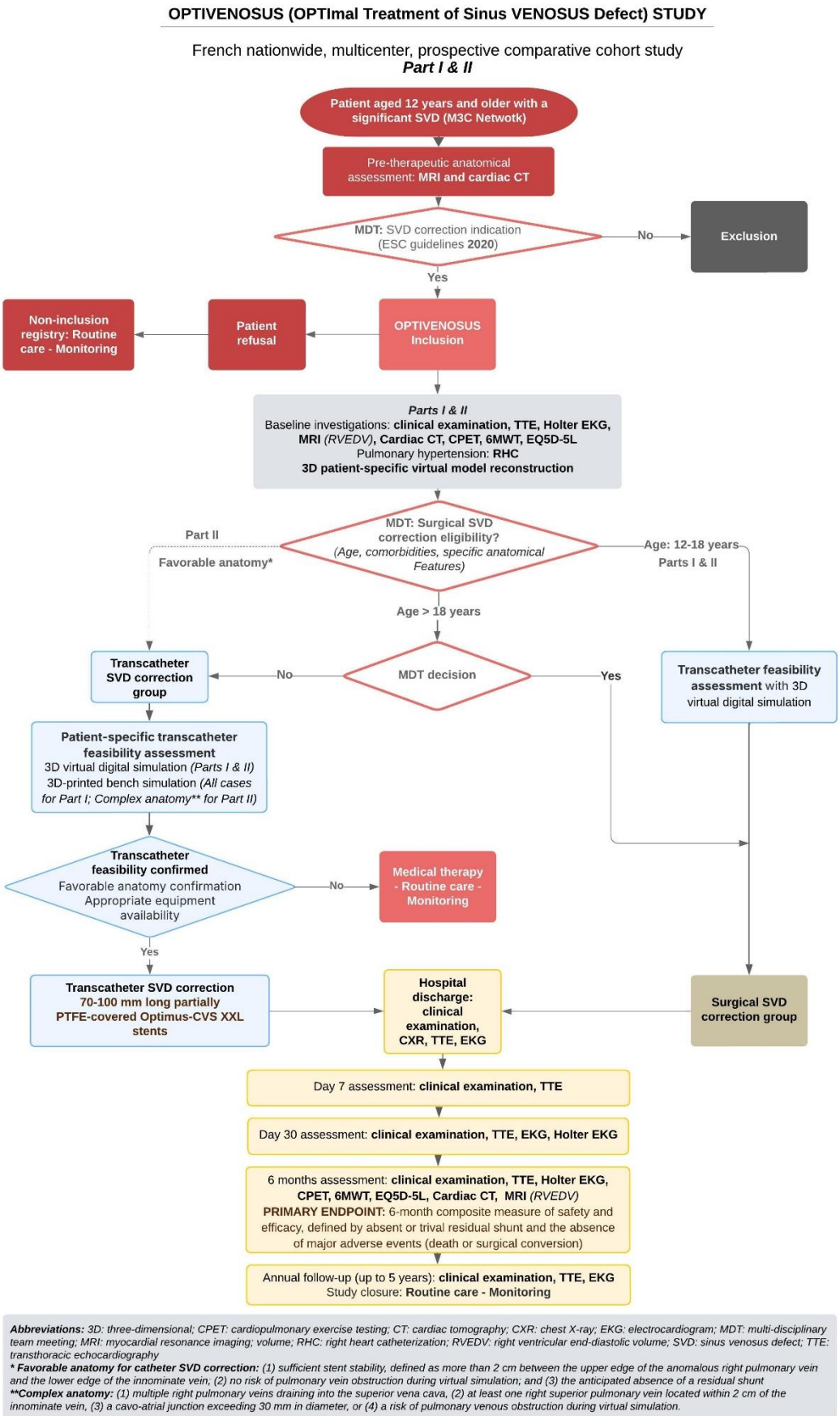

Abbreviations: *3D: three-dimensional; CPET: cardiopulmonary exercise testing; CT: cardiac tomography; CXR: chest X-ray; EKG: electrocardiogram; MDT: multi-disciplinary team meeting; MRI: myocardial resonance imaging; volume; RHC: right heart catheterization; RVEDV: right ventricular end-diastolic volume; SVD: sinus venosus defect; TTE: transthoracic echocardiography*

** **Favorable anatomy for catheter SVD correction:** (1) sufficient stent stability, defined as more than 2 cm between the upper edge of the anomalous right pulmonary vein and the lower edge of the innominate vein; (2) no risk of pulmonary vein obstruction during virtual simulation; and (3) the anticipated absence of a residual shunt*

*** **Complex anatomy:** (1) multiple right pulmonary veins draining into the superior vena cava, (2) at least one right superior pulmonary vein located within 2 cm of the innominate vein, (3) a cavo-atrial junction exceeding 30 mm in diameter, or (4) a risk of pulmonary venous obstruction during virtual simulation.*

Fig. 2

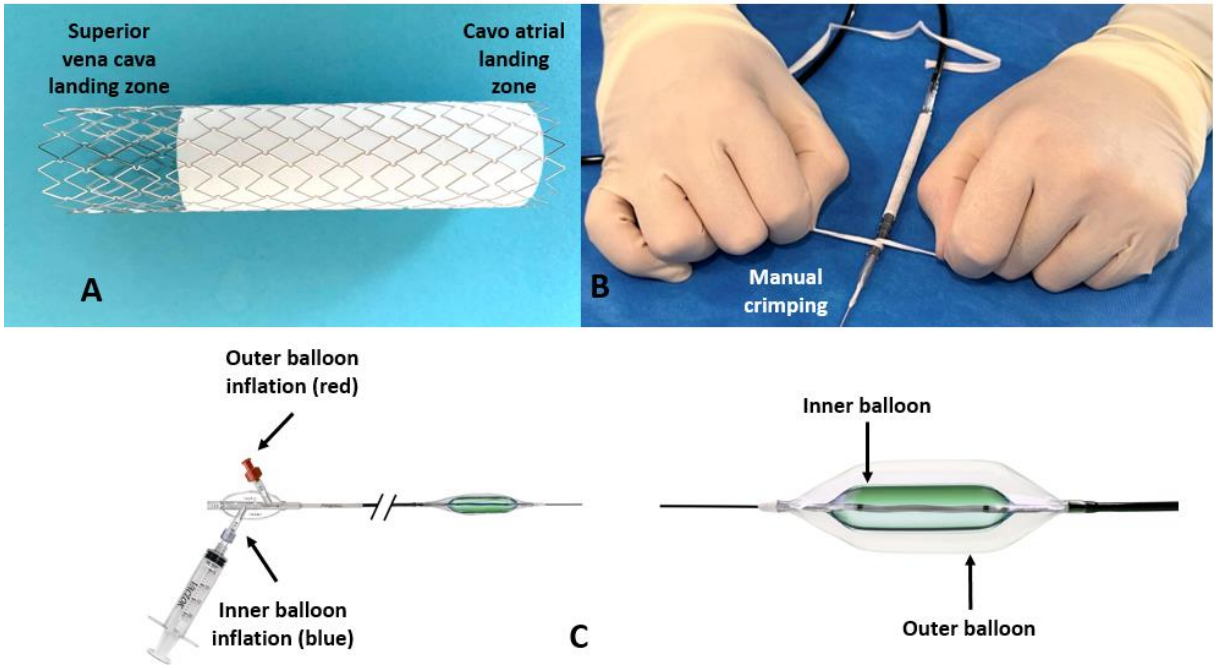
Superior
vena cava
landing zone
Cavo atrial
landing
zone
A
B
Manual
crimping
Outer balloon
inflation (red)
Inner balloon
inflation (blue)
C
Inner balloon
Outer balloon

Fig. 3

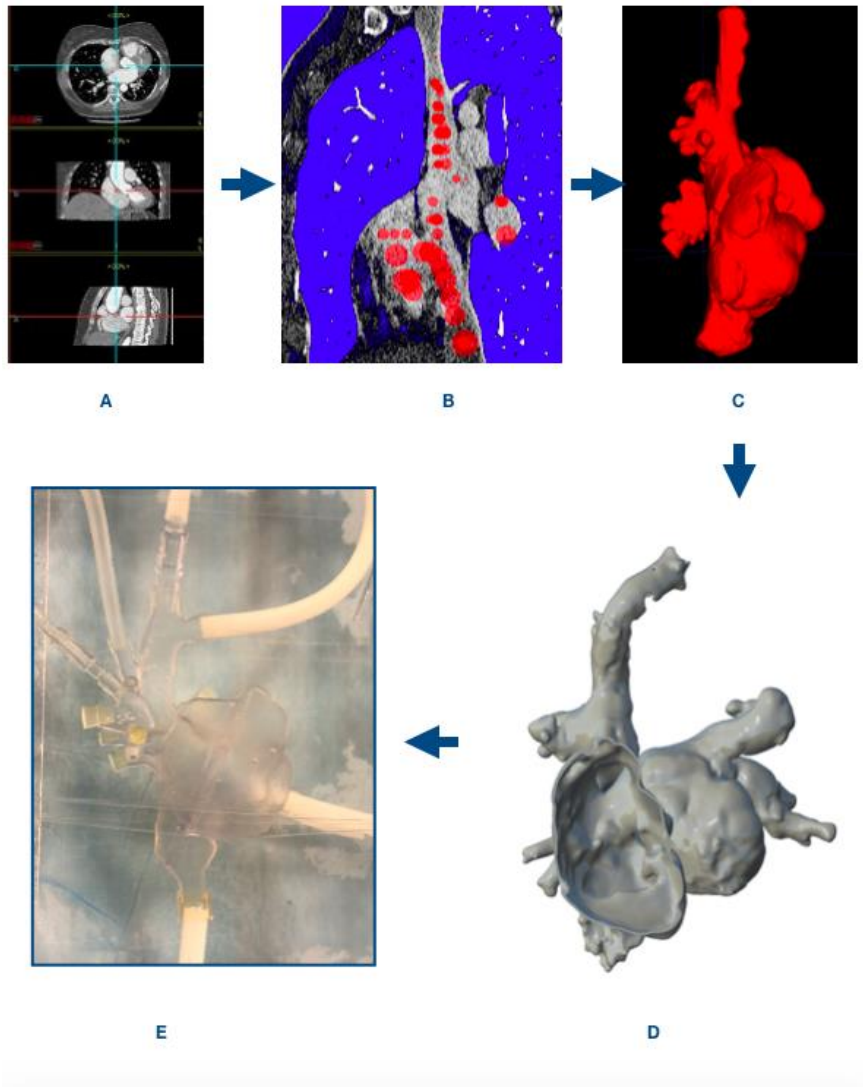

Fig. 4

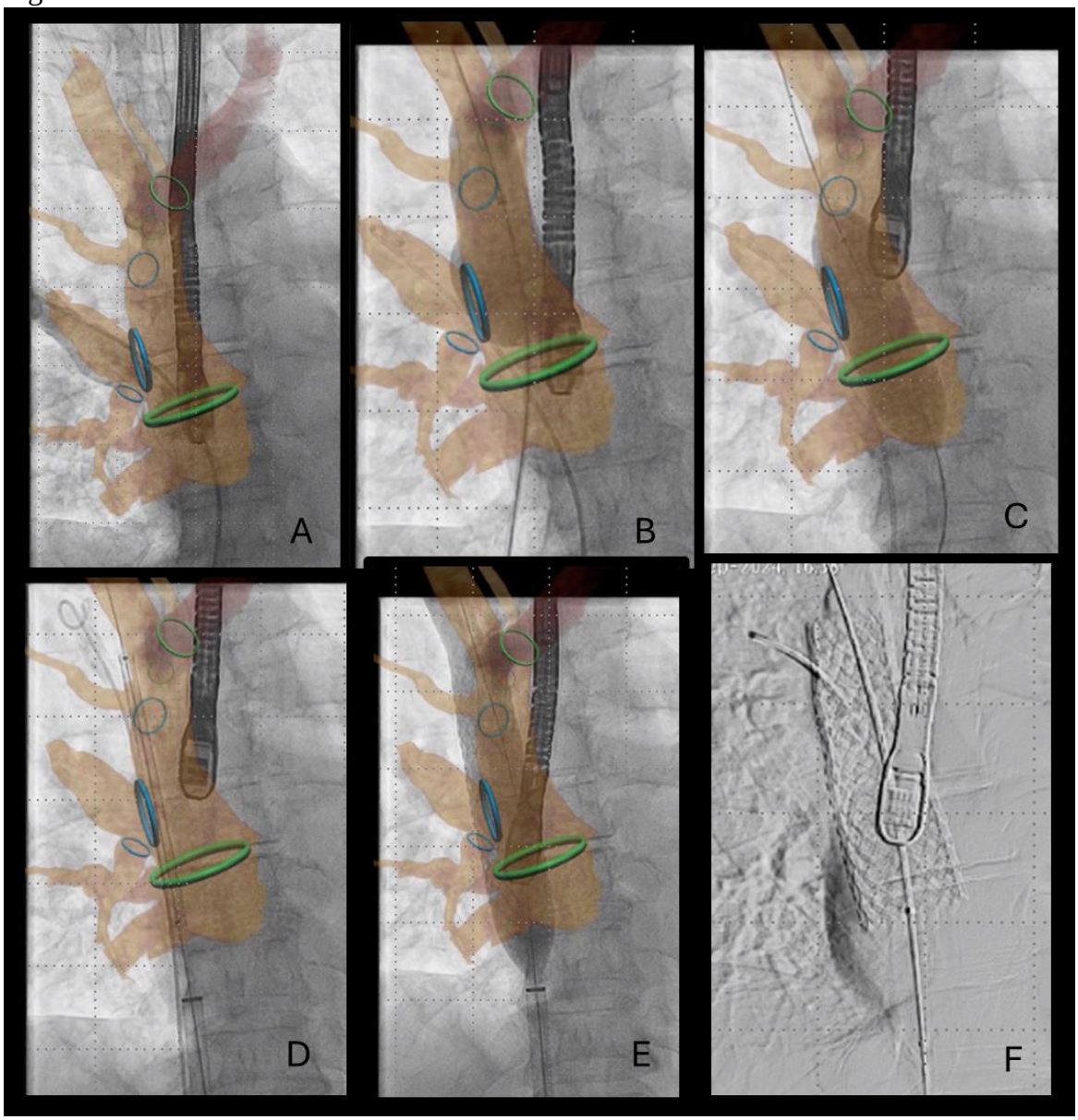

7. Résultats préliminaires

Flow-chart actualisé (novembre 2024) des RCP, inclusions, patients traités et follow-up de l'étude Optivenosus.

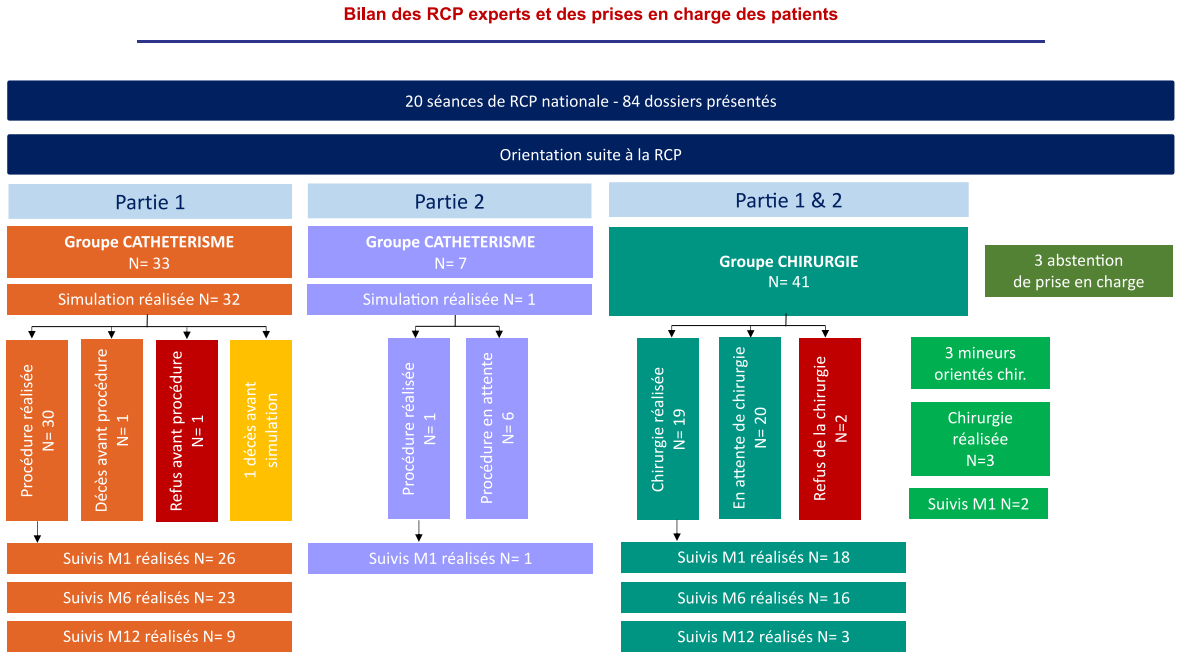

Figure 58 : Flow-chart actualisé (novembre 2024) de l'étude OPTIVENOSUS

8. Abstract de la publication à venir sur les résultats

Background: Transcatheter correction has been a new innovative treatment for superior sinus venosus defects (SVDs). A dedicated long partially covered XXL stent has been developed specifically for this procedure. Its safety and efficacy have to be investigated.

Objectives: This study aims to evaluate the efficacy and safety of transcatheter SVDs correction with the OTIMUS XXL® partially covered stent.

Material and Methods: A prospective, nationwide, multi-center cohort study with approval to include 60 consecutive patients started in June 2023. Preliminary early and mid-term (6 months) outcomes were collected.

Results: Thirty adults were enrolled over one year in 5 centers (mean age 61 years; female, 73%; dyspnea, 90%; history of atrial arrhythmia, 43%; pulmonary hypertension, 40%; heart failure, 47%; mean indexed right ventricular end-telediastolic volume= 140mL/m² on MRI). Simulation of transcatheter SVD correction was done on virtual twin and on 3D printed models in all cases. All procedures were successful. Pulmonary vein pathway was protected in 57% of cases. Stents of 100mm and 80mm

were implanted in 67% and 33% of cases respectively, using Gemini balloons. Additional stents were implanted at the upper part in 3 patients (10%). An ostium secundum atrial septal defect was closed during the same procedure in 2 patients (6.7%). No stent embolization, pulmonary vein compression, significant residual shunt or tamponade were observed. No peri-procedural death was reported during the follow-up. In one patient, a moderate pericardial effusion was observed 7 days after the procedure and resolved spontaneously. A flat thrombus of 4x22mm was fortuitously observed upholstering the bottom part of the covered stent on the systematic computed tomography scan control at 6 months. No other stent related adverse event.

Conclusion: Transcatheter SVDs correction using OPTIMUS XXL® covered stents is safe and effective with excellent early and mid-term outcomes.

V. Coopérations internationales

1. 1ère correction percutanée de CIA sinus venosus en Allemagne

L'intérêt puis l'expertise acquise par l'équipe de cardiopathie congénitale de l'Hôpital Marie Lannelongue concernant cette nouvelle intervention et sa planification préopératoire a permis de tisser des liens professionnels avec plusieurs équipes à travers l'Europe voir le Monde.

L'équipe du Pr Nick Hass et du Dr Andre Jakob (Hôpitaux Universitaires de Munich) nous a ainsi sollicité en 2021 afin de les accompagner dans la première correction percutanée allemande. C'est donc en octobre 2021 que nous sommes allés avec le Dr Hascoet proctorer cette première nationale au cours de laquelle 2 patients ont été opérés avec succès.

Cette démarche a consolidé les liens entre nos deux équipes de manière certaine, preuve en est, la présence du Dr Andre Jakob au récent Workshop 2024 tenu à l'Hôpital Marie Lannelongue en Octobre 2024.

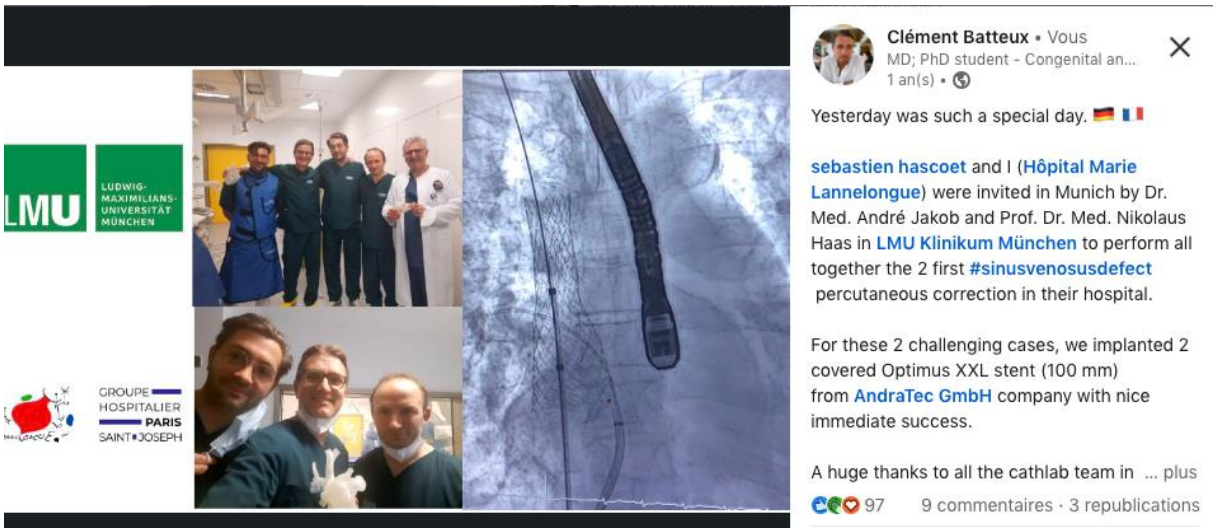

Figure 59 : post Link dn consécutif à la première correction percutanée allemande de CIA sinus venosus.

2. Modélisation 3D et simulation virtuelle pour évaluation de la faisabilité de la correction transcutanée

Suite à la reconnaissance des publications de l'équipe sur le sujet, nous avons eu le plaisir et l'honneur d'être sollicités à l'échelle internationale afin d'apporter notre expertise dans le domaine de la simulation préopératoire de la correction percutanée des CIA sinus venosus.

Via ce paragraphe, sont remerciées les équipes qui nous ont fait confiance dans cette expertise.

-Hôpitaux Universitaires de Lausanne, Suisse (Dr Rutz et Dr Ladouceur)

-Hopital de Coimbra, Portugal (Dr Santos)

-Deutsch Heart Centrum de Munich, Allemagne (Dr Georgiev)

-Hôpital Universitaire de Padoue, Italie (Dr Sirico et Dr Castaldi)

-Hôpital Universitaire de Téhéran, Iran

-Hôpital Universitaire de Mexico, Mexique

3. Publications internationales

LETTER TO THE EDITOR 1 : multicenter experience of transcatheter correction of superior sinus venosus defect using the covered stent Optimus XXL[117].

ARTICLE ORIGINAL: Covered stent correction for Sinus Venosus Atrial Septal Defects - an emerging alternative to surgical repair: Results of an International Registry.

Publication acceptée dans Circulation (novembre 2024).

Covered stent correction for Sinus Venosus Atrial Septal Defects - an emerging alternative to surgical repair: Results of an International Registry.

Eric Rosenthal MD, FRCP[1], Shakeel A Qureshi MBChB, FSCAI[1], Kothandam Sivakumar MD[2], Matthew Jones MBBS[1], San-Fui Yong MBBS [1], Saleha Kabir PhD[1], Pramod Sagar MD[2], Puthiyedath Thejaswi MD [2], Sebastien Hascoet MD[3], Clement Batteux MD[3], Younes Boudjemline MD, PhD[4], Ziyad M Hijazi, MD, MPH, MSCAI[4], Jamil A Aboulhosn MD[5], Daniel S Levi MD[6], Morris M Salem MD[6], Edwin Francis MD[7], Aleksander Kempny MD[8], Alain Fraisse MD[8], Carles Bautista-Rodriguez MD[8], Kevin Walsh MD [9], Damien Kenny MD, FSCAI [9], Brian Traynor MD [9], Salim N Al Maskari FRCPCH[10], James R Bentham MD PhD[11], László Környei MD PhD[12], Muthukumaran C Sivaprakasam MRCPCH[13], Ata Firouzi MD[14], Zahra Khajali MD[14], Lee Benson MD[15], Mark Osten MD[15], Alban-Elouen Baruteau MD[16], Matthew A Crystal MD[17], Thomas J Forbes MD[18], Stanimir Georgiev MD, FPICS[19], Horst Sievert MD[20], Tin Do Nguyen MD[21], Daniel Springmuller MD[22], Anand Subramanian MD[23], Hussein A M Abdullah MD[24], Radwa Bedair MD[25], Francisco Chamié, MD, FSCAI, FPICS[26], Ahmet Celebi MD[27], Jesus Damsky Barbosa MD[28], Pieter De Meester, MD, PhD[29], Luca Giugno MD[30], Zakaria Jalal MD, PhD [31], Clement Karsenty MD PhD[32], Anastasia Schleiger MD[33], Gregory Fleming MD, MSCI, FSCAI, FPICS[34], Andre Jakob MD[35], Tevfik Karagoaz MD[36], Gur Mainzer MD[37], Gareth J Morgan MD[38], Nazmi Narin MD[39], Shabana Shahanavaz MD[40], Zachary L. Steinberg MD[41], Osamah Aldoss MD[42], Elnur Alizade MD[43], Oliver Aregullin MD[44], Hélène Bouvaist MD[45], Thilo Fleck MD[46], Francois Godart MD[47], Sophie Malekzadeh-Milani MD[48], Paulo Motta MD[49], Angel Sanchez-Recalde MD [50], Juan Pablo Sandoval MD[51], Weiyi Tan MD, MPH[52], John Thomson MD, FSCAI[53], Pablo Tome MD[54], Evan M Zahn MD, MSCAI[55]

1. Paediatric & Adult Congenital Heart Disease, Evelina London Children's Hospital, Guy's & St Thomas' Hospital Trust, London, UK.
2. Department of Pediatric Cardiology, Institute of Cardio Vascular Diseases, Madras Medical Mission, Chennai, India.
3. Department of Congenital Heart Diseases, Centre de Reference Cardiopathies Congenitales Complexes M3C, Hospital Marie Lannelongue, Groupe Hospitalier Paris, Saint Joseph, Universite Paris-Saclay, Paris, France.
4. Sidra Heart Center, Sidra Medicine, Doha, Qatar.
5. Division of Cardiology, Ahmanson/UCLA Adult Congenital Heart Disease Center, Los Angeles, California, USA.
6. Division of Pediatric Cardiology, Mattel Children's Hospital at UCLA, Los Angeles, California, USA.
7. Aster Medcity Hospital, Kochi, India
8. Adult Congenital Heart Disease, Royal Brompton Hospital, Guy's & St Thomas' Hospital Trust, London, UK.
9. Department of Cardiology, Mater Misericordiae University Hospital, Dublin, Ireland.
10. Paediatric Cardiology, National Heart Centre, Muscat, Oman.
11. Department of Congenital Cardiology, Leeds General Infirmary, Leeds, UK.
12. Gottsegen National Cardiovascular Center, Budapest, Hungary.
13. Department of Paediatric Cardiology, Apollo Children's Hospital, Chennai, India.
14. Cardiovascular Intervention Research Center, Rajaie Cardiovascular Medical and Research Institute, Iran University of Medical Sciences, Tehran, Iran.

15. The Labatt Family Heart Center, The Hospital for Sick Children, The Toronto General Hospital, University of Toronto School of Medicine, Toronto, Ontario, Canada.
16. Nantes Université, CHU Nantes, Department of Pediatric Cardiology and Pediatric Cardiac Surgery, FHU PRECICARE, F-44000 Nantes, France.
17. Congenital Interventional Catheterization, Columbia University Vagelos College of Physicians and Surgeons | Morgan Stanley Children's Hospital of NewYork-Presbyterian, New York, USA.
18. Joe DiMaggio Children's Hospital, Hollywood, FL, USA.
19. Department of Congenital Heart Diseases and Pediatric Cardiology, German Heart Center, Munich 80636, Germany.
20. CardioVascular Center (CVC) Frankfurt, Frankfurt, Germany.
21. Department of Pediatrics, University of Medicine and Pharmacy, Ho Chi Minh City, Vietnam.
22. Departamento de Cardiología Pediátrica, División de Pediatría. Facultad de Medicina, Pontificia Universidad Católica de Chile. Unidad de Cardiopatías Congénitas del Adulto, Instituto Nacional del Tórax, Santiago, Chile.
23. Pediatric Cardiology, Sri Jayadeva Institute of Cardiovascular Sciences, Bangalore, India.
24. Ibn- Albitar Center for Cardiac Surgery, Baghdad, Iraq.
25. Adult Congenital Cardiology, Bristol heart institute, Bristol, UK.
26. INTERCAT - Interventional Cardiology, Rio de Janeiro, Brazil.
27. Department of Pediatric Cardiology, Dr. Siyami Ersek Hospital for Cardiology and Cardiovascular Surgery, Istanbul, Turkey.
28. Cardiology and Hemodynamics, Pedro de Elizalde Children's Hospital, Buenos Aires, Argentina.
29. Division of Congenital and Structural Cardiology, UZ Leuven and Department of Cardiovascular Sciences, KU Leuven, Belgium.
30. IRCCS Policlinico San Donato, Milano, Italy.
31. University Hospital of Bordeaux - Department of Pediatric and Adult Congenital Cardiology; LIRYC Electrophysiology and Heart Modeling Institute, Fondation Bordeaux Université; INSERM, Centre de recherche Cardio-Thoracique de Bordeaux, U1045; 33600 Pessac, France.
32. Pediatric and Congenital Cardiology, Children's Hospital CHU Toulouse, Institut des Maladies Métaboliques et Cardiovasculaires, Université de Toulouse, Institut National de la Santé et de la Recherche Médicale (INSERM), U1048, Clinique Pasteur, Toulouse, France..
33. Dept. of Congenital Heart Disease – Pediatric Cardiology, Deutsches Herzzentrum der Charité, Campus Virchow Klinikum, Berlin, Germany.
34. Division of Pediatric Cardiology, Duke University Medical Center, USA.
35. Department of Paediatric Cardiology and Paediatric Intensive Care, University Hospital, LMU Munich, Germany.
36. Department of Pediatric Cardiology, Faculty of Medicine, Hacettepe University; Ankara, Turkey.
37. Pediatric Cardiology Department, Hadassah Medical Center, Jerusalem, Israel.
38. The Heart Institute, Children's Hospital of Colorado, University of Colorado Hospital, Denver, Colorado, USA.
39. Department of Pediatric Cardiology, Faculty of Medicine, Izmir Katip Çelebi University, Izmir, Turkey.
40. Department of Pediatrics Heart Institute Cincinnati Children's Hospital University of Cincinnati College of Medicine Cincinnati OH.

41. Division of Cardiology, Department of Medicine, University of Washington Medical Center, Seattle, Washington, USA.
42. Division of Pediatric Cardiology, Stead Family Children's Hospital, University of Iowa, Iowa City, IA, USA.
43. Kosuyolu Heart, Research and Education Hospital, Department of Cardiology, Istanbul, Turkey.
44. Congenital Cardiology, Congenital Heart Center, Spectrum Health Helen DeVos Children's Hospital, Grand Rapids, Michigan, USA.
45. Service de Cardiologie –CHU Grenoble Alpes 38043 Grenoble cedex 09
46. Department of Congenital Heart Disease and Pediatric Cardiology, University Heart Center Freiburg – Bad Krozingen, Medical Center - University of Freiburg, Germany.
47. CHRU de Lille, university Lille Nord-de-France, Faculté de Médecine, Institut Cœur Poumon, Service des Maladies Cardiovasculaires Infantiles et Congénitales, Boulevard Pr.-Leclercq, 59037 Lille Cedex, France.
48. M3C-Necker, Hôpital Universitaire Necker-Enfants malades, Assistance Publique-Hôpitaux de Paris (AP-HP), Paris, France.
49. Interventional Cardiology, Home Hospital, Brasilia, Brazil.
50. University Hospital Ramon y Cajal, Madrid.
51. Imaging and Intervention in Congenital and Structural Heart Disease, Ignacio Chavez National Institute of Cardiology, Mexico City, Mexico.
52. Adult Congenital Heart Disease, UT Southwestern, Dallas, TX, USA.
53. Blalock-Taussig-Thomas Pediatric and Congenital Heart Center, Johns Hopkins Children's Center, Baltimore, MD, USA.
54. Hospital Fornecedores de Cana de Piracicaba, Piracicaba, São Paulo, Brazil.
55. The Department of Pediatrics, The Smidt Heart Institute, Cedars Sinai Medical Center, Los Angeles, California, USA.

Short title: Covered stent correction for Sinus Venosus ASDs

Corresponding author: Prof Eric Rosenthal MD FRCP
Consultant Paediatric and Adult Congenital Cardiologist
Evelina London Children's Hospital
School of Biomedical Engineering and Imaging Sciences
King's College London
London
United Kingdom
Tel: +44 02071884559
Eric.Rosenthal@kcl.ac.uk

Word Count: Total – 8625; Abstract – 331; Text - 4216

Covered stent correction for Sinus Venosus Atrial Septal Defects - an emerging alternative to surgical repair: Results of an International Registry.

Abstract:

Background

Covered stent correction (CSC) for a Sinus Venosus Atrial Septal Defect (SVASD) was first performed in 2009. This innovative approach was initially viewed as experimental and was reserved for highly selected patients with unusual anatomic variants. From 2016, increasing numbers of procedures began to be performed and in several centers, it is now offered as a standard of care option alongside surgical repair. CSC for SVASD is however, not recognized by regulatory authorities and in the minds of many pediatric and adult congenital cardiologists and surgeons, the condition is viewed as only treatable by cardiac surgery using cardiopulmonary bypass.

Methods

In April 2023, all centers identified from international conferences, publications and colleague networks to be undertaking CSC for SVASD were invited to participate in a retrospective audit of their procedures.

Results:

Data were received on 381 patients from 54 units over a 12-year period with 90% of procedures being performed over the past 5 years. Balloon-expandable stents (eight types) were used in the majority while self-expanding stents (four types) were used in 4.5%. The commonest stent was the 10-zig covered Cheatham Platinum stent in 62% of cases. In 10 procedures, the stent embolized requiring surgical retrieval and repair of the defect resulting in technically successful implantation in 371/381 (97.4%). Major complications (surgical drainage of tamponade, pacemaker implantation, surgery for pulmonary vein occlusion and late stent removal) occurred in 5 patients (1.3%). Repeat catheterization to correct residual leaks was required in 7 patients (1.8%). Thus 359/381 (94.2%) of the patients had successful correction without major complications or additional catheter interventions.

Conclusions

This paper details the exponential uptake of CSC for SVASD during the past 5 years. Cardiopulmonary bypass was avoided in the majority of patients, whilst major complications were infrequent. Prospective registries with standardized definitions, inclusion criteria and follow-up as well as comparative studies with surgery are now required to help support the extension of covered stent correction as an alternative standard of care option for patients with a SVASD.

Key Words: Covered stent, Sinus Venosus Atrial Septal Defect

Clinical Perspective:

What is new?

- There has been an exponential increase in the number of Covered Stent Corrections in patients with a Sinus Venosus ASD over the past 5 years.
- In this international Registry, the success rate of stent implantation in 381 patients was 97.4% with major complications in 1.3% and repeat catheter interventions for residual leaks in 1.8%.
- In high frequency units, Covered Stent Correction is currently offered routinely as an alternative to surgery in patients with a Sinus Venosus ASD.

What are the clinical implications?

- The high success rate and low complication rate of Covered Stent Correction in patients with a Sinus Venosus ASD, suggest that prospective comparative studies with surgery are now indicated.
- Covered Stent Correction in patients with a Sinus Venosus ASD may come to rival surgical repair as the standard of care.

Nonstandard Abbreviations and Acronyms:

ASD = Atrial Septal Defect
CCP = Covered Cheatham Platinum
CP = Cheatham Platinum
CSC = Covered stent correction
IRB = Institutional Review Board
LA = Left Atrium
QP:QS = Pulmonary to systemic flow ratio
RA = Right Atrium
RVEDV = Right ventricular end diastolic volume
RV/LV = Right ventricular end diastolic volume/ Left ventricular end diastolic volume
SVASD = Sinus Venosus Atrial Septal Defect
SVC = superior vena cava
TEE = Transesophageal echocardiography
TTE = Transthoracic echocardiography

Introduction:

Covered stent correction (CSC) for a Sinus Venosus Atrial Septal Defect (SVASD) was first performed in 2009 and briefly alluded to in a manuscript describing anatomical variations of the defect in 2011[1]. The first detailed case report was published in 2014, whilst an earlier oral presentation from 2013 was formally published in 2020[2, 3]. Subsequently several further case reports were published using different stents[4-6]. From 2016, significant numbers of procedures began to be performed in two centers - published in 2020 - and in 2021, data on 75 procedures using covered CP stents (CCP) were published[7-9]. In several centers, CSC is currently regarded as a standard of care option routinely offered to anatomically suitable patients as an alternative to surgical repair. CSC for SVASD is however, not recognized by any regulatory authorities and no stents repurposed or newly developed for this procedure have received approval. In the absence of randomized comparisons[10], in the minds of many pediatric and adult congenital cardiologists and surgeons, the condition is viewed as only treatable by cardiac surgery using cardiopulmonary bypass. This paper informs on the uptake of CSC from contributors to the SVASD CSC Registry to provide real-world data on the success rates and complications from multiple institutions using a variety of stents.

Methods:

All centers known to be undertaking CSC using any type of stent were invited to join the Registry. Centers were identified from participants in the original 10-zig CCP Registry[9], conference proceedings, publications[1-24], stent manufacturers' databases and through colleague networks. Invitations were issued in April 2023, preliminary results were presented at the CSI conference in June 2023 and data accepted until 31 August 2023. Data were anonymized - each center identified their patients by a center code and number and the age in years and months. Demographics included age, weight, height, symptoms and MRI findings. Procedural details included the procedure date, type and size of stent/s, implantation technique and procedure duration.

Inclusion: Patients with a SVASD who had no additional reasons for cardiac surgery (valve repair, coronary revascularization etc.) were assessed for anatomical suitability with cross-sectional imaging (CT or MRI) supplemented by 3D reconstruction[11]. When the drainage of the anomalous right pulmonary veins to the left atrium was predicted to be adequate after covered stent placement in the superior vena cava, and there were no high non-divertible pulmonary veins amenable to surgical redirection, the patient proceeded to cardiac catheterization. Final assessment for suitability was made during balloon interrogation of the defect. A balloon was inflated in the SVC to occlude the defect so that the pulmonary venous pathway to the left atrium could be assessed by TEE, angiography and pressure measurements. When the pulmonary venous pathway was confirmed to be unobstructed, CSC proceeded[7-9]. Patients, who were unsuitable on cross-sectional imaging or at cardiac catheterization (pulmonary venous pathway obstruction or inability to eliminate the shunt during balloon interrogation) or who were not considered for CSC due to patient or physician preference, were excluded from this retrospective audit.

Definitions: CSC was considered to be technically successful after stent implantation without embolization requiring cardiopulmonary bypass to remove the stent and correct the defect. Major complications were those requiring additional cardio-thoracic surgery. Moderate complications were those requiring intra-procedural interventions, vascular access site interventions or cardioversion. Minor complications were those that required medication alone or resolved without treatment. Additional catheter interventions were catheterization procedures performed after the initial procedure. Early complications were those occurring intra-procedurally or during the initial hospital stay up to 30 days. Late complications occurred after the hospital stay and beyond 30 days to 1 year. Complications included procedure-specific and general catheterization complications occurring acutely and during follow up to the census date of 31 August 2023. Residual leaks on angiography and/or echocardiography were qualitatively described as trivial, small and moderate – the latter possibly needing a further procedure.

Statistics: Fisher's Exact Test was used to test differences between groups

The audit was approved by the audit committee of Guy's & St Thomas' NHS Hospital Trust. Individual institutional approval was not mandated, but obtained at the discretion of the submitting centers. Results are presented in accordance with the Strengthening the Reporting of Observational Studies in Epidemiology (STROBE) cohort reporting guidelines. The checklist is provided in the Supplemental Material[25]. Data that supports the findings of this study are available from the corresponding author upon reasonable request.

Results:

Data capture:

Of the 12 centers in the 10-zig CCP registry[9], all but one participated, extending follow-up and adding new patients. The twelfth center could not obtain IRB permission and withdrew their single patient. Of the additional 47 centers invited to participate, data were submitted by 43 centers; institutional approval was not obtained in time at 3 centers (4 patients) and 1 institution (1 patient) failed to respond. One center could only obtain data from their primary hospital, but not their secondary hospital (2 patients) due to IRB constraints and one center could not track data on one earlier patient after a personnel change. Thus, of a potential 59 centers, 54 submitted data on 381 patients with 3 missing patients and 5 centers with 6 patients did not participate. Data were analyzed on 381/390 (97.8%) known procedures (Fig. 1).

Patient details:

The age at the time of the procedure ranged from 4.75 - 87 years (median 44 years) with a weight of 17 - 145 kg (median 70 kg). Thirty-seven patients were aged 18 years or younger of whom 14 were aged 4.75 - 10 years (Table 1). Symptoms were present in 307, absent in 65 and not stated in 9 patients. More than one symptom was common. In 2 patients previous surgical repair had left a residual shunt - one identified when a post-operative pacemaker was needed[11]. A non-divertible accessory right upper pulmonary vein was present in 72 (18.9%) patients and bilateral SVCs in 58 (15.2%) patients. Shunt calculations (cardiac catheterization or MRI) confirmed a left to right shunt in 198 patients . In only one patient was there a right to left shunt .

Procedural uptake:

The first procedure was in 2011 and the last on 31 August 2023 with fewer than 5 procedures annually until 2016 followed by a year on year increase so that from 2021, over 70 procedures were performed annually (Fig 2A). During the first 8 months of 2023 over 80 procedures were reported, suggesting the final tally will significantly surpass the preceding years. Mirroring the increased procedure frequency was an increase in centers undertaking CSC. In 2 centers more than 50 procedures were performed while 14 centers had only undertaken 1 procedure (Fig. 2B). The largest number of procedures was in India (Fig 3) using balloon-expandable stents in 103 of 117 patients and the United Kingdom, using balloon-expandable stents in all 77 patients. The highest crude rate per million of population was in Qatar at 6.7, whilst only Oman, Ireland and the United Kingdom had more than 1 procedure per million of population (Table I, Data Supplement).

Stents:

The different stents are illustrated in Fig 4. Balloon-expandable stents (8 types) were used in 364/381 cases (95.5%) [3, 7 – 9, 12 – 16]. The majority of centers (33) used only balloon-expandable stents of one type, but 15 used more than one type (Table 2A). A mixture of balloon-expandable and self-expanding stents was used in 4 centers and only self-expanding stents in 2 centers[4, 17, 18]. The 10-zig CCP stent (Numed Inc., Hopkinton, NY, USA) was the commonest stent 237/381 (62%) - 19 centers only using this stent.

Additional stents (1.8 stents per procedure) were used in 180 (47.2%) procedures (Table 2B). Anchoring the covered stent in the SVC because of actual or threatened instability

was the commonest reason. Additional covered stents sealed residual shunts - usually at the RA or SVC end of the stent and less commonly for a mid-stent endoleak [19]. Overlapping stents were mounted on one longer balloon in 17 cases due to unavailability of a longer stent or when combined with an uncovered stent to avoid blocking small very high veins above the covered stent [8] (Figure I, Data Supplement). Two stents were sutured together to form a longer initial stent in 3 cases - the stents separated in 2 requiring an overlap stent in the middle[20].

Implantation Techniques:

The femoral venous approach for balloon-expandable stents was predominantly over a femoral to internal jugular vein guidewire rail, with occasional placement of the guidewire tip in a brachial vein. A single stent was used this way in 187 patients (49.1%). Preliminary landing zone stents were placed in the SVC prior to siting the covered stent in 74 procedures (19.4%); a third locking stent in the SVC "sandwiched" the covered stent in 33 (8.7%) of these (Table 2B)[9]. A suture threaded through a zig at the cranial end of the stent and exiting the jugular vein sheath to control stent positioning was used in 48 (12.6%) patients[9, 13, 21]. Self-expanding stents were used in 17 (4.5%) of the patients - from the femoral vein in 12 and the jugular vein in 5.[4, 17, 18]. A single stent was used in 14 patients. In 3, a landing zone stent was placed (balloon-expandable in 2 and self-expanding in 1) and in one patient a third self-expanding stent was needed[4].

A concomitant secundum ASD was closed with an ASD occluder in 8 patients[15]. In one patient, transvenous pacing leads were extracted and new ones sited immediately after CSC.

Procedure monitoring:

Transesophageal (TEE) monitoring was used as an adjunct to pulmonary vein access in 266 (69.8%), as the sole monitoring technique in 46 (12.1%) and not used in 69 (18.1%) of the procedures (Table 2B). Pulmonary vein access to assess suitability and monitor the procedure (pressure and angiography) was obtained in 335 (87.9%) of procedures. Trans-septal access was used in 239 (62.7%) - via a trans-septal puncture in 166 (43.6%) or via a patent foramen ovale or secundum ASD in 73 (19.2%). A retrograde femoral arterial approach was used in 43 (11.3%) and both antegrade and retrograde access in 5 procedures[7, 8]. Direct access from the femoral vein via the SVASD with removal of the pulmonary vein catheter before, during or after stenting was performed in 53 (13.9%) procedures.

Pulmonary vein protection:

A balloon was inflated in the pulmonary vein after trans-septal access in 113 cases (29.6%) to prevent pulmonary venous pathway compromise during stent implantation [7] (Figure II, Data Supplement). The pulmonary vein protection balloon deflated inadvertently during stent implantation in 2 cases. In one, re-inflation of the pulmonary vein balloon re-established pulmonary venous flow (Fig II, Data Supplement). In the other, this went unnoticed and pulmonary venous obstruction caused hemoptysis requiring a thoracoscopic partial upper lobectomy at 3 months[9]. In 8 cases (2.1%), obstruction of the pulmonary venous pathway occurred without previous pulmonary vein protection and subsequent balloon inflation in the pulmonary vein molded the covered stent to allow unobstructed pulmonary venous pathway flow[14].

Procedural outcome

Stent implantation was technically successful in 371 of 381 procedures (97.4%). In 10 patients (2.6%) at 8 different centers, the stent embolized to the right atrium or right ventricle. All underwent surgical retrieval and standard surgical repair with uneventful recovery. In 6 patients this was intra-procedural and in 4 after leaving the catheter laboratory or by the next day. Most occurred during the first 6 procedures at 7 different centers and continued to occur throughout the study period as new centers joined (Table 3; Figure 2A). Embolization occurred with balloon-expandable stents in 9/364 (2.5%), self-expanding stents in 1/17 (5.9%), after an initial landing zone stent in 3/77 (3.9%), using the suture holding technique in 1/48 (2.1%) and in children in 1/37 (2.7%). There was no significant difference in the frequency of embolization based on stent length (7/176 with stents < 7 cm long and 3/205 with stents >/ 7 cm long).

Immediately after the procedure, there was no leak in 194 (51%), a trivial leak in 121 (31.8%), a small leak in 36 (9.4%), a moderate leak in 7 (1.8%) with no comment in 13 (3.5%). High non-diverted veins were left draining above the level of the covered stent in 22 patients, through a bare metal anchoring stent in 23 patients (Fig I, Data Supplement), were covered over in 12 patients without apparent sequelae and not recorded in 15 patients. Procedural times (n = 312; 81.9%) ranged from 50 to 450 minutes (median 143.5) with fluoroscopy times (n = 305; 80.1%) of 9.31 to 123 minutes (median 33.4).

Complications:

There were 5 major (1.3%) and 39 moderate and minor (10.2%) complications and 7 catheter re-interventions for residual leaks (1.8%). The combined incidence in children was 4/37 (10.8%) and 47/344 (13.7%) in adults.

Early complications (Table 4A).
Major Complications

Cardiac tamponade in 2 patients required surgical drainage in the first week. The trans-septal puncture was assumed to be the cause in one patient[7]. The anchoring hooks of a self-expanding stent penetrated the aorta in another and were covered with pledgets[22].
Sinus node dysfunction developed in one patient hours after the procedure necessitating a pacemaker 3 days later. At one year, there were signs of sinus node recovery[23].

Moderate & Minor Complications – the majority resolved during the procedure or during the hospital stay.
Innominate vein obstruction in 2 patients, from stents placed too high in the SVC resolved with balloon dilation – in one after needle puncture of the covered stent[8].
Pulmonary venous pathway narrowing was relieved with intra-procedural balloon dilation in 8 patients (2%).
Intra-procedural thrombus in 6 patients (1.57%) resolved with intra-procedural heparin.
Access site: A significant jugular hematoma resolved uneventfully but a femoral haematoma underwent surgical exploration. A superficial femoral puncture site infection responded to antibiotics. A self-expanding stent delivery mechanism was trapped by a second stent and removed by jugular vein cut down. In 4 patients, a femoral artery pseudoaneurysm responded to compression and thrombin injections.
Atrial fibrillation in 2 patients reverted with cardioversion. One patient developed atrial flutter that was cardioverted 2 days later.

Pulmonary hemorrhage due to a guide wire injury required intensive care but resolved over 2 weeks in one patient. One patient had a minor pulmonary vein dissection without extravasation and stent implantation proceeded uneventfully.
*Pericardial effusions r*esolved with conservative management in two patients - in one by day 3 and in one after a course of colchicine.
Arm neuropraxia: Prolonged procedures and poor patient positioning led to a neuropraxia in 4 patients that resolved completely over several weeks.
In stent thrombus was detected in 1 patient and resolved after changing anti-platelet agents to anticoagulation during the in-hospital stay.

Late complications (Table 4B).
Major Complications
Pulmonary vein obstruction of an accessory right upper lobe pulmonary vein caused ongoing hemoptysis in one patient, who underwent thoracoscopic partial upper lobectomy at 3 months[9].
Stent removal with residual leak - a patient with a moderate residual shunt, tricuspid regurgitation and newly detected coronary artery disease, had surgical correction of all his defects with stent removal at 1 year.

Additional Catheter Interventions
Significant residual shunting required an additional stent or ASD occluder during the first year in 7 patients (1.8%).

Minor Complications
In stent thrombus was detected in 3 patients by routine TEE in the weeks after the procedure. These resolved after changing anti-platelet agents to anticoagulation [24].

Deaths:

There was no procedural mortality but three patients died after successful procedures. A 60-year-old man in congestive heart failure with pulmonary hypertension had a cerebral bleed (mechanism not ascertained), developed pneumonia and died 3 weeks after the procedure. A 73-year-old woman died from a brain tumor more than 12 months after the procedure. A 70-year-old man died 2 years after the procedure from complications of Crohn's disease.

Follow-up:
At many centers, follow-up was rarely available for more than a post-operative visit with subsequent follow-up at the referral centers, especially when the patient had travelled from abroad. Follow-up ranged from one day to 12.4 years, with a median of 1.7 years. The leak had resolved in a further 44/121 with a trivial leak, 12/36 with a small leak and 3/7 with a moderate leak. The 1-year follow up was still awaited in 118 patients. A formal MRI shunt calculation was available in 51 (13.4%) patients, documenting a fall in QP:QS from 2.5 +/- 0.68 to 1.2 +/- 0.3.
One patient had a pacemaker for asymptomatic pauses on Holter monitoring, but it was unclear if this predated CSC 14 months previously.

Discussion:

CSC for SVASD was initially viewed as an experimental approach in highly selected patients with unusual anatomic variants, but unlikely to be applicable to the majority of patients [1-6]. Over the past few years, there has been an exponential rise in the volume of procedures and number of units offering CSC[7-24]. This Registry included data from 54 centers with their respective learning curves over 12 years. CSC was successful in 371/374 patients (97.4%) and free from major complications or repeat catheter interventions in 359/381 patients (94.2%). The majority of moderate and minor complications resolved or were corrected during the procedure or in-hospital stay, and were typical of general cardiac catheterization procedures. The relatively long procedural times of an unfamiliar procedure during the learning curves contributed to their occurrence.

Stenting technique:

A range of stents and implantation techniques were used. One larger center used 5 different balloon-expandable stents, whilst another used only a single type. Newer and longer stents (custom length 10-zig CCP, Optimus, G-Armor) with less shortening (Zephyr) are increasingly used and should reduce the risk of complications and residual leaks. "Innovative" strategies to elongate a stent by suturing two stents together are no longer needed. Overlapping covered and uncovered stents to avoid occluding high non-divertible pulmonary veins can be replaced with purpose designed stents that are partially covered. Whilst attractive conceptually – and frequently discussed in interventional meetings - self-expanding stents were used far less frequently than anticipated. Nevertheless, newer self-expanding stents continue to emerge and may yet have a role in specific anatomic subsets (VB, Nano).

Monitoring during the procedure also varied considerably. Transesophageal monitoring was used most frequently, commonly accompanied by pulmonary vein monitoring. The majority of operators used trans-septal access, for pulmonary vein monitoring, to facilitate pulmonary venous pathway "protection" when needed or as a rescue route for pathway obstruction after stent implantation. Some centers, in carefully selected patients, avoided this thereby simplifying the procedure considerably. That balloon dilation of the pulmonary venous pathway after stenting was still occasionally required, suggests pulmonary venous access needs to be considered carefully when the pulmonary venous pathway appears borderline and when new operators commence CSC. It is important to emphasize that although ostensibly a straight forward procedure once the anatomy is understood and the concept accepted, it remains technically challenging. Most embolization occurred during the first 6 procedures undertaken in a unit, but there was also late embolization in the two most experienced centers. New operators and centers may benefit from observing procedures and guidance from proctors.

Comparison with surgery:

As with many new procedures that develop in the face of an established technique, CSC for SVASD has not been formally compared to surgical repair. Avoidance of sternotomy and cardiopulmonary bypass with a short hospital stay – the majority of patients going home the day after the procedure and returning to normal activities and work within a few days - are major advantages of CSC. Particularly in the developing world, lower costs and length of hospital stay would benefit many.

Complications reported after surgical repair (residual defects, SVC and pulmonary vein stenosis and sinus node dysfunction) vary between centers and with surgical techniques. . One patch, two patch and the Warden repair have their proponents and different complication profiles and also have "modifications" that differ across centers. The Warden procedure can cause SVC obstruction requiring re-operation or stent implantation in as many as 22%[31]. Sinus node dysfunction ranges from 14 – 55% after the two patch repair, depending on the era and center[32-34].

The impetus to perform comparative studies depends on evidence of non-inferiority and potential superiority that are slow to accrue with small case reports and limited series. Modifications during the learning curve and experience with different stents in different centers also impede this by introducing variations. This Registry highlights that CSC using a range of stents and techniques successfully avoided the morbidity of open cardiac surgery in the vast majority. Minor and resolvable catheter complications were not infrequent during the learning curves of multiple institutions, but are anticipated to decrease as the technique becomes established; e.g. femoral pseudoaneurysms (1%) are avoidable if retrograde catheterization of the pulmonary vein is replaced by direct or trans-septal access, whilst arm neuropraxia (1%) should be reduced with shorter procedures as the technique becomes familiar. Stent embolization in 2.6% required cardiac surgery with cardiopulmonary bypass but is anticipated to decrease with greater experience of the procedure and the availability of longer and newer stents. The incidence of stent embolization was too low to confirm that longer stents embolized less frequently and data on the length of stent apposition to the SVC as a possible cause of embolization were not available.

Two of the patients in this registry had residual shunts following surgical repair, and underwent successful CSC. Cross-over of patients between the modalities highlights the interdependence of congenital interventional cardiology and cardiac surgery. A small non-randomized, era-based comparison, showed similar rates (and different types) of complications but the output of this Registry indicates that larger formal prospective studies should now be considered[10]. Such studies in patients with secundum ASDs have shown shorter hospital stay, lower costs and fewer complications in the catheter closure group compared with the surgical group[35-37].

Uptake of the procedure:

This Registry highlights the uneven uptake of CSC. Whilst the crude rates per million of population do not take into account equity of health opportunities, socioeconomic factors, health tourism and population movements, it is apparent that large parts of the world have not engaged with this procedure and many patients are not considered for it. Currently many pediatric and adult congenital cardiologists and surgeons still view the SVASD as a wholly surgical condition. The aim of the Registry was to inform practitioners of our specialty on the current state of CSC and has now collected data showing upward of 100 procedures annually in the past 2 years and upward of 54 centers that now offer the procedure. The number of centers and procedures is likely to continue to rise despite the absence of formal regulatory approval, which is surely needed now. The absence of either FDA approval for the procedure itself or CE marking for any custom made stents currently in use, are an important obstacle to wider uptake.

Limitations:

Whilst identification of centers, as described, may not have included every center undertaking CSC, it is likely that the vast majority will have been invited. Only a few centers with small numbers of patients did not submit data, so that 98% of known procedures were included. Data collection accuracy depended on the goodwill of the participants as did the reporting of complications. The indications for SVASD closure, procedural approach, stent implantation techniques, anticoagulation regimen and follow-up were not standardized in this retrospective study. Neither was the definition of residual shunting by either TEE or angiography at implant or by TEE, TTE, CT or MRI scanning during follow-up. Routine TEE was obtained at one large and several smaller centers in the first 1 - 6 months; whereas another large center performed a CT scan at 2 months and an MRI scan at a year. Many centers discharged patients to local care after the first follow-up. The absence of rigorous quantification of residual shunts and documentation of the timing of complete closure is the most limiting aspect of this study, although typically this is not performed after surgical repair currently. Unlike surgery, where high draining veins can be diverted with patches or the Warden procedure (though in some cases they are left behind), during CSC, these veins are typically left draining to the SVC. Quantification of the amount of residual shunting through these smaller veins was not undertaken although the overall shunt in those with follow up MRIs was negligible. Sinus node function was not systematically evaluated before or after the procedure. The single acute instance of sinus node dysfunction requiring a pacemaker after CSC was considerably lower than that seen after surgery[26-28] and appeared to recover during further follow up[23]. While 9.7% of the patients were children, further data and longer follow up are required to assess fully the effects of growth. Finally the proportion of patients who were considered unsuitable for CSC is unknown and should be addressed in future studies.

Conclusions:

CSC for SVASD was performed in 381 patients at 54 units over a 12-year period with more than 90% in the past 5 years. Cardiopulmonary bypass was avoided in the majority of patients, whilst complications were infrequent. Longer and newer stents and evolving techniques are likely to reduce the incidence of complications and residual shunts further and streamline the procedure. Therefore, CSC has moved from being a restricted investigational option in rare highly selected patients to an increasingly commonly performed procedure. Indeed in several centers, when the anatomy appears favorable, it is now offered as a standard of care option alongside surgical repair. Prospective registries with standardized definitions, inclusion criteria and follow-up as well as comparative studies with surgery are required before recommending CSC more widely as an alternative option to surgical repair.

Acknowledgments, Sources of Funding, & Disclosures:

a) Acknowledgements

We are grateful to the following for support of this project with data collection and procedural assistance: Dr Neha Ahluwalia, Children's Hospital of Michigan Detroit Medical Center, Detroit, USA. Prof. Felix Berger MD, Dept. of Congenital Heart Disease – Pediatric Cardiology, Deutsches Herzzentrum der Charité, Berlin, Germany; Dr Mario Carminati MD, IRCCS Policlinico San Donato, Milano, Italy; Dr Ivan Casserly MD, Mater Misericordiae University Hospital, Dublin; Prof Peter Ewert MD, Department of Congenital Heart Diseases and Pediatric Cardiology, German Heart Center, Munich, Germany; Dr Marc Gewillig MD, Division of Congenital and Structural Cardiology, UZ Leuven, Belgium; Dr Albenque Grégoire MD, Department of Congenital Heart Diseases, Hospital Marie Lannelongue, Paris, France; Dr. Nikolaus Haas MD, Kinderkardiologie und Pädiatrische Intensivmedizin, Klinikum der Universität München, München, Germany; Dr Raymond N Haddad, M3C-Necker Enfants Malades, AP-HP, Paris, France; Dr Berhan Keskin MD, Kosuyolu Heart, Research and Education Hospital, Department of Cardiology, Istanbul, Turkey; Dr Brian Morray MD, Cardiac Catheterization Laboratories, Seattle Children's Hospital, Seattle, WA, USA; Dr Dao Anh Quoc MD, University Medical Center, HCMC, Vietnam; Dr Kolja Sievert MD, CardioVascular Center (CVC) Frankfurt, Frankfurt, Germany; Dr Murat Sürücü, Department of Pediatric Cardiology, Dr. Siyami Ersek Hospital for Cardiology and Cardiovascular Surgery, Istanbul, Turkey; Dr Mark Turner MD, Adult Congenital Cardiology, Bristol heart institute, Bristol, UK.

b) Sources of funding

No funding received for this study

c) Disclosures:

GJM, SAQ & ZH are consultants for Numed; DSL and ZL are consultants for B Braun. AF and AK are consultants for AndraTec. ER is a proctor for BVMedical.

References:

1) Butts RJ, Crean AM, Hlavacek AM, Spicer DE, Cook AC, Oechslin EN, Anderson RH. Veno-venous bridges: the forerunners of the sinus venosus defect. Cardiol Young. 2011;2:623-30.
2) Garg G, Tyagi H, Radha AS. Transcatheter closure of sinus venosus atrial septal defect with anomalous drainage of right upper pulmonary vein into superior vena cava–an innovative technique. Catheter Cardiovasc Interv. 2014;84:473–477.
3) Abdullah HAM, Alsalkhi HA, Khalid KA. Transcatheter closure of sinus venosus atrial septal defect with anomalous pulmonary venous drainage: Innovative technique with long-term follow-up. Catheter Cardiovasc Interv. 2020;95:743-747.
4) Crystal MA, Vincent JA, Gray WA. The wedding cake solution: a percutaneous correction of a form fruste superior sinus venosus atrial septal defect. Catheter Cardiovasc Interv. 2015;86:1204–1210.
5) Thakkar AN, Chinnadurai P, Breinholt JP, Lin CH. Transcatheter closure of a sinus venosus atrial septal defect using 3D printing and image fusion guidance. Catheter Cardiovasc Interv. 2018;92:353–357.
6) Gertz ZM, Strife BJ, Shah PR, Parris K, Grizzard JD. CT angiography for planning of percutaneous closure of a sinus venosus atrial septal defect using a covered stent. J Cardiovasc Comput Tomogr. 2018;12:174-175.
7) Hansen JH, Duong P, Jivanji SGM, Jones M, Kabir S, Butera G, Qureshi SA, Rosenthal E. Transcatheter correction of superior sinus venosus atrial septal defects as an alternative to surgical treatment. J Am Coll Cardiol. 2020;75:1266–1278.
8) Sivakumar K, Qureshi S, Pavithran S, Vaidyanathan S, Rajendran M. Simple Diagnostic Tools May Guide Transcatheter Closure of Superior Sinus Venosus Defects Without Advanced Imaging Techniques. Circ Cardiovasc Interv. 2020;13:e009833.
9) Rosenthal E, Qureshi SA, Jones M, Butera G, Sivakumar K, Boudjemline Y, Hijazi ZM, Almaskary S, Ponder RD, Salem MM, et al. Correction of sinus venosus atrial septal defects with the 10 zig covered Cheatham-platinum stent - An international registry. Catheter Cardiovasc Interv. 2021;98:128-136.
10) Brancato F, Stephenson N, Rosenthal E, Hansen JH, Jones MI, Qureshi S, Austin C, Speggiorin S, Caner S, Butera G. Transcatheter versus surgical treatment for isolated superior sinus venosus atrial septal defect. Catheter Cardiovasc Interv. 2023;101:1098-1107.
11) Velasco Forte MN, Byrne N, Valverde I, Gomez Ciriza G, Hermuzi A, Prachasilchai P, Mainzer G, Pushparajah K, Henningsson M, Hussain T, Qureshi S, Rosenthal E. Interventional Correction of Sinus Venosus Atrial Septal Defect and Partial Anomalous Pulmonary Venous Drainage: Procedural Planning Using 3D Printed Models. JACC Cardiovasc Imaging. 2018;11:275-278.
12) Pascual-Tejerina V, Sánchez-Recalde Á, Cantador JR, López EC, Gómez-Ciriza G, Gutiérrez-Larraya F. Transcatheter repair of superior sinus venosus atrial septal defect with partial anomalous pulmonary venous drainage with the chimney double stent technique. Rev Esp Cardiol (Engl Ed). 2019;72:1088-1090.
13) Haddad RN, Bonnet D, Gewillig M, Malekzadeh-Milani S. Modified safety techniques for transcatheter repair of superior sinus venosus defects with partial anomalous pulmonary venous drainage using a 100-mm Optimus-CVS® covered XXL stent. Catheter Cardiovasc Interv. 2022;99:1558-1562.

14) Batteux C, Ciobotaru V, Bouvaist H, Kempny A, Fraisse A, Hascoet S. Multicenter experience of transcatheter correction of superior sinus venosus defect using the covered Optimus XXL stent. Rev Esp Cardiol (Engl Ed). 2023;76:199-201.
15) Thejaswi P, Sagar P, Sivakumar K. Simultaneous Transcatheter Closure of Coexistent Superior Sinus Venosus Defects and Oval Fossa Defects. Pediatr Cardio. 2023;44:1591-1598.
16) Morgan GJ, Zablah J. A new FDA approved stent for congenital heart disease: First-in-man experiences with G-ARMORTM. Catheter Cardiovasc Interv 2022. 100:1261-1266.
17) Muthukumaran CS, Ganesan R, Reddy RV, Yalamanchi RP, Showkathali R, Srinivasan KN. Transcatheter self-expanding stent closure of sinus venosus atrial septal defects with indigenous method of determining appropriate stent length without advanced imaging techniques -A case series of single center experience. IHJ Cardiovasc Case Rep. 2022;6:8-12.
18) Vettukattil J, Subramanian A, Barthur A, Mahimarangaiah J. Transcatheter closure of sinus venosus defect: First-in-human implant of a dedicated self-expanding VB stent system. Catheter Cardiovasc Interv. 2023;102:1088-1094.
19) Qureshi F, Sivakumar K, Sagar P. Endoleak in covered CP stent causes procedural failure during transcatheter closure of sinus venosus defects. Catheter Cardiovasc Interv. 2024;103:317-321.
20) Tan W, Levi D, Perens G, Aboulhosn J. Suture connection of overlapping covered CP stents for transcatheter treatment of sinus venosus atrial septal defect with anomalous pulmonary venous connection. Catheter Cardiovasc Interv. 2022;100:399-403.
21) Hejazi Y, Hijazi ZM, Saloos HA, Ibrahim H, Mann GS, Boudjemline Y. Novel technique for transcatheter closure of sinus venosus atrial septal defect: The temporary suture-holding technique. Catheter Cardiovasc Interv. 2022;100:1068-1077.
22) Yalamanchi R, Sivaprakasam MC, Janke RVR, Chandrasekharan K, Sadhasivam VS, Showkathali R. Unanticipated complication of transcatheter correction of superior sinus venosus atrial septal defect. J Cardiol Cases. 2021;25 99-102.
23) Sandoval JP, Rosenthal E, Arias E, García-Montes JA, Rodríguez-Zanella H, Zabal C, Kabir S, Yong SF, Jones M, Qureshi S. Sinus node dysfunction during transcatheter assessment and stent correction of sinus venosus atrial septal defects. Catheter Cardiovasc Interv. 2023;102:683-687.
24) Sagar P, Thejaswi P, Sivakumar K. A rare unreported complication following transcatheter correction of sinus venosus defect. Ann Pediatr Cardiol. 2023;16:215-218.
25) von Elm, E, Altman, DG, Egger, M, Pocock, SJ, Gotzsche, PC, Vandenbroucke, JP. The Strengthening the Reporting of Observational Studies in Epidemiology (STROBE) Statement: guidelines for reporting observational studies. 2007;18:800–804.
26) Bentley receives CE mark for new BeGraft aortic stent graft - Vascular News https://vascularnews.com/bentley-receives-ce-mark-for-new-begraft-aortic/
27) Andramed GmbH; www.andramed.com
28) Haddad RN, Hascoet S, Karsenty C, Houeijeh A, Baruteau AE, Ovaert C, Valdeolmillos E, Jalal Z, Bonnet D, Malekzadeh-Milani S. Multicentre experience with Optimus balloon-expandable cobalt-chromium stents in congenital heart disease interventions. Open Heart. 2023;10:e002157.
29) Sagar P, Puthiyedath T, Sivakumar K. First-in-man use of an Indian-made balloon-expandable covered Zephyr stent and intermediate-term follow‐up. Ann Pediatr Card 2023;16:48-51

30) Illig KA, Ohki T, Hughes GC, Kato M, Shimizu H, Patel HJ, Shahriari A, Mehta S; Zenith TX2 Low Profile study investigators. One-year outcomes from the international multicenter study of the Zenith Alpha Thoracic Endovascular Graft for thoracic endovascular repair. J Vasc Surg. 2015;62:1485-94.
31) Said SM, Burkhart HM, Dearani JA, Eidem B, Stensrud P, Phillips SD, Schaff HV. Outcome of caval division techniques for partial anomalous pulmonary venous connections to the superior vena cava. Ann Thorac Surg. 2011;92:980-4.
32) Okonta KE, Agarwal V. Does Warden's procedure reduce sinus node dysfunction after surgery for partial anomalous pulmonary venous connection? Interact Cardiovasc Thorac Surg. 2012;14:839-42.
33) Elzein C, Abdulkarim M, Abbas U, Vricella L, Ilbawi M. Repair of Superior Sinus Venosus Atrial Septal Defect Using a Modified Two-Patch Technique. Ann Thorac Surg. 2020;109:583-587.
34) Stephens EH, Mongé MC, Eltayeb O, Patel A, Webster G, Cornicelli MD, Kennedy C, Popescu AR, Rigsby CK, Backer CL. Evolution and Current Results of a Unified Strategy for Sinus Venosus Surgery. Ann Thorac Surg. 2021;111:980-986.
35) Du ZD, Hijazi ZM, Kleinman CS, Silverman NH, Larntz K; Amplatzer Investigators. Comparison between transcatheter and surgical closure of secundum atrial septal defect in children and adults: results of a multicenter nonrandomized trial. J Am Coll Cardiol. 2002;39:1836-44.
36) Mylotte D, Quenneville SP, Kotowycz MA, Xie X, Brophy JM, Ionescu-Ittu R, Martucci G, Pilote L, Therrien J, Marelli AJ. Long-term cost-effectiveness of transcatheter versus surgical closure of secundum atrial septal defect in adults. Int J Cardiol. 2014;172:109-14.
37) Ooi YK, Kelleman M, Ehrlich A, Glanville M, Porter A, Kim D, Kogon B, Oster ME. Transcatheter Versus Surgical Closure of Atrial Septal Defects in Children: A Value Comparison. JACC Cardiovasc Interv. 2016;9:79-86.

Figure Legends

Fig. 1 Study enrolment
Study enrolment flow chart showing the majority of procedures were undertaken by 11/12 of the centers from the original 10-zig CCP registry[9]. The 42 new centers contributed 39% of the procedures.

Fig. 2 Number of procedures by year and by center
The yearly number of procedures is in the blue bars while the total number of centers undertaking procedures is in the orange bars in A. Only 8 months of data are available in 2023. The number of cases that embolized are in the red bars. The number of cases and centers is shown in B.

Fig. 3 World uptake of Covered Stent Correction for Sinus Venosus ASDs
The color-coded graphic shows the world uptake of the procedure as well as the large parts of the world that have not yet undertaken procedures. Actual case numbers are in Table I Data Supplement. (https://datawrapper.dwcdn.net/0BIJU/1/)

Fig. 4 Stents
Stents used included (A) 10-zig covered CP (Numed Inc, Hopkinton, NY), (B) 10-zig G-Armor (uncovered in illustration) stent (Numed), (C) B-graft (Bentley InnoMed GmbH | Germany), (D) Covered Andrastent (Andramed GmbH, Reutlingen, Germany), (E) Optimus Covered Stent (AndraTec GmbH, Koblenz, Germany), (F) Zephyr Covered Stent (Sahajan and Laser Technology Limited, India), (G) Zenith Stentgraft (Medtronic), (H) Endurant Stentgraft, (I) VB Stent, (J) Nano Self-Expanding Stent. The 8-zig versions of (A) and (B) are not shown.

Table I: Patient details

	Total (n = 381)
Age, median (range), years	**44 (4.75 – 87)**
Age, n (%)	
5 – 10 years of age	14 (3.7)
11 – 16 years of age	16 (4.2)
17 – 18 years of age	7 (1.8)
> 18 years of age	344 (90.3)
Weight, median (range), kg	70 (17 – 145) *
Sex, n (%)	
Male	188 (49.4)
Female	193 (50.6)
Symptoms, n (%)	307 (81)
Shortness of breath	206 (54)
Palpitations	85 (12)
Chest pain (atypical)	36 (9.5)
Syncope/presyncope	13 (3.4)
Miscellaneous	15 (3.9)
Asymptomatic	65 (17)
Not stated	9 (2.4)
Other Cardiovascular findings, n (%)	
Bilateral SVCs	58 (15.2)
Accessory / non-diverted RUPV	72 (18.9)
Atrial flutter or fibrillation	25 (6.6)
Pulmonary vascular disease	8 (2.1)
Previous surgical repair	2 (0.5)
MRI and/or Catheterization findings	
QP:QS, median (range)	2.5:1 (1.2 – 5.4) **
RVEDV (ml/m^2), median (range)	161 (91 – 295) ***
RV/LV, median (range)	2.7 (1.5 – 4.15) ****

QP:QS = Pulmonary to systemic flow ratio on MRI or at cardiac catheterization
RVEDV = Right ventricular end diastolic volume; & available in 106 (27.8%)
RV/LV = Right ventricular end diastolic volume/ Left ventricular end diastolic volume
SVC = superior vena cava
* Weight available in 370/381 (97.1%) of the patients
** QP:QS available in 198 (52.0%) of the patients with a left to right shunt
*** RVEDV available in 106 (27.8%) of the patients
**** RV/LV available in 72 (18.9%) of the patients

Table 2 Stent and Procedure details

A)	Number of cases	Number of centers using this stent	Number of centers using only this stent
Balloon expandable stents			
10 zig CCP [7, 9]	237	34	19
Optimus [13, 14]	39	12	7
Zephyr [15]	27	2	
8 zig CCP [3]	25	9	2
Andramed [8]	22	1	
10 zig G-Armor CCP [16]	7	7	
B-Graft [11]	4	4	2
8 zig G-Armor CCP [16]	3	3	3
Self-expanding stents			
Endurant [17]	10	2	
VB stent [18]	5	2	1
Zenith [4]	1	1	
Nano	1	1	1

B)	Patients, n (%)
Number of Stents	
One	201 (52.8%)
Two	117 (30.7%)
Three	51 (13.4%)
Four	10 (3.2%)
Five	2 (0.5%)
Technique	
Single balloon mounted stent	187 (49.1%)
Initial landing zone stent	74 (19.4%)
"Sandwich technique" [9]	33 (8.7%)
Suture assisted delivery [12, 19]	48 (12.6%)
Overlapping stents on single balloon [8]	17 (4.5%)
Stents sutured together [18]	3 (7.9%)
Self-expanding stents	17 (4.5%)
Additional ASD or PFO occluder	8 (2.1%)
Pulmonary vein and procedure monitoring	
Pulmonary vein access	335 (87.9%)
Retrograde arterial	43 (11.3%)
Trans-septal	239 (62.7%)
Direct femoral vein	53 (13.9%)
TEE & Pulmonary Vein access	266 (69.8%)
TEE alone	46 (12.1%)
TEE not used	69 (18.1%)
Echonavigator fusion[14]	14 (3.6%)
Pulmonary vein protection balloon	113 (29.6%)
Pulmonary vein rescue balloon	8 (2.1%)

Table 3 Embolization of Covered Stent/s

Center Number *	Cases in center	Case number embolized	Type of Stent	Length of Stent (cm)	Technique of implantation	Year of procedure
1	92	1	8 zig CCP	4.5 x 2	Two stents on one balloon	2015
		6	Andrastent	4.8		2017
		77	Zephyr	7.9	Additional stent for instability	2023
2	53	20	10 zig CCP	7.0		2019
8	10	4	10 zig CCP	6.0	Suture control & 2 additional stents	2020
10	9	6	10 zig CCP	6.0	Initial landing zone stent; additional stent for leak	2022
13	7	2	Optimus	5.7	Initial landing zone stent; additional stent for leak	2022
23	4	2	VB Stent	7.5		2023
27	3	2	10 zig CCP	6.0	Initial landing zone stent; additional stent for leak	2021
30	3	3	10 zig CCP	6.0	Additional stent for instability	2022

* Centers were ranked first by volume of procedure and if equal then by earliest date of commencing procedures. CCP = Covered Cheatham Platinum (stent)

Table 4 Complications after successful CSC

	Patients, n (%)
A) Early (Intraprocedural and in-hospital)	
Major	**3 (0.79%)**
Pericardial tamponade requiring surgical relief	2 (0.5%)
Severe bradycardia after procedure – pacemaker implanted	1 (0.25%)
Moderate & minor - transient & resolved	**36 (9.4%)**
Innominate vein obstruction – relieved during procedure	2 (0.5%)
Pulmonary venous pathway narrowing – relieved with balloon dilation during procedure	8 (2.1%)
Pulmonary vein dissection – uncomplicated – resolved during procedure	1 (0.25%)
Procedural thrombus – resolved with heparin during procedure	
In stent	1 (0.25%)
Clot on guidewire – resolved with aspiration and heparin	1 (0.25%)
Clot on trans-septal puncture site	1 (0.25%)
Jugular, innominate vein or superior vena cava – right atrial junction clot	3 (0.79%)
Atrial fibrillation during the procedure – cardioversion at end procedure	2 (0.5%)
Atrial flutter – cardioverted 2 days later	1 (0.25%)
Access site	
Femoral artery pseudoaneurysm – resolved with thrombin injections	4 (1.05%)
Jugular cut down to retrieve self-expanding stent mechanism	1 (0.25%)
Jugular hematoma - resolved	1 (0.25%)
Femoral vein hematoma – surgical exploration – no active bleeding found	1 (0.25%)
Femoral puncture site infection – resolved on antibiotics	1 (0.25%)
Pulmonary hemorrhage requiring intensive care – resolved	1 (0.25%)
Pericardial effusion – conservative management	2 (0.5%)
Arm neuropraxia - resolved	4 (1.05%)
Clot in stent – antiplatelet drugs changed to oral anticoagulation - resolved	1 (0.25%)
B) Late (30 days - 1 year)	
Major	**2 (0.5%)**
Pulmonary vein obstruction - thoracoscopic partial upper lobectomy	1 (0.25%)
Late stent removal – moderate leak, tricuspid regurgitation & need for coronary artery bypass grafting for new onset coronary disease	1 (0.25%)
Additional catheter intervention	**7 (1.84%)**
Additional stent for residual shunt	4 (1.05%)
Atrial septal occluder for residual shunt	3 (0.79%)
Minor - resolved	**3 (0.79%)**
Clot in stent – antiplatelet drugs changed to oral anticoagulation	3 (0.79%)

Fig. 1 Study enrolment

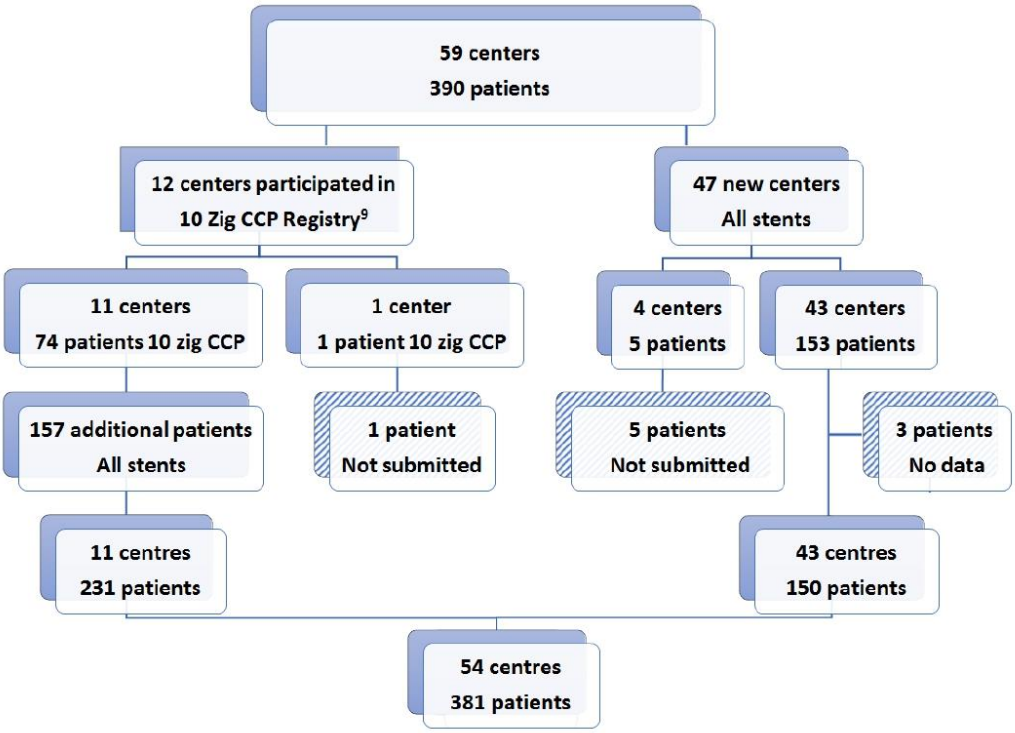

Study enrolment flow chart showing the majority of procedures were undertaken by 11/12 of the centers from the original 10-zig CCP registry[9]. The 43 new centers contributed 39% of the procedures. Of 390 known patients data were submitted on 381. CCP = Covered Cheatham Platinum (stent)

VI. Travaux connexes

1. « cas frontières »

Pendant ces 4 années de thèse, la modélisation 3D des CIA sinus venosus a permis la découverte et l'analyse de certains cas frontières, n'étant pas des CIA sinus venosus, mais dont l'anatomie semblait s'en rapprocher.

Ces raretés anatomiques ont été finalement d'une grande richesse dans la recherche et l'évaluation liée à cette cardiopathie singulière, et méritent d'être présentées ci-après.

CASE REPORT 3 : Inferior sinus venosus defect and anomalous hepatic venous return to the coronary sinus leading to Eisenmenger syndrome **(publié dans Cardiology In the Young, Avril 2022)**

Référence bibliographique 119

A Tajouri, C Batteux, R Ly, L Houyel, S Hascoet

Cardiology in the Young

cambridge.org/cty

Brief Report

Cite this article: Tajouri A, Batteux C, Ly R, Houyel L, and Hascoet S (2023) Inferior sinus venosus defect and anomalous hepatic venous return to the coronary sinus leading to an Eisenmenger syndrome. *Cardiology in the Young* **33**: 136–137. doi: 10.1017/S1047951122001354

Received: 30 November 2021
Revised: 4 March 2022
Accepted: 7 April 2022
First published online: 28 April 2022

Author for correspondence:
Sebastien Hascoet, Hôpital Marie Lannelongue, 133 avenue de la résistance, 92350, Le Plessis-Robinson, France.
Tel: 0033 1 40 94 28 00.
E-mail: s.hascoet@ghpsj.fr

Inferior sinus venosus defect and anomalous hepatic venous return to the coronary sinus leading to an Eisenmenger syndrome

Asma Tajouri[1], Clément Batteux[1,2], Reaksmei Ly[3], Lucile Houyel[4] and Sebastien Hascoet[1,2]

[1]Marie-Lannelongue Hospital, Paediatric and Congenital Cardiac Surgery Department, Centre de Référence des Malformations Cardiaques Congénitales Complexes M3C Groupe Hospitalier Saint-Joseph, Paris-Saclay University, Plessis-Robinson, France; [2]UMRS 999, INSERM, Marie-Lannelongue Hospital, Paris-Saclay University, Le Plessis Robinson, France; [3]Hôpital Européen Georges Pompidou, adult congenital Cardiology Unit, Centre de Référence des Malformations Cardiaques Congénitales Complexes M3C, Paris, France and [4]Hôpital Necker-Enfants Malades, Congenital and Pediatric Cardiology Unit, Centre de Référence des Malformations Cardiaques Congénitales Complexes M3C, Paris, France. Université de Paris, Paris, France

Abstract

Inferior sinus venosus defect associated with left hepatic vein drainage to the coronary sinus is an extremely rare condition. We report the case of a 41-year-old man suffering from pulmonary arterial hypertension related to this unusual CHD. Planning of heart–lung transplantation in this case required accurate anatomical description.

A 41-year-old man with pulmonary arterial hypertension due to an inferior sinus venosus defect was referred for heart–lung transplantation. He complained of congestive heart failure and WHO 3 dyspnoea. Right ventricle ejection fraction on MRI was lowered to 18% with enlarged right cardiac cavities (end diastolic right ventricle volume: 228 ml/m^2, right atrium area: 50 mm^2). Under advanced pulmonary arterial hypertension therapy (tadalafil and ambrisentan), pulmonary vascular resistance was 6.2 Wood unit.m^2. Mean atrial pressures were highly elevated at 22 mmHg. Inferior sinus venosus defect consisted of overriding of the inferior caval vein over the interatrial septum, nicely depicted on a 3D model (panels E and F), with a large interatrial defect (panels A, B, E, and F ; star) and continuity between the inferior caval vein and the posterior wall of the left atrium (panel A).[1] A prominent Eustachian valve (panel A; arrow) on the right side of the inferior caval vein directed the flow preferentially to the left atrium. An intriguing left hepatic vein anomalous return to a dilated coronary sinus was diagnosed (panels C and D).[2,3] There was an intrahepatic small connection between the inferior caval vein and the left hepatic vein (panel D). The patient died of terminal heart failure while on the waiting list. Autopsy confirmed the diagnosis of inferior sinus venosus defect by visualising partial anomalous connection of the two right lower pulmonary veins to the inferior caval vein at its junction with the right atrium, and the anomalous drainage of the left hepatic vein to coronary sinus (panels G and H).

Left hepatic vein drainage to the coronary sinus is an extremely rare and benign congenital vascular anomaly often associated with other vascular malformations such as persistent left superior vena cava, anomalous pulmonary venous drainage, interrupted inferior caval vein with azygos continuation.[4] In this case, its recognition was important to plan the heart–lung transplantation.[5,6] Pulmonary arterial hypertension was likely to be related to the sinus venosus defect and the right ventricle volume overload. Genetic study did not identify at-risk anomaly to date. The left hepatic vein drainage to the coronary sinus was not associated with porto-caval fistula.

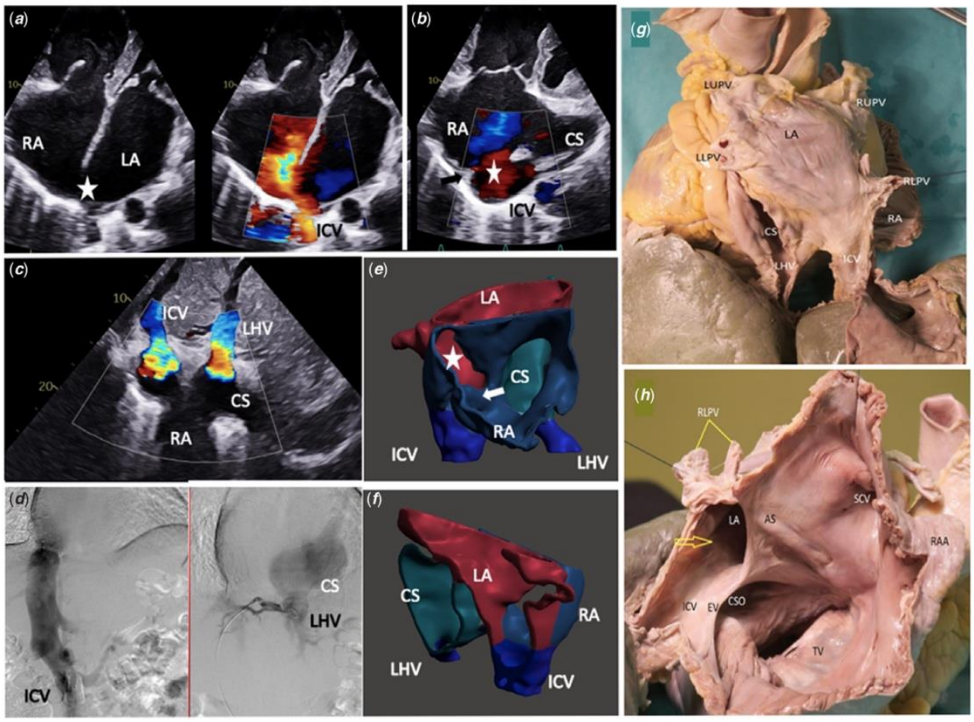

Figure 1. (***a***) Trans-thoracic echocardiography TTE (4 chambers view): vizualisation of the atrial septal defect (star), and the left and right atriums (LA and RA) dilated. The atrial septum overrides the inferior caval vein (ICV). (***b***) Trans-thoracic echocardiography TTE (modified 4 chambers view): vizualisation of the coronary sinus (CS) opening in right atrium (RA). Septal defect is marked by the star, and the septum (arrow) overrides the inferior caval vein (ICV). (***c***) Trans-thoracic echocardiography TTE (sub-costal view): vizualisation of the inferior caval vein (ICV) drainage to the right atrium (RA), overriding the atrial septum. Vizualisation of the left hepatic vein (LHV) drainage to the coronary sinus (CS) opened in the RA. (***d***) Angiographic face view during catheterization. Vizualisation of the inferior caval vein (ICV) drainage to right atrium (RA) and the left hepatic vein (LHV) drainage to the coronary sinus (CS). Note the small vein communication between these two venous returns just above the diaphragm area. (***e*** and ***f***) Three-dimensional view of the malformation built from cardiac CT using open-sources modelling softwares (ITK-snap®, Meshmixer®). E: front view. F: posterior view. Coronary sinus (CS) appears in green. Inferior caval vein (ICV) and left hepatic vein (LHV) appear in royal-blue. Right atrium (RA) appears in dark-blue. Left atrium (LA) appears in red. The atrial defect is marked by a star. The arrow shows the prominent Eustachian valve. (***g***) Posterior view of the heart specimen. CS, coronary sinus; ICV, inferior caval vein; LA, left trium; LHV, left hepatic veins; LLPV, left lower pulmonary vein; LUPV, left upper pulmonary vein; RA, right atrium; RLPV, right lower pulmonary veins; RUPV, right upper pulmonary vein. (***h***) Right atrium. The atrial septum overrides the inferior caval vein (inferior sinus venosus defect). AS, atrial septum; CSO, coronary sinus orifice; EV, Eustachian valve; ICV, inferior caval vein; LA, Left atrium; RAA, right atrial appendage; RLPV, right lower pulmonary veins; SCV, superior caval vein; TV, tricuspid valve. Yellow arrow: inferior sinus venosus defect.

Supplementary material. To view supplementary material for this article, please visit https://doi.org/10.1017/S1047951122001354

Financial support. This research received no specific grant from any funding agency, commercial or not-for-profit sectors.

Conflicts of interest. None.

References

1. Chen CA, Wang JK, Hsu JY, Hsu HH, Chen SJ, Wu MH. Diagnosis of inferior sinus venosus atrial septal defects using transthoracic three-dimensional echocardiography. J Am Soc Echocardiogr 2010; 23: 457.e4–6.
2. Sanders SP. Anomalous hepatic venous connection to the coronary sinus diagnosed by two-dimensional echocardiography. Am J Cardiol 1984; 54: 458–459. doi: 10.1016/0002-9149(84)90225-x. PMID: 6465037.
3. Lee C, Saremi F. Anomalous left hepatic vein draining into coronary sinus imaged with multidetector computed tomography. Clin Anat 2013; 26: 987–989. doi: 10.1002/ca.22257. Epub 2013 Jul 30. PMID: 23908095.
4. Morshuis WG, de Lind van Wijngaarden RA, Kik C, Bogers AJ. Drainage of the left hepatic vein into the coronary sinus, a rare intraoperative finding. J Card Surg 2015; 30: 817–818. doi: 10.1111/jocs.12645. Epub 2015 Sep 29. PMID: 26420740.
5. Vuran C, Ozker E, Gumus B, Turkoz R. Anomalous hepatic vein draining into the coronary sinus. Pediatr Cardiol 2011; 32: 1256–1257. doi: 10.1007/s00246-011-0063-0. Epub 2011 Jul 30. PMID: 21805201.
6. Rao RK, Varadaraju R, Girish B, Singh N. Anomalous left hepatic vein to coronary sinus in a patient with atrial septal defect: Minimally invasive approach; technical challenges. J Card Surg 2021; 36: 4390–4392. doi: 10.1111/jocs.15906. Epub 2021 Aug 8. PMID: 34365681.

https://doi.org/10.1017/S1047951122001354 Published online by Cambridge University Press

***CASE REPORT 4 : Transcatheter correction of a rare combined anomalous pulmonary and systemic venous return in an adult* (cardiovascular flashlight publié dans European Heart Journal, octobre 2024)**

Référence bibliographique 120

G Albenque, C Batteux, S Hascoet

CARDIOVASCULAR FLASHLIGHTS https://doi.org/10.1093/eurheartj/ehae732

Transcatheter correction of a rare combined anomalous pulmonary and systemic venous return in an adult

Grégoire Albenque [1,2], Clément Batteux [1,2], and Sébastien Hascoët [1,2,*]

[1]Department of Congenital Heart Diseases, Centre de Référence Malformations Cardiaques Congénitales Complexes M3C, Hôpital Marie Lannelongue, Faculté de médecine, Université Paris-Saclay, 133 Avenue de la Résistance, 92350 Le Plessis-Robinson, France; and [2]Université Paris-Saclay, INSERM, UMR_S 999, Hypertension Pulmonaire: Physiopathologie et Innovation Therapeutique (HPPIT), AP-HP, Hôpital Bicêtre, Hôpital Marie Lannelongue, ERN-Lung, 92350 Le Plessis-Robinson, France
*Corresponding author. Tel: +33 140 942 800, Fax: +33140 948 718, Email: s.hascoet@ghpsj.fr

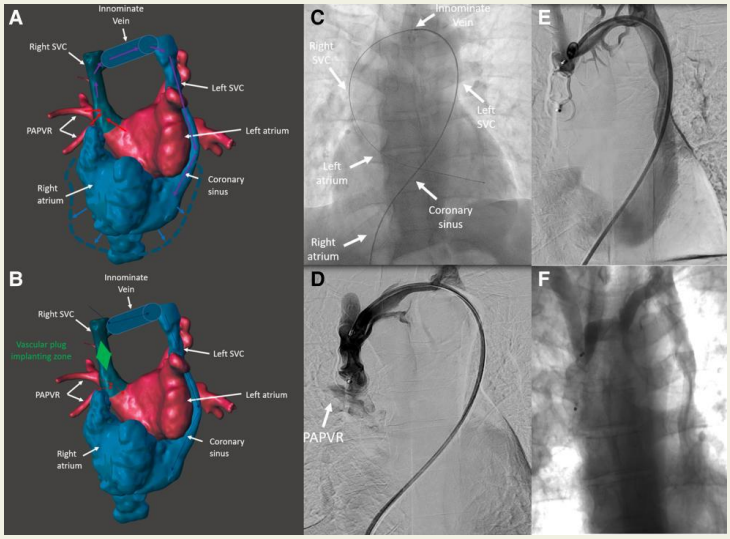

A 50-year-old patient with a history of cerebral abscess was referred following the incidental discovery of right heart cavities dilation. A computed tomography scan (see Supplementary data online, *Video S1*) with 3D reconstruction (*Panels A* and *B*) identified a very unusual congenital heart disease combining anomalous systemic and pulmonary venous return. A left superior vena cava (SVC) drained into the coronary sinus, while the right SVC connected to the left atrium. Additionally, a partial anomalous pulmonary venous return (PAPVR) included a right upper lobar pulmonary vein connecting to the termination of the right SVC without defect of the interatrial septum. A pathophysiology of left-to-right shunt was observed with oxygenated blood flow going from left to right atrium through the SVC circuit leading to right heart dilation (*Panel A*—arrows in the veins). An original mini-invasive transcatheter option was deemed feasible (*Panel B*). The procedure was performed via the inferior vena cava, where a wire-loop was established through the right atrium, coronary sinus, left SVC, innominate vein, right SVC, and finally into the left atrium (*Panel C*). A 7 Fr long sheath was advanced allowing for the placement of a 20 mm Amplatzer Vascular Plug II® in the right SVC, positioned between the i.v. and the PAPVR (*Panel D*). Post-procedural angiography (*Panel E*) confirmed the successful redirection of deoxygenated venous flow into the innominate vein and oxygenated blood from the PAPVR into the left atrium (*Panel E*). At 6 months of follow-up, no residual shunt and proper blood flow redirection were confirmed (*Panel F*).

Supplementary data are available at *European Heart Journal* online.

S.H. is a proctor for Abbott Vascular, Edwards Lifesciences, and Venus Medtech. The other authors have no disclosure.

The data underlying this article will be shared on reasonable request to the corresponding author.

a. *CIA sinus venosus inférieur isolée*

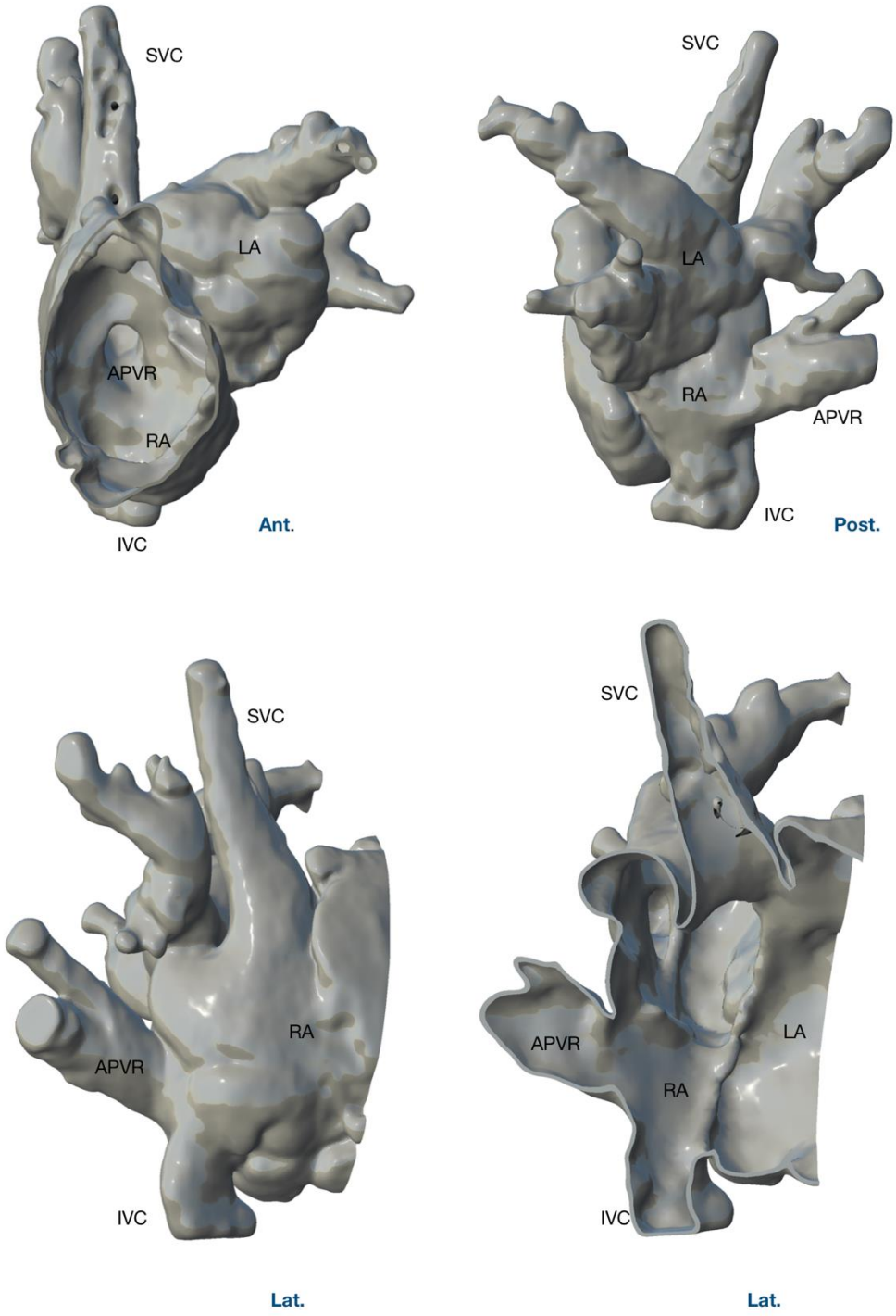

Figure 60 : modélisation 3D de la CIA sinus venosus inférieure

Jeune patiente de 17 ans ayant une CIA OS large associée à une anomalie type sinus venosus inférieure. La veine pulmonaire inférieure droite s'abouche à la jonction cavo-atriale inférieure avec un défect en regard. Patiente opérée par tunnélisation avec double patch en 2023 avec un bon résultat.

b. *Forme avortée de CIA sinus venosus ?*

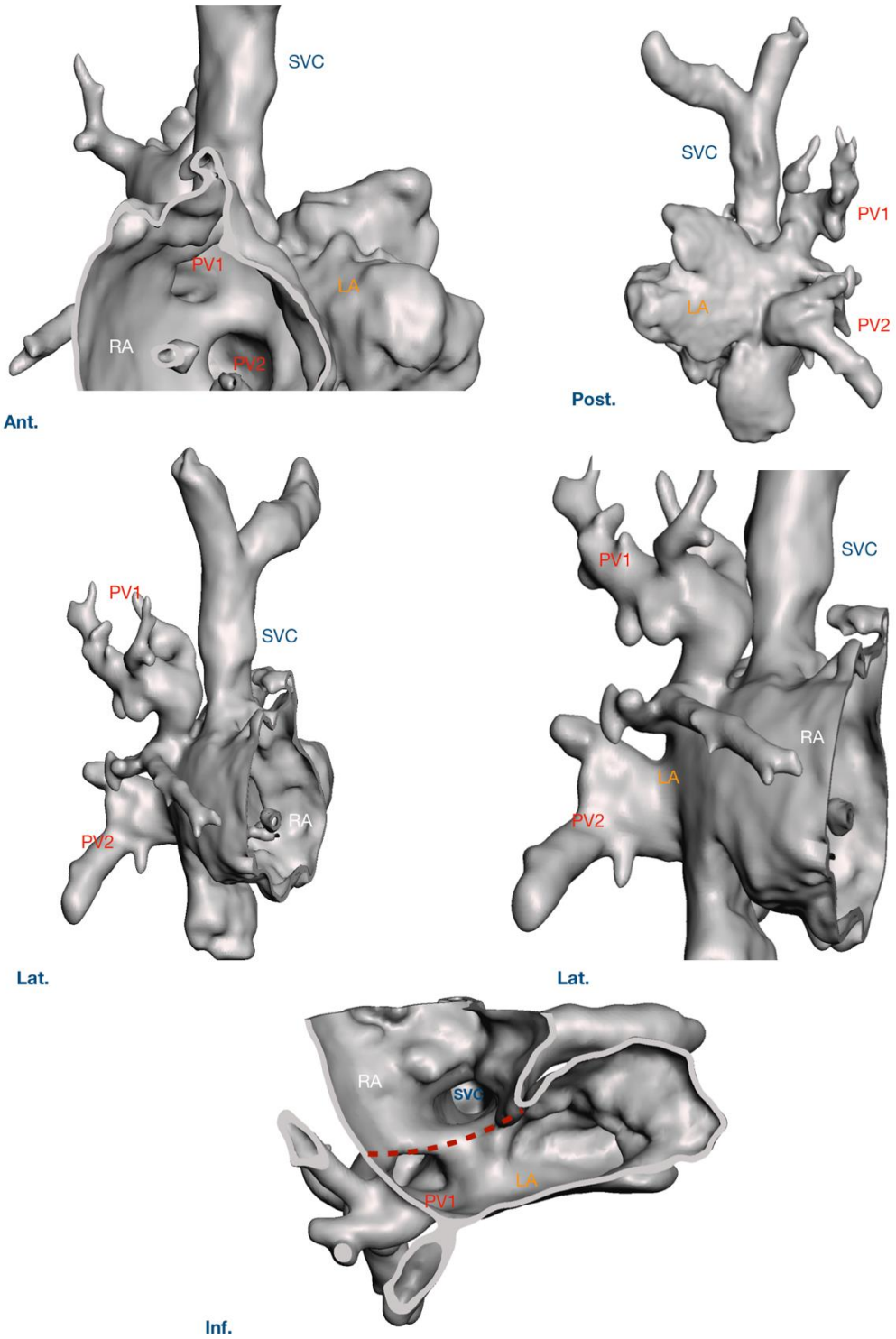

Figure 61 : modélisation 3D d'une forme anatomique semblant « avortée » de CIA sinus venosus.

La jeune patiente de 8 ans présente une CIA ostium secundum large avec un aspect de veines pulmonaires supérieures droites semblant s'orienter vers la VCS. Finalement, les VPSD se jettent au toit de l'OG, avec respect de la jonction cavo-atriale.

c. *RVPA dans veine cardinale*

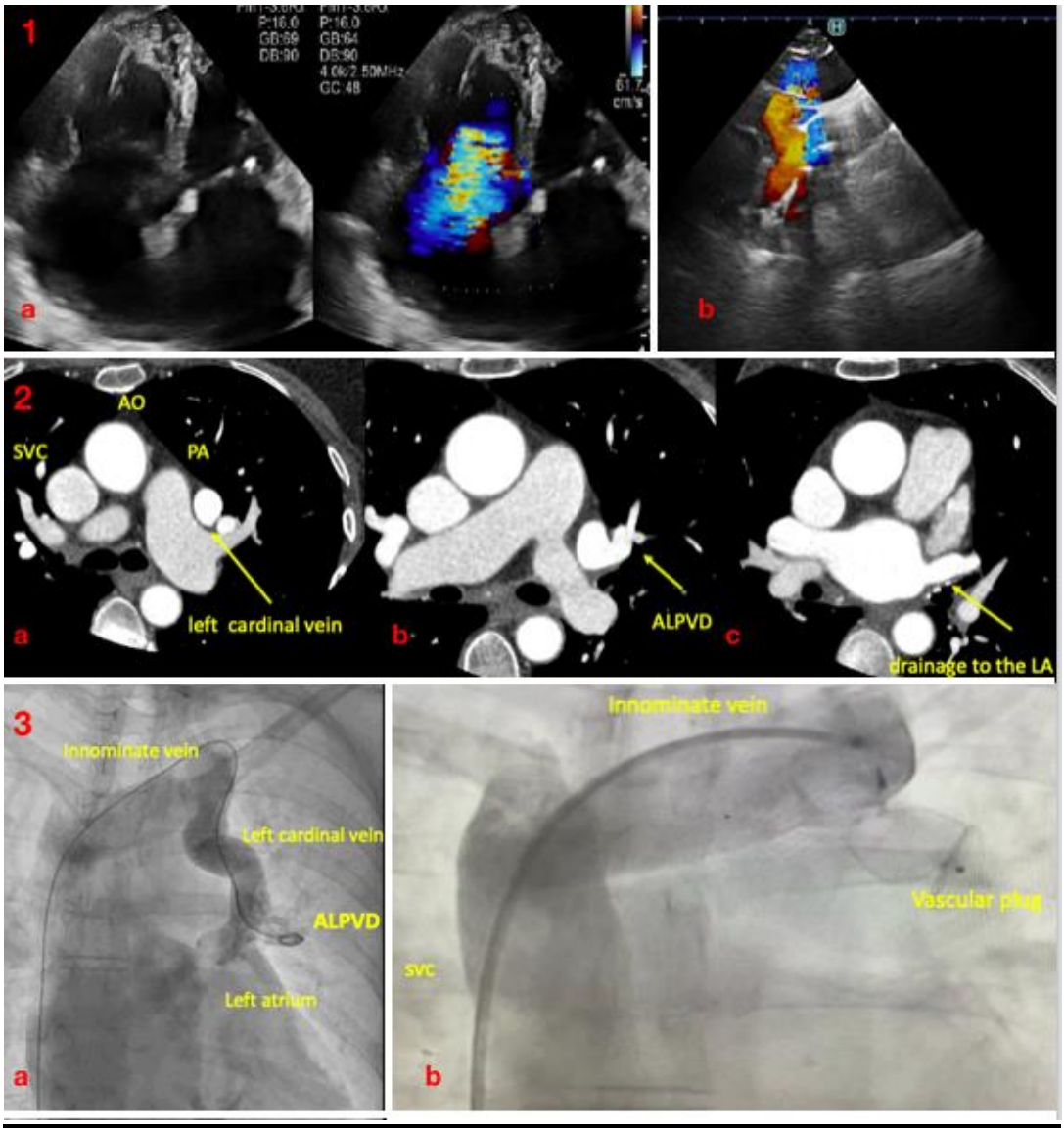

Figure 62 : retour veineux pulmonaire anormal dans une veine cardinale s'abbouchant à l'oreillette gauche.

Diagnostic échographique, scannographique puis traitement par embolisation par plug d'un retour veineux pulmonaire anormal dans une veine cardinale s'abouchant à l'oreillette gauche. La veine cardinale est abouchée à l'oreillette gauche et reçoit un retour veineux pulmonaire anormal du poumon gauche. Cette conformation semble être un miroir d'une CIA sinus venosus avec VCSG. Ici, la présence d'un TVI permet d'emboliser la veine cardinale au-dessus du RVPA par un plug ; ainsi Le RVPA à la veine cardinale reste drainé à l'OG et le TVI ne se draine plus que dans la VCSD, rétablissant une situation circulatoire physiologique.

VII. Communications, diffusions

1. Marie Lannelongue workshop

Ce travail de thèse a été mené en équipe, et accompagné sur le plan scientifique, institutionnel, technique et tout simplement humain, par de nombreuses personnes salariées de l'Hôpital Marie Lannelongue.

Un des aboutissements les plus concrets de ce travail de thèse a été la création d'un workshop par notre équipe, dédié au cathétérisme interventionnel complexe des cardiopathies congénitales. Ce workshop a été initié en octobre 2023 et ré-édité en octobre 2024, et a maintenant vocation à se renouveler chaque année.

Nous avons pu y convier des experts de renommée internationale pour la correction percutanée des CIA sinus venosus, dans un cadre permettant le partage d'expérience et d'expertise. Nous avons également souhaité y convier des juniors européens après diffusion d'appel à candidature par l'Association Européenne de Cardiologie Pédiatrique (AEPC) afin de leur permettre d'approcher de manière didactique et conviviale cette nouvelle intervention complexe.

Au cours de ces workshop, des ateliers de simulation virtuelle, de simulation sur banc d'essai et des cas live ont été proposés aux intervenants, avec des retours très positifs de tous les participants, nous encourageant à sa poursuite dans les années futures.

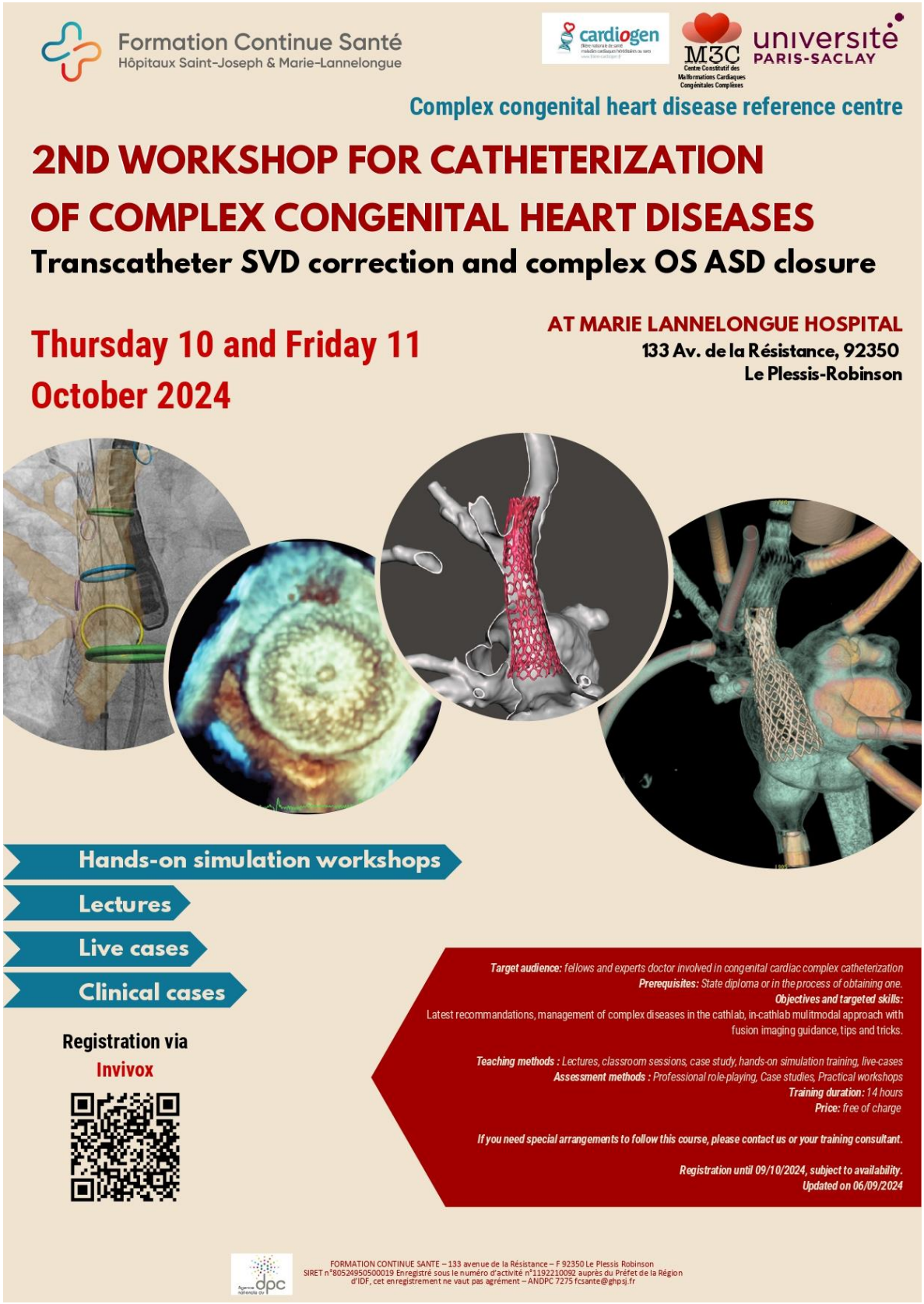

Figure 63 : flyer du work shop Marie Lannelongue sur le cathétérisme interventionnel des cardiopathies congénitales complexes (édition 2024)

2. Communications scientifiques et diffusion (Dr Batteux)

Journées européennes de la SFC (société française de cardiologie)

2023

- CIA type Sinus Venosus : Caractéristiques anatomiques par l'imagerie multi-modalités

- Multicenter Experience of Transcatheter Correction of Sinus Venosus Defect Using the Covered Optimus XXL Stent

-Transcatheter Correction of Sinus Venosus Defect : From Bench Testing to Clinical Success

2021

-Modélisation tridimensionnelle et simulation multimodalité de la fermeture percutanée des communication inter-atriales type sinus venosus

Lauréat Bourse Hélène de Marsan

Worl Congress de cardiologie pédiatrique et congénitale

2023

-Rethinking sinus venosus defect anatomy using 3D reconstruction

Congrès de la FCPC (fédération de cardiologie pédiatrique et congénitale)

2024 **:** *4D Flow Magnetic Resonance Imaging Evaluation after Transcatheter Correction Of Sinus Venosus Defects*

2023 ***:*** *Early Multicenter experience of transcatheter correction of superior sinus venosus defect using the covered Optimus XXL stent*

2022 ***:*** *atelier : correction percutanée des CIA sinus venosus sur banc d'essai*

Congrès de l'AEPC (association européenne de cardiologie pédiatrique)

2022

-Transcatheter Correction of Sinus Venosus Defect : From Bench Testing to Clinical Success.

Lauréat du prix : Young Investigator Award

Japanese Society of Pediatric Cardiology

2022 : *Transcatheter Correction of Sinus Venosus Defect : From Bench Testing to Clinical Success*

Cardiogen

2023 : *Sinus venosus defect : anatomic analysis 3D modeling*

Live case de correction percutanée de CIA sinus venosus (équipe HML)

*CSI Frankfurt **2024***

*CSI Frankfurt **2023***

3. Chapitre de livre d'enseignement Masson

Rédaction d'un chapitre d'enseignement sur les communications inter-atriales pour le traité de cardiologie édité aux éditions Masson (publication prochainement).

4. Magazine de la santé (France 5)

Tournage à l'Hôpital Marie Lannelongue d'un documentaire à destinée du grand public pour l'émission « le magazine de la santé » permettant de suivre le parcours patient d'une patiente ayant une CIA sinus venosus. Le documentaire suit la patiente et l'équipe médicale depuis l'annonce diagnostic jusqu'au traitement endovasculaire ainsi qu'au cours de son suivi postopératoire. Un chapitre est dédié à la simulation préopératoire de l'intervention sur modèle imprimé perfusé sur banc d'essai, afin de préparer au mieux l'intervention de manière ciblée et adaptée à la malformation de la patiente.

https://www.youtube.com/watch?v=Beh5O8Rr9o0

PRIX ET BOURSES EN RELATION AVEC LA THÈSE

2020/2021

Bourse Hélène de Marsan (Cardiologie Pédiatrique ou congénitale) soutenue par l'AREMCAR de la Société Française de Cardiologie.

"*Modélisation tridimensionnelle et simulation multi-modalité de la fermeture percutanée des communication inter-atriales type sinus venosus"*

Montant : 15 000 euros

2022

Lauréat du prix Young Investigator Award de l'Association Européenne de Cardiologie Pédiatrique (AEPC).

Transcatheter Correction of Sinus Venosus Defect : From Bench Testing to Clinical Success.

Montant : 1500 euros

PERSPECTIVES, LIMITES, DISCUSSIONS

I. Anatvenosus

Continuum embryologique ?

Les controverses embryologiques relatives à l'explication développementale des CIA sinus venosus sont nombreuses[66-68].

Une tendance actuelle semble évoquer comme origine un pont veno-veineux ou une collatérale entre les veines pulmonaires et la veine cave supérieure[72, 121].

D'après notre travail anatomique sur une cohorte conséquente et la classification proposée, il est possible d'imaginer un continuum embryologique entre toutes les formes rencontrées. En effet, aussi bien les formes fenestrations que les formes cavo-atriales pourraient provenir d'une origine commune liée au retour veineux pulmonaire anormal dans la VCS droite et ensuite s'étendre soit vers le haut (forme floride), soit vers le bas (forme cavoatriale pure), soit vers le haut et le bas (forme cavoa-atriales florides)

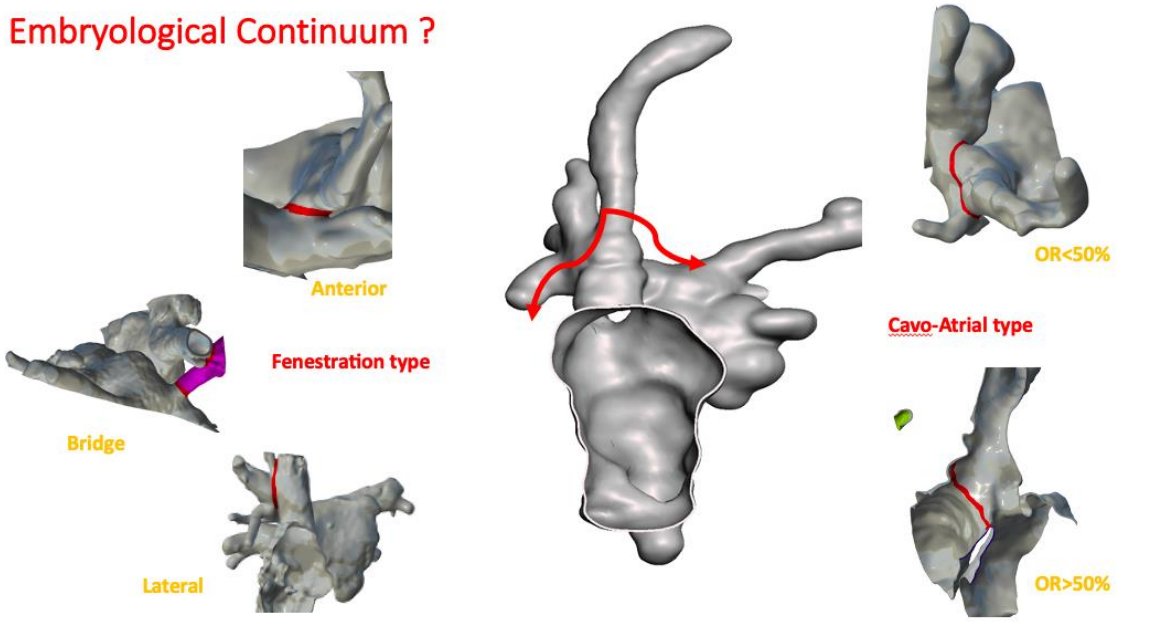

Figure 64 : possibilité d'un continuum embryologique entre les formes de cia sinus venosus

Concepts anatomiques

L'étude anatomique des CIA sinus venosus, motivée par les connaissances tirées de la modélisation 3D a permis d'introduire de nouveaux concepts et d'affiner ceux déjà décrits.

Étant donné la variabilité anatomique des retours veineux pulmonaires dans la population générale, et plus particulièrement chez les patients présentant une CIA sinus venosus, nous avons choisi de nous concentrer sur les ostia des veines pulmonaires droites, plutôt que sur le nombre précis de veines impliquées. Le concept d'ostium principal anormal veineux pulmonaire simplifie la compréhension et la description de la variabilité du retour veineux pulmonaire anormal associé aux CIA sinus venosus.

La caractérisation du défect en tant que tel reste un sujet de débat, car son apparence peut varier en fonction du point de vue. Il peut en effet être visualisé sous forme d'un orifice, ou plus couramment, sous la forme d'un volume conique, en fonction de sa relation avec le RVPA, de l'extension caudale et du degré d'over-riding de la veine cave supérieure. Par exemple, dans la fenestration, ce qui est qualifié défect peut apparaître comme un orifice plan, tandis que dans la forme cavo-atriale, il peut se présenter sous la forme d'un grand volume conique. Nous pensons ainsi que le défect lui-même ne devrait pas être considéré comme un paramètre primaire dans l'évaluation des CIA sinus venosus, mais plutôt comme une conséquence des facteurs anatomiques mentionnés précédemment.

Dans ce contexte, nous avons choisi d'évaluer la distance entre l'ostium des veines pulmonaires anormales supérieures et le bord inférieur de la communication entre les deux oreillettes, afin de définir la zone de shunt, plutôt que de tenter de définir le défect lui-même.

Notre définition de l'extension caudale repose sur une analyse en 3D de la jonction cavo-atriale, qui ne peut être correctement évaluée dans des vues orthogonales 2D en raison de l'orientation variable de la VCS lorsqu'elle s'abouche à l'OD. Nous avons arbitrairement choisi de nous concentrer sur un plan de coupe au niveau de la partie supérieure cette jonction, car cela semblait être la méthode la plus reproductible. Dans ce contexte, nous avons toléré une extension de 10 mm la forme fenestration étant donné que l'orientation oblique de la SVC entraîne automatiquement une extension caudale « artificielle » du défect.

Le concept d'over-riding, précédemment décrit à l'aide d'une méthode comparable à celle utilisée pour la tétralogie de Fallot[72], impliquait une prolongation plane et supposée du septum inter-atrial afin de déterminer le degré d'over-riding de la VCS avec l'OG. Nous avons modifié cette méthode en prolongeant virtuellement la VCS en 3D, après l'avoir sectionnée suivant le plan de la veine azygos. Cette modification a

permis de révéler une plus grande proportion de cas sans over-riding en comparaison aux études précédentes.

Comme indiqué dans les publications antérieures[71, 72], nous maintenons que l'over-riding n'est pas un critère obligatoire pour caractériser une CIA sinus venosus.

Nécessité d'une classification

Notre objectif principal était de proposer une classification des CIA sinus venosus, car les descriptions et implications thérapeutiques varient souvent de manière significative entre les praticiens. Cette classification vise à standardiser le langage anatomique utilisé pour décrire la cardiopathie, facilitant ainsi la communication et permettant un ciblage plus précis des stratégies thérapeutiques anatomo-dépendantes. En définissant des points clés tels que l'over-riding, l'extension caudale et le nombre d'ostia des veines pulmonaires anormales, nous espérons répondre par une classification simple et didactique, aux défis spécifiques posés par chaque anatomie singulière.

Implications pour la correction percutanée

Formes « Single »

Single Fenestration : Cette forme implique une zone de communication haute entre les deux chambres atriales. Étant donné que la région cavo-atriale n'est pas affectée, la protection des veines pulmonaires n'est généralement pas nécessaire dans l'approche initiale. La stratégie d'implantation du stent doit se concentrer sur les faits suivants :

-Assurer une bonne impaction du stent au niveau de la région du TVI pour prévenir l'embolisation du dispositif (la distance entre les ostia des veines pulmonaires et la veine innominée doit être évaluée pour s'assurer qu'elle est suffisante).

-Assurer une bonne impaction du stent au niveau de la jonction cavo-auriculaire (sous l'ostia anormal des veines pulmonaires) afin d'éviter un shunt résiduel.

-Une forme en « 8 » du stent est souvent attendue dans les procédures de correction percutanée pour ce type particulier.

Single cavo-atrial : Ce type est fréquemment rencontré, impliquant la jonction cavo-atriale et l'ostium de la veine pulmonaire anormale situé relativement bas. Pour la correction percutanée, la stabilité du stent n'est généralement pas un problème si la distance entre le RVPA et TVI est suffisante. Toutefois, il existe un risque de shunt résiduel, qui doit être mis en balance avec risque d'occlusion de la veine pulmonaire,

car l'excès de flairing du stent dans sa partie caudale peut entraîner l'occlusion de la veine pulmonaire en regard. La protection de la veine pulmonaire doit alors se discuter en raison de cette balance sus-citée.

Formes florides : Lorsqu'un ostium supplémentaire de veine pulmonaire anormal est impliqué dans la CIA-SV, sa position par rapport à l'ostium principal de la veine pulmonaire est cruciale. Si l'ostium supplémentaire est situé en dessous de l'ostium principal, il ne pose généralement pas de problème majeur pour la TCSVD, car la redirection de la veine pulmonaire principale redirigera également la veine supplémentaire. Cependant, si l'ostium supplémentaire se trouve au-dessus du principal, une attention particulière est requise. Une stratégie de protection par ballon ou de maintien de la veine dans dans la VCS doit être considérée. Une étude précise utilisant l'IRM 4D avec une analyse sélective du rapport qp/qs peut aider à déterminer la meilleure approche en fonction du rôle hémodynamique attendu pour la veine supplémentaire additionnelle.

VCSG associée : Comme nous l'avons démontré, lorsque la veine cave supérieure gauche (VCSG) est présente, le diamètre de la SVC droite est beaucoup plus petit dans sa partie supérieure que dans la région cavo-auriculaire. Dans de tels cas, un stent hautement conformable devrait être utilisé pour la correction, car il devra être impacté à petit diamètre dans la portion haute de la VCS, tout en s'élargissant à la base plus large afin d'éviter un shunt résiduel.

<u>Perspectives liées à la cohorte 3D</u>

En construisant une base de données 3D significative des CIA-SV, nous programmons de réaliser des corrections virtuelles de CIA sinus venosus sur nos jumeaux numériques, en testant différents stents pour évaluer les challenges et la faisabilité du traitement endovasculaire en fonction de l'anatomie et du stent utilisé. Cela aidera à déterminer les taux de succès attendus des différents dispositifs en fonction de chaque type anatomique rencontré.

Concernant la sélection des patients pour la correction percutanée, nous suggérons que l'âge minimum pour envisager cette procédure doit probablement réduit à 15 années, car nos mesures 3D montrent que la croissance de la VCS se stabilise en diamètre autour de cet âge.

<u>Limites</u>

Une limite à notre étude anatomique est que la modélisation 3D par segmentation semi-automatique est chronophage et peu accessible aux non-initiés. De plus, ces

outils nécessitent une expertise en cardiopathies congénitales pour être utilisés de manière efficace. D'autre part, l'alternative de l'analyse 2D ou les processus de segmentation automatique peuvent manquer de précision et ne sont pas entièrement adaptés à la pratique clinique.

II. Simuvenosus

La mise en place d'un programme de simulation globale de correction percutanée a été un long chemin. Partis d'un modèle imprimé opaque permettant une implantation à la main du stent lui-même cousu artisanalement pour le rendre étanche sur sa couverture, nous sommes parvenus à un banc d'essai quasiment complet intégrant tous les outils de guidage et monitoring semblables à ceux présents en salle de cathétérisme interventionnel aujourd'hui.

Si l'on souhaite être exhaustif, peut-être ne maquerait il maintenant plus qu'une reproductibilité exacte des conditions de charge et de pression, permettant de monitorer les variations de pressions avant ou après un obstacle éventuel, risque notoire de l'intervention testée, toutefois aisément diagnostiqué sur le cone-beam post-test.

Le banc d'essai est maintenant familier à l'équipe de l'hôpital et permet de tester les interventions pour les médecins moins expérimentés dans la correction percutanée des CIA sinus venosus.

Son coût reste conséquent car il implique un nombre non négligeable de personnes (technicien de salle, nettoyage, ingénieur, médecin) et des consommables (modèle imprimé, circuit de tubing, stent, sondes, ballons etc.) dont certains ne peuvent être réutilisés à l'infini.

Sa permanence repose donc maintenant sur un pivot concernant son utilisation car il ne devrait être maintenant utilisé par notre équipe, qui a acquis son expérience, que pour les cas complexes avec des formes anatomiques borderline de CIA sinus venosus.

Pour les formes simples, il devra pouvoir être loué à d'autres praticiens ou hôpitaux souhaitant initier un programme de correction percutanée des CIA sinus venosus, dans le but de les familiariser avec la technique, de les réassurer dans la démarche procédurale, et de pouvoir évaluer leur intervention sur un modèle imprimé avant de se lancer dans la vraie vie. Il permettra à ces équipes secondairement de progresser

dans leur pratique avec une montée en puissance quand à la complexité des cas à tester et simuler.
Le banc pourra être aussi adapté pour accueillir d'autres pathologies cardiaques où un traitement novateur endovasculaire est possible, comme par exemple les autres communications inter-atriales, les valvulations pulmonaires percutanées, les embolisations de fistule ou les fermetures d'auricule.
Il pourrait enfin servir à l'industrie pour permettre le développement de nouveaux stents visant à corriger les CIA sinus venosus, dans le cadre d'un partenariat commercial, comme l'a fait Andratec, afin de tester leurs matériaux, évaluer leur forces et faiblesses, dans des conditions proches de celles du réelles, chose semblant être le feedback le plus efficace concernant les problématiques d'ingénierie spécifiques pouvant être rencontrées.

Les limites identifiées du banc d'essai sont l'observation de facteurs non contrôlables dans le processus de création du modèle. La distensibilité du tissu cave et atrial est difficile à prévoir car varie probablement selon les personnes sans que cela ne soit ni évaluable ni quantifiable. Cette distensibilité semble varier de manière intra-individuelle en fonction de l'âge, qui quand il est avancé, entraine une perte d'élasticité du tissu, entrainant sa plus grande distensibilité, impression confirmée par les chirurgiens de notre équipe sur le sujet précis des CIA sinus venosus.
L'hémodynamique, la précharge et l'état d'hydratation du patient, semblent également être des facteurs influant les dimensions (diamètres surtout) de la région anatomique étudiée à partir des examens scannographiques. Ces facteurs sont peu contrôlables dans la pratique quotidienne.
Les tests de sizing au ballon de la veine cave supérieure au cours de la procédure in-vivo doivent donc rester indispensables, du fait de ce degré d'incertitude des procédures réalisées sur banc d'essai.

III. Optivenosus

2ème phase de l'étude : 30 corrections percutanées supplémentaires

En Septembre 2024, l'agence nationale de sécurité du médicament (ANSM) a donné son accord pour la prolongation de l'étude Optivenosus qui est entrée dans sa phase 2, permettant à 30 patients supplémentaires par bras, d'être inclus. Les critères de sélection pour le bras percutané ont été allégés car le fait d'être récusé pour la

chirurgie ne devient plus un critère obligatoire pour être inclus dans le bras percutané. Ainsi, des patients bien portants sans comorbidités pourront être inclus dans le groupe cathétérisme à condition que la correction percutanée soit évaluée « facilement » faisable (forme verte).

Poursuite du proctoring de nouveaux centres

Prochainement, notre équipe se rendra à Padoue en Italie afin d'accompagner les Drs Castaldi et Sirico dans leurs premières corrections percutanées de CIA sinus venosus. Un support préopératoire par modélisation 3D et simulation virtuelle, ainsi que per-opératoire au cours de l'intervention, leur sera fourni.

Eurovenosus

Projet d'extension européenne de l'étude française Optivenosus, avec traduction des eCRF en anglais, organisation de RCP internationales, et comité de pilotage également international.

Dépôt de dossier de PRME (projet de recherche médico-économique)

Suite logique et naturelle d'Optivenosus, son objectif est de poursuivre l'évaluation de la nouvelle technique par le biais de critères médicaux et économiques, comme par exemple la réduction des complications postopératoires, l'amélioration de la qualité de vie et la réduction de la durée d'hospitalisation, sans perte d'efficacité en comparaison avec le gold-standard chirurgical.

Ce projet se fera via un essai randomisé ouvert multicentrique impliquant les centres Français experts en cardiopathies congénitales complexes du réseau maladies rares M3C.

Les critères de jugement associent au critère médico-économique, des critères cliniques incluant l'efficacité, la sécurité, la capacité fonctionnelle et la qualité de vie, et des critères sur les conséquences hospitalières des stratégies, durée de séjour totale, et durée de séjour en réanimation.

L'essai tentera d'apporter des preuves solides pour redéfinir l'algorithme de traitement de la CIA-SV. Ses résultats seront déterminants pour les recommandations internationales et l'amélioration de la prise en charge des patients.

Il participera également au processus de marquage CE des nouveaux dispositifs médicaux relatifs à cette technique, notamment les stents Optimus XXL de Andratec.

IV. Perspectives associées

Co-encadrement de thèse

Inscription en thèse de science à partir de 2024 d'un nouveau doctorant dont le co-encadrement au cours de son master 2 a été effectué pendant ce travail de thèse.

Grégoire Albenque : innovations thérapeutiques dans le traitement des communications inter-atriales (IFTA U999)

Projet Malic

MALIC (Marie Lannelongue Innovation Center) est une plateforme nouvellement créée au sein de l'hôpital Marie Lannelongue, qui vise à proposer des services d'accompagnement pour la conception, le développement et l'évaluation de nouveaux dispositifs médicaux.

Véritable « Tiers-lieux d'expérimentation médecins-ingénieurs », il sera ouvert aux acteurs clé de la filière : start-up, PME et industriels, mais également médecins et chirurgiens des hôpitaux du territoire de l'Université Paris-Saclay. Le projet MALIC capitalise sur l'expérience de l'Hôpital Marie Lannelongue qui, depuis sa création, a développé un savoir-faire dans le développement d'outils et concepts chirurgicaux innovants dans le domaine des pathologies coeur-poumon-vaisseaux de l'enfant à l'adulte. Avec le support de la SATT Paris-Saclay et CentraleSupélec, MALIC est l'opportunité de consolider cette expertise existante et reconnue, et de la déployer plus largement auprès des acteurs de la filière de la Région Île-de-France.

CONCLUSIONS

Ce travail de thèse a rempli les 3 objectifs qu'il s'était fixé à son commencement.

L'analyse anatomique approfondie en 3 dimensions d'une cohorte significative de patients devrait améliorer la description et classification de cette maladie singulière. Elle devrait également servir à envisager la correction percutanée de manière ciblée et adaptée aux challenges anatomiques spécifiques, propres à chaque patient.

Le programme de simulation de correction percutanée des CIA sinus venosus a été mis en place, développé et amélioré au cours de cette thèse. Il a servi de référence dans le lancement de l'étude Française Optivenosus concernant la sélection préopératoire des patients, et dans la confirmation de leur éligibilité à la nouvelle thérapeutique.

L'aide à la mise en place et au lancement de l'étude clinique thérapeutique prospective Optivenosus et la participation du doctorant en tant qu'investigateur pour l'Hôpital Marie Lannelongue à cette étude a permis de traiter à date, 30 patients avec la solution percutanée innovante. L'étude se poursuit et les prochaines publications porteront seront les résultats de cette étude.

Ce travail de thèse a participé de manière pragmatique et novatrice, à une progression globale dans la compréhension et le traitement percutané des CIA sinus venosus.
Les perspectives concernant cette pathologie et son traitement endovasculaire sont prometteuses, avec entre autres, l'ouverture de l'étude Optivenosus au niveau européen, la développement de nouveaux stents dédiés (qui pourront être eux aussi testés sur banc d'essai), et l'élargissement des indication via l'augmentation des cas étiquetés faisables.

A titre personnel, les perspectives du doctorant concernant les futurs encadrements de projets de recherche liées aux cardiopathies congénitales à l'Hôpital Marie Lannelongue, sont aussi stimulantes que réjouissantes.

LETTER TO THE EDITOR 2 : Treatment of sinus venosus defects : time to tune **(editorial publié dans International Journal of Cardiology, décembre 2023)**

S Hascoet, R Roussin, C Batteux

International Journal of Cardiology 399 (2024) 131630

Contents lists available at ScienceDirect

International Journal of Cardiology

journal homepage: www.elsevier.com/locate/ijcard

Editorial

Treatment of sinus venosus defect: Time to tune

Transcatheter therapy of congenital heart disease has seen major advances over the last 40 years with the development of prostheses for cardiac shunts occlusion, followed by the development of stents, particularly valved stents for transcatheter pulmonary valve replacement. More recently, transcatheter correction of sinus venosus defect (SVD) has emerged, taking minimally invasive treatment options for congenital heart disease to a new level.

SVD is a combination of an interatrial communication and an anomalous pulmonary venous return, usually in the superior vena cava (SVC) and rarely in the inferior vena cava. [1] Surgical correction is the gold-standard treatment, using a single patch, a double patch or a caval division technique (Warden procedure). Transcatheter correction seemed conceptually highly challenging but it has benefited from a three-dimensional understanding of the anatomical relationships between the anomalous pulmonary venous return, the SVC and the defect. [2–4] Transcatheter correction has been developed consisting of implanting a long and large tailored covered stent in the SVC, which does not occlude the defect but rather channels the anomalous pulmonary venous return flow posteriorly to the left atrium through the defect. The stent is then widened at the cavo-atrial junction to avoid a residual shunt. Following the first implantations, transcatheter SVD correction is being developed worldwide and more than 380 cases are currently being analysed in an international registry. [3,5–9]

Comparing the results of this new technique with the reference method is needed. [10] While the transcatheter technique, like all minimally invasive procedures, has the potential to allow a fast recovery, the result must be comparable to those of the surgical method and sustainable over time. In fact, potential adverse events have been identified with the transcatheter method: instability and embolization of the stent with the need for surgical conversion, stenosis of the pulmonary venous channel, stent thrombosis, SVC lesion, sinus node dysfunction and residual shunt. [6,11–13]

It is in this context that the study by Muroke and his colleagues is interesting. [14] They assessed long-term outcomes after surgical correction of SVD in a Finnish nationwide register-based cohort study including 182 patients with a majority of children (77.5%) compared to 593 age-matched controls. The median follow-up was of 18.2 years. First, no surgery-related death was reported, reminding us that surgical SVD correction is at low-risk. [15,16] However SVD patients had an elevated risk for new-onset atrial fibrillation, heart failure, ischemic heart disease, migraine, sick sinus syndrome, atrio-ventricular block or pacemaker implantation. However, there is little data provided about surgical technique to identify its influence on long-term morbidity. [15–21]

Patients with new onset atrial fibrillation were older at surgery (40.8 years versus 18.0 years) reminding us that SVD should be corrected during childhood to prevent irreversible atrial remodelling. However, when atrial fibrillation is diagnosed before SVD correction, ablation should be performed first. [22] This is particularly the case when transcatheter SVD correction is indicated since the stent may prevent from doing an efficient ablation of a trigger coming from the anomalous pulmonary venous return. If the incidence of new onset atrial fibrillation will be lower with transcatheter SVD correction is unclear. Irreversible atrial remodelling may already occur prior to correction. On the other hand, surgical SVD correction with atrial scars, can also lead to complex re-entrant atrial tachycardia that may not be seen with the transcatheter approach. This risk seems higher with the double patch surgical technique compared to single-patch or modified warden techniques. [20]

In this study, surgical correction was mainly performed in children. To date transcatheter is mainly indicated in adults or older children. Indeed, there is currently no stent with the ability to enlarge with children growth and recurrent stent dilation would be needed in that case. However, some anatomical studies suggest that by the age of 6, the diameter of the SVC can be of adult size. One may expect that in future, transcatheter procedure will be offered in selected children. [23]

On the other hand, the under-representation of adults in this study may be related to a conservative approach in adults diagnosed lately, in agreement with European guidelines suggesting that conservative approach is an alternative option to surgery. [24] This is exactly where the transcatheter option offers its major interest to date. Similarly to transcatheter ostium secundum atrial septal defect closure performed lately, transcatheter SVD correction is associated with a significant improvement of symptoms and hemodynamic.

In this study, a higher incidence of pace-maker and sick sinus syndrome was reported following surgical SVD correction compared to general population. [20] A 2%–8.6% rate of sinus node dysfunction has been reported in a meta-analysis. [20] Sick sinus syndrome may be related to the position of right atriotomy and meticulous attention should be paid to the incision position, considering the sino-atrial nodal artery position. [18,25] To date, one case of sick sinus syndrome has been reported after transcatheter SVD correction. [12]

Unfortunately, there is no data reported in this study on the incidence of reintervention, obstruction of the SVC and obstruction of the pulmonary venous pathway that are reported after SVD correction in 2.7%–7.7%. [10,15–21]

All these considerations are merely hypothesis and a randomized

DOI of original article: https://doi.org/10.1016/j.ijcard.2023.131433.

https://doi.org/10.1016/j.ijcard.2023.131630
Received 12 November 2023; Received in revised form 26 November 2023; Accepted 29 November 2023
Available online 2 December 2023

control study of transcatheter treatment versus surgery is needed. However, this study design is limited by its poor potential acceptability. This is why so far, we are conducting an open multicentre prospective comparative study with similar preprocedural planning and long-term follow-up (OPTIVENOSUS study, NCT05865119) to further assess the position of transcatheter SVD correction in the therapeutic algorithm.

Disclosures

Sebastien Hascoet is a proctor for Edwards lifesciences, Venus medtech and Abbott vascular. Clement Batteux and Régine Roussin have no relationship to disclose.

CRediT authorship contribution statement

Sebastien Hascoët: Conceptualization, Supervision, Validation, Visualization, Writing – original draft, Writing – review & editing. **Régine Roussin:** Validation, Visualization, Writing – review & editing. **Clément Batteux:** Validation, Visualization, Writing – review & editing.

References

[1] A. Tajouri, C. Batteux, R. Ly, L. Houyel, S. Hascoet, Inferior sinus venosus defect and anomalous hepatic venous return to the coronary sinus leading to an Eisenmenger syndrome, Cardiol. Young (2022), https://doi.org/10.1017/S1047951122001354.

[2] C. Batteux, A. Azarine, C. Karsenty, J. Petit, V. Ciobotaru, P. Brenot, S. Hascoet, Sinus venosus ASDs: imaging and percutaneous closure, Curr. Cardiol. Rep. 23 (2021), https://doi.org/10.1007/s11886-021-01571-7.

[3] C. Batteux, A. Meliani, P. Brenot, S. Hascoet, Multimodality fusion imaging to guide percutaneous sinus venosus atrial septal defect closure, Eur. Heart J. 41 (2020), https://doi.org/10.1093/eurheartj/ehaa292.

[4] G. Butera, F. Sturla, F.R. Pluchinotta, A. Caimi, M. Carminati, Holographic augmented reality and 3D printing for advanced planning of sinus Venosus ASD/partial anomalous pulmonary venous return percutaneous management, JACC Cardiovasc. Interv. 12 (2019) 1389–1391, https://doi.org/10.1016/J.JCIN.2019.03.020.

[5] C. Batteux, V. Ciobotaru, H. Bouvaist, A. Kempny, A. Fraisse, S. Hascoet, Multicenter experience of transcatheter correction of superior sinus venosus defect using the covered Optimus XXL stent, Revista Española de Cardiología (English Edition) 76 (2023) 199–201, https://doi.org/10.1016/j.rec.2022.08.004.

[6] E. Rosenthal, S.A. Qureshi, M. Jones, G. Butera, K. Sivakumar, Y. Boudjemline, Z. M. Hijazi, S. Almaskary, R.D. Ponder, M.M. Salem, K. Walsh, D. Kenny, S. Hascoet, D.P. Berman, J. Thomson, J.J. Vettukattil, E.M. Zahn, Correction of sinus venosus atrial septal defects with the 10 zig covered Cheatham-platinum stent – an international registry, Catheter. Cardiovasc. Interv. 98 (2021), https://doi.org/10.1002/ccd.29750.

[7] J.H. Hansen, P. Duong, S.G.M. Jivanji, M. Jones, S. Kabir, G. Butera, S.A. Qureshi, E. Rosenthal, Transcatheter correction of superior sinus Venosus atrial septal defects as an alternative to surgical treatment, J. Am. Coll. Cardiol. 75 (2020), https://doi.org/10.1016/j.jacc.2019.12.070.

[8] G. Garg, H. Tyagi, A.S. Radha, Transcatheter closure of sinus venosus atrial septal defect with anomalous drainage of right upper pulmonary vein into superior vena cava-an innovative technique, Catheter. Cardiovasc. Interv. 84 (2014) 473–477, https://doi.org/10.1002/ccd.25502.

[9] J. Vettukattil, A. Subramanian, A. Barthur, J. Mahimarangaiah, Transcatheter closure of sinus venosus defect: first-in-human implant of a dedicated self-expanding VB stent system, Catheter. Cardiovasc. Interv. (2023), https://doi.org/10.1002/ccd.30814.

[10] F. Brancato, N. Stephenson, E. Rosenthal, J.H. Hansen, M.I. Jones, S. Qureshi, C. Austin, S. Speggiorin, S. Caner, G. Butera, Transcatheter versus surgical treatment for isolated superior sinus venosus atrial septal defect, Catheter. Cardiovasc. Interv. 101 (2023) 1098–1107, https://doi.org/10.1002/ccd.30650.

[11] R. Yalamanchi, M.C. Sivaprakasam, R.V.R. Janke, K. Chandrasekharan, V. S. Sadhasivam, R. Showkathali, Unanticipated complication of transcatheter correction of superior sinus venosus atrial septal defect, J. Cardiol. Cases 25 (2022), https://doi.org/10.1016/j.jccase.2021.07.005.

[12] J.P. Sandoval, E. Rosenthal, E. Arias, J.A. García-Montes, H. Rodríguez-Zanella, C. Zabal, S. Kabir, S.F. Yong, M. Jones, S. Qureshi, Sinus node dysfunction during transcatheter assessment and stent correction of sinus venosus atrial septal defects, Catheter. Cardiovasc. Interv. 102 (2023) 683–687, https://doi.org/10.1002/ccd.30790.

[13] P. Sagar, P. Thejaswi, K. Sivakumar, A rare unreported complication following transcatheter correction of sinus venosus defect, Ann. Pediatr. Cardiol. 16 (2023) 215–218, https://doi.org/10.4103/apc.apc_41_23.

[14] V. Muroke, M. Jalanko, J. Haukka, V. Anttila, T. Pätilä, J. Sinisalo, Long-term outcome after surgical correction of sinus venosus defect in a nationwide register-based cohort study, Int. J. Cardiol. (2023) 131433, https://doi.org/10.1016/j.ijcard.2023.131433.

[15] R.D. Stewart, F. Bailliard, A.M. Kelle, C.L. Backer, L. Young, C. Mavroudis, Evolving surgical strategy for sinus venosus atrial septal defect: effect on sinus node function and late venous obstruction, Ann. Thorac. Surg. 84 (2007) 1651–1655, https://doi.org/10.1016/j.athoracsur.2007.04.130.

[16] C.H. Attenhofer Jost, H.M. Connolly, G.K. Danielson, K.R. Bailey, H.V. Schaff, W.-K. Shen, C.A. Warnes, J.B. Seward, F.J. Puga, A.J. Tajik, Sinus Venosus atrial septal defect: : long-term postoperative outcome for 115 patients, Circulation. 112 (2005) 1953–1958, https://doi.org/10.1161/CIRCULATIONAHA.104.493775.

[17] S.M. Said, H.M. Burkhart, J.A. Dearani, B. Eidem, P. Stensrud, S.D. Phillips, H. V. Schaff, Outcome of caval division techniques for partial anomalous pulmonary venous connections to the superior vena cava, Ann. Thorac. Surg. 92 (2011) 980–985, https://doi.org/10.1016/j.athoracsur.2011.04.110.

[18] L. Ait-Ali, A. Ravaglioli, P. Festa, A. Tamburrini, C. Marrone, M. Cuman, C. Farnetani, V. Pak, M. Chiavarelli, D. Federici, The different surgical impact of the superior cavoatrial incision in children and adults, Cardiol. Young 31 (2021) 751–755, https://doi.org/10.1017/S1047951120004540.

[19] A.P. Iyer, K. Somanrema, S. Pathak, P.Y. Manjunath, S. Pradhan, S. Krishnan, Comparative study of single- and double-patch techniques for sinus venosus atrial septal defect with partial anomalous pulmonary venous connection, J. Thorac. Cardiovasc. Surg. 133 (2007) 656–659, https://doi.org/10.1016/j.jtcvs.2006.08.076.

[20] K.E. Okonta, M. Sanusi, Superior sinus Venosus atrial septal defect: overview of surgical options, open journal of thoracic, Surgery. 03 (2013) 114–122, https://doi.org/10.4236/ojts.2013.34024.

[21] H. Lin, J. Yan, Q. Wang, S. Li, H. Sun, Y. Zhang, L. Zhang, W. Liu, Outcomes of the Warden procedure for partial anomalous pulmonary venous drainage, Pediatr. Cardiol. 41 (2020) 134–140, https://doi.org/10.1007/s00246-019-02235-8.

[22] J.A. Milstein, D. Beer, J. Thomson, A. Cedars, K. Konstantinidis, Atrial fibrillation ablation in a patient with SV ASD and PAPVR preceding transcatheter septal closure, JACC Case Rep. 15 (2023) 101862, https://doi.org/10.1016/J.JACCAS.2023.101862.

[23] K. Sivakumar, S. Qureshi, S. Pavithran, S. Vaidyanathan, M. Rajendran, Simple diagnostic tools may guide transcatheter closure of superior sinus venosus defects without advanced imaging techniques, Circ. Cardiovasc. Interv. 13 (2020), https://doi.org/10.1161/CIRCINTERVENTIONS.120.009833.

[24] H. Baumgartner, J. De Backer, S.V. Babu-Narayan, W. Budts, M. Chessa, G.P. Diller, B. Lung, J. Kluin, I.M. Lang, F. Meijboom, P. Moons, B.J.M. Mulder, E. Oechslin, J. W. Roos-Hesselink, M. Schwerzmann, L. Sondergaard, K. Zeppenfeld, E.S.C.S.D. Group, 2020 ESC Guidelines for the management of adult congenital heart disease, Eur. Heart J. 42 (2021) 563–645, https://doi.org/10.1093/eurheartj/ehaa554.

[25] J. Vikse, B.M. Henry, J. Roy, P.K. Ramakrishnan, W.C. Hsieh, J.A. Walocha, K. A. Tomaszewski, Anatomical variations in the sinoatrial nodal artery: a meta-analysis and clinical considerations, PLoS One 11 (2016) e0148331, https://doi.org/10.1371/journal.pone.0148331.

Sebastien Hascoët[a,b,*], Régine Roussin[a], Clément Batteux[a,b,*]

[a] *Hôpital Marie Lannelongue, Groupe Hospitalier Paris Saint Joseph, Faculté de médecine, Université Paris-Saclay, BME laboratory, 133 avenue de la résistance, 92350 Le Plessis Robinson, France*

[b] *Inserm UMR-S 999, Marie Lannelongue hospital, Paris-Saclay university, 92350 Le Plessis Robinson, France*

[*] Corresponding authors at: Hôpital Marie Lannelongue, Groupe Hospitalier Paris Saint Joseph, Faculté de médecine, Université Paris-Saclay, BME laboratory, 133 avenue de la résistance, 92350 Le Plessis Robinson, France.

E-mail address: s.hascoet@hml.fr (S. Hascoët).

REFERENCES BIBLIOGRAPHIQUES

1. Botto LD, Correa A, Erickson JD. Racial and temporal variations in the prevalence of heart defects. Pediatrics 2001;107(3):E32.
2. Maury P, Gandjbakhch E, Baruteau AE, Bessiere F, Kyndt F, Bouvagnet P, Rollin A, Bonnet D, Probst V, Maltret A. Cardiac Phenotype and Long-Term Follow-Up of Patients With Mutations in NKX2-5 Gene. J Am Coll Cardiol 2016;68(21):2389-2390.
3. Caputo S, Capozzi G, Russo MG, Esposito T, Martina L, Cardaropoli D, Ricci C, Argiento P, Pacileo G, Calabro R. Familial recurrence of congenital heart disease in patients with ostium secundum atrial septal defect. Eur Heart J 2005;26(20):2179-84.
4. Chen J, Qi B, Zhao J, Liu W, Duan R, Zhang M. A novel mutation of GATA4 (K300T) associated with familial atrial septal defect. Gene 2016;575(2 Pt 2):473-477.
5. Schott JJ, Benson DW, Basson CT, Pease W, Silberbach GM, Moak JP, Maron BJ, Seidman CE, Seidman JG. Congenital heart disease caused by mutations in the transcription factor NKX2-5. Science 1998;281(5373):108-11.
6. Lee SA, Lee SG, Moon HS, Lavulo L, Cho KO, Hyun C. Isolation, characterization and genetic analysis of canine GATA4 gene in a family of Doberman Pinschers with an atrial septal defect. J Genet 2007;86(3):241-7.
7. Hirayama-Yamada K, Kamisago M, Akimoto K, Aotsuka H, Nakamura Y, Tomita H, Furutani M, Imamura S, Takao A, Nakazawa M, Matsuoka R. Phenotypes with GATA4 or NKX2.5 mutations in familial atrial septal defect. Am J Med Genet A 2005;135(1):47-52.
8. Ching YH, Ghosh TK, Cross SJ, Packham EA, Honeyman L, Loughna S, Robinson TE, Dearlove AM, Ribas G, Bonser AJ, Thomas NR, Scotter AJ, Caves LS, Tyrrell GP, Newbury-Ecob RA, Munnich A, Bonnet D, Brook JD. Mutation in myosin heavy chain 6 causes atrial septal defect. Nat Genet 2005;37(4):423-8.
9. Okubo A, Miyoshi O, Baba K, Takagi M, Tsukamoto K, Kinoshita A, Yoshiura K, Kishino T, Ohta T, Niikawa N, Matsumoto N. A novel GATA4 mutation completely segregated with atrial septal defect in a large Japanese family. J Med Genet 2004;41(7):e97.
10. Elliott DA, Kirk EP, Yeoh T, Chandar S, McKenzie F, Taylor P, Grossfeld P, Fatkin D, Jones O, Hayes P, Feneley M, Harvey RP. Cardiac homeobox gene NKX2-5 mutations and congenital heart disease: associations with atrial septal defect and hypoplastic left heart syndrome. J Am Coll Cardiol 2003;41(11):2072-6.
11. Hamanoue H, Rahayuningsih SE, Hirahara Y, Itoh J, Yokoyama U, Mizuguchi T, Saitsu H, Miyake N, Hirahara F, Matsumoto N. Genetic screening of 104 patients with congenitally malformed hearts revealed a fresh mutation of GATA4 in those with atrial septal defects. Cardiol Young 2009;19(5):482-5.
12. Holt M, Oram S. Familial heart disease with skeletal malformations. Br Heart J 1960;22:236-42.
13. Correa A, Gilboa SM, Besser LM, Botto LD, Moore CA, Hobbs CA, Cleves MA, Riehle-Colarusso TJ, Waller DK, Reece EA. Diabetes mellitus and birth defects. Am J Obstet Gynecol 2008;199(3):237 e1-9.

14. Parker SE, Werler MM, Shaw GM, Anderka M, Yazdy MM, National Birth Defects Prevention S. Dietary glycemic index and the risk of birth defects. Am J Epidemiol 2012;176(12):1110-20.
15. Miller A, Riehle-Colarusso T, Siffel C, Frias JL, Correa A. Maternal age and prevalence of isolated congenital heart defects in an urban area of the United States. Am J Med Genet A 2011;155A(9):2137-45.
16. Reefhuis J, Honein MA, Schieve LA, Correa A, Hobbs CA, Rasmussen SA, National Birth Defects Prevention S. Assisted reproductive technology and major structural birth defects in the United States. Hum Reprod 2009;24(2):360-6.
17. Schleich JM, Abdulla T, Summers R, Houyel L. An overview of cardiac morphogenesis. Arch Cardiovasc Dis 2013;106(11):612-23.
18. Fuse S, Tomita H, Hatakeyama K, Kubo N, Abe N. Effect of size of a secundum atrial septal defect on shunt volume. Am J Cardiol 2001;88(12):1447-50, A9.
19. Hascoet S, Fournier E, Jais X, Le Gloan L, Dauphin C, Houeijeh A, Godart F, Iriart X, Richard A, Radojevic J, Amedro P, Bosser G, Souletie N, Bernard Y, Moceri P, Bouvaist H, Mauran P, Barre E, Basquin A, Karsenty C, Bonnet D, Iserin L, Sitbon O, Petit J, Fadel E, Humbert M, Ladouceur M. Outcome of adults with Eisenmenger syndrome treated with drugs specific to pulmonary arterial hypertension: A French multicentre study. Arch Cardiovasc Dis 2017;110(5):303-316.
20. Geibel A. Echokardiographische Diagnostik angeborener Herzfehler im Erwachsenenalter [Echocardiographic evaluation in unoperated congenital heart disease in adults]. Herz. 1999 Jun;24(4):276-92. German. doi: 10.1007/BF03043879. PMID: 10444707.
21. Acar P, Saliba Z, Bonhoeffer P, Aggoun Y, Bonnet D, Sidi D, Kachaner J. Influence of atrial septal defect anatomy in patient selection and assessment of closure with the Cardioseal device; a three-dimensional transoesophageal echocardiographic reconstruction. Eur Heart J 2000;21(7):573-81.
22. Hascoet S, Hadeed K, Marchal P, Dulac Y, Alacoque X, Heitz F, Acar P. The relation between atrial septal defect shape, diameter, and area using three-dimensional transoesophageal echocardiography and balloon sizing during percutaneous closure in children. Eur Heart J Cardiovasc Imaging 2015;16(7):747-55.
23. Hanslik A, Pospisil U, Salzer-Muhar U, Greber-Platzer S, Male C. Predictors of spontaneous closure of isolated secundum atrial septal defect in children: a longitudinal study. Pediatrics 2006;118(4):1560-5.
24. Helgason H, Jonsdottir G. Spontaneous closure of atrial septal defects. Pediatr Cardiol 1999;20(3):195-9.
25. McMahon CJ, Feltes TF, Fraley JK, Bricker JT, Grifka RG, Tortoriello TA, Blake R, Bezold LI. Natural history of growth of secundum atrial septal defects and implications for transcatheter closure. Heart 2002;87(3):256-9.
26. Blom NA, Gittenberger-de Groot AC, Jongeneel TH, DeRuiter MC, Poelmann RE, Ottenkamp J. Normal development of the pulmonary veins in human embryos and formulation of a morphogenetic concept for sinus venosus defects. Am J Cardiol 2001;87(3):305-9.
27. Batteux C, Meliani A, Brenot P, Hascoet S. Multimodality fusion imaging to guide percutaneous sinus venosus atrial septal defect closure. Eur Heart J 2020.

28. Snarr BS, Liu MY, Zuckerberg JC, Falkensammer CB, Nadaraj S, Burstein D, Ho D, Gardner MA, Butto A, Ewing SG, Pandian NG, Banerjee A. The Parasternal Short-Axis View Improves Diagnostic Accuracy for Inferior Sinus Venosus Type of Atrial Septal Defects by Transthoracic Echocardiography. J Am Soc Echocardiogr 2017;30(3):209-215.
29. Crystal MA, Al Najashi K, Williams WG, Redington AN, Anderson RH. Inferior sinus venosus defect: echocardiographic diagnosis and surgical approach. J Thorac Cardiovasc Surg 2009;137(6):1349-55.
30. Cossor W, Addetia K, Balkhy HH, Spencer KT, Patel AR. Unroofed coronary sinus atrial septal defect: a multi-modality imaging approach. Eur Heart J Cardiovasc Imaging 2015;16(11):1263.
31. Santoro G, Gaio G, Russo MG. Transcatheter treatment of unroofed coronary sinus. Catheter Cardiovasc Interv 2013;81(5):849-52.
32. Torres A, Gersony WM, Hellenbrand W. Closure of unroofed coronary sinus with a covered stent in a symptomatic infant. Catheter Cardiovasc Interv 2007;70(5):745-8.
33. Berger F, Vogel M, Kramer A, Alexi-Meskishvili V, Weng Y, Lange PE, Hetzer R. Incidence of atrial flutter/fibrillation in adults with atrial septal defect before and after surgery. Ann Thorac Surg 1999;68(1):75-8.
34. Teuwen CP, Ramdjan TT, Götte M, Brundel BJ, Evertz R, Vriend JW, Molhoek SG, Dorman HG, van Opstal JM, Konings TC, van der Voort P, Delacretaz E, Houck C, Yaksh A, Jansz LJ, Witsenburg M, Roos-Hesselink JW, Triedman JK, Bogers AJ, de Groot NM. Time Course of Atrial Fibrillation in Patients With Congenital Heart Defects. Circ Arrhythm Electrophysiol. 2015 Oct;8(5):1065-72. doi: 10.1161/CIRCEP.115.003272. Epub 2015 Aug 14. PMID: 26276884.
35. O'Neill L, Floyd CN, Sim I, Whitaker J, Mukherjee R, O'Hare D, Gatzoulis M, Frigiola A, O'Neill MD, Williams SE. Percutaneous secundum atrial septal defect closure for the treatment of atrial arrhythmia in the adult: A meta-analysis. Int J Cardiol 2020.
36. Fujii Y, Akagi T, Nakagawa K, Takaya Y, Eto K, Kuroko Y, Kotani Y, Ejiri K, Ito H, Kasahara S. Clinical impact of transcatheter atrial septal defect closure on new onset atrial fibrillation in adult patients: Comparison with surgical closure. J Cardiol. 2020 Jul;76(1):94-99.
37. Garg J, Shah K, Turagam MK, Janagam P, Natale A, Lakkireddy D. Safety and efficacy of catheter ablation for atrial fibrillation in patients with percutaneous atrial septal closure device: Electrophysiology Collaborative Consortium for Meta-analysis-ELECTRAM Investigators. J Cardiovasc Electrophysiol 2020.
38. Combes N, Derval N, Hascoët S, Zhao A, Amet D, Le Bloa M, Maltret A, Heitz F, Thambo JB, Marijon E. Ablation of supraventricular arrhythmias in adult congenital heart disease: A contemporary review. Arch Cardiovasc Dis. 2017 May;110(5):334-345. doi: 10.1016/j.acvd.2017.01.007. Epub 2017 Mar 27. PMID: 28359691.
39. Wasmer K, Köbe J, Dechering DG, Bittner A, Mönnig G, Milberg P, Baumgartner H, Breithardt G, Eckardt L. Isthmus-dependent right atrial flutter as the leading cause of atrial tachycardias after surgical atrial septal defect repair. Int J Cardiol. 2013 Oct 3;168(3):2447-52.
40. Houck CA, Lanters EAH, Heida A, Taverne YJHJ, van de Woestijne PC, Knops P, Roos-Serote MC, Roos-Hesselink JW, Bogers AJJC, de Groot NMS. Distribution of Conduction Disorders in Patients With Congenital Heart Disease

and Right Atrial Volume Overload. JACC Clin Electrophysiol. 2020 May;6(5):537-548.
41. Dallaglio PD, Anguera I, Jiménez-Candil J, Peinado R, García-Seara J, Arcocha MF, Macías R, Herreros B, Quesada A, Hernández-Madrid A, Alvarez M, Di Marco A, Filgueiras D, Matía R, Cequier A, Sabaté X. Impact of previous cardiac surgery on long-term outcome of cavotricuspid isthmus-dependent atrial flutter ablation. Europace. 2016 Jun;18(6):873-80.
42. Jalal Z, Hascoet S, Baruteau AE, Iriart X, Kreitmann B, Boudjemline Y, Thambo JB. Long-term Complications After Transcatheter Atrial Septal Defect Closure: A Review of the Medical Literature. Can J Cardiol 2016;32(11):1315 e11-1315 e18.
43. Sachweh JS, Daebritz SH, Hermanns B, Fausten B, Jockenhoevel S, Handt S, Messmer BJ. Hypertensive pulmonary vascular disease in adults with secundum or sinus venosus atrial septal defect. Ann Thorac Surg 2006;81(1):207-13.
44. Vogel M, Berger F, Kramer A, Alexi-Meshkishvili V, Lange PE. Incidence of secondary pulmonary hypertension in adults with atrial septal or sinus venosus defects. Heart 1999;82(1):30-3.
45. Goetschmann S, Dibernardo S, Steinmann H, Pavlovic M, Sekarski N, Pfammatter JP. Frequency of severe pulmonary hypertension complicating "isolated" atrial septal defect in infancy. Am J Cardiol 2008;102(3):340-2.
46. Smilowitz NR, Subashchandran V, Berger JS. Atrial Septal Defect and the Risk of Ischemic Stroke in the Perioperative Period of Noncardiac Surgery. Am J Cardiol. 2019 Oct 1;124(7):1120-1124.
47. Lena T, Amabile A, Morrison A, Torregrossa G, Geirsson A, Tesler UF. John H. Gibbon and the development of the heart-lung machine: The beginnings of open cardiac surgery. J Card Surg. 2022 Dec;37(12):4199-4201
48. King TD, Thompson SL, Steiner C, Mills NL. Secundum atrial septal defect. Nonoperative closure during cardiac catheterization. JAMA. 1976 Jun 7;235(23):2506-9. PMID: 946659.
49. Butera G, Carminati M, Chessa M, Youssef R, Drago M, Giamberti A, Pomè G, Bossone E, Frigiola A. Percutaneous versus surgical closure of secundum atrial septal defect: comparison of early results and complications. Am Heart J. 2006 Jan;151(1):228-34.
50. Masura J, Gavora P, Podnar T. Long-term outcome of transcatheter secundum-type atrial septal defect closure using Amplatzer septal occluders. J Am Coll Cardiol. 2005 Feb 15;45(4):505-7. doi: 10.1016/j.jacc.2004.10.066.
51. Brida M, Chessa M, Celermajer D, Li W, Geva T, Khairy P, Griselli M, Baumgartner H, Gatzoulis MA. Atrial septal defect in adulthood: a new paradigm for congenital heart disease. Eur Heart J. 2022 Jul 21;43(28):2660-2671.
52. Zwijnenburg RD, Baggen VJM, Witsenburg M, Boersma E, Roos-Hesselink JW, van den Bosch AE. Risk Factors for Pulmonary Hypertension in Adults After Atrial Septal Defect Closure. Am J Cardiol. 2019 Apr 15;123(8):1336-1342.
53. Takaya Y, Akagi T, Sakamoto I, Kanazawa H, Nakazawa G, Murakami T, Yao A, Nanasato M, Saji M, Hirokami M, Fuku Y, Hosokawa S, Tada N, Matsumoto K, Imai M, Nakagawa K, Ito H. Efficacy of treat-and-repair strategy for atrial septal defect with pulmonary arterial hypertension. Heart. 2022 Mar;108(5):382-387.
54. Gazengel P, Hascoët S, Amsallem M, Savale L, Montani D, Mercier O, Humbert M, Fadel E, Le Pavec J. Double-lung transplantation followed by delayed

percutaneous repair for atrial septal defect-associated pulmonary arterial hypertension. Eur Respir J. 2022 Jan 20;59(1):2102388.
55. Humenberger M, Rosenhek R, Gabriel H, Rader F, Heger M, Klaar U, Binder T, Probst P, Heinze G, Maurer G, Baumgartner H. Benefit of atrial septal defect closure in adults: impact of age. Eur Heart J. 2011 Mar;32(5):553-60.
56. Schwerzmann M, Pfammatter JP. Approaching atrial septal defects in pulmonary hypertension. Expert Rev Cardiovasc Ther. 2015 Jun;13(6):693-701.
57. Kijima Y, Akagi T, Takaya Y, Akagi S, Nakagawa K, Kusano K, Sano S, Ito H. Treat and Repair Strategy in Patients With Atrial Septal Defect and Significant Pulmonary Arterial Hypertension. Circ J. 2016;80(1):227-34.
58. Yong G, Khairy P, De Guise P, Dore A, Marcotte F, Mercier LA, Noble S, Ibrahim R. Pulmonary arterial hypertension in patients with transcatheter closure of secundum atrial septal defects: a longitudinal study. Circ Cardiovasc Interv. 2009 Oct;2(5):455-62.
59. Egidy Assenza G, Krieger EV, Baumgartner H, Cupido B, Dimopoulos K, Louis C, Lubert AM, Stout KK, Valente AM, Zeppenfeld K, Opotowsky AR. AHA/ACC vs ESC Guidelines for Management of Adults With Congenital Heart Disease: JACC Guideline Comparison. J Am Coll Cardiol. 2021 Nov 9;78(19):1904-1918.
60. Stout KK, Daniels CJ, Aboulhosn JA, Bozkurt B, Broberg CS, Colman JM, Crumb SR, Dearani JA, Fuller S, Gurvitz M, Khairy P, Landzberg MJ, Saidi A, Valente AM, Van Hare GF. 2018 AHA/ACC Guideline for the Management of Adults With Congenital Heart Disease: A Report of the American College of Cardiology/American Heart Association Task Force on Clinical Practice Guidelines. Circulation. 2019 Apr 2;139(14):e698-e800.
61. Humbert M, Kovacs G, Hoeper MM, Badagliacca R, Berger RMF, Brida M, Carlsen J, Coats AJS, Escribano-Subias P, Ferrari P, Ferreira DS, Ghofrani HA, Giannakoulas G, Kiely DG, Mayer E, Meszaros G, Nagavci B, Olsson KM, Pepke-Zaba J, Quint JK, Rådegran G, Simonneau G, Sitbon O, Tonia T, Toshner M, Vachiery JL, Vonk Noordegraaf A, Delcroix M, Rosenkranz S; ESC/ERS Scientific Document Group. 2022 ESC/ERS Guidelines for the diagnosis and treatment of pulmonary hypertension. Eur Heart J. 2022 Oct 11;43(38):3618-3731. doi: 10.1093.
62. Landi F, Cipriani L, Cocchi A, Zuccala G, Carbonin P. Ostium secundum atrial septal defect in the elderly. J Am Geriatr Soc. 1991 Jan;39(1):60-3.
63. Peacock TB. Malformations dependent on arrest of development at an early period of fetal life. In: Peacock TB, ed. Malformations of the human heart. London: John Churchill, 1858:24-5.
64. Lewis F J, Taufic M, Vacro R L, Niazi S. The surgical anatomy of atrial septal defects: experiences with repair under direct vision. Ann Surg 1955;142:401-17.
65. Ross D N. The sinus venosus type of atrial septal defect. Guy's Hospital Report 1956;105:376-81.
66. Shaner RF. The high defect in the atrial septum. Can Med Assoc J 1958;78:688-9.
67. Li J, Al Zaghal AM, Anderson RH. The nature of the superior sinus venosus defect. Clin Anat. 1998;11(5):349-52.
68. Van Praagh S, Carrera ME, Sanders SP, Mayer JE, Van Praagh R. Sinus venosus defects: unroofing of the right pulmonary veins--anatomic and

echocardiographic findings and surgical treatment. Am Heart J. 1994 Aug;128(2):365-79.
69. al Zaghal AM, Li J, Anderson RH, Lincoln C, Shore D, Rigby ML. Anatomical criteria for the diagnosis of sinus venosus defects. Heart. 1997 Sep;78(3):298-304. doi: 10.1136/hrt.78.3.298. PMID: 9391294.
70. Anderson RH, Ettedgui JA, Devine WA. Sinus venosus defect. Am Heart J. 1995 Jun;129(6):1229-32. doi: 10.1016/0002-8703(95)90423-9. PMID: 7754966.
71. Relan J, Gupta SK, Rajagopal R, Ramakrishnan S, Gulati GS, Kothari SS, Saxena A, Sharma S, Rajashekar P, Anderson RH. Clarifying the anatomy of the superior sinus venosus defect. Heart. 2022 May;108(9):689-694. doi: 10.1136/heartjnl-2021-319334.
72. Chowdhury UK, Anderson RH, Pandey NN, Sharma S, Sankhyan LK, George N, Goja S, Arvind B. A reappraisal of the sinus venosus defect. Eur J Cardiothorac Surg. 2022 May 27;61(6):1211-1222. doi: 10.1093/ejcts/ezab556. PMID: 35090016.
73. Hansen JH, Duong P, Jivanji SGM, Jones M, Kabir S, Butera G, Qureshi SA, Rosenthal E. Transcatheter Correction of Superior Sinus Venosus Atrial Septal Defects as an Alternative to Surgical Treatment. J Am Coll Cardiol. 2020 Mar 24;75(11):1266-1278. doi: 10.1016/j.jacc.2019.12.070. PMID: 32192652.
74. Batteux C, Azarine A, Karsenty C, Petit J, Ciobotaru V, Brenot P, Hascoet S. Sinus Venosus ASDs: Imaging and Percutaneous Closure. Curr Cardiol Rep. 2021 Aug 19;23(10):138. doi: 10.1007/s11886-021-01571-7. PMID: 34410510.
75. Kirklin JW, Ellis FH, Wood EH. Treatment of anomalous pulmonary venous connections in association with interatrial communications. Surgery 1956;39:389-98.
76. Schuster SR, Gross RE, Colodny AH. Surgical management of anomalous right pulmonary venous drainage to the superior vena cava, associated with superior marginal defect of the atria1 septum. Surgery 1962;51:805-8.
77. Laboux L, Bouhour JB, Dupon H, Cornet E. Retours veineux anormaux. Arch Mal Coeur 1968;61:1035–42.
78. Enjalbert A, Calazel P, Eschapasse H. Un unequivalent du type cave superieur des communications interauriculaires: retour veineux pulmonaire anormal droit associe a un gros vaisseau unissant la veine cave superieure a loreillette gauche. Ann Chir Thorac Cardiovasc 1967;6: 785–90.
79. Warden HE, Gustafson RA, Tarnay TJ, Neal WA. An alternative method for repair of partial anomalous pulmonary venous connection to the superior vena cava. Ann Thorac Surg 1984;38:601-5.
80. Muroke V, Jalanko M, Haukka J, Anttila V, Pätilä T, Sinisalo J. Long-term outcome after surgical correction of sinus venosus defect in a nationwide register-based cohort study. Int J Cardiol. 2024 Jan 15;395:131433. doi: 10.1016/j.ijcard.2023.131433. Epub 2023 Oct 11. PMID: 37827284.
81. Abdullah HAM, Alsalkhi HA, Khalid KA. Transcatheter closure of sinus venosus atrial septal defect with anomalous pulmonary venous drainage: Innovative technique with long-term follow-up. Catheter Cardiovasc Interv. 2020 Mar 1;95(4):743-747. doi: 10.1002/ccd.28364. Epub 2019 Jun 14. PMID: 31197932.
82. Garg G, Tyagi H, Radha AS. Transcatheter closure of sinus venosus atrial septal defect with anomalous drainage of right upper pulmonary vein into superior vena cava--an innovative technique. Catheter Cardiovasc Interv. 2014

Sep 1;84(3):473-7. doi: 10.1002/ccd.25502. Epub 2014 Apr 23. PMID: 24753393.
83. Rosenthal E, Qureshi SA, Jones M, Butera G, Sivakumar K, Boudjemline Y, Hijazi ZM, Almaskary S, Ponder RD, Salem MM, Walsh K, Kenny D, Hascoet S, Berman DP, Thomson J, Vettukattil JJ, Zahn EM. Correction of sinus venosus atrial septal defects with the 10 zig covered Cheatham-platinum stent - An international registry. Catheter Cardiovasc Interv. 2021 Jul 1;98(1):128-136. doi: 10.1002/ccd.29750. Epub 2021 May 7. PMID: 33909945.
84. Sandoval JP, Rosenthal E, Arias E, García-Montes JA, Rodríguez-Zanella H, Zabal C, Kabir S, Yong SF, Jones M, Qureshi S. Sinus node dysfunction during transcatheter assessment and stent correction of sinus venosus atrial septal defects. Catheter Cardiovasc Interv. 2023 Oct;102(4):683-687. doi: 10.1002/ccd.30790. Epub 2023 Jul 28. PMID: 37506123.
85. Sivakumar K. How to do it? Transcatheter correction of superior sinus venosus defects. Ann Pediatr Cardiol. 2022 Mar-Apr;15(2):169-174. doi: 10.4103/apc.apc_92_21. Epub 2022 Aug 19. PMID: 36246755; PMCID: PMC9564414.
86. Houck CA, Evertz R, Teuwen CP, Roos-Hesselink JW, Duijnhouwer T, Bogers AJJC, de Groot NMS. Time course and interrelationship of dysrhythmias in patients with surgically repaired atrial septal defect. Heart Rhythm. 2018 Mar;15(3):341-347. doi: 10.1016/j.hrthm.2017.10.020. Epub 2017 Oct 14. PMID: 29038089.
87. Milstein JA, Beer D, Thomson J, Cedars A, Konstantinidis K. Atrial Fibrillation Ablation in a Patient With SV ASD and PAPVR Preceding Transcatheter Septal Closure. JACC Case Rep. 2023 May 1;15:101862. doi: 10.1016/j.jaccas.2023.101862. PMID: 37283841; PMCID: PMC10240272.
88. Kéchichian R, Valette S, Sdika M, Desvignes M. Automatic 3D multiorgan segmentation via clustering and graph cut using spatial relations and hierarchically-registered atlases, MICCAI Medical Computer Vision: Algorithms for Big Data, 2014, pp. 201-209.
89. Withey, D. J. & Koles, Z. J. A review of medical image segmentation : methods and available software. International Journal of Bioelectromagnetism, 2008.
90. Kéchichian R, Valette S, Desvignes M, Prost R : Shortest-Path Constraints for 3D Multiobject Semiautomatic Segmentation via Clustering and Graph Cut, IEEE Trans. on Image Processing, vol. 22, no. 11, pp. 4224-4236, 2013.
91. Giehl-Brown E, Dennler S, Garcia SA, Seppelt D, Oehme F, Schweipert J, Weitz J, Riediger C. 3D liver model-based surgical education improves preoperative decision-making and patient satisfaction-a randomized pilot trial. Surg Endosc. 2023 Jun;37(6):4545-4554. doi: 10.1007/s00464-023-09915-w. Epub 2023 Feb 27. PMID: 36849565; PMCID: PMC9970129.
92. Isikay I, Cekic E, Baylarov B, Tunc O, Hanalioglu S. Narrative review of patient-specific 3D visualization and reality technologies in skull base neurosurgery: enhancements in surgical training, planning, and navigation. Front Surg. 2024 Jul 16;11:1427844. doi: 10.3389/fsurg.2024.1427844. PMID: 39081485; PMCID: PMC11287220.
93. Manrique M, Mondragón IF, Flórez-Valencia L, Montoya L, García A, Mera CA, Kuhlmann A, Guillén F, Cortés M, Gutiérrez Gómez ML. Haptic experience to significantly motivate anatomy learning in medical students. BMC Med Educ. 2024 Aug 30;24(1):946. doi: 10.1186/s12909-024-05829-w. PMID: 39215247; PMCID: PMC11363654.

94. Xiong J, Dai X, Zhang Y, Liu X, Zhou X. Augmented reality for basic skills training in laparoscopic surgery: a systematic review and meta-analysis. Surg Endosc. 2024 Nov 12. doi: 10.1007/s00464-024-11387-5. Epub ahead of print. PMID: 39532736.
95. Hou X, Xu RX, Tang J, Yin C. A novel 3D multimodal fusion imaging surgical guidance in microvascular decompression for primary trigeminal neuralgia and hemifacial spasm. Head Face Med. 2024 Oct 10;20(1):56. doi: 10.1186/s13005-024-00442-0. PMID: 39390456; PMCID: PMC11465763.
96. Cheng F, Qiao Z, Zhao L, Pu J. Real-time 3D-3D image fusion of CTA/CBCT roadmap fluoroscopy in the transcatheter mitral intervention. Catheter Cardiovasc Interv. 2024 Jan;103(1):230-233. doi: 10.1002/ccd.30826. Epub 2023 Sep 5. PMID: 37668044.
97. Zendjebil S, d'Angelo L, Doguet F, Dumont N, Benamer H, Fourchy D, Djebbar M, Garot J, Vaillant R, Garot P. Computed Tomography/Fluoroscopy Fusion and 3D Transesophageal Echocardiography-Guided Percutaneous Paravalvular Leak Closure. JACC Case Rep. 2022 Dec 1;5:101690. doi: 10.1016/j.jaccas.2022.101690. PMID: 36636511; PMCID: PMC9830464.
98. Vukicevic M, Mosadegh B, James K. Min et al. Cardiac 3D printing and its future directions. JACC Cardiovasc Imaging 2017, vol 10, No. 2, pp 171 à 184.
99. Batteux C, Haidar MA, Bonnet D. 3D-Printed Models for Surgical Planning in Complex Congenital Heart Diseases: A Systematic Review. Front Pediatr. 2019 Feb 11;7:23. doi: 10.3389/fped.2019.00023. PMID: 30805324; PMCID: PMC6378296.
100. Gomez-Ciriza G, et al. Affordable Three-Dimensional Printed Heart Models. Front. Cardiovasc. Med 8:642011.
101. Farooqi KM, Cooper C, Chelliah A, Saeed O, Chai PJ, Jambawalikar SR, Lipson H, Bacha EA, Einstein AJ, Jorde UP. 3D Printing and Heart Failure: The Present and the Future. JACC Heart Fail. 2019 Feb;7(2):132-142. doi: 10.1016/j.jchf.2018.09.011. Epub 2018 Dec 12. PMID: 30553901.
102. Wang C, Zhang L, Qin T, Xi Z, Sun L, Wu H, Li D. 3D printing in adult cardiovascular surgery and interventions: a systematic review. J Thorac Dis. 2020 Jun;12(6):3227-3237. doi: 10.21037/jtd-20-455. PMID: 32642244; PMCID: PMC7330795.
103. Abudayyeh I, Gordon B, Ansari MM, Jutzy K, Stoletniy L, Hilliard A. A practical guide to cardiovascular 3D printing in clinical practice: Overview and examples. J Interv Cardiol. 2018 Jun;31(3):375-383. doi: 10.1111/joic.12446. Epub 2017 Sep 25. PMID: 28948646.
104. James M. Otton, Roberto Spina, Romina Sulas et al. Left Atrial Appendage Closure Guided by Personalized 3D-Printed Cardiac Reconstruction. JACC: Cardiovasc Interv vol. 8, No. 7, 2015 : pp 1004 à 1006.
105. Orly Goitein, Noam Fink, Victor Guetta et al. Printed MDCT 3D models for prediction of left atrial appendage (LAA) occluder device size: a feasibility study. EuroIntervention 2017 ; 13 : pp 1076 à 1079.
106. Michaela M. Hell, Stephan Achenbach, In Seong Yoo et al. 3D printing for sizing left atrial appendage closure device: head-to-head comparison with computed tomography and transoesophageal echocardiography. EuroIntervention 2017 ; 13 : pp 1234 à 1241.

107. Vlad Ciobotaru, Nicolas Combes, Claire A. Martin et al. Left atrial appendage occlusion simulation based on three-dimensional printing: new insights into outcome and technique. EuroIntervention 2018 ; 14 : pp 176 à 184.
108. Odemis E, Aka İB, Ali MHA, Gumus T, Pekkan K. Optimizing percutaneous pulmonary valve implantation with patient-specific 3D-printed pulmonary artery models and hemodynamic assessment. Front Cardiovasc Med. 2024 Jan 8;10:1331206. doi: 10.3389/fcvm.2023.1331206. PMID: 38259310; PMCID: PMC10800937.
109. Jivanji SGM, Qureshi SA, Rosenthal E. Novel use of a 3D printed heart model to guide simultaneous percutaneous repair of severe pulmonary regurgitation and right ventricular outflow tract aneurysm. Cardiol Young. 2019 Apr;29(4):534-537. doi: 10.1017/S1047951119000106. Epub 2019 Apr 10. PMID: 30968796.
110. Ciobotaru V, Tadros VX, Batistella M, et al. 3D-Printing to Plan Complex Transcatheter Paravalvular Leaks Closure. J Clin Med. 2022 Aug 15;11(16):4758. doi: 10.3390/jcm11164758. PMID: 36012997; PMCID: PMC9410469.
111. Li WD, Keyoumu R, Wang C, Liu Z. 3D Printing-guided endovascular repair of enormous twisted thoracoabdominal aortic aneurysm with branch stenosis and occlusion. Catheter Cardiovasc Interv. 2023 Mar;101(4):813-816. doi: 10.1002/ccd.30578. Epub 2023 Feb 5. PMID: 36740232.
112. Baruteau AE, Hascoet S, Malekzadeh-Milani S, Batteux C, Karsenty C, Ciobotaru V, Thambo JB, Fraisse A, Boudjemline Y, Jalal Z. Transcatheter Closure of Superior Sinus Venosus Defects. JACC Cardiovasc Interv. 2023 Nov 13;16(21):2587-2599. doi: 10.1016/j.jcin.2023.07.024. Epub 2023 Oct 18. PMID: 37855807.
113. Paul A. Yushkevich, Joseph Piven, Heather Cody Hazlett, Rachel Gimpel Smith, Sean Ho, James C. Gee, and Guido Gerig. User-guided 3D active contour segmentation of anatomical structures: Significantly improved efficiency and reliability. Neuroimage 2006 Jul 1;31(3):1116-28.
114. Butera G, Sturla F, Pluchinotta FR, Caimi A, Carminati M. Holographic Augmented Reality and 3D Printing for Advanced Planning of Sinus Venosus ASD/Partial Anomalous Pulmonary Venous Return Percutaneous Management. JACC Cardiovasc Interv. 2019 Jul 22;12(14):1389-1391. doi: 10.1016/j.jcin.2019.03.020. Epub 2019 May 15. PMID: 31103542.
115. Batteux C, Abakka S, Gaudin R, Vouhé P, Raisky O, Bonnet D. Three-dimensional geometry of coronary arteries after arterial switch operation for transposition of the great arteries and late coronary events. J Thorac Cardiovasc Surg. 2021 Apr;161(4):1396-1404. doi: 10.1016/j.jtcvs.2020.06.036. Epub 2020 Jun 29. PMID: 32713644.
116. Batteux C, Ciobotaru V, Arditi W, Decante B, Karsenty C, Combes N, Hascoet S. Transcatheter correction of sinus venosus defect in a patient with a challenging anatomical configuration: From bench testing to clinical success. Catheter Cardiovasc Interv. 2023 Dec;102(7):1265-1270. doi: 10.1002/ccd.30898. Epub 2023 Nov 17. PMID: 37975208.
117. Batteux C, Ciobotaru V, Bouvaist H, Kempny A, Fraisse A, Hascoet S. Multicenter experience of transcatheter correction of superior sinus venosus defect using the covered Optimus XXL stent. Rev Esp Cardiol (Engl Ed). 2023 Mar;76(3):199-201. English, Spanish. doi: 10.1016/j.rec.2022.08.004. Epub 2022 Aug 30. PMID: 36055641.

118. Haddad RN, Hascoet S, Karsenty C, Houeijeh A, Baruteau AE, Ovaert C, Valdeolmillos E, Jalal Z, Bonnet D, Malekzadeh-Milani S. Multicentre experience with Optimus balloon-expandable cobalt-chromium stents in congenital heart disease interventions. Open Heart. 2023 Jan;10(1):e002157. doi: 10.1136/openhrt-2022-002157. PMID: 36631173; PMCID: PMC9835936.
119. Tajouri A, Batteux C, Ly R, Houyel L, Hascoet S. Inferior sinus venosus defect and anomalous hepatic venous return to the coronary sinus leading to an Eisenmenger syndrome. Cardiol Young. 2023 Jan;33(1):136-137. doi: 10.1017/S1047951122001354. Epub 2022 Apr 28. PMID: 35481445.
120. Albenque G, Batteux C, Hascoët S. Transcatheter correction of a rare combined anomalous pulmonary and systemic venous return in an adult. Eur Heart J. 2024 Oct 29:ehae732. doi: 10.1093/eurheartj/ehae732. Epub ahead of print. PMID: 39471415.
121. Devine WA, Anderson RH. Superior caval to pulmonary venous fistula: the progenitor of the sinus venosus defect? Pediatr Path01 1989;9:345-9.33.